THE SEDIMENTOLOGY, MINERALOGY AND METAL CONTAMINATION OF SEDIMENTS IN THE APEX OF THE NEW YORK BIGHT, NY, USA: AN INTEGRATED LABORATORY AND FIELD STUDY OF TRACE METAL BEHAVIOR IN AN URBAN ESTUARY

by

NOUREDDIN H. AMAACH

A dissertation submitted to the Graduate Faculty in Earth and Environmental Sciences in partial fulfillment of the requirements for the degree of Doctor of Philosophy,The City University of New York

2008

INFORMATION TO USERS

The quality of this reproduction is dependent upon the quality of the copy submitted. Broken or indistinct print, colored or poor quality illustrations and photographs, print bleed-through, substandard margins, and improper alignment can adversely affect reproduction.

In the unlikely event that the author did not send a complete manuscript and there are missing pages, these will be noted. Also, if unauthorized copyright material had to be removed, a note will indicate the deletion.

ProQuest LLC
789 East Eisenhower Parkway
P.O. Box 1346
Ann Arbor, MI 48106-1346

This manuscript has been read and accepted for the

Graduate Faculty in Earth and Environmental Sciences in satisfaction of the

dissertation requirement for the degree of Doctor of Philosophy.

Dr. Stephen Aja

Date **Chair of Examining Committee**

Dr. Yehuda Klein

Date **Executive Officer**

Dr. David Seidemann

Dr. Cecilia McHugh

Supervisory Committee

THE CITY UNIVERSITY OF NEW YORK

Abstract

THE SEDIMENTOLOGY, MINERALOGY AND METAL CONTAMINATION OF SEDIMENTS IN THE APEX OF THE NEW YORK BIGHT, NY, USA: AN INTEGRATED LABORATORY AND FIELD STUDY OF TRACE METAL BEHAVIOR IN AN URBAN ESTUARY

By

Noureddin Amaach

Advisor: Professor Stephen Aja

Owing to past and present discharge of industrial and chemical wastes in the New York Bight, sediments and biota of the NYB have been shown to contain elevated levels of enviro-toxic trace metals. These trace metals, produced by anthropogenic activities, persist at elevated levels and pose health risks to humans and the ecosystem.

In this study, two sets of sediment samples collected over a period of 20 years have been studied to evaluate the health of the Bight system. The first series of samples were collected in summer of 1976 during the time of active dumping and the second series were collected in summer of 1997.

The samples were analyzed by flame atomic absorption spectrophotometry (AAS) to determine sediment Pb, Cr, Cu, Zn, Cd and Ni concentrations. Estimated mineral composition of these samples was determined by powder X-ray diffractometry analysis (XRD).

This study found greater Pb, Cr, Cu, Zn, Cd, and Ni concentrations in clay-silt fraction from sewage sludge, mud dumpsite and near shore mud-patches than their

background values and greater than those of USEPA sediment quality guidelines. Zn had the highest concentration followed by Pb,Cr, Cu, Ni, and Cd.

XRD analysis of the sediments showed that the dominant clay minerals were illite, chlorite, and kaolinite. The percentage of clays and trace metal levels showed the same trends, being highest within sewage sludge and mud dumpsites. These levels were slightly lower south and north of these dumpsites, and near shore environment. This indicates contaminants-laden clays on the floor of the NYB are being reworked by currents, transported, and scattered within the Bight.

Statistical analysis showed weak correlation and nonnormal distribution of trace metals. This suggests that the geochemical behavior of these metals has been affected by pH, Eh, clay-metal cations selectivity, and hydrodynamics of the Bight.

Therefore, result from this study may be useful in the development of management plans to clean up polluted sites and curtail sources of contamination.

ACKNOWLEDGMENTS

First of all, I would like to thank my advisor, Professor Stephen Aja, for sticking it out with me all these years and giving liberally of his time. Professor Aja is responsible for involving me in this project in the first time. During my independent studies with Aja, I learned about the properties of clays and the significant role they play in a diverse range of environmental problems. He taught me how to ask questions and express ideas. He also showed me different ways to approach a research problem and the need to be consistent to accomplish any goal. Professor Aja is an excellent scientist-he surely will be a role model in my academic career.

Beside my advisor, I would like to thank the rest of my committee: Professor Cecilia McHugh from Queens College and Professor David Seidemann form Brooklyn College, who have been very helpful in their academic and personal advisements. Special thanks go to professor McHugh who I met several times at Columbia University-Lomont Doherty Research Laboratories and Queens College. She provided me with sections of two core samples and invaluable literature on the New York Bight and the Hudson River Estuary. She also helped me understand the sedimentology and the physical processes involved in the New York Bight and the Hudson River Estuary. I deeply appreciate the assistance of Professor David Seidemann for his comments, encouragement and his kind words. Seidemann in one of his emails says: “your thesis approved itself, in a sense. Good work is good work”.

There are so many people at Brooklyn College, my home college, to whom I owe much. Let me say "thank you" to the following Professors who taught me geology: William Harris, Somedev Battacharji, Gerard Friedman, Nehru Cherukupalli, John Chamberlain, David Seidemann and Stephen Aja. Thanks to my friend Guillermo Rocha in the Geology department for his technical assistance in using AAS. Many thanks also go to Ms Lina McCain, the graduate program assistant from EES, who is an invaluable asset to the Ph.D. program and all the graduate students.

I owe my thanks to family: my parents, Haddou Amaach, and Mahjouba Elalami, for giving me life in the first place, for educating me, for support and encouragement to pursue my interests, even when the interest went beyond boundaries of language, field and geography.

Last but not least, I owe my loving thanks to my wife Hayat Barakat, for her listening to my complaints and frustrations, and for believing in me. Without her encouragement and understanding it would have been impossible for me to finish this work. And thanks to God, "our dwelling place through all generations"

Table of Contents

List of Tables

Page

List of Tables

Page

List of Figures

List of Figures (continued)

Page

CHAPTER 1

Some Environmental Issues in the New York Bight

The marine environments of the New York Bight have been used for navigation, dredging, recreation, and commercial fishing**.** These coastal environments have, moreover, served as major waste disposal sites for well over a century as records of ocean disposal activities in the Bight region date back to the late 1800s' (Gross, 1976; Mueller and Anderson 1978; Squire, 1983; Butman et al., 1998, Butman et al., 2002; Butman, 2003). The NYB sediments are contaminated by various substances that are potentially toxic (Metzger, 1998). The anthropogenic activities are the major sources of these enviro-toxic substances. The environmental impacts of disposal in the Bight are discussed in Mayer (1982), HydroQual (1989), Munns and Rubinstein (1990), Swanson and others (1991), EPA (1990B), NOAA (1995), and EPA and others (1996).

The New York –New Jersey Harbor is shallow and needs constant dredging just to facilitate navigation and preserve existining channel depths. The annual volume of sediments that needs to be dredged is approximately 3 to 5 million m^3 (~ 4 to 6 million $yard^3$) . The dredged sediments have been found to contain elevated substances that are potentially toxic (Medzger, 1998).

The commercial market of the port of the New York has declined as a result of concerns over costs, securities and above all, the lack of dredging of contaminated sediments. Delays in dredging have caused ocean carriers to divert cargo to other ports. Thus, the port's share of North Atlantic shipping trade has dropped from 60% in 1967 to 40% in 1990 (Raymond,1998; Friedman et al, 2000).

The degradation of the NYB environment is further exacerbated by the high population density of the New York-New Jersey metropolitan area, which is the most populated coastal region in the United States (Figure 1). For instance, for over a period of 64 years, sewage sludge from New York's twenty sewage treatment plants was dumped at the '12-Mile Mud-Dump Site' in the apex of the New York Bight, where the water is about 50m deep, 10 million t $year^{-1}$ of sludge was disposed there (Clarke, 1997). In addition, the Mud DumpSite (MDS) received 200 million m^3 of dredged material between 1936 and 1980 (Dayal 1981). In what follows, an abbreviated history of disposal activities in the Bight area is provided (Massa et al., 1996).

1800 to late 1960s: Though ocean disposal had become a common practice by the late 1800s, there was very little regulation of such activities. The primary concerns, during this period, centered on transportation and navigation needs rather than on environmental concerns. Congressional acts (such as the New York Harbor Act of 1899) gave the United State Army Corporation of Engineers (USACE) authorities to select disposal sites and issue permits for ocean disposal. During this period (1890-1971), a great variety of wastes (including municipal waste, industrial waste, construction and demolition debris, municipal sewage, and dredge material) totaling about 1,100 million cubic yard of solid wastes were estimated to have been disposed off in the Bight (Gross, 1976). The first major ban of ocean disposal activities occurred in the 1930s. Following lengthy litigation between New York City and communities along the New Jersey shore, the Supreme Court banned ocean disposal of municipal waste and floatable debris in U.S. waters after 1934.

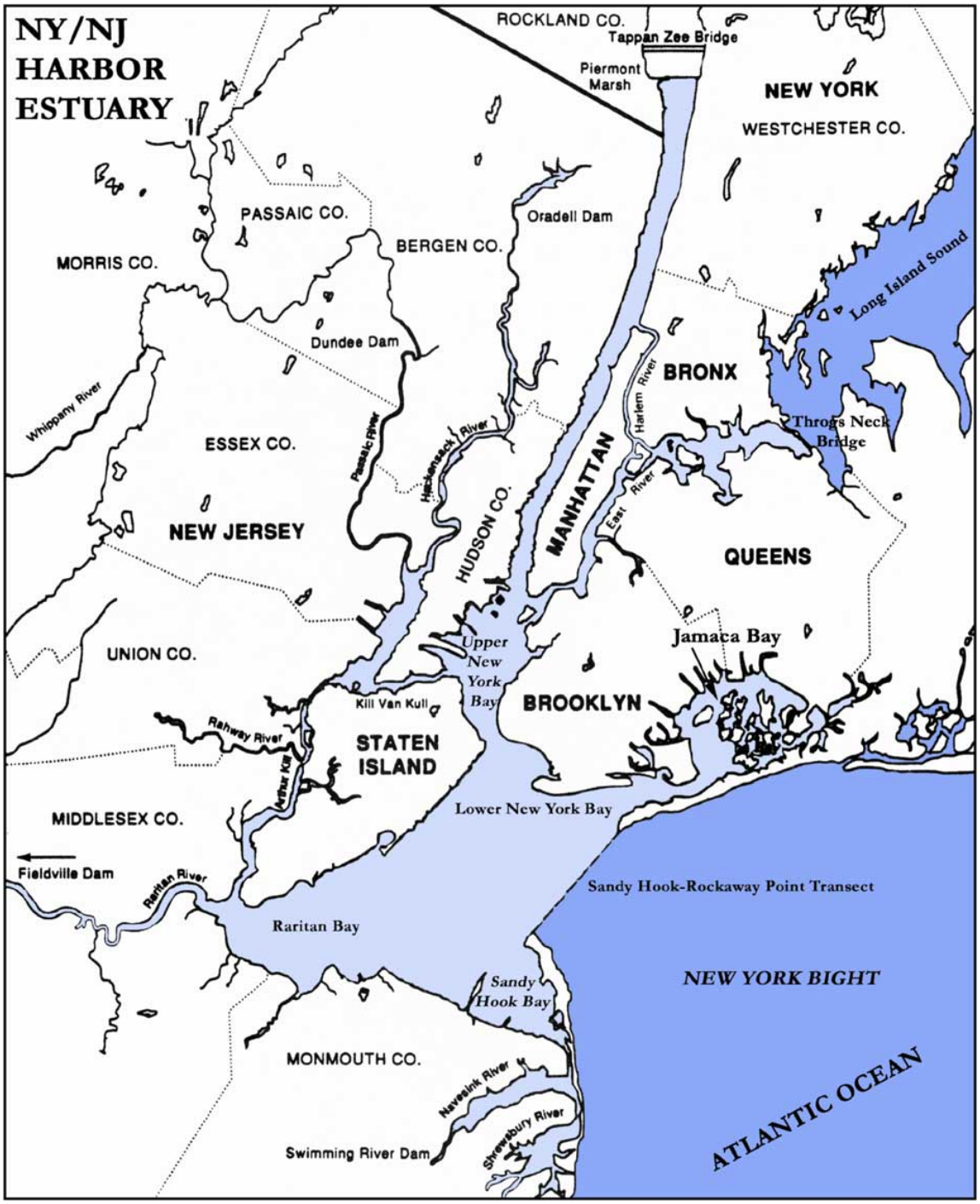

Figure 1: New York-New Jersey metropolitan area.

(White color is land; light blue color represents NY/NJ harbor waters and dark blue color for NYB water) (Source: NOAA, 2003)

Late 1960s to late 1980s: Public and Congressional awareness of the environmental impacts of ocean disposal increased in the late 1960s and early 1970s. These concerns led to laws that greatly increased research, public involvement, and government oversight. The Congress passed the National Environmental Policy Act (NEPA) in 1969. This act provided for the formation of a Council of Environmental Quality Report (1970) which identified the poor regulation of ocean disposal as a potential environmental danger. This Act also led to the establishment of the EPA in 1970, and EPA was subsequently given oversight responsibility for many ocean disposal activities.

In 1972 the London Dumping Convention (LDC) was negotiated and went into effect in 1975. The LDC is an international agreement among nations to control materials leaving their shores for the purpose of ocean disposal. The Marine Protection, Research, and Sanctuaries Act (MPRSA) (Public Law 92-532), also referred to as the Ocean Dumping Act, were passed in 1972 (and subsequently amended). MPRSA declares that "it is the policy of the United States to regulate the dumping of all types of materials into ocean waters." It prohibits the ocean disposal of any material which would unreasonably degrade or endanger human health, welfare, amenities, the marine environment, ecological systems, or economic potentialities. The research, monitoring, evaluation and designation of ocean disposal sites are the shared responsibility of EPA and the National Oceanic and Atmospheric Administration (NOAA). Site designation involves preparation of a voluntary Environmental Impact Statement (EIS) and a thorough environmental review in accordance with the site designation criteria that the EPA first issued in October 1973. The disposal operations may take place only if an ocean dumping permits is issued. The permitting program established under MPRSA is

administered by EPA and USACE. It has been and continues to be EPA's policy that no permit should be issued for ocean disposal of any waste if there is a technically feasible and environmentally acceptable alternative disposal method. Surveillance and enforcement activities to ensure lawful ocean dumping practices are the responsibility of the U.S.Coast Guard working in cooperation with the EPA.

Late 1980s to Mid-1990s: The increased public concern about disposal of wastes in the ocean, during this time period, resulted in legislation that banned the disposal of certain wastes in ocean waters. This period also saw increasing government monitoring, more stringent permit conditions, and increased use of beneficial and other non-ocean alternatives so that the quantities of ocean-disposal wastes degrading the health of the Bight continued to decline. The average annual volume of dredged material removed between 1980 and 1987 from the port of New York and New Jersey was 4.4 million cubic meters (Bokuniewicz et al., 1991). Almost all ocean disposal activities in the Bight were phased out by the early 1990s; disposal of industrial waste, acid waste, cellar dirt, wood incineration and sewage sludge ended in 1987, 1988, 1989, 1991, and 1992, respectively.

1986s to 1990s: The waste was taken to the 106-mile site, 185 km offshore and with a water depth of 2200-2700 m. Despite this, waste disposal at this site was prohibited after 1991 (Clarke, 1997) and commercial fishing were discontinued and waste disposal alternatives were evaluated.

On July 24, 1996, the Clinton Administration mandated the closure of the Mud DumpSite or MDS. In September 1997 the MDS was closed as an official ocean disposal site by the U.S. Environmental Protection Agency, and the MDS and surrounding areas

were designated as Historic Area Remediation Site (HARS). The sea floor of the HARS, approximately 9 square nautical miles in area, is being remediated by placing at least a one-meter cap of Category I (clean) dredged material on the top of the existing surface sediments that exhibit varying degrees of degradation. About 1.1 million cubic yards of dredged material for remediation was placed in the HARS in 1999, and 2.5 million cubic yards in 2000 to avoid further pollution (Friedman, 1996a, b).

A summary of history of uses and regulations of ocean disposal sites in the NYB are tabulated in Appendix A.

1.1. Sources and Types of Waste in the New York Bight

Historically, a great variety of wastes have been disposed in the apex of New York Bight (Figure 2). There are five major waste disposal sites in the New York Bight. These sites are all located within the Bight apex (Figure 3 & Table 1). They include the sewage sludge site, the Mud Dump Site (MDS), the cellar dirt (rubble and debris) site, the acid wastes site, and the wreck (derelict vessel) site. A sixth dump site, the chemical wastes site is just outside the New York Bight (Figure 4). Roughly 70% of the municipal wastes and 60% of the industrial wastes are dumped at these six sites (USEPA, 1974). Descriptions of prior ocean disposal activities dating back to the late 1800 s may be found in Gross (1976), Mueller and Anderson (1978), and Squires (1983).

1.1.1. Sources of waste

Waste disposal at the Acid Wastes Site consisted almost entirely of liquid, highly acidic (pH<1) waste generated from industries in New Jersey. For instance, sulfuric acid and ferrous sulfates were generated from the processing of titanium dioxide pigment, and hydrochloric acid was produced during the manufacture of refrigerant like Freon.

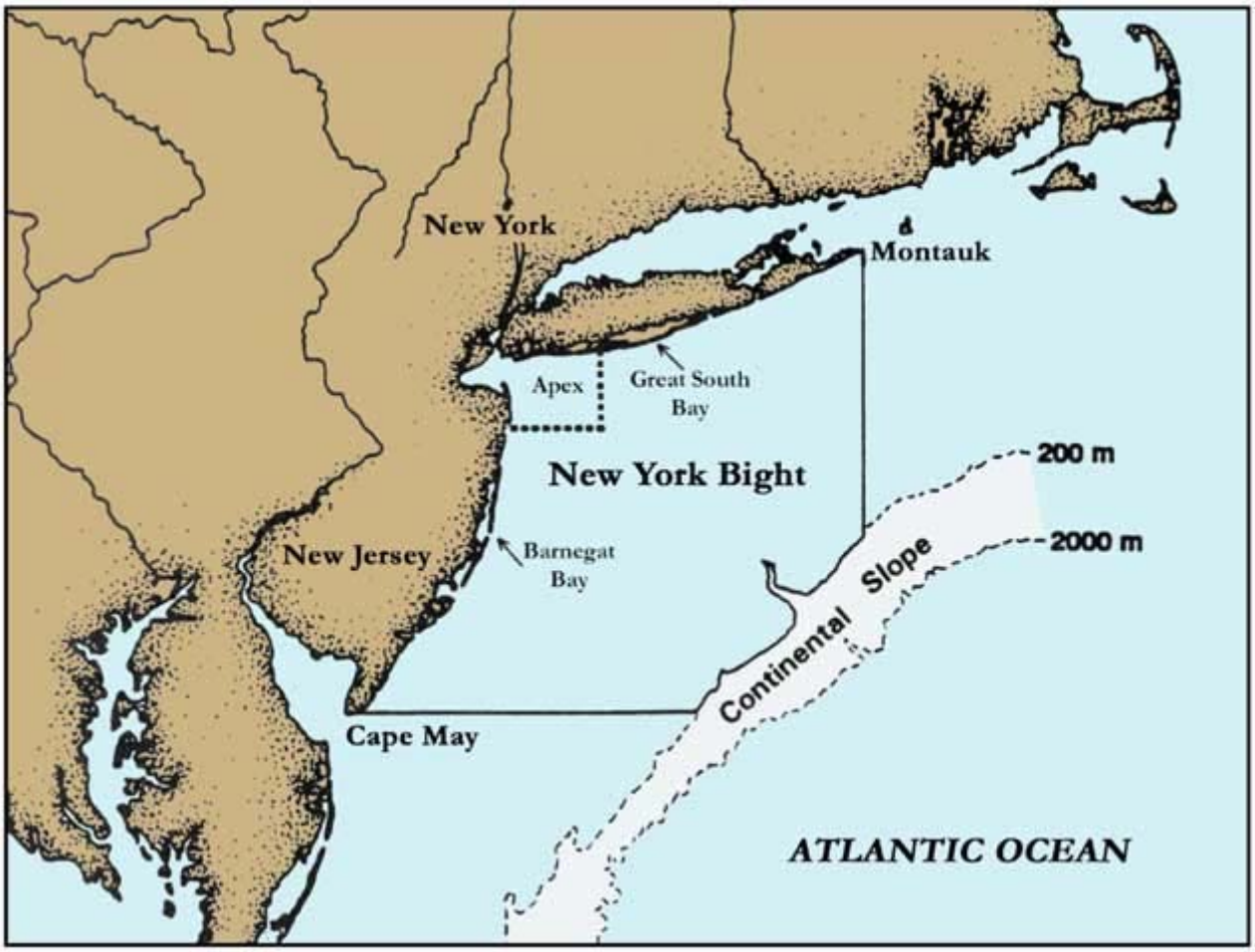

Figure 2: The Bight.
(Brown color represents land and blue are waters)
Source: NOAA 2003

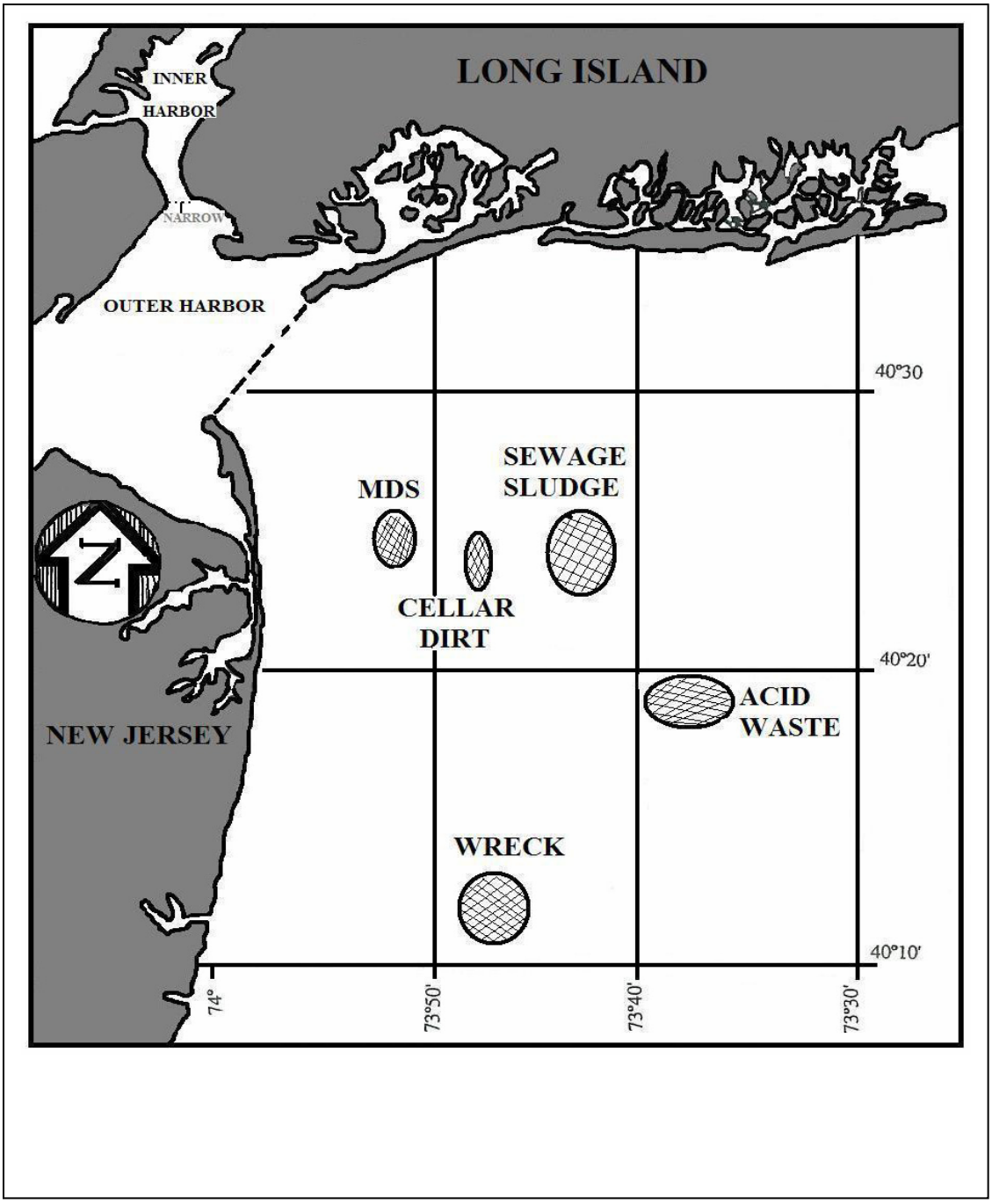

Figure 3: Bight apex and waste disposal sites (Dark gray color is land & white color is water). Note that all the waste disposal sites lie within the confines of the Bight Apex (Adapted from EPA 1980b, modified)

Table 1: Dump sites in and adjacent to the New York Bight

Dump Site	Coordinates Latitude & Longitude	Area Sq km	Depth (meters)	Approximate Distance (km)	
				L.I.	N.J.
Sewage Sludge	40°22' 30" N to 40°25'00" N 73°41' 30" W to 73°45'00"W	22.7	27	20	20
Dredge Spoil (Mud Dump Site)	40 °24'10" N to 73°49'00" W[1]	6.9	27	20	9
Cellar Dirt	40°23'00" N to 40° 20'00"W[1]	6.9	31	22	11
Acid Wastes	40°16'00" N to 40°20'00" N 73°36'00" N to 73°40'00" N	41	24	27	27
Wreck	40° 13'00" N to 73°46'00" W[1]	6.9	26	30	20
Chemical Waste	38°40'00" N to 39°00'00" N 72°00'00" N to 72°30'00" N	1,500	1,800	-	-

[1]Center Coordinates
USEPA, November 15, 1975
Note: History of Dump sites and regulations: See Appendix A

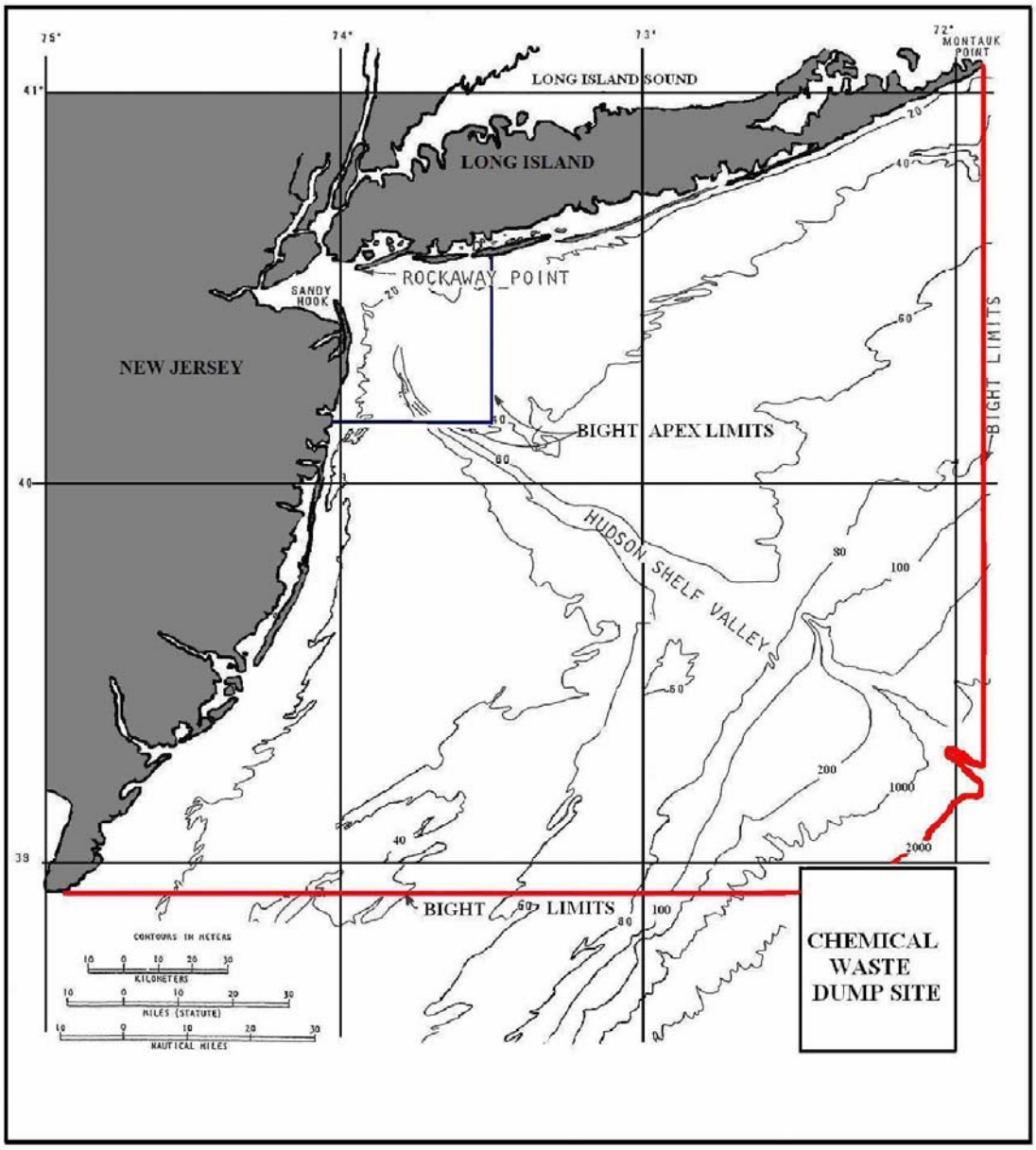

Figure 4: New York Bight showing the bight limits in red .
Note that the chemical waste dump lies outside the Bight limits.
Modified from USEPA (APRIL, 1975)

Industrial wastes consisted of solid, semi solid, or liquid byproduct generated by manufacturing or processing plants, such as by product produced during the manufacture of paint or chemicals and by-product hydrochloric acid from Allied Chemical and by-product sulfuric acid-iron waste from the manufacture of titanium dioxide by NL Industries (Monahan et al., 1987).

Municipal sewage sludge consisted of the solid and semi solid or liquid residues generated during the treatment of domestic sewage. The disposed sewage sludge was mostly water and consists of about 5% solids on dry basis and 95% liquid. The solid fraction is a heterogeneous mixture of a variety of solids, including microorganisms, organic detritus or aggregates, fibers (including hair), plastics, metals, petrochemicals, petroleum-combustion products, plants debris, mineral grains, animal waste and food residue. The liquid part of sewage contains industrial wastes, atmospheric fallout, and vehicular wastes (oils and greases) (Gross, 1976). Today most of the solid residues are eliminated during the primary and the secondary treatment processes; however some of the solid particles remain in sewage during emergency release.

Dredged material consists of the sediments deposited naturally in water ways so in this sense it is not an anthropogenically generated waste. Sediments are dredged from the New York Harbor region to assure that the navigation channels and berths can accommodate the cargo-, container-, and passenger ships coming into the port. The sediments dredged from the harbor have been predominantly fine-grained. Based on the data accumulation from 1980 to 1990, on average, material disposed off in the ocean consists of approximately 33% sand, 44% silt, and 23% clay (USACE and EPA, 1994). Before dredged material can be disposed off in the ocean, it must undergo rigorous

physical, chemical and biological testing to ensure that the materials will not unacceptably degrade the ocean environment. These tests are described in handbooks commonly known as the old and new Green Books (EPA and USACE, 1977 and 1991) and revised regional guidance documents for implementing the new Green Book (EPA and USACE, 1992). Based on the tests, the sediments pass or fail the ocean disposal criteria and are classified by EPA region 2 and the USACE New York district into one of the three categories.

Category 1: Sediments which meet ocean disposal criteria; they are acceptable for "unrestricted" ocean disposal.

Category 2: Sediments which meet ocean disposal criteria. To protect against the potential for bioaccumulation, appropriate techniques such as capping with layer of clean material are commonly required. This is referred to as "restricted" ocean disposal.

Category 3: Sediments which do not meet ocean disposal criteria; even with the application of management techniques they are not acceptable for ocean disposal.

1.1.2. Type of Pollutants in the New York Bight

The contaminant loading in the Bight can be attributed to dumping and non-dumping pollutant sources. The non-dumping loading comes from three major sources: 1) atmospheric fallout, 2) waste water (municipal and industrial discharges), and 3) surface (gauged and urban) and groundwater runoff. Three separate zones have been identified for wastes loading into the Bight: the Sandy Hook-Rockaway Point transect zone, the New Jersey coastal zone, and the Long Island coastal zone. According to Muller and Jeris (1975), the greatest pollutants input to the Bight originate in the Sandy Hook-Rockaway Point transect zone. Inputs from the New Jersey and Long Island

coastal zones are small, contributing less than 6% of the total contaminant loading to the Bight. A summary of sources of pollutants in the New York Bight are presented in Figure 5.

Barging sources include dredged material, sewage sludge, cellar dirt and acid wastes dumped directly into the waters of the Bight. The pollutant loading from the wreck was considered to be insignificant. In term of absolute volumes, dredged material constituted the major source of pollutants dumped in the Bight.

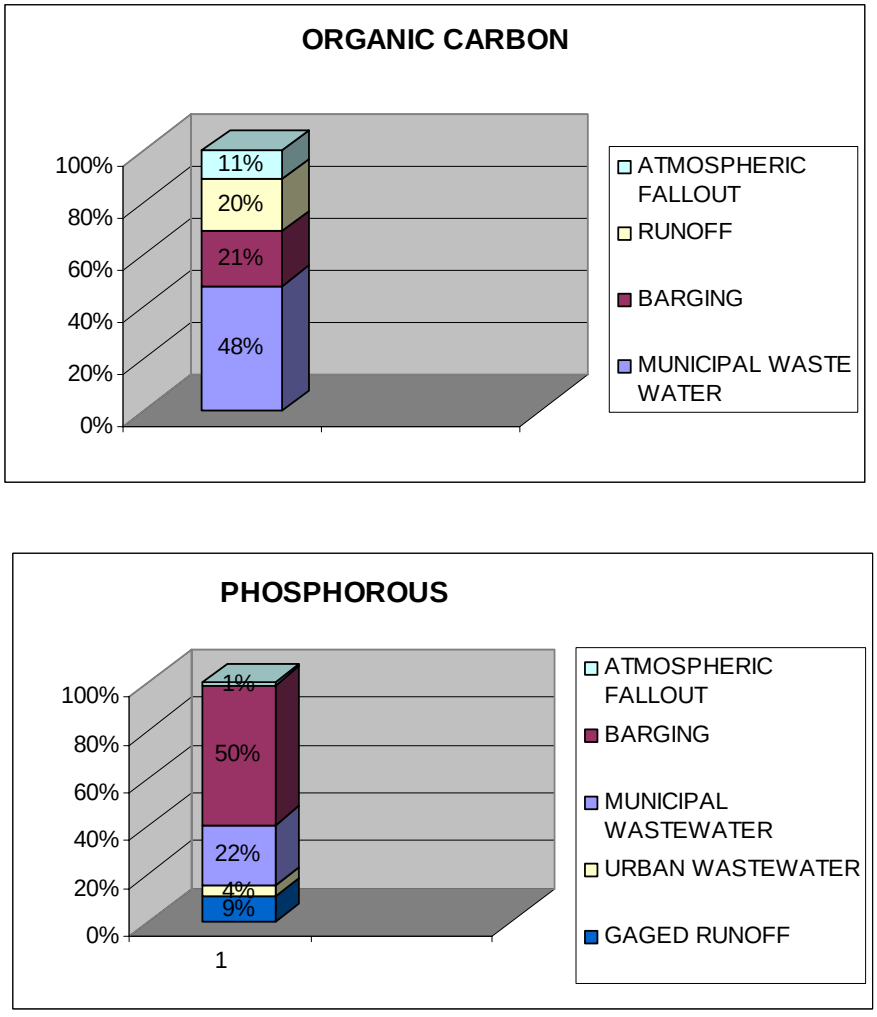

Figure 5: Types and sources of pollutants in NYB. Modified from Gross (1976)

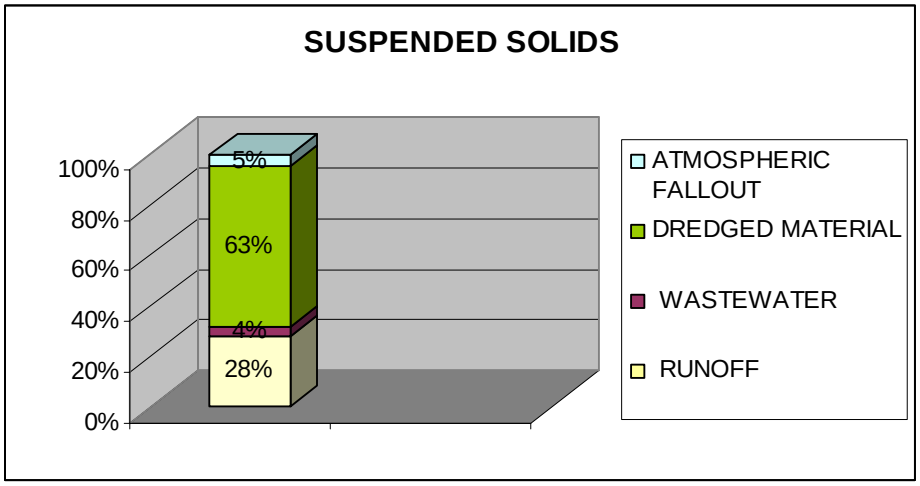

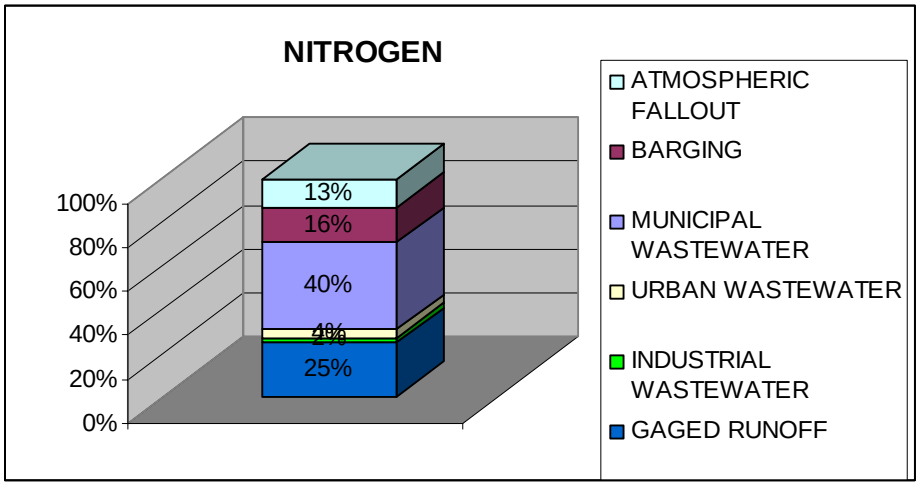

Figure 5: Types and sources of pollutants in NYB (continued). Modified from Gross (1976)

Suspended Solids

The major input of suspended solids to the New York Bight waters (63%) is derived from barged sources, especially dredged material (54%), and is followed by cellar dirt (6.8%) and sludge material (2.1%). Atmospheric fallout contributes approximately 5% of the total, while runoff contributes about 28%. Wastewater discharge contributes the remaining 4% (Muller et al, 1975, Gross 1976)

Carbonaceous Materials

Municipal wastewater discharges are the source of about half (48%) of the biochemical oxygen demand (BOD) loading reaching the Bight. Barging (21%), runoff (20%), and atmospheric fallout (9%) account for most of the remaining load. Barging and municipal wastewater discharge loadings account for approximately 67% of the carbon oxygen demand (COD) and 50% of the total oxygen carbon (TOC) loading in the Bight. The COD and TOC loadings from atmospheric fallout are approximately 11 % and 15%, respectively. Likewise, the COD and TOC loadings from runoff are approximately 11 % and 15%, respectively (Mueller et al, 1975, Gross 1976)

Heavy Metals

Barging appears to be the major source of heavy metals contamination to the New York Bight, with exception of Hg (from municipal wastewater discharges). Runoff and municipal wastewater discharges are the second and third largest sources. Almost all of the barge-related heavy metal loadings are the result of dredged material dumping; sewage sludge account for less than 6% of these loadings (Mueller et al, 1975, Gross 1976)

Nitrogen and Phosphorous

Approximately half of the oxidizable nitrogen (ammonia, organic nitrogen, and nitrate-nitrogen) in the Bight appears to result from municipal wastewater discharges. Runoff and barging, almost equally, account for the remaining oxidizable nitrogen. Gauged runoff (60%) is by far the largest source of nitrites and nitrates in the Bight. Atmospheric fallout (33%) is the second major source of these contaminants. Municipal wastewater discharges account for 72% of the dissolved phosphorous (Ortho-P) loading in the New York Bight. The remainder of the dissolved phosphorous results from runoff. Barging, primarily of dredged material, accounts for 50% of the total phosphorous loading to the Bight (Mueller et al, 1975, Gross 1976)

Microbial Contamination

Municipal wastewater discharges appear to be the major source (84 to 91 %) of microbial contamination (fecal and total coliform) to the Bight. The remaining coliform loading results from urban runoff. Barging is an insignificant source of fecal contamination of the New York Bight (Mueller et al, 1975, Gross 1976)

1.2. Previous Studies of Metal Contamination in the New York Bight

Numerous studies (Shepard et al., 1936; Emery et al., 1952; Chave et al., 1960 ; Friedman et al., 1968; Gross, 1970; Pearce, 1972; Carmody, 1973; Harris, 1976 and 1982; Gross et al. 1979; Dayal et al., 1981; Scott et al., 1990; NOAA, 1991; Huntley et al., 1993; Schimmel et al., 1994, Butchholtz ten Brink et al., 1997) have been carried out on sediments, seawater, and dredged material on the continental shelf of the New York Bight. From an examination of the New York Bight sediment samples, Shepard (1936) reported a lack of correlation between grain size and distance from the

shore and in a further study of more than 700 sediment samples from the continental shelf, Shepard and Cohee (1936) found that the sediments of New Jersey shelf were derived from the erosion of Tertiary Formations. From a comparative study of the mineral compositions of recent marine sediments and ancient marine sedimentary rocks, Chave et al. (1960) concluded that chemical reactions took place at solid-water interface subsequent to the settling of sediment on the sea floor; however, the rate and types of chemical reactions were not fully understood. The relationship between bottom sediments, microorganisms, and the waters on the continental shelf of the New York Bight has been studied by Friedman and Sanders (1968) who concluded that the distribution of trace metals within the depositional system is a function of Eh, pH and other chemical factors. Changes of these parameters will result in variations in trace-metals concentration and distribution. Emery and Rittenberg (1952) reported that the Eh and pH of interstitial waters result from bacterial degradation of sulfate ions. Friedman et al. (1968) studied the chemical characteristics of interstitial waters from cores of shelf sediments from the inner and outer shelf off Long Island. They compared these chemical characteristic with those of the overlying seawaters and found that the chlorinity (Cl) and Ca/Cl, K/Cl, and Rb/Cl ratio are higher on the inner shelf than the outer shelf. They also noted that the values of pH and Eh are lower in interstitial waters than in overlying waters and attributed the decrease in Eh and pH below the water-sediment interface to the activity of anaerobic bacteria. Studies of organic matter content (Hunt, 1961; Gross, 1970; Froelich et al. 1971) have shown that the total organic carbon (TOC) content is inversely related to the mean size distribution of the sediments particles. Furthermore, in a study of the Bight Apex sediments, Pearce (1972) determined that the concentration of

total organic matter is in the order of 10%-20% in the mud and silt deposits of the Christiansen Basin; this organic material (i.e., Christiansen Basin) and those found in mud patches near Long Island have been shown to be predominantly of sewage origin (Gross et al., 1976). Sewage-derived organic matter wanes at the seaward side of the Bight Apex as the organic matter becomes less influenced by sewage-derived organic matter and oceanic organic matter becomes more significant. Owing to the disposal of raw-sewage and the discharge of municipal and industrial wastewater onto the New York Harbor waters, much of the sediment dredged from these areas is contaminated with hydrocarbons and heavy metals (Gross, 1970; Mueller et al., 1976; Conner et al., 1979). Heavy metals concentrations (Pb, Cu, Zn, Ni, and Cr) in the Bight sediments were investigated by Carmody (1973) in a study of 400 sediment samples; he documented a horizontal distribution of the five metals in a similar pattern around the dumping site and a considerable vertical variation of the metals in the sediments. The movement of wastes, down the Hudson Submarine Valley, also suggested by Carmody's data may be due to a gravity-induced flow of the gelatinous contaminants. Additional studies of environmentally-sensitive metals (Pb, Zn, Mn, Cr) by Harris (1976) showed temporal and spatial variations in the distribution of fine-grained deposits and in the concentration ratios for certain metals especially Zn and Cr; these metal ratios were then used by Harris (1976) to determine the sources of these materials. He also noted that bottom currents can resuspend Christiansen Basin mud derived from the sludge disposal site in the apex and actively transport these materials containing high concentrations of trace metals; hence, the mud patches near Long Island are cyclic and the settling of these patches takes place during summer time. A detailed study of metals in interstitial waters of the New

York Bight Dredged-Material Deposits was conducted by Dayal et al., (1981); they found that for dredged material deposits, a sediment-derived diffuse flux of dissolved Fe and Mn to overlying water exists. The estimated fluxes for Fe and Mn are at least two to three orders of magnitude lower than the input of Mn and Fe associated with dredged-material dumping, while the concentration of Zn in interstitial water is equivalent to those reported for the bottom water at the dredged-material dump site. Hence, the diffusional flux of Zn is minor. The extremely low concentration of other metals (such as Cu, Cd, and Hg) in the interstitial waters indicates that their diffusional flux is negligible. In 1982, Harris reported that during ocean disposal only a small fraction of the sludge particles penetrates the pycnocline to accumulate in the disposal area; most are rapidly dispersed in the water.

Other studies have described elevated levels of contaminants in sediments (NOAA 1991; Huntley et al., 1993) and sediment toxicity (Scott et al., 1990; Schimmel et al. 1994). Some of the waste disposed within the New York Bight and New York harbor estuary now appears to reside in the Hudson Shelf Valley, based on elevated concentrations of lead and other metals in shelf valley sediments (e.g., Butchholtz ten Brink et al. 1996; Butchholtz ten Brink et al., 1998; Mecray et al., 1999; Mercay et al., 2001). Most of these studies have shown that water and bottom sediments of the New York Bight have been polluted as a result of ocean dumping of industrial and municipal wastes.

1.3. Objectives and Significance of Study

The disposal of waste materials onto the NYB environment certainly produced some environmental contamination which may have been dispersed and diluted over time. However, past studies have described elevated contaminant in sediments and these

earlier studies focused primarily on the concentrations and distribution of the trace metals without adequate consideration of the mineralogy of the sediments hosting the contaminant and the nature of the interaction of metal contaminants with sediments. Whilst the problem of metal pollution in the New York Bight is a long-standing one, there is still a considerable lack of information about the mineralogy of clays, the concentrations and distribution of trace metals in clay fractions, and mobility and behavior of trace metals in this unique environment. Such an understanding of the factors controlling mobility of metal pollutant in a dynamic hydrodynamic environment is necessary for predicting the fate of substances introduced into such aquatic environments. According to Gibbs et al. (1990), a uniform composition along the Hudson River estuary was found for illite (65%), chlorite (24%), and kaolinite (10%). Smectite being absent in the upper estuary above 60 km and being <5% in the lower estuary. The percentages of clay minerals are remarkably constant throughout the entire Hudson River estuary. Other studies of estuaries showed some trend in the mineral changing along the length of the estuary (Gibbs, 1997; Allen, 1991). Clays play a significant role in a diverse range of environmental problems and awareness of this role is growing (Parker and Rae, 1998). A particular important property of clays is the chemical activity of their surfaces which arises due to surface charge. This charge is caused by a combination of broken bonds, surface-growth defect and cation substitutions in the lattice. The negatively charged mineral surfaces can have two important consequences for environmental studies. Firstly, when riverine clays meet saline solutions, as for example in estuarine system, charge reversal occurs and particles form aggregates (a process referred as flocculation). When the floccules become large enough to settle out of the suspension, large scale

deposition of clays can occur. In this case the clays themselves can be said to be the pollutants. Further, any anthropogenic contaminants reacted with clays will accumulate in the area of flocculation. Other important problems issues in which clay minerals feature include contaminated land studies, the transport and reactivity of nutrients and the behavior of ^{137}Cs in upland soils following the Chernobyl nuclear disaster of 1986. Some problems are only just beginning to emerge, for example the role of clays in transporting viruses in coastal waters and in protecting absorbed viruses from degradation by sunlight. There will no doubt an endless plethora of new and in some case currently unimagined environmental problems in years to come. Clays therefore, may play a major role in the mobility toxic substance in aqueous environments such as, New York Bight. Hence, the principal objectives of this research are therefore:

1. To determine trace metal concentrations and Enrichment Factors (EF) as a function of particle size.
2. To obtain a better understanding of the mineralogy and sedimentology of the New York Bight sediments.
3. To quantify metal-mineral interactions in these marine environments.
4. To understand the dispersion pattern of dumped waste.
5. To understand the importance of clays in the transport and storage of trace metals.
6. To evaluate 1997 and 1976 sediment trace metal contaminant concentrations of selected sites.
7. To compare the trace metal concentrations with sediment quality standards values (USEPA ERL / ERM) of Logan and Morgan (1990) and Canadian EPA (1976).

8. To analyze the statistical significance of trace metal correlation in the apex of New York Bight sediments.

Aquatic sediments play a commanding role in regulating the concentration of most dissolved reactive trace metals in soils and natural water systems and in the coupling of the components of hydrogeochemical cycles. Thus, aquatic sediments constitute the most important reservoir or sink of metals and other pollutants. Sediments often uniquely preserve the history of pollution. One of the most important issues regarding the presence of contaminants in aquatic environments, according to Förstner (1987) is the potential availability of the contaminants in the sediments for aquatic life. It is important to determine trace metal concentrations in marine sediments, because these could be important sources of contamination of marine organisms that reside there. It has been known for several decades that trace quantities of certain elements exert a positive or negative influence on plant, animal, and human life. Thereby, the trace metal concentration will answer how toxic are the sediments. Knowledge of particle size distribution (PSD) may contribute a good deal of information to this research. The PSD may help clarify what controls the contaminant distribution and which fraction of sediment serves as the major sink for the trace metals. The trace elements chosen in this study are, lead (Pb), zinc (Zn), copper (Cu), cadmium (Cd), nickel (Ni), chromium (Cr), and manganese (Mn). Contamination of sediments by toxic metals has become an issue of concern in many areas of the United States. This concern is justified by the fact that these sediment concentrations of heavy metals which exceed designated thresholds have proven hazardous to biological system, including humans. The effect of heavy metals on biosphere is often evidenced by declines in once-abundand biota and modification of

biota residence. These metals are frequent and important contaminants in aquatic sediments. They are subject to a number of reactions in the system including sorption and precipitation. As a consequence of changing environment condition, heavy metals can be released from these sediments. This disturbance will be then marked as Chemical Time Bomb (CTB). A clear understanding of the mobility of trace elements in this marine environment is therefore needed. The mobility and bioavailability of trace metals in bottom sediments strongly depend on their specific chemical and mineralogical forms and their binding characteristics. Therefore, the process of sequential extractions helps establish the strength with which trace metals are bound to aquatic sediments.

When the relationships between these objectives have been determined, they can provide a sound basic for making future management decision on the disposal at coastal marine environment of waste materials. Therefore, insights gained from this study may be of universal application.

CHAPTER 2

Geology & Sedimentology of the New York Bight

The New York Bight refers to the expanse of shallow Ocean between Long Island and New Jersey; it extends 150 to 189 km offshore to the continental shelf edge (Figure 2). The general east to west trend of Long Island, relative to the mainland, creates a great right angle in the general geometry of the Atlantic coastline; along the coastline, the Bight is bounded by Cape May, Sandy Hook, and Montauk Point on the southwest, northwest and northeast, respectively. Its outer limits are defined by the 200 meters contour line. Morphologically, the Bight is bounded to the northeast by the Block Shelf Valley, and is divided into two sections by the Hudson Shelf Valley which extends from the Bight Apex to the outer shelf and Hudson Canyon (Figure 6); at 170 km, the Hudson shelf Valley is the largest physiographic feature on the continental shelf (Sinderman and Swanson, 1979). The Hudson Shelf Valley flattens at about 120 km from the entrance to the New York Harbor, and becomes indistinct owing to repeated deltaic deposition on the southeast end of the Hudson Canyon. The deltaic sand is transported by littoral drift from the nearby coast and frequently forms gills across valley heads; more extensive sand banks (or sand massifs) form on seaward shoals near estuary mouths. Besides the Hudson Shelf Valley, the Christiansen Basin (a broad shallow basin) also forms a prominent natural depression in the Bight area (Williams and Duane, 1974; Freeland and Swift, 1978; Massa et al., 1996). Though the morphology of the Bight has been attributed to sea level fluctuations, anthropogenic activities have introduced some

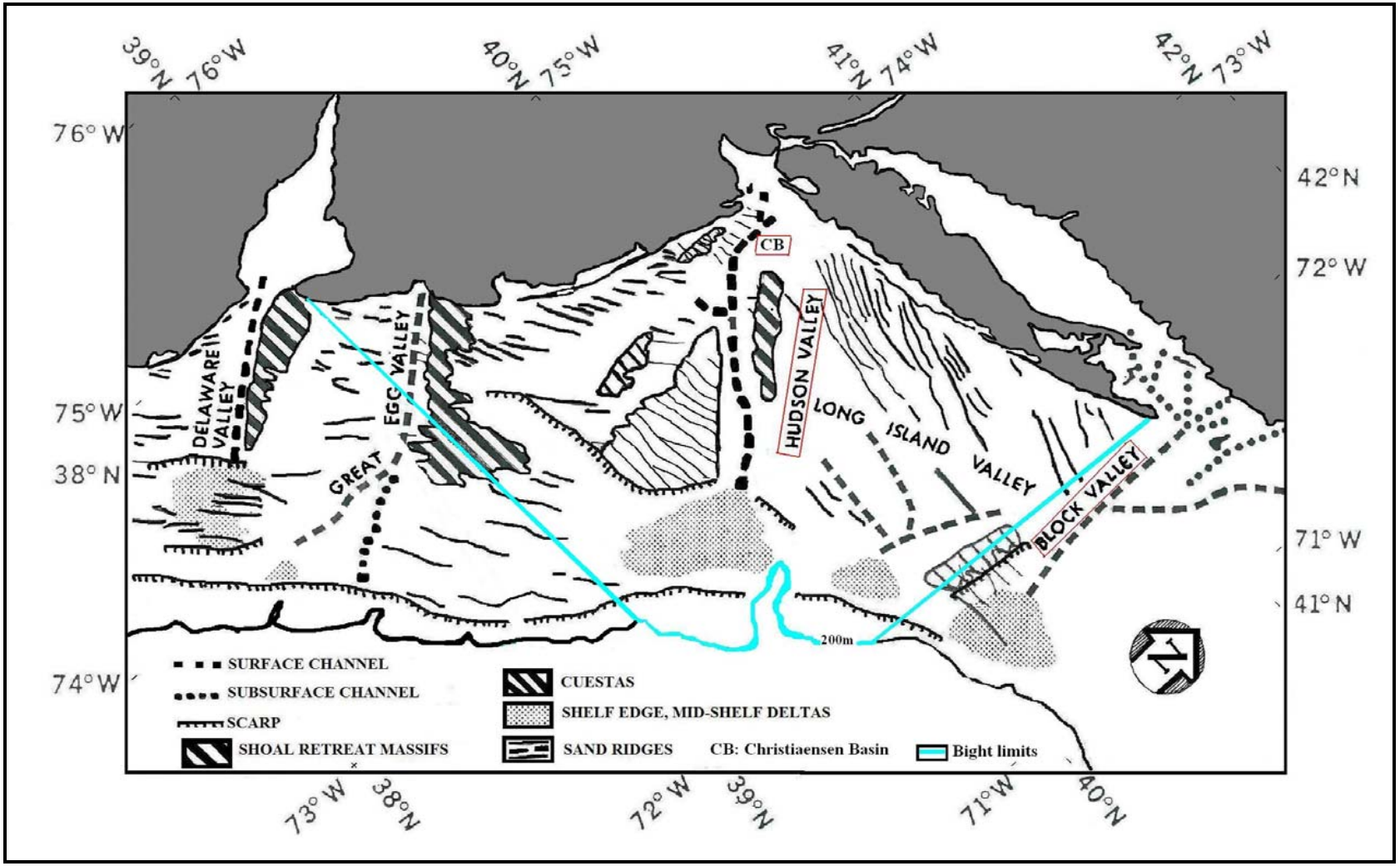

Figure 6: Morphological framework of the New York- New Jersey shelf. Modified from Swift (1974).

morphological modifications as evidenced by the Ambrose and Sandy Hook channels created for navigational purposes.

2.1. Evolution and Settings of the New York Bight Landscape

The Hudson Shelf Valley is the submerged seaward extension of the ancestral Hudson River drainage system that, unlike most incised valleys on the Atlantic shelf, has not been filled with sediments. The valley head is located in Christiansen Basin and extend offshore 5-40 m below the shelf surface to a seaward terminus at a shelf-edge delta (Ewing and others, 1963; Williams and Duane, 1974; Freeland and Swift, 1978; Massa et al., 1996; Emery and Uchupi and others, 2001).

The Hudson valley is a bedrock valley that is hypothesized to have formed over at least several tens of millions of years. Rifting commenced in late Triassic (Grow and Sheridan, 1988), and seafloor spreading began by the Middle Jurassic (~ 165Ma; Sheridan, Gradstein et al., 1983; Klitgord et al., 1988). Sedimentation rates were generally low during late Cretaceous to Paleogene, when the continental margin became starved of sediment and the shelf subsided by several hundreds of meter below sea level (Poag, 1985). The subsidence has caused an increase in sediment supply, as evidenced by a 1 km-thick wedge of Oligocene-Pleistocene sediment on the adjacent passive margin (Newman et al., 1969; Ridge et al., 1991; Steckler et al., 1990; Austin et al., 1998; McHugh et al., 2004).

A common accepted model for the evolution of continental margins links sediment erosion, transport and deposition to eustasy (sea level change) (Christie-Blick et al., 1998; McHugh et al., 2002; McHugh et al., 2004). The New Jersey continental margin is an ideal location to test the effect on sedimentation due to its tectonic stability

and thick undisturbed sediment facies (Steckler and Watts, 1978; Poag and Ward, 1993; Pazzaglia and Gardner, 1994; Steckler et al., 1996). Multiple drilling legs were required to date and correlate the stratigraphic events and associated surfaces that might be related to sea-level change, and to investigate how sedimentary facies and textures are related to sea level variations. As a part of the effort, the Deep Sea Drilling Program (DSDP) and Ocean Drilling Program (ODP) carefully drilled sites on the coastal plain (Legs 150X and 174AX), as well as on the outer shelf, slope and continental rise (Legs 95, 150, and 174A). Detailed studies of these ODP Legs may be found in Poag (1987), Miller et al. (1994, 1996a, 1998a), Mountain et al (1994), Austin et al (1998) and McHugh et al (2002).

The entire present path and shape of the valley were formed or modified during the last glaciation when Laurentide Ice Sheet covered this area and the ice formed a deep valley. As the ice-sheet retreated, from ca. 15 to 13 ka, this deep valley was occupied by a series of glacial lakes and filled with glacial and lake deposits (Newman et al., 1969; Ridge et al., 1991; McHugh et al., 2004; Nitsche et al., 2007). These lakes were gradually drained in a series of event after the last glacial maximum (Weiss, 1974; Swift et al., 1980; Uchupi et al., 2001; Donnelly et al., 2005). With rising sea level, from ca 12-10 ka the Hudson River estuarine conditions were established (Weiss, 1974). Due to sea level fluctuation, sediment derived from both the Hudson River and adjacent shelf was deposited within the estuary from 10 ka to present, (Olsen et al., 1978, Peltier, 1999).

The modern Hudson River Estuary crosses different geologic units; in what follows from north to south, the name of the formations: alluvial and sedimentary rocks of Mohawk Lowlands, the shale and the sandstone formation of the Catskills, the slightly

metamorphosed carbonates, sandstones and shales of the Taconic Sequence of the Shawangunk Mountains, the Precambrian igneous and Metamorphic rocks of the Hudson Highlands, the Manhattan pong including the Manhattan Schist, Inwood marble and Fordham gneiss, the Pallisades Diabase, the sandstone and shale of the Newark basin, and finally the coastal plain sediments including outwash sands and the Harbor hill moraine (Sanders, 1974; Coch and Bokuniewicz, 1986; Isachen et al., 2000). The Estuary is unusual for its narrowness and length. Its width varies from 0.3 to 3.7 km. The present lower Hudson River Estuary is dominated by tidal currents with an average of 0-5-1m/s (Abood, 1974; Olsen et al., 1978). The salinity ranges from 25 ‰ just north of the harbor to 5 ‰ 100 km from the harbor (Geyer et al., 2001). The majority of freshwater in the modern Hudson River estuary is from the upper Hudson River and the Mohawk River, which merge with the upper Hudson just above the Troy Dam (Cooper et al., 1988).

2.2. Sedimentology of the New York Bight

The New York Bight sediments were hypothesized to be deposited as result of the break up of the glacial lakes in upstate New York after the last glacial maximum (Weiss, 1974; Swift et al., 1980; Peltier, 1994; Peltier, 1999; McHugh et al, 2004; Nitsche et al., 2007).

Sediments covering the floor of the New York Bight consist mainly of silt and clay mineral particles. Coarse sediments (sand and gravel) consist mainly of quartz and feldspar grains, rock fragments and anthropogenic particles (Gross, 1976). A large field of sand waves is located in the lower valley in 70-80 water depth that covers an area approximately 30 km long and 4 km wide. Current activity formed ribbons, dunes, and

sand ridges as much as 10 m in amplitude on the inner and middle shelves as the shore migrated during the Holocene (Swift et al., 1972).

The New York Bight shelf is covered by sand sized sediment with isolated gravel particles (Shlee, 1973, 1975; Williams and Duane, 1974; Williams, 1976; Freeland and Swift, 1978). In deeper waters, of the Hudson Shelf Valley, and in lagoons and estuaries where wave's action is less pronounced, silt is the predominant sediments. Muds and sandy muds rich in organic carbon and trace metals floor the dredge spoil banks, the bathymetrically-low Christiansen basin, depression on the Cholera Bank in and east of off the sewage sludge disposal area, and mud patches near the shore of the New Jersey and Long Island west and north of the Christiansen Basin and disposal areas (Harris, 1974), whereas the rest of the area contains assorted sizes of sand both anthropogenic (artifact) and natural gravel deposits (Freeland and Swift, 1978). The most common sediments in the apex are silty fine sand and slightly gravelly fine to medium sand (Harris, 1976).

Sand: Sand make 75% of sediments and decreases below 50% only in region where there is gravel exposed (off north central NJ) or there is mud deposits (in the Hudson Shelf Valley). Beyond the shelf edge the sand content decreases drastically (bellow 25%) and the percentage of fines increases (Freeland and Swift, 1978).

Gravel: The distribution of gravel varies from none to 75% off central north New Jersey. Most of the gravel deposits are thought to be river-borne terrace gravels that were deposited on the exposed shelf by glacial melt waters, probably from the Hudson River system (Freeland and Swift, 1978).

Silt: Silt occurs in the low percentages on the shelf except to the northeast. The almost complete absence of silt on the inner Long Island Shelf was due to the removal of fine-grained material during Holocene transgression. Silt content increase within the Hudson Shelf valley (75%) and continental slope (40%) (Freeland and Swift, 1978).

Clay: Clay is almost negligible on the shelf because storm-generated waves and currents constantly winnow fine silt- and clay-size material out of shelf surficial sediment. The only exception is the Hudson Shelf Valley, where small amount of clay have been found, and in shelf muds to the northeast (Freeland and Swift, 1978).

Organic material: Organic matter is low in shelf sediments, but increases in the fine sediments of the Hudson Shelf Valley, on the slope and continental rise. Percentage of organic carbon from natural and anthropogenic sources increases seaward of the shelf edge. High concentrations (>1%) are observed around dumpsites and close to Cape May which contrast with the rest of the continental shelf which is characterized by a low percentage of organic carbon (<0.24%) (Freeland and Swift, 1978)

The sources of suspended sediments into the Bight are shown in Appendix A. Suspended fluvial sediments discharged onto the shelf are composed of 85% inorganic and 15% combustible organic materials (Hathaway, 1972). Particles derived from biogenic processes are also significant component suspended matter in estuaries and on shelf (Appendix A). Concentration of combustible biogenic matter decreases rapidly with depth, and little of this material is preserved in sediment deposits (Folger, 1972a; Gross, 1972). Atmospheric fall out over New York Bight is small relative to other sediment sources (Appendix A).

The US Geological Survey (USGS) has conducted extensive studies in mapping the surficial sedimentary environment of the Hudson Shelf Valley and adjacent shelf from its head in the Christiansen basin at 40° 25' N and 73° 48' W to where it crosses the outer shelf at about 39° 40' N and 72° 50' W. The detailed maps of the sedimentary environment offshore New York have guided sampling and process studies carried out as part of a USGS study of the transport and long-term fate of sediments and contaminants in the New York Bight environment (Butchholtz ten Brink et al., 1998). In Christiansen Basin at water depth of about 38m, the sediment texture is sand or silty sand, with the bulk of sediment being very fine sand (Butchholtz ten Brink, 1998; Butman et al., 2002). In the upper part of the Hudson Shelf valley, about 8.4 km south of Christiansen basin, at a water depth about 56m, the sediments texture is sandy silty clay (Butchholtz ten Brink, 1998; Butman et al., 2002). The eastern side of the axis of the Hudson Shelf valley, about 41.4 km down valley from Christiansen Basin, at water depths of about 71m, the sediment is silty sand, with about 50% of the sediments being very fine sand (Butchholtz ten Brink, 1998; Butman et al., 2002). In the axis of the Hudson Shelf valley, about 77.4 km down-valley from Christiansen basin, at about 74 m water depth, the sediments texture is silty sand with about 35 % of the material is very fine sand (ten Brink, 1998; Butman et al., 2002).

Austin et at (1998) concluded that the adjacent continental shelf is sand rich and sediments starved, and the sediments are effectively transported by tide- and longshore-wave current and storms. Evidence shows that the modern Hudson River estuary is now effectively filled at or near sea level (McHugh et al., 2004). Delta progradation may take place as available shelf accommodation is filled, but these sediments accumulation are

likely to be eroded once the sea level begins to fall (McHugh et al., 2004). On the basis of radionuclide dating profiles, measured by gamma spectrometry and alpha sepectrometry (Simpson et al., 1977; Simpson et al., 1978; Olsen et., 1979; Olsen et al., 1981; Austin et al, 1998; Friedman et al., 2000; McHugh et al., 2004), that much of the total surface area of the Hudson River estuary has little or no accumulation of recent sediments. At the head of the shelf valley, about 30 km from the mouth of the estuary, "recent" sedimentation is mostly the result of anthropogenic activities (Massa et al., 1996). The absence of significant sediment accumulation for the latest Holocene (ca. 3 ka to present) is also indicated by radiocarbon dating of oyster shells and wood, and the presence of coal and other relicts of coal burning that are found on the estuary (McHugh et., 2004). Sediment younger than 1965, defined as recent as revealed by the presence of ^{137}Cs, are presented by layers no more than 50 cm thick that accumulated at rates as high as 5-10 mm/yr (McHugh et al., 2004). Radionuclide dating (^{137}Cs) activity also shows that the total rate sedimentation in the upper Hudson River and lower estuary is ~ 50×10^3 t/yr and ~ 3.0×10^3 t/yr, respectively (Geyer et al., 2001) . Recent studies (Nitsche et al., 2007), showed that the distribution pattern of sedimentary facies along the Hudson River estuary is strongly influenced by, bed rock types, morphology, tributaries and human activities. The marine end of the upper and lower estuary is dominated by marine sand, strongly influenced by marine waves and currents; the central part of the estuary is dominated by muddy sediments and the upper estuary is dominated by fluvial sand. The overall, regional sediment distribution of the Hudson River Estuary is similar to the model described by Dalrymple et al. (1992), which applies best to the coastal plain estuaries.

2.3. Mineralogy of the New York Bight Sediments

Sediment types in the Bight are a result of geological processes on the adjacent land (Figure 7). The particle sizes have been governed by transportation agents such as streams, waves, and currents and storms. Quartz and feldspar dominate the sand-size fraction, which is a primary indicator of a terrigenous source. In the Bight, quartz and feldspar combined are usually 90% of the sand-size fraction and decreases down the slope to less than 50% on the continental rise. Quartz is predominant in the Pleistocene (McHugh et al., 2002).

Carbonate content in the Bight is generally less than 5% with small area of up to 25%. The major carbonate constituents are mollusk and echinoid shell fragments and foraminifera (Freeland and Swift, 1978).

Most of the shelf area contains less than 2% glauconite, but there are glauconite – rich patches which suggests reworking of the glauconite-rich Cretaceous or lower Tertiary strata exposed in either subareal or submarine outcrops (Freeland and Swift, 1978). The outer shelf is characterized by a glauconite-rich lag typically no more than few centimeters thick (Christie-Blick et al., 2002). ODP leg 150 showed that Glauconite beds are up to 8 m thick and is predominant in Oligocene and lower Miocene (McHugh et al., 2002)

Heavy minerals in the Bight are represented by amphiboles, epidote, garnet, and staurolite. The amount of each varies. For instance, in the area off southern New Jersey shelf, the distribution ranges from 4% to 16% of heavy mineral concentration. The high garnet to staurolite ratio off the southern New Jersey shelf decreases sharply toward

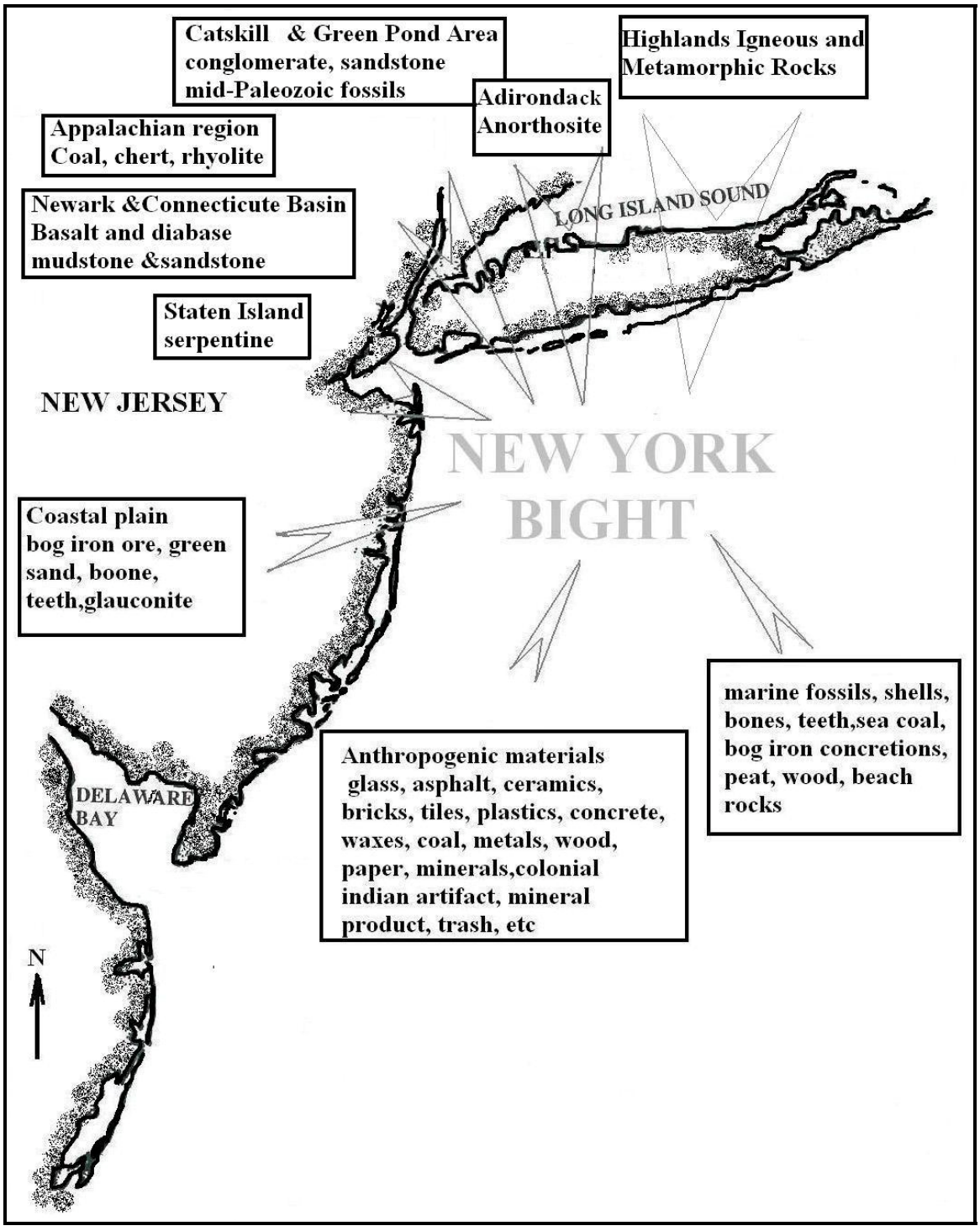

Figure 7: Possible sources of sediments found in the Bight.
Modified from Stoffer and Messina (1996)

eastern Long Island, suggesting northeastward transport (Freeland and Swift, 1978). The heavy minerals from the New Jersey shelf consist mostly of hornblende and garnet (Frank et al., 1972).

Clay minerals in the Bight sediments include illite, chlorite, vermiculite, and kaolinite. Similarities between clay minerals on the upper shelf and those on the outer shelf suggest that they migrated shoreward by winnowing from clayey areas on the outer shelf. Deposited in New York Bight early Holocene, lagoonal clays are considered to be one of the sources of organic matter in the New York Bight surficial sediments. The ratio of terrigenous organic matter over the pelagic marine organic matter decreases down the continental rise (Freeland and Swift, 1978). The organic-rich fine-grained material concentrated in the Christiansen Basin and the Hudson Shelf Valley area came from the dumping events in the past as well as from recent waste release along the shore (Schwab et al., 1997).

The clays identified in ODP leg 150 showed different colors. The greenish chlorite predominate in the Pleistocene-age clays. Whereas the brownish kaolinite is common in the Miocene-age clays (McHugh et al., 1996). Kaolinite, chlorite and illite are considered of detrital origin in marine sediments (Biscay, 1965; Griffin et al., 1968; Singer, 1984). Chlorite in marine sediment is associated with mechanical weathering and glacial erosion of high-latitude climatic conditions. Whereas kaolinite is associated with extreme leaching and is commonly today in the tropics. The chlorite present in sediment came from times of cold climate (McKinney and Friedman, 1970). The presence of kaolinite in Miocene and Oligocene sediments indicates weathering and erosion of continental sources. Illite in marine environment is associated with river and eolian input

(McHugh et al., 1996). A classification of sediment facies recovered on leg 150 can be found in (McHugh et al., 1996; 2002).

2.4. Sediment Transport (Hydrodynamics)

An understanding of the processes that resuspend and distribute sediment is essential both for predicting the fate of contaminants found in the New York Bight, and explaining the geomorphic evolution of the area. Past studies have shown that the general surface ocean circulation is mostly southwest and parallel to the coast (Bumpus et al, 1965). However, northerly counter currents along both New Jersey and Long Island exist, particularly in spring and autumn. Powers and Ayers (1951) found from drift bottle studies, that a series of alternating clockwise and counterclockwise gyres exit along the Long Island and the New Jersey shores. Pearce (1969) found that the bottom currents are more important to the dispersion of waste than surface currents. A year round bottom current was found up to the Hudson Submarine Valley in a northwesterly direction (Bumpus, 1965; Pearce, 1969). Past studies also showed that sediment transport on many continental shelves is dominated by resuspension during energetic wave events (Butman et al., 1979, Lyne et al., 1978; Drake and Cacchione, 1985). In the New York Bight the transport of sediments is dominated by storm events where wave activity close to the bed, combined with the mean currents produce the conditions under which bed load and suspended load transport can occur. Sediment resuspension was correlated with waves whose height exceeds 2 m, based on evidence from cameras near the bed over historic dumpsites (SAIC, 1995). Observations made on the New Jersey shelf also indicated that sediment transport on the shelf is dominated by resuspension during energetic wave's events (Butman et al., 1979; Lyne et al., 1987). In 1994, Manning et al measured

currents over several months within the Hudson Shelf Valley; their measurements yielded mean velocities in the range of 0.10-0.2 m/s with maximums of 0.2-0.6 m/s. These studies concluded that winds producing setup at the coast create offshore velocities in the shelf valley, with setdown-favorable winds are correlated with shoreward directed velocities (Lavelle et al., 1975; Nelsen et al., 1978; Manning et al., 1994). Harris and Signell (1999) used numerical models of circulation and sediment transport to predict that winds from the northwest could generate up-valley directed currents energetic enough to resuspend and transport sediments within the Hudson Shelf Valley. These winds occur frequently, and Harris and Signell (1999) concluded that resuspension and transport by the associated up-valley currents may dominate sediment flux within the Hudson Shelf Valley. Harris and Signell (1999) circulation calculation were consistent with Manning and others (1994) observation. Sediment transport predictions could not be verified because simultaneous measurements of suspended sediment concentration and flux were lacking. In the winter of 1999-2000, Butman et.al. measured the current velocities and sediment transport along the axis of the shelf valley and about 26 m on the adjacent shelves offshore of New Jersey and Long Island, New York. These were the first direct near-bed measurements of suspended sediment concentration and sediment flux from the region. Current and sediment transport were coherent over tens of kilometers during both up-valley and down-valley, and usually aligned with the axis of the shelf valley. Up-valley transport (shoreward) coincided with times of winds from the northwest, low wave energy, high current velocities (0.2-0.4 m/s), and sea-level set-down at the coast. Down-valley (off-shore) transport was associated with energetic waves, winds from the northeast, moderate current velocities (0.5-1 m/s), and sea level setup at Sandy Hook, NJ.

Wave forcing has been shown to dominate sediment transport in many continental shelves (Drake and Cacchione, 1985). Within the Hudson Shelf valley however, sediment fluxes were dominated by resuspension and transport by energetic currents (Butman et al., 2003). In the shelf valley, circulation overwhelmed wave effects for transporting sediment. The coastline configuration, shelf bathymetry, and predominant wind patterns combine to reinforce the circulation patterns (Butman et al., 2003).

CHAPTER 3

Experimental Methods

3.1. Sample Collection

The sediment samples (see Appendix A for description) used in this study was collected by Harris (1976) and McHugh (1997); details of their sampling techniques have been summarized in the Appendix A. Figure 8 and Table 2 show location of the sampling stations in the study area. The samples provided by Harris were already in metal-free "Whirl Pack" (2-Oz; 3 by 5 inches) plastic bags and in metal- free plastic jars and stored frozen at Brooklyn College. Portions of the core AC 97-9 and core AC 97-1 provided by McHugh, stored-refrigerated at Columbia University-Lamont Doherty Research Laboratories, were extracted with a metal-free plastic spoon and transferred to metal-free "Whirl Pack" (2-Oz; 3 by 5 inches) plastic bags.

3.2. Materials and Reagents

All chemical reagents used in this study were all trace metal grade and included nitric, hydrochloric, hydrofluoric and perchloric acids. Stock solutions were diluted to appropriate concentrations using 18 milli-Q water to give the following; 70% HNO_3, 37% HCl, 45-51% HF, and 70% $HClO_4$.

The samples were processed in HDPE Nalgene bottles (60 and 125mL), Pyrex flasks (25, 50, and 100 mL), 100 mL Teflon beakers and polypropylene funnels. These wares were initially washed with tap water and a cleaning solution ("Micro detergent"), rinsed with 25% hydrochloric solution, and rinsed twice with 18 milli-Q water.

Subsequently, the containers and all laboratory glassware were bathed overnight in a Nalgene rectangular tank containing 25% hydrochloric solution and then rinsed twice with 18 milli-Q water.

The filter paper used in the filtration process was Whatman Nos.542 and 40 or 540, which is hardened ashless circles of 185 and 150 mm in diameter, respectively.

3.3. Methods

3.3.1. Particle Size Distribution (PSD)

Particle size distributions were determined by dry sieve analysis. Prior to each analysis, the sample was dried for 4 to 5 hours in glass beaker in a drying oven at 60°C and then cooled to room temperature in an environmental hood. Extraneous matter such as fragments of plant matter, pieces of rubber and glass were then removed from the samples. For the sieve analysis, the weight of sediment samples used varied from 99.50 grams to 204.00 grams depending on sample availability. A selected nest of sieves was used to separate the different particle sizes and the grain size abundances were calculated as weight percentage. The sieve sizes used covered the following range:

Sieve Size (mm)	Diameter (ϕ)	Grain Size
> 2 mm	-1	Gravels
2 - 1 mm	0	Very coarse sand
1 - 0.5 mm	1	Coarse sand
0.5 - 0.25 mm	2	Medium sand
0.25 - 0.125 mm	3	Fine sand
0.125 - 0.0625 mm	4	Very fine sand
< 0.0625 mm	5	Silt & clay

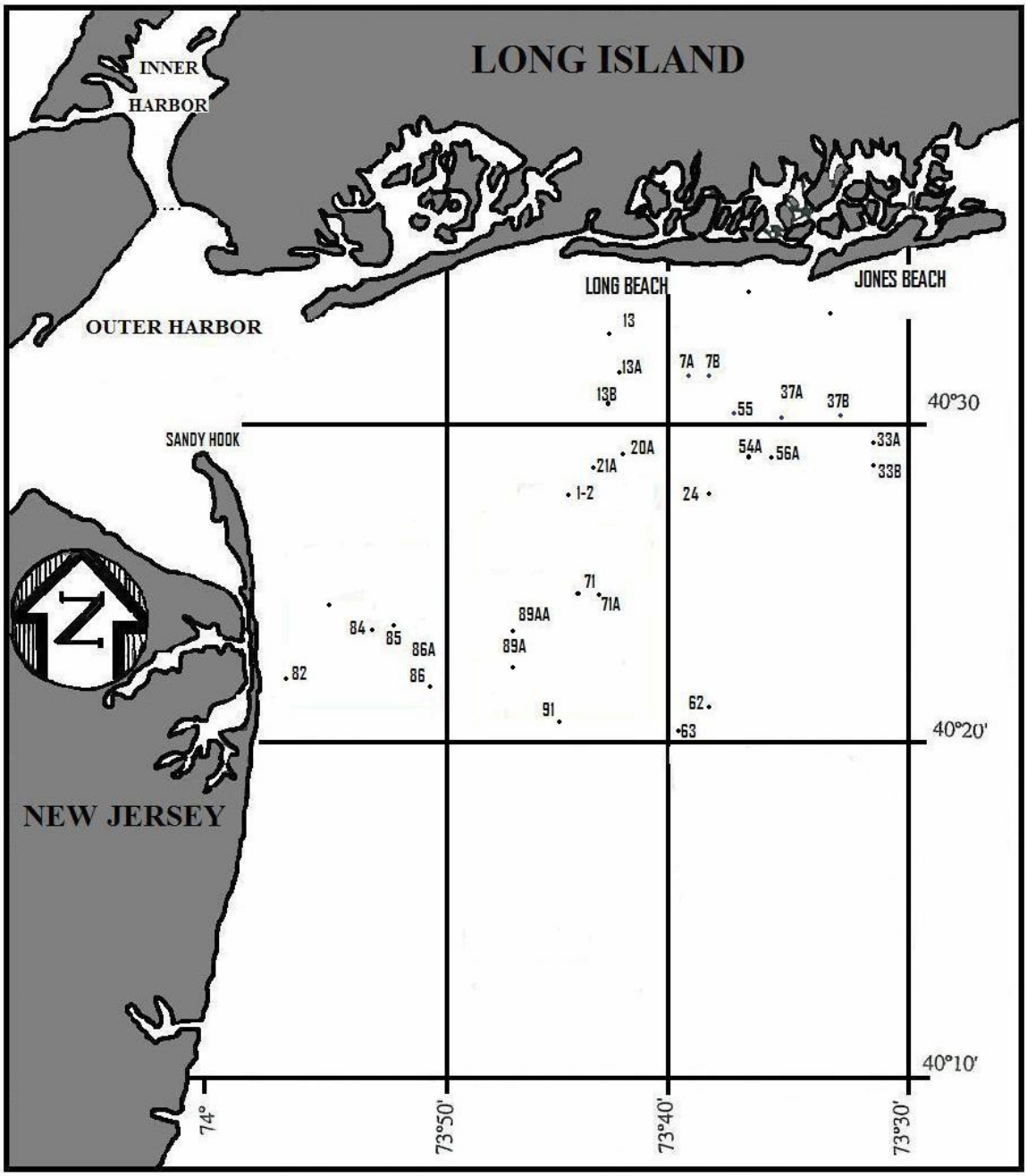

Figure 8: Location of the sampling sites in the study area.

Note: All the sites lie within the NYB Apex

Table 2: Sampling locations

Sample #	Coordinates	
	Latitude	**Longitude**
Mud Dump Site		
82	40° 22' 30"	73° 55' 00"
86	40° 22' 20"	73° 51' 30"
84	40° 23' 00"	73°47' 00"
85	40° 23' 50"	73° 51' 00"
86A	40° 22' 40"	73°50' 00"
Sewage sludge		
89A	40° 22' 30"	73° 47' 30"
89AA	40° 22' 40"	73° 47' 00"
91	40° 21' 30"	73° 44' 30"
71	40° 23' 30"	73° 43' 00"
71A	40° 23' 00"	73° 43' 00"
1-2	40° 27' 00"	73° 44' 00"
Near shore mud patches		
7A	40° 31' 00"	73° 39' 00"
7B	40° 31' 00"	73° 38' 00"
13A	40° 32' 00"	73° 42' 00"
13B	40° 31' 30"	73° 42' 00"
South of Long beach		
54A	40° 28' 30"	73° 36' 00"
56A	40° 28' 10"	73° 35' 00"
55	40° 29' 00"	73° 36' 00"
21A	40° 28' 00"	73° 42' 00"
24	40° 27' 30"	73° 39' 00"
20A	40° 28' 20"	73° 41' 00"
37A	40° 30' 10"	73° 35' 00"
37BB	40° 30' 30"	73° 33' 30"
South of Jones Inlet		
33A	40°29'00"	73° 31' 00"
33B	40° 28' 00"	73° 31' 00"
Cholera Bank		
62	40° 21' 00"	73° 38' 00"
63	40° 20' 10"	73° 39' 30"

3.3.2. X-ray Diffraction Analysis

Clay fractions of selected samples for XRD were processed and analyzed at K/T GeoServices, Inc. Argyle TX. X-ray diffraction is the best available techniques for the identification and quantification of all minerals present in the clay fractions. XRD

methods can quantify crystalline material only. Organic non-crystalline material in large concentrations can be detected but not quantified. Therefore, any organic and/or non-crystalline material is not included in the results. Detection limits for XRD are on the order of one to five weight percent. The detection limits differ for each mineral species. Mineral standards used to determine calibration factors are often different from the actual minerals analyzed. Minerals such as feldspars that undergo solid solution are especially problematic. Clay minerals also have a wide range of crystallinities (poorly to well crystallized) and variable chemical composition. These variations result in large differences in the intensities of XRD reflection between different specimens of the same mineral. Such variable intensities can result in large analytical errors in quantitative analysis if intensities are selected improperly. Clay minerals are problematic for these reasons. Whereas mineral identification is relatively simple if modern software and good mineral databases are available, accurate quantitative analysis of clay remain a formidable challenge (see reviews by Brindley, 1980; Reynolds, 1989, Snyder and Bish, 1989; Mc Manus, 1991; Moore and Reynolds, 1997).

Sample Preparation

Samples for XRD analysis were first disaggregated using a mortar and pestle, weighed and dispersed in de-ionized water using a sonic probe. The samples were next centrifugally size-fractionated into a bulk (>4 microns) and a clay-size <4 microns ESD (Equivalent Spherical Diameter) fraction. The clay suspensions were then decanted and vacuum-deposited on nylon membrane filters to produce oriented mounts. Clay mounts were attached to glass slides and exposed to ethylene glycol vapor for a minimum of 24 hours to aid in detection and characterization of expandable clays. The bulk fractions of

each sample were dried and weighed in order to determine weight loss due to removal of clay-size materials.

Analytical Procedures

XRD analysis of the clay-size fractions of the samples were performed by K/T GeoServices, Inc., using a Siemens D500 automated powder diffractometer equipped with CuKa radiation source (40 Kv, 35mA) and a solid state or scintillation detector. The air-dried (AD) and ethylene glycol-solvated (EG) oriented clay mounts were analyzed over an angular range of 2-36 degrees 2 theta at a scan rate of 1 degree/minute.

Quantitative analyses of the diffraction data were done using integrated peak areas (derived from peak deconvolution / profile-fitting techniques) and empirical reference intensity ratio (RIR) factors determined specifically for the diffractometer used for data collection. Determinations of mixed-layer clay types, ordering and percent expandable interlayers were done by comparing experimental diffraction data from the glycol-solvated clay aggregates with simulated one dimensional diffraction profiles generated using the program NEWMOD (Reynolds, 1989).

3.3.3. Extraction of Trace Metals

Fractions of the sieved samples, as discussed above, were digested for trace metals determination using a two step procedure. In the first instance, the metals were extracted with 50% HNO_3 leach; presumably, this removes weakly-bound and exchangeable metals without decomposing the mineral structure. In the second step, the filter cake (residue from step one) is digested using a combination of HF/$HClO_4$/ HNO_3; this releases the total metal concentration from sediment samples. For comparative

purposes, a single step digestion using the mixed reagents consisting of the three acids, $HF/HClO_4/ HNO_3$ was also conducted.

Extraction with 50% nitric acid

0.500 grams of the <0.0625 mm dry sediment was mixed with 20 mL of the 50% nitric acid solution in 60 mL Nalgene bottle. The sample-acid mixture was shaken vigorously for two hours (at room temperature) on a wrist action shaker (Model 75). The suspension was then filtered into 100 mL volumetric flasks fitted with polypropylene funnels, using Whatman Nos. 542 and 540 (or 40) filter paper for muddy samples and sandy samples, respectively. After filtration, the solution was brought to volume (100 mL) with 18 milli-Q water and then poured in 125 mL Nalgene bottle and stored in a refrigerator. The residues held by the filter paper were then transferred and saved in metal-free "Whirl Pack" plastic bags for further chemical analysis.

Extraction from different particle size fractions

Owing to the simplicity of a single-pass extraction of trace metals with 50% concentrated HNO_3, many researchers have adopted this method (Carmody, 1972). The trace metal contents of each fraction isolated by the sieve analyses were extracted by this single leach method. Typically, 0.500 grams of each fraction (clay and silt, very fine sand, fine sand, medium sand, coarse sand and very coarse sand) is mixed in 60 mL HDPE bottle with 20 ml 50% concentrated HNO_3. The sample-acid mixture was shaken vigorously for two hours at room temperature on wrist action shaker. The sediment and acid extract of each fraction were transferred to polypropylene filter funnel and the acid extract was filtered through Whatman filter paper. After filtration, the solution was

brought to volume 100 ml with 18 milli-Q water in a glass volumetric flask and analyzed for trace metals by Atomic Absorption Spectrophotometer (AAS).

Total Sample Digestion

The digestion technique described here represents a modification of the procedures outlined by Johnson and Maxwell (1981), and Langmuir and Paus (1968). The digestion procedure described subsequently were applied both to the residues of the single leach extraction (50% HNO_3 leach) and to virgin samples. For the latter, 0.500 grams of finely ground (<0.0625 mm) untreated samples were transferred to 100 ml Teflon beaker. To each Teflon beaker, 6 ml nitric acid solution was added and the beakers were placed on a Thermolyne (type 2000) hot plate for 30 minutes in a metal-free environmental hood; the hot plate was adjusted to produce a surface temperature of 200 °C. After 30 minutes the Teflon beakers were cooled for 5 minutes in the environmental hood. 6 mL hydrofluoric acid (HF) and 2 mL perchloric acid ($HClO_4$) solutions were then added to each Teflon beaker and returned to the hot plate. The beakers were heated until the evolution of gray to white fumes (perchloric fumes) and the residues became just moist without being baked. The beakers were then removed from the hot plate, cooled for 5 minutes and the digestion process was repeated again. Subsequently, 2ml of 50 % hydrochloric acid solution and 10 ml 18 milli-Q water were added to the beakers and these were then returned to hot plate until the residues were dissolved. The beakers were then cooled at room temperature in the environmental hood.

The resulting aqueous solutions (i.e., the acid extract) were then filtered in order to preclude clogging of the atomic absorption spectrophotometer nebulizer. The Whatman filter paper was doubled and folded into polypropylene funnels. The filtrates

were then transferred into 100 mL in glass volumetric flasks and brought to volume. The solutions were poured into HDPE bottle for storage in a refrigerator.

3.3.4. Analysis of Aqueous Extracts

The chemical compositions of the aqueous extracts were determined using a Perkin-Elmer atomic absorption spectrophotometry (Model 3300). The concentration of Pb, Cu, Zn, Ni, Cd, Cr and Mn in the extracts was measured at the following wavelengths 283.3, 324.8, 213.9, 232.0, 228.8, 357.9 and 279.5 nm, respectively. The standard reference solutions for the metals were matrix matched with the aqueous extracts (using HNO_3) and prepared in the following batches:

(1) Pb, Cu, Zn, Ni and Cr standards range between 0-100ppm.

(2) Mn standard ranges between 0-1000ppm.

A blank solution, free of trace metals, was prepared with 18 milli-Q water and matrix matched with an appropriate amount of HNO_3. During the analysis, optimization of the instrument (with regard to sensitivity and range linearity) was achieved for each element separately. A brief discussion of AAS techniques, instrumental parameters precision and accuracy of the analysis are presented in Appendix A.

Table 3 compares the percent accuracy between trace element concentrations in these standards as determined for all the metals analyzed in this study and those published as certified values. Instrumental precision (repeatability of analysis) was based on analysis of eleven replicate measurements. The analytical precision in the reported concentration due to change in instrumental conditions during analysis describes the closeness of a measurement to other measurement made in same way (Table 3). The analytical procedure (accuracy of procedure) was inter-calibrated by analysis of NBS

SRM (Table 3). Accuracy (standard deviation) indicates the closeness of a measurement between a result and its true value. The accuracy can never be determined exactly because the true value of a quantity can never be known. An accepted value is used instead. Concentrations of Cu (99.9 %), Mn (93.5%), Ni (91%), Cr (90%), Zn (109.6%) and Pb (82%) in NBS-SRM 1646 as determined in this study show that the recovery rates for metals in acid digestion are generally good when compared to certified reference material values (Table 3). The deviation of measured trace metal values from certified concentrations of analytical standards are shown in Figure 9. The percentage accuracy for Zn shows that 9.6% more analyte is recovered than its certified concentration. The increased analytical concentration can be attributed to addition of the analyte metal to the sample during sample preparation probably from the reagent used.

3.4. Statistical Analysis

Correlation analysis is undoubtedly one of the most widely used of statistical methods. It enables us to assess the strength of the relationship (correlation) among the variables. Statistical analysis was performed using the computer application JMP version 5.1.2, the Statistical Discovery Software from the SAS Institute Inc., Cary, NC, USA (2002). The sediment data for each metal were subjected to various tests, including, One-Way by station analysis of variance (ANOVA), bivariate analysis and Cluster Analysis and tests for normal distribution (Normalcy). The data were further analyzed: all metals concentrations in sediments were subjected to Kendall Tau-b and Spearman Rho non-parametric measures and pairwise correlations to test the relationship among pairs of trace metals.

Table 3: Accuracy of the procedure utilized for metal studied-NBS estuarine sediments 1646a

Analytical Values	Mean Analytical Value	Certified Values	Accuracy
		Pb (ppm)	
10.01 ± 0.72	9.6 ± 0.65	11.7 ± 1.2	18 %
9.7 ± 0.5			
10.00 ± 1.5			
9.75 ± 0.52			
9.55 ± 0.34			
10.00 ± 1.25			
9.75 ± 0.55			
9.44 ± 1.25			
9.4 ± 0.125			
8.98 ± 0.04			
9.01 ± 0.4			
		Cu (ppm)	
10.00 ± 0.11	10.00 ± 0.18	10.01 ± 0.34	0.1%
9.66 ± 0.125			
9.88 ± 0.1			
11.01 ± 0.42			
10.00 ± 0.75			
9.57 ± 0.2			
10.8 ± 0.11			
9.75 ± 0.12			
9.51 ± 0.2			
10.48 ± 0.1			
9.34 ± 0.15			
		Ni (ppm)	
21.04 ± 0.7	21 ± 1.05	23 ± 3	8.7%
21.00 ± 1			
21.00 ± 1.9			
22.00 ± 1.09			
21.01 ± 1.52			
21.00 ± 0.9			
21.5 ± 1.04			
20.36 ± 1.05			
20.00 ± 0			
20.00 ± 1.2			
		Zn (ppm)	
53.00 ± 0.48	53.6 ± 1.22	48.9 ± 1.6	-9.6 %
54.01 ± 1.2			
52.14 ± 1.93			
53.05 ± 1.34			
55.76 ± 1.12			
53.7 ± 1.9			
55.34 ± 1.09			
53.9 ± 2.01			
53.00 ± 1.12			
52.7 ± 0.33			
53.00 ± 1			
		Cd (ppm)	
0.14 ± 0.06	0.125 ± 0.024	0.148 ± 0.007	15.5 %
0.125 ± 0.012			
0.135 ± 0.06			
0.129 ± 0.009			
0.125 ± 0.01			
0.12 ± 0.005			
0.116 ± 0.01			
0.135 ± 0.0125			
0.12 ± 0.001			
0.115 ± 0.034			
90.115 ± 0.055			

Table 3: Accuracy of the procedure utilized for metal studied-NBS estuarine sediments 1646a (continued)

Analytical Values	Mean Analytical Value	Certified Values	Accuracy
		Cr (ppm)	
36.05 ± 0.7	36 ± 0.69	40.9 ± 1.9	10 %
36.00 ± 0.74			
34.09 ± 0.61			
35.01 ± 0.19			
36.70 ± 1.125			
36.00 ± 0.09			
35.55 ± 0.59			
35.12 ± 1.00			
36.00 ± 1.00			
37.88 ± 0.69			
37.6 ± 0.88			
		Mn (ppm)	
220.1 ± 7	219 ± 6.6	234.5 ± 2.8	6.6 %
219.5 ± 5.7			
219.01 ± 7			
220.9 ± 3.46			
218.5 ± 9.64			
220.34 ± 11			
221.01 ± 3.01			
219.6 ± 6.34			
215.70 ± 10.2			
217.00 ± 5.125			
217.34 ± 4.01			

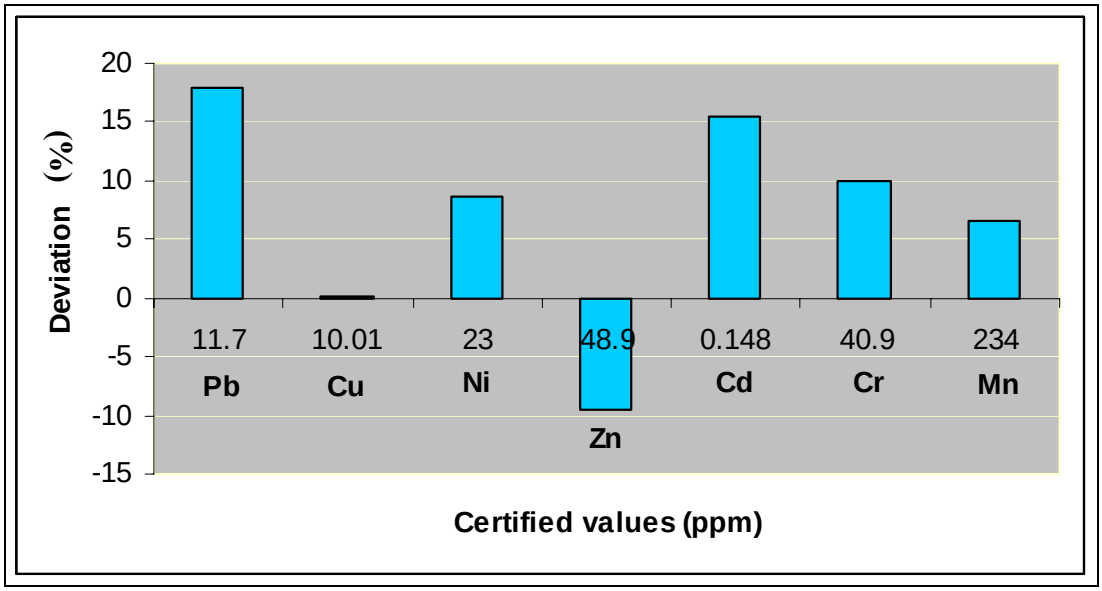

Figure 9: Comparison of certified concentrations of analytical standards with measured values.

CHAPTER 4

Results

4. 1. Sediments Particle Size

The particle size distribution of samples (PSD) from New York Bight apex is shown in Figure 10 & Appendix B. The sediment samples from the study area consist predominantly of sand (from 53.09 to 99.96%) (about 94.64% average), followed by silt and clay (from 0.0039 to 46.90%). The most frequent occurring populations for the majority of samples is fine sand, medium sand and very fine sand (Figure 10 & Appendix B). The average weight percent of each sediment fraction within each dumpsite of the NYB are presented as frequency graphs in Figure 11. The average weight percent of each fraction varies among NYB dumpsites. For instance, silt and clay fractions are highest in MDS with an average of 24.73%, followed by sewage sludge and near shore mud-patches with an average of 6.5% and 1.3 % respectively. In general, the granulometry of each dumpsite is dominated by fine sand (Figure 11).

The frequency-distribution, cumulative-distribution and arithmetic-distribution curves were plotted for each of the twenty-four sediment of the New York Bight samples (Appendix B). All the frequency-distribution curves deviate from the normal distribution; some of them are bimodal, which suggest different sources of sediment. The frequency-distribution curves show very small or no occurrence of grains with diameter more than 2mm (-1 Phi). When present, the grains consist of skeletal debris, wood, and other anthropogenic materials dumped in this area.

Sediments Particle Size
Mud Dump Site

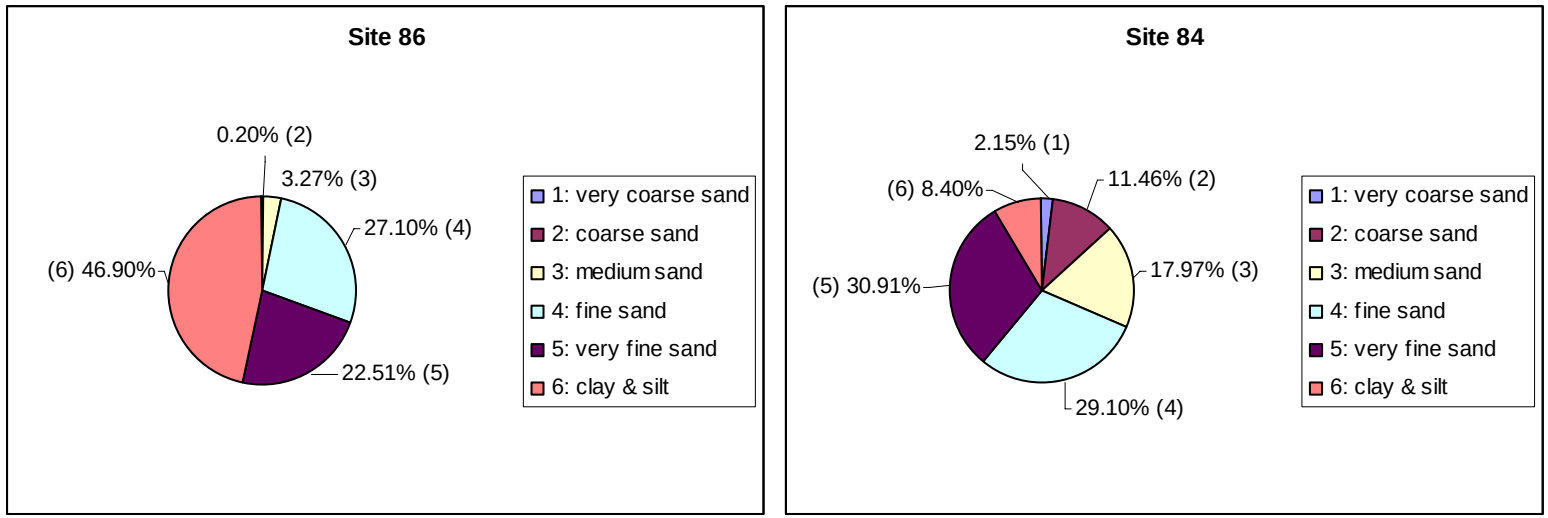

Figure: 10

Sediments Particle Size

Sewage Sludge Dumpsite

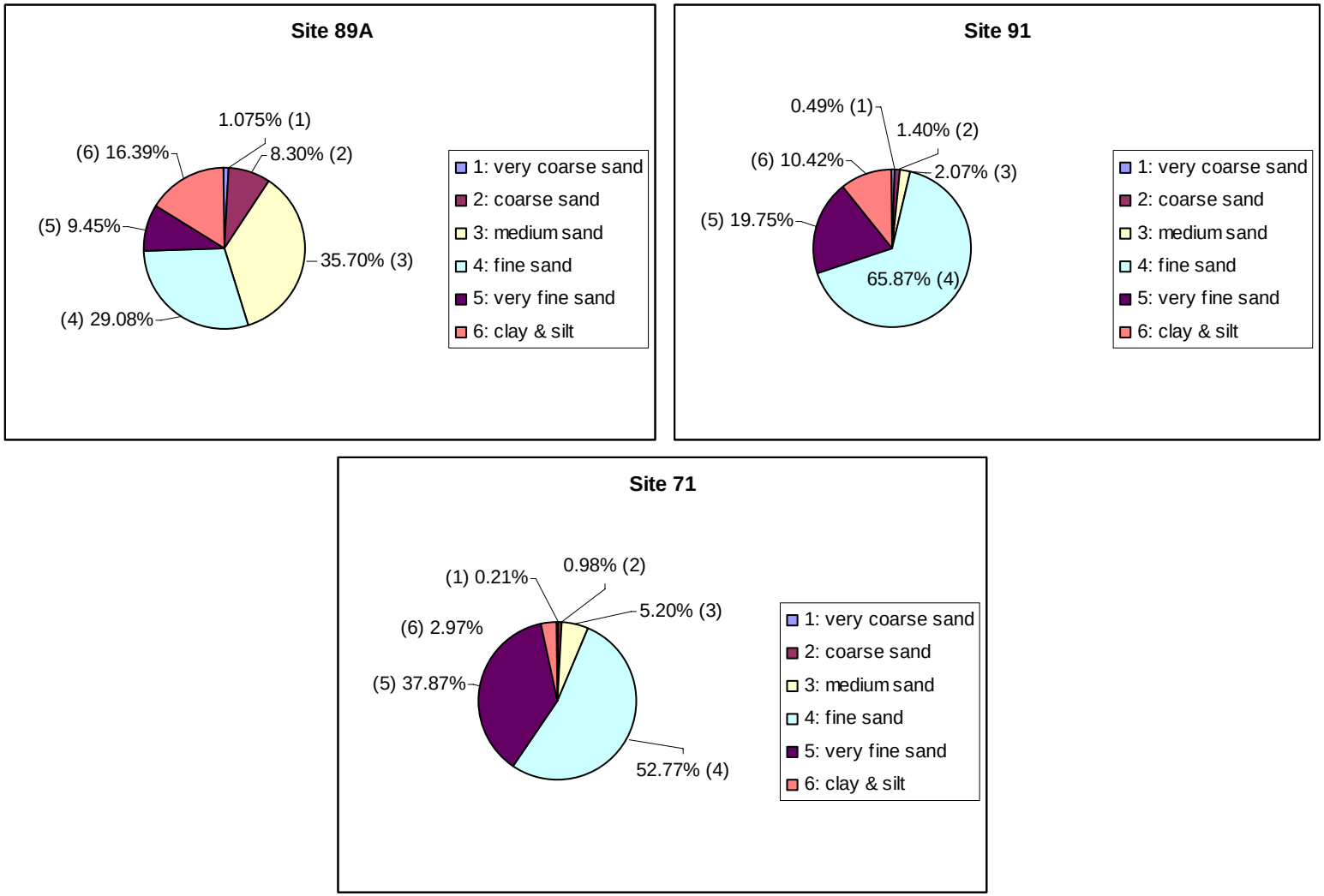

Figure: 10

Sediments Particle Size (continued)

Near shore mud-patches

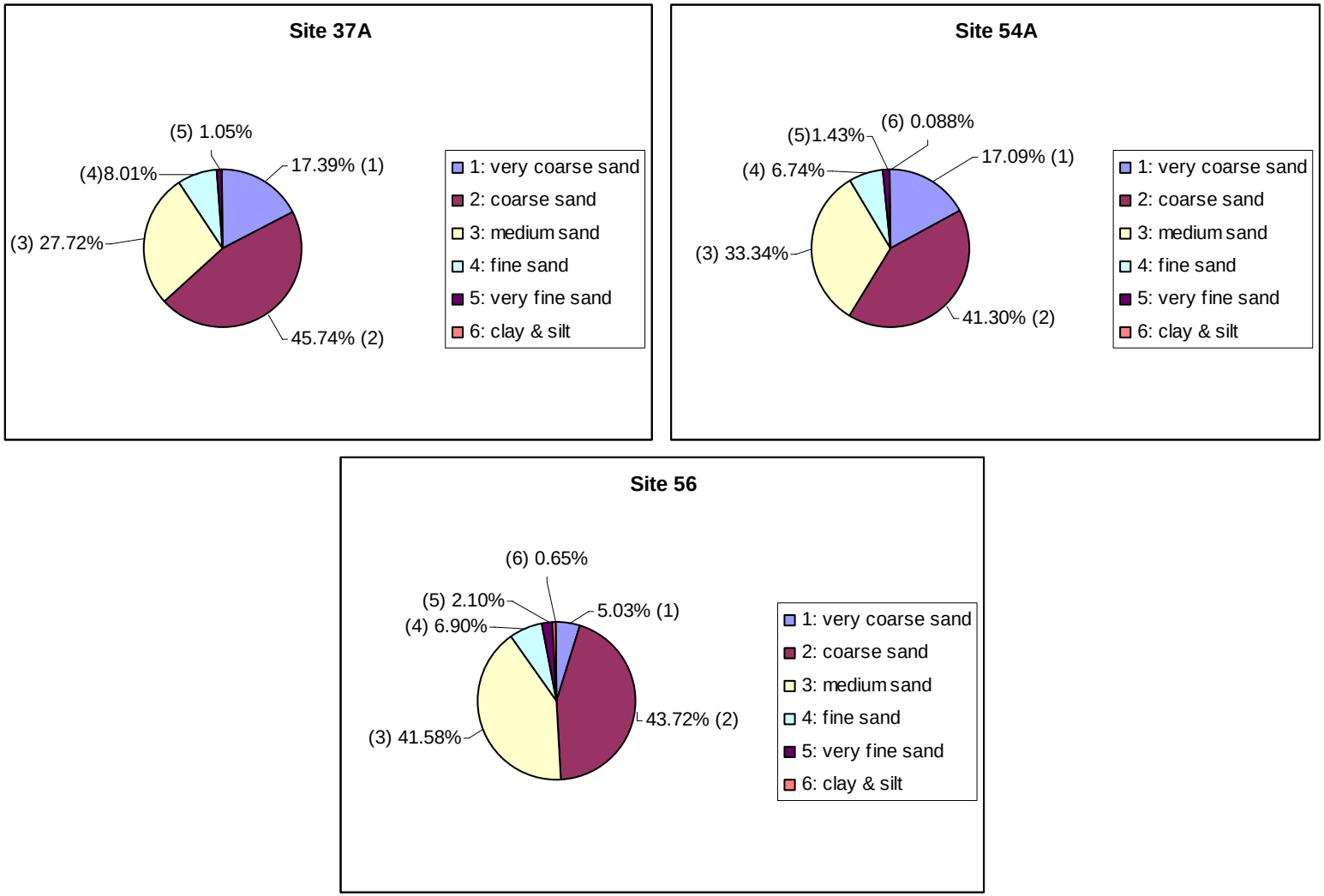

Figure: 10

Sediments Particle Size (continued)

Nearshore mud-patches

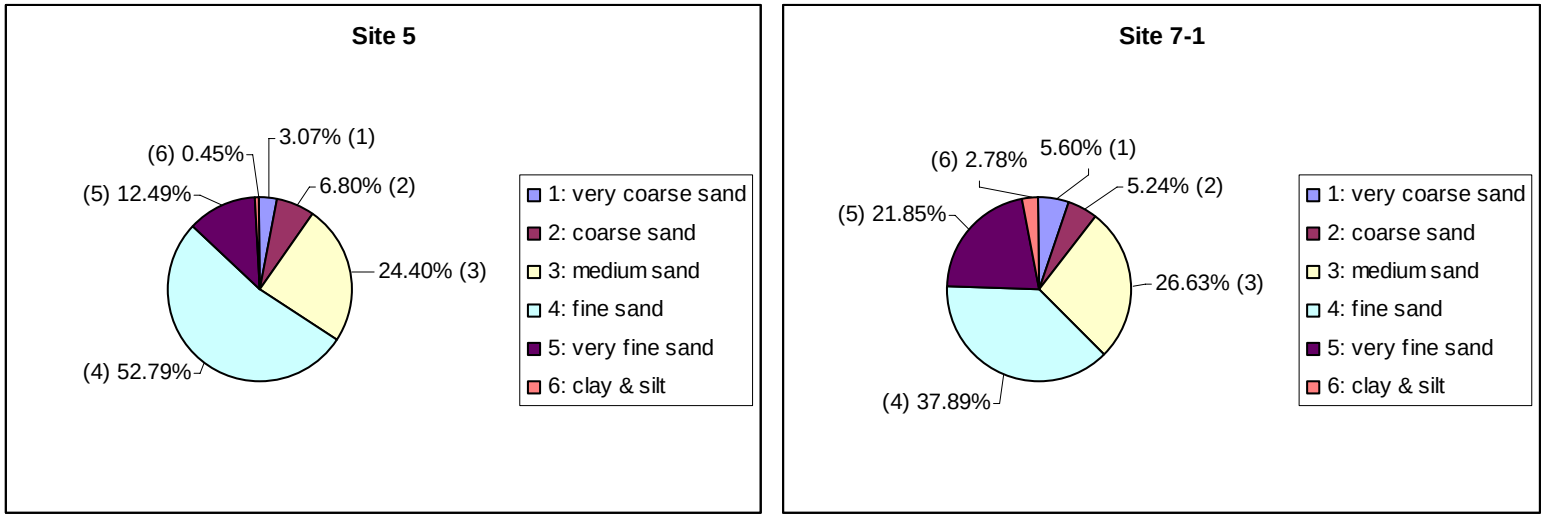

Figure: 10

Sediments Particle Size (continued)

Cholera Bank

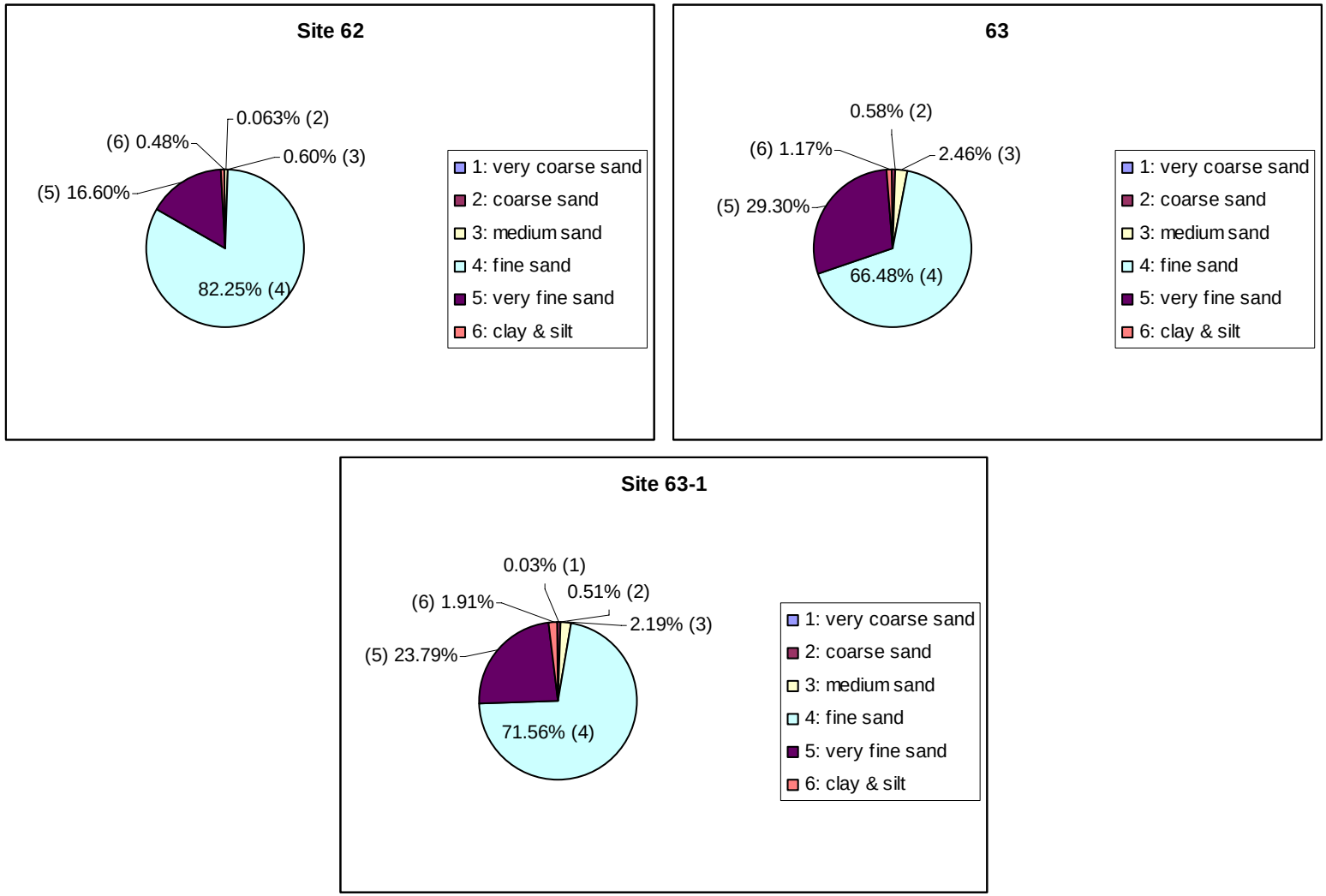

Figure: 10

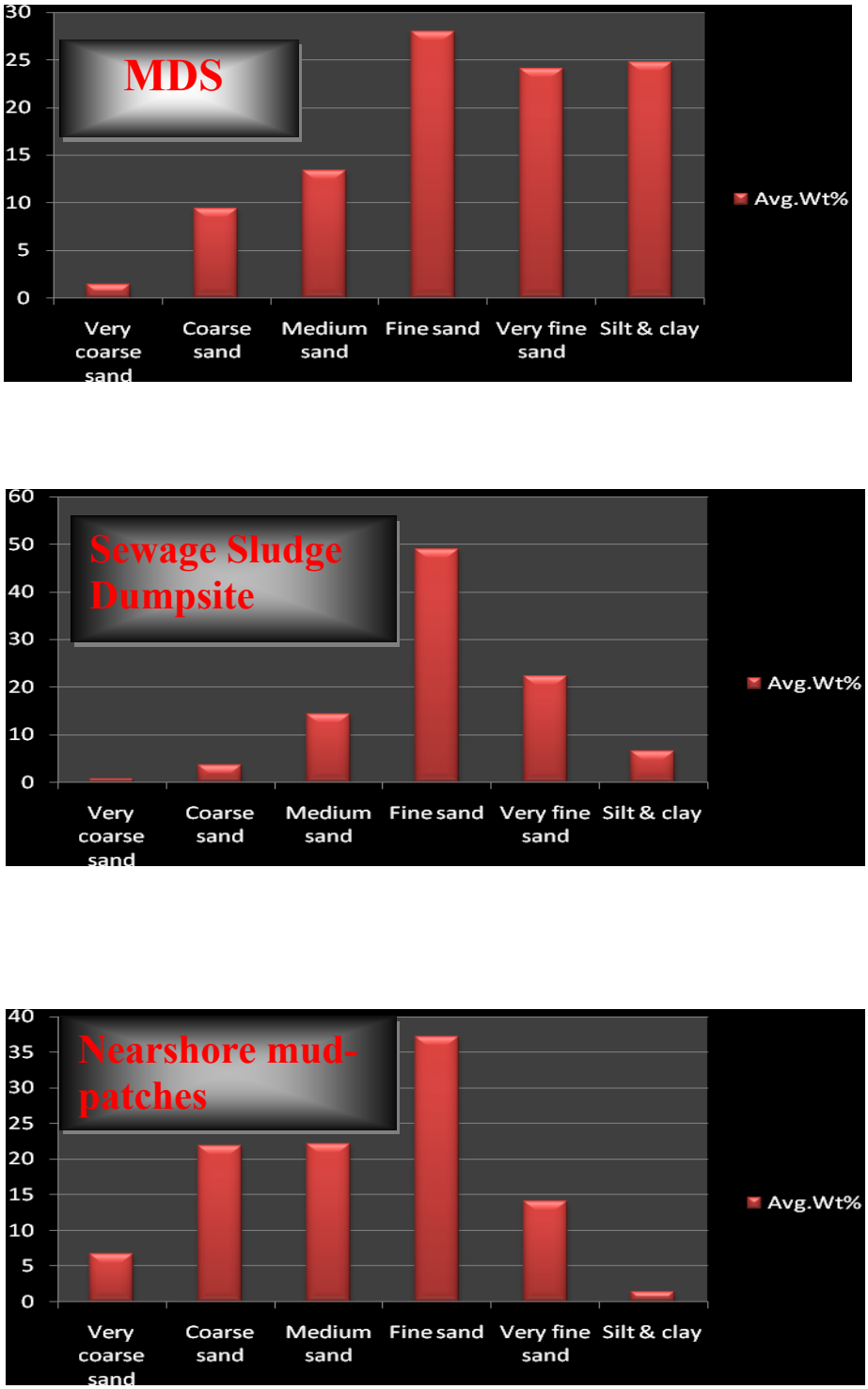

Figure 11: Weight percentage of sediment fractions from the apex of the NYB .

The mean size, standard deviation, skewness, and kurtosis for each sample were computed from the cumulative-distribution curve using the graphic formulae of Folk and Ward (1957). The mean size values calculated varies from 0.75 Phi to 3.6 Phi (Table 4). The average mean size is 2.33 Phi, which points to fine sand. The highest mean sizes occur at sites 86 and 89A (3.60 Phi and 3.48 Phi respectively). The coarsest sediment samples contain relatively high amount of silt and clay (46.90 and 16.39% respectively). The lowest mean sizes were observed in samples at sites 37 and 37A (0.75 Phi and 0.83 Phi respectively). These sediment samples contain high amount of coarse sand (48.26 and 45, 74% respectively).

In general grain-size distribution varies from one site to another. Most of the samples show high percentage of fine sand. For instance, sample 62 consists mostly of fine sand (82.25%). A very similar situation occur at sites 63-1, 63, 13-1 and 13 where fine sand dominate other size fractions (71.56, 66.48, 61.63, and 54.00 % respectively). In contrast, clay and silt fraction dominate the grain size population at the site 86 (46.90 %) (Appendix B and Figure 10).

The standard deviation is an important parameter in statistical analysis. In populations of particles, the standard deviation provides information on the extent to which particle sizes are clustered about the mean, and hence defines the concept of the sorting (Friedman and Sanders, 1978). The standard deviation for the twenty-four of the New York Bight sediment samples varies from 0.36 Phi to 1.34 Phi (Table 4). Sorting which can be expressed by the standard deviation indicates that most of the sediment samples are moderately well sorted moderately sorted and well sorted (Table 4). This finding shows that the particle size are clustered about the mean of the samples studied, which indicate also that the sediments have been reworked and recycled within the Bight.

Skewness is important in the study of particle size as indicates that particles in excess of the normal distribution are present in the coarser fraction or finer fraction, especially in the extremes (the so-called tails) of the distribution. This information can be used in interpreting the deposition of sediments. The skewness is said to be negative when the distribution posses a coarse tail portion relative to the finer sizes, whereas if there is a tail portion in the finer size relative to the coarser sizes, the skewness is positive (Friedman et al., 1992). In the New York Bight sediment samples the skewness was calculated from the cumulative-distribution curves; however it can be determined using the frequency distribution as well. The skewness varies from -0.38 to 0.61. Most of the samples are positively skewed, which means that fine-grained material (sand size particles) dominates over the coarse-grained material (gravels). Five samples from sites 54A, 56, 37A and 37 are characterized by negative skewness, which mean there is excess of coarse particles.

Kurtosis measures the peakdness or broadness of the curve from the "normal" frequency or cumulative curve. A high kurtosis distribution has a sharper "peak', while a low kurtosis distribution has a more rounded peak with wider "shoulders". In the twenty-four sediment samples studied kurtosis ranges from 0.48 to 1.89Phi. The kurtosis indicates that the grain size distribution is leptokurtic, mesokurtic and platykurtic. Some grain size distribution becomes very platykurtic and very leptokurtic (Table 5).

In general, skewness seems to be sedimentologically significant, but the significance of kurtosis is unclear. The peakdness or broadness of the frequency-distribution curves shows that the central part of the curves is usually sorted and that of the flanks are poorly sorted. High peakedness is not observed in the sediment samples studied, which confirm that the sediments are not poorly sorted (Appendix B).

The cumulative-frequency distribution curves plotted on probability paper shows that the curves are divided into segments. All curves show that there are more than two straight-line segments present, each having a different slope and sharp break between segments (Appendix B). The slope of each straight-line segment and its position are functions of the geological mechanism of deposition. The cumulative-frequency curves help to define the main population of particle sediments. The central and larger segments of the curves may represent a subpopulation that moved by saltation, the segment at the fine end of the distribution resulted from deposition of particles carried in suspension and that at the coarser end from the particles deposited by rolling or sliding. The saltation, sliding and rolling transport are non- submarine processes therefore, no definite conclusion can be made on these subpopulations. When these populations are present, they are presented mostly by coarse artificial particles, which are not natural for marine depositional environments. The materials of this population consist of wood, skeleton, shells, ceramics and other anthropogenic material dumped in this area. The fragile shell fragments found preserved in certain samples could indicate a low energy environment. The suspension population is well developed for most of the curves, which indicate that the depositional environment of these samples is predominantly low energy. For instance, the cumulative-frequency distributions of the particle size sediments from the site 91, 89A, 62, 63, 71, 63-1 and 86 show well developed suspension population, which indicate that the depositional environment of these samples is predominantly low energy, where finer materials can be deposited (Appendix B). The presence of suspension population may indicate the disturbance of the low energy environment where finer material accumulates.

Table 4: Sediment textural properties

Sample	ϕ 5%	ϕ 6%	ϕ 25%	ϕ 50%	ϕ 75%	ϕ 84%	ϕ 95%	Mean	Stand.dev.	Skwn.	Kurt.	Sorting Class
63	2.10	2.35	2.50	2.78	3.05	3.20	3.60	2.78	0.44	0.04	1.11	well sorted
71	2.10	2.45	2.60	2.90	3.25	3.45	3.85	2.93	0.51	0.093	0.88	moderately well sorted
87	0.40	1.05	1.55	2.60	3.7	4.05	4.30	2.57	1.34	-0.08	0.74	moderately sorted
86	2.50	2.75	2.90	3.80	4.15	4.25	4.40	3.60	0.66	-0.38	0.62	moderately well sorted
89a	0.70	1.30	1.55	2.15	3.10	3.98	4.25	3.48	1.21	0.27	0.93	moderately sorted
91	2.05	2.35	2.50	2.80	4.25	3.65	4.18	2.93	0.64	0.30	0.49	moderately well sorted
54A	0.00	0.00	0.25	0.80	1.40	1.68	2.35	0.83	0.77	0.18	0.83	moderately well sorted
56	0.00	0.40	0.62	1.03	1.52	1.75	2.60	1.06	0.73	0.13	1.18	moderately well sorted
62	2.25	2.48	2.55	2.75	2.95	3.25	3.40	2.83	0.36	0.30	0.94	well sorted
37A	0.00	0.00	0.20	0.75	1.35	1.68	2.35	0.81	0.77	0.095	0.83	moderately well sorted
7-1	0.00	1.30	1.65	2.35	3.25	3.35	3.80	2.33	1.08	-0.13	0.97	moderately sorted
5	0.40	1.35	1.70	2.28	2.73	2.92	3.33	2.18	0.83	-0.23	1.16	moderately sorted
20A-1	0.98	1.90	2.15	2.58	2.95	3.20	3.60	2.56	0.72	-0.13	1.34	moderately well sorted
37	0.00	0.00	0.52	0.80	1.15	1.45	2.05	0.75	0.67	0.095	1.33	moderately well sorted
33-1	0.05	0.90	1.65	2.40	2.90	3.10	3.80	2.13	1.11	-0.30	1.23	moderately sorted
1-2	1.65	2.20	2.40	2.92	3.35	3.55	3.98	2.89	0.69	-0.37	1.00	moderately well sorted
84	0.42	1.18	1.70	2.68	3.40	3.68	4.12	2.51	1.18	-0.21	0.89	moderately sorted
20A	1.32	2.02	2.22	2.70	3.10	3.32	3.75	2.68	0.69	-0.023	1.13	moderately well sorted
13	1.68	2.18	2.40	2.80	3.20	3.40	3.85	2.79	0.63	-0.30	0.85	moderately well sorted
21A	1.12	1.70	1.95	2.40	2.80	3.00	3.60	2.37	0.70	-0.05	1.19	moderately well sorted
13-1	1.48	2.09	2.25	2.65	3.00	3.15	3.42	2.63	0.50	-0.13	1.06	well sorted
37B	0.30	0.60	0.72	1.00	1.50	1.75	2.25	1.12	0.58	0.19	1.00	moderately well sorted
63-1	2.12	2.40	2.50	2.78	3.00	3.25	3.70	2.81	0.45	0.61	1.30	well sorted
5-1	0.00	1.75	2.15	2.58	2.95	3.15	3.69	2.49	0.90	-0.29	1.89	moderately sorted

Stand.dev: Standard deviation; Skwn: Skewness; Kurt: kurtosis; ϕ 5%: Phi value at 5%; ϕ 16%: Phi value at 16%; ϕ 25%: Phi value at 25% ϕ 50%: Phi value at 50%; ϕ 75%: Phi value at 75%; ϕ 84%: Phi value at 84%; ϕ 95%: Phi value at 95%

Table 5: Kurtosis values

Site	Lowest	to	Highest	Equal
91, 86	0.41		0.67	very platykurtic
71, 87, 54A, 37A, 84, 13	0.67		0.90	platykurtic
13-1, 37B, 1-2, 7-1, 62, 89A	0.90		1.11	mesokurtic
63.1, 21A, 20A, 33-1, 20A-1, 56, 63	1.10		1.50	leptokurtic
5-1	1.50		3.00	very leptokurtic

Core 97-9 consists mostly of sticky dark brown mud, which indicate deep environment (low energy setting). This core shows gravelly sand injections within the mud. These injections indicate storm events, especially at depth of 59-60cm and 68-. 69cm. Core 97-1 shows the predominance of clean sand with scattered shell fragment and anthropogenic materials. This clean sand could be deposited by one single storm event.

4.2. XRD Analysis of the Clay Fractions

The experimental XRD patterns of the Air Dried (AD) and Ethylene Glycol (EG) solvation of the oriented clay mounts are shown in Appendix C. All the samples from the apex of NYB exhibit similar XRD patterns, whatever their sampling site. As evident (Appendix C), the peaks intensities of the XRD patterns reflect the presence of clay minerals (illite,chlorite, kaolinite) and non clay minerals (quartz, K-feldspar, plagioclase, pyrite and amphibole). The reflection peaks in the EG state correspond exactly to those of AD state, which indicate that clay fractions from NYB are similar in mineral composition regardless their location. The difference in XRD pattern of AD and EG of clays from site 7-1-2 is reflected by the presence of mixed layer illite/smectite phases in addition to illite, chlorite and kaolinite.

The estimated mineral compositions of the XRD data of the selected samples studied in the apex of the NYB from which the clay separations were taken is shown as weight percent in Table 6. As the data shows, the major contributors to the non-clay phase composition are quartz,

K-feldspar, plagioclase and pyrite, whereas the clay minerals are illite, kaolinite, chlorite and mixed layer illite/smectite. The comparative mineral composition of clay fraction of selected site is shown in Figure 12. Illite concentrations in clay fraction from the apex of the NYB are almost constant throughout the sampling area. However, illite percentages are slightly higher in dredge spoil samples and sewage sludge samples than those of near shore mud-patches. Station 87-1(dredge spoil) showed the highest value of 48.5% and station 54A (South of Long beach) the lowest (28.6%).The second highest clay minerals are chlorite, followed by kaolinite and mixed layer illite/smectite. As evident (Figure 12), the weight percent of chlorite showed constant distribution in MDS and sewage sludge sites. However, the weight percent of chlorite in clay fractions of near shore mud-patches varied with sites. For instance, station 56A (south of long beach) showed highest amount of chlorite content (24%) and the lowest amount of chlorite occurred at station 7-1-2 south of Long Beach (3.2%). Kaolinite represents the third highest clay minerals in clay fraction of the apex of the NYB. The highest kaolinite values occurred at station 84-1, 7-1-2 and 91 with a weight percent of 10.6 and 10.4 respectively. In general the weight percent of mixed layer illite/smectite was significantly low to absent in most of NYB clay fractions, with an exception of site 7-1-2, which showed the highest value of 16.6 %.

Table 6: Clay fraction mineralogy from quantitative X-ray diffraction analysis

XRD	Site	Qtz	Kspar	Plag	Amph	Py	RO M-L I/L 90S	Illite	Kao	Chl	Total	Clay Wt% <4μm
1	1-1	21.5	2.8	15.8	0	5.4	0	36.5	3.3	14.7	100	14.1
2	1-2	16.4	4.1	22.6	0	4.4	0	33.3	3.3	15.9	100	20.7
3	7-1	15.5	2.7	20.9	0	10.4	0	32.6	5.8	12.1	100	21.2
4	7-1-2	17	1	7.2	0	0.5	16.6	44.1	10.4	3.2	100	33.5
5	33-1	14.2	3.8	24.8	4.6	3.4	1.2	28.7	4	15.3	100	21
6	54A	18.9	4.1	25.2	0	1.9	0	28.6	6.5	14.8	100	26.5
7	55-1	14.6	4.3	15.5	0	3.4	0	39	5.4	17.8	100	27.5
8	56A	15	1.8	11.9	0	4.3	0	41.1	1.9	24	100	14.2
9	63	14.2	2.7	18.7	0	10.7	0	33.8	10.5	9.4	100	24.5
10	84-1	13.4	1.2	10.7	0	4.8	1.1	45.3	6.4	17.1	100	25.9
11	85-1	12.1	2.1	11.8	0	4.3	1.6	45.2	5.3	17.6	100	22.2
12	86	12.3	1.3	9.8	0	3.9	1	46.2	6.9	18.6	100	18.4
13	86-1	9.6	1	10.7	0	3.8	1.1	47.9	7.3	18.6	100	15.8
14	87-1	13	0.8	9.9	0	5.2	1.6	48.5	3.7	17.3	100	18.5
15	88-1	9.3	1.3	10.9	0	4.3	1.5	48.2	8.3	16.2	100	23.4
16	89A	12.4	0.9	9.4	0	5.4	2.5	47.2	5.2	17	100	37.6
17	91	15.2	1.5	20.4	0	3.8	0	35	10.4	13.7	100	22.9

Qtz = quartz; Plag: plagioclase; Kspar: K-feldspar; Py: pyrite; Amph: amphibole; Kaol: kaolinite; Chl: chlorite; I/S: illite/smectite
RO M-L I/S 90S - Randomly Oriented Mixed-Layer Illite/smectite with 90% Smectite Layer

Figure 12: Comparative clay faction mineralogy
Mud Dump Site (MDS)

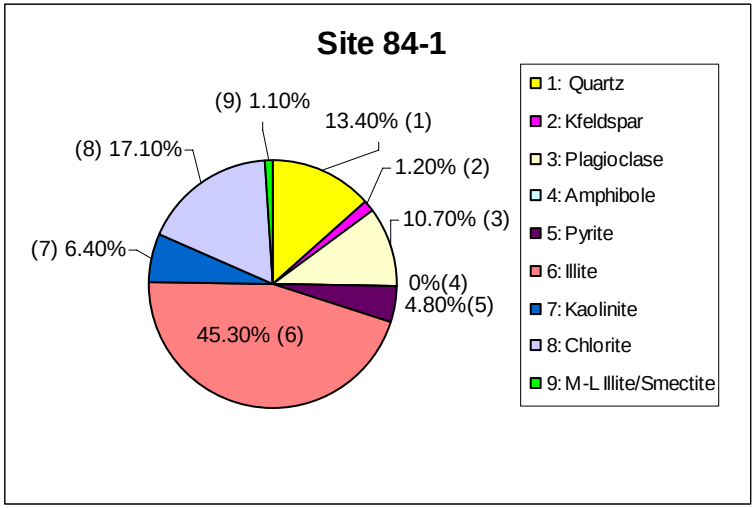

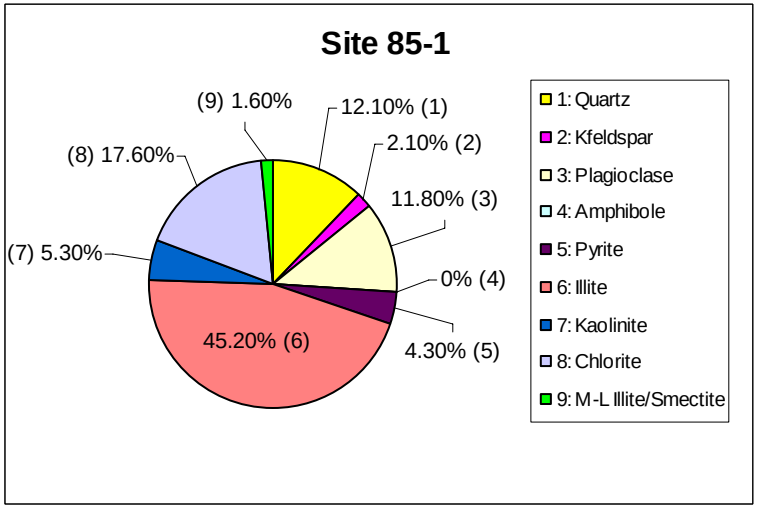

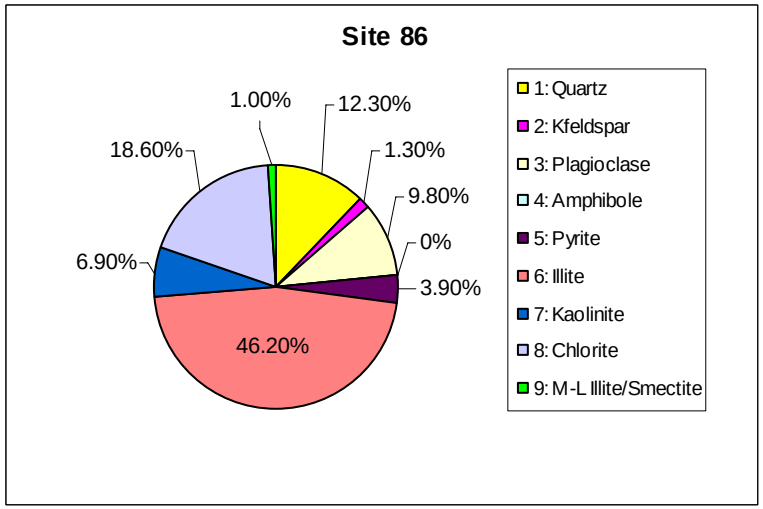

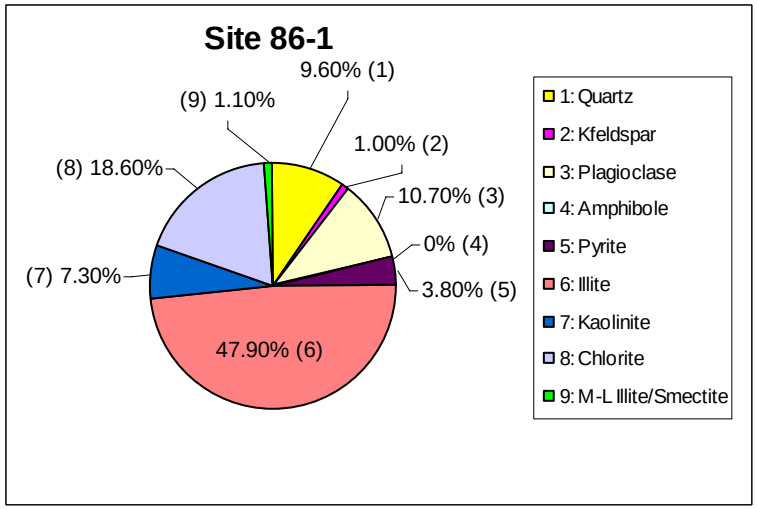

Figure 12: Comparative clay faction mineralogy
Mud Dump Site (MDS) (continued)

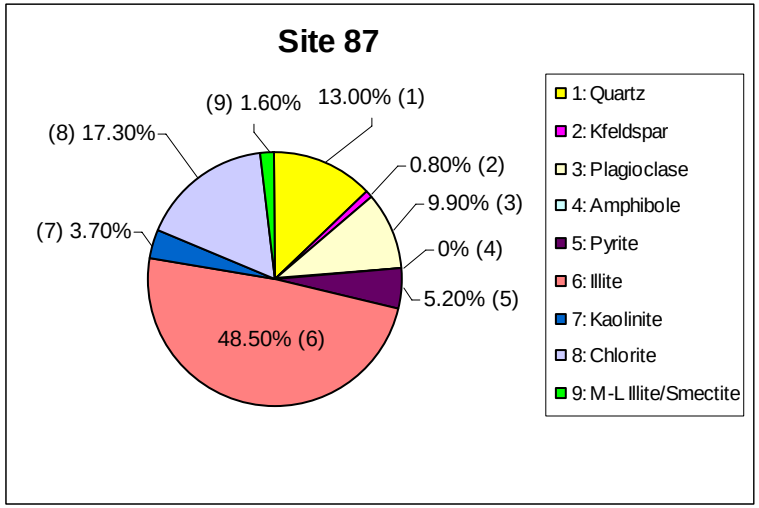

Figure 12: Comparative clay faction mineralogy
Sewage Sludge Dumpsite -southern Christiansen Basin

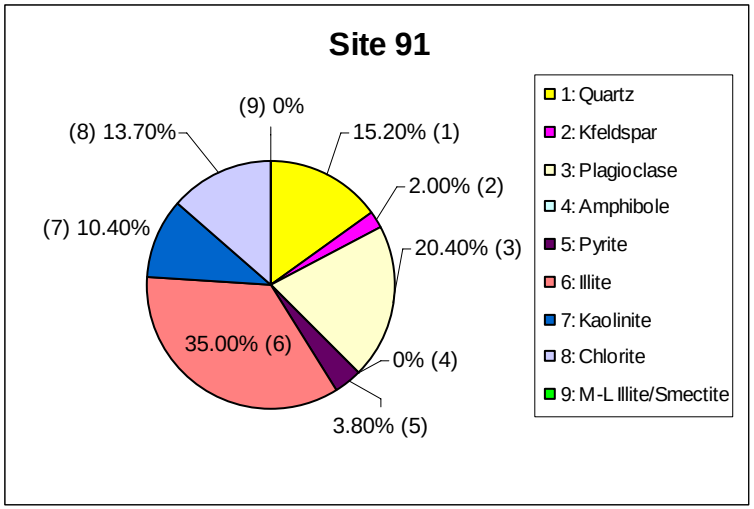

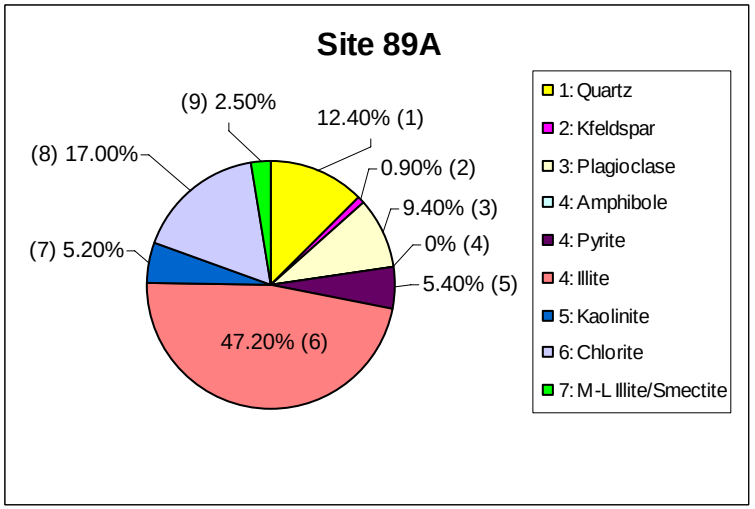

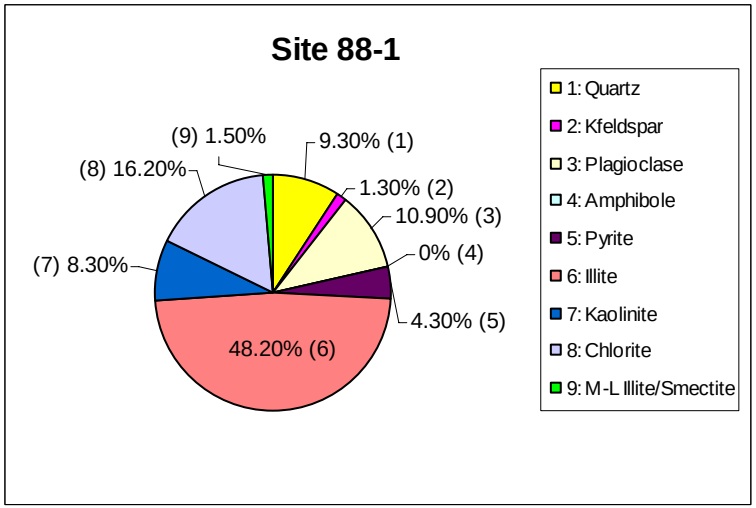

Figure 12: Comparative clay faction mineralogy
Sewage Sludge Dumpsite-northen Christiansen Basin

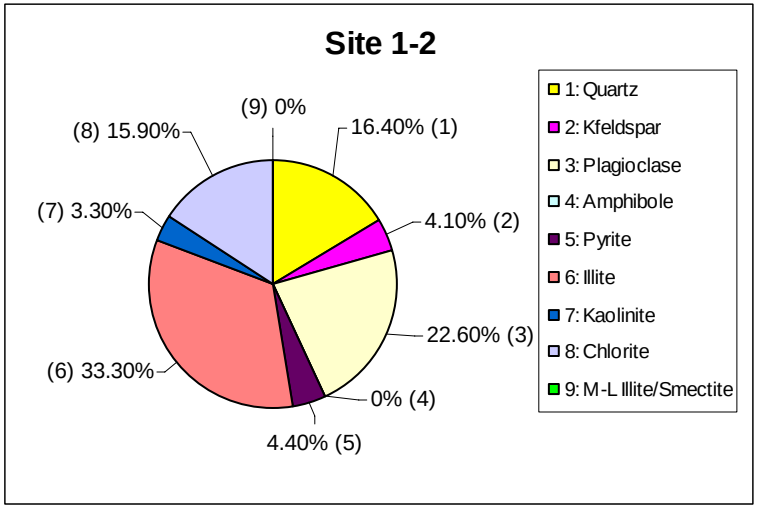

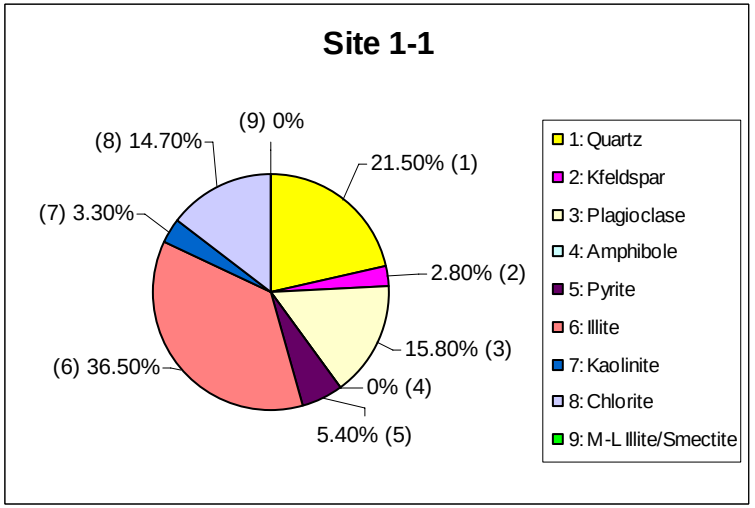

Figure 12: Comparative clay faction mineralogy
Nearshore Mud Patches- South of Long Beach

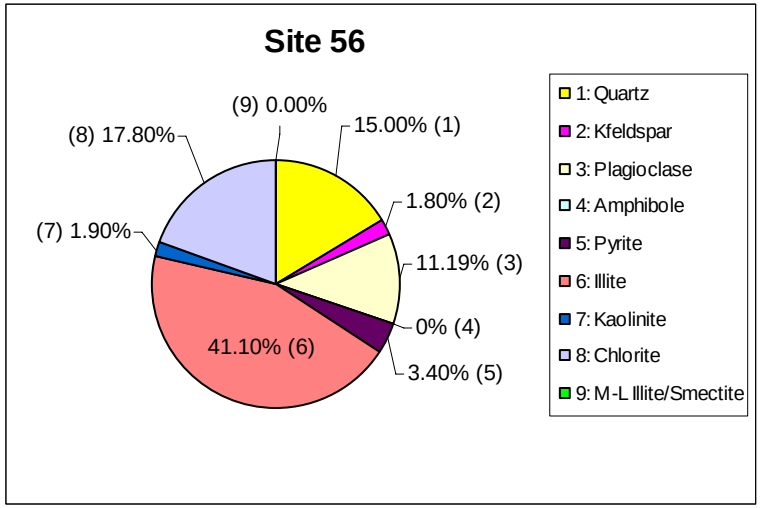

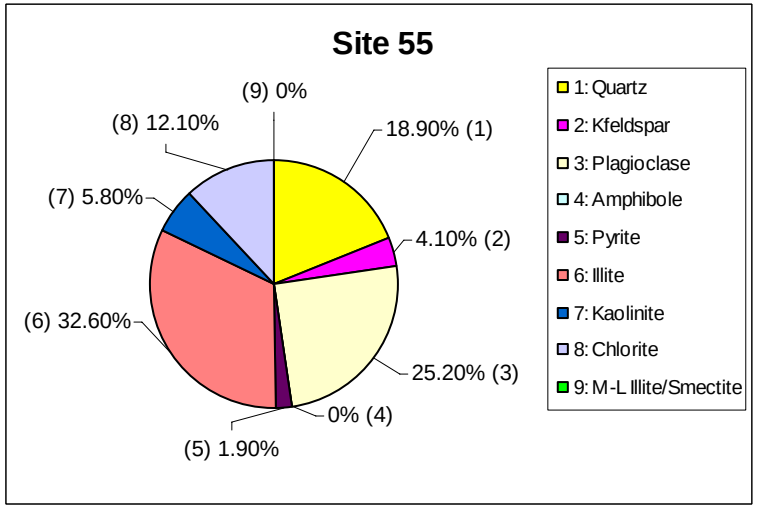

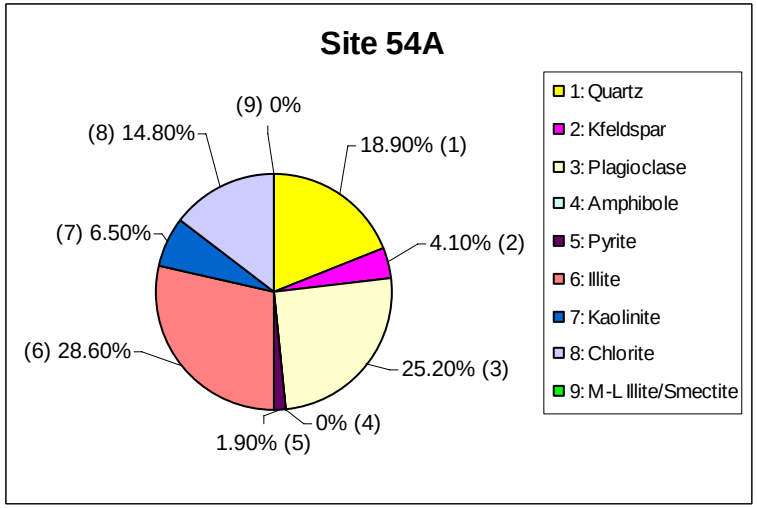

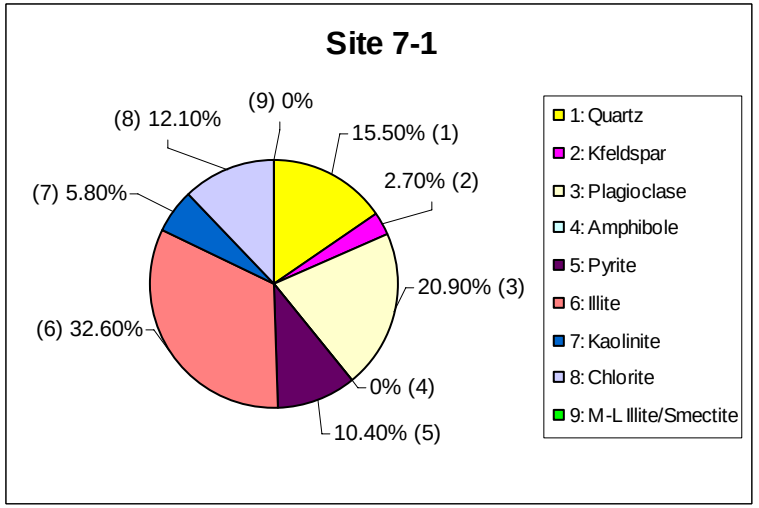

Figure 12: Comparative clay faction mineralogy (continued)

Nearshore Mud Patches- South of Long Beacch

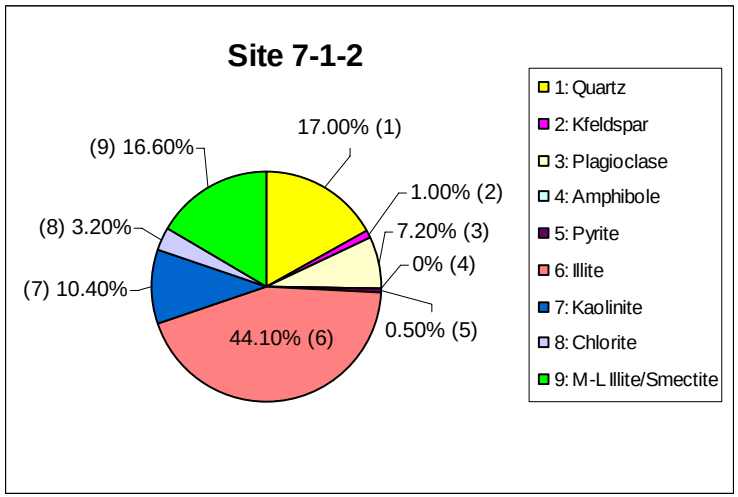

Nearshore Mud Patches- South of Jones Inlet

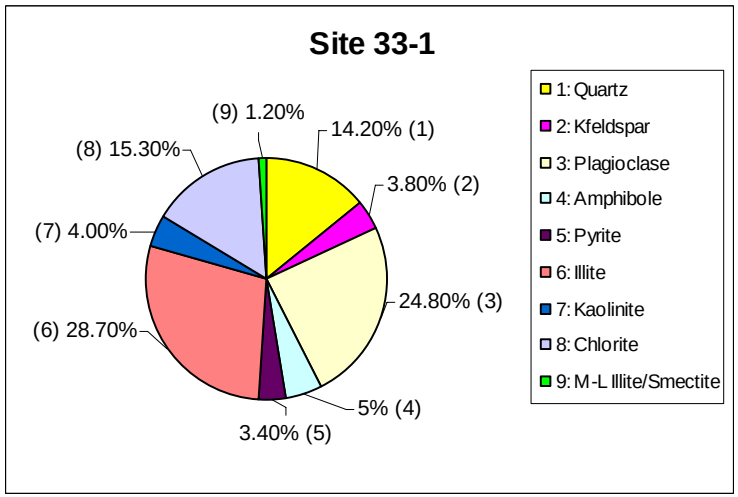

Cholera Bank

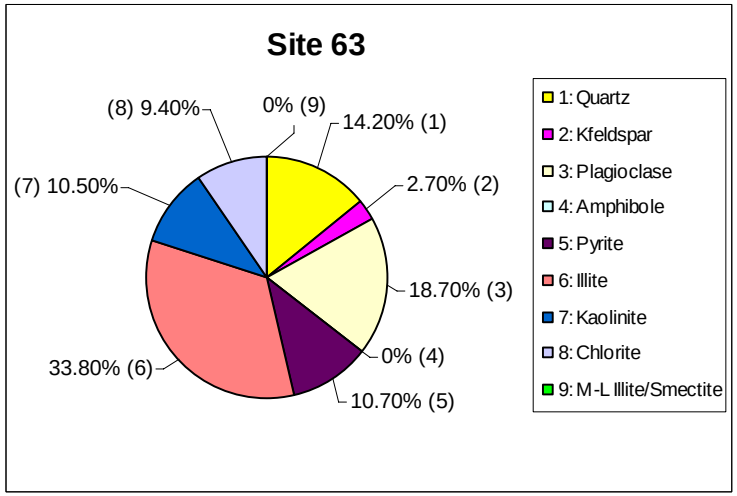

4.3. Concentration and Distribution of Trace Metals in the Apex of the NYB

The trace metals were extracted with a single 50% HNO_3 leach and for comparative purposes, a single step digestion using the mixed reagents consisting of three acids, $HF/HClO_4/HNO_3$ was also conducted. The trace metal levels extracted by this procedure are shown in Figure 13**.**

The AAS was used to measure the level of trace metalsl. The average concentration of each metal in the acid extract (Pb, Cu, Zn, Ni, Cr and Mn) was calculated from three readings. Each reading was delayed by three seconds until the system was stabilized. A matrix standard and blank were analyzed every 10 samples. The instrumental settings and detection limits for trace elements by AAS analysis are listed in Appendix A.

4.3.1. Variability of Trace Metal Concentrations

The comparative results of trace metal concentration in New York Bight sediments are shown in (Appendix D) and graphically in Figure 14. The concentrations are in mg/kg (ppm) dry weight; ± values indicate the analytical error (standard deviation or precision) in the reported concentration due to change in instrumental conditions during sample analysis. The relative standard deviation (RSD was calculated using the mean standard deviation (precision), divided by the mean concentration, and multiplying by 100 to give the percent precision. The precision or standard deviation was calculated by using 11 replicate measurements of NBS Estuarine Sediment 1646a. The analytical precision varied depending on the metal selected (Table 3).

4.3.1.1. Variability of Cd

Cadmium concentration in clay fraction did not vary significantly with site. The maximum occurred at station 91 (Christiansen Basin) and 71 (north of Christiansen Basin) (15 ppm) with the next highest at station 85 (MDS), 63 (Cholera Bank) and 7-1 (near shore mud-

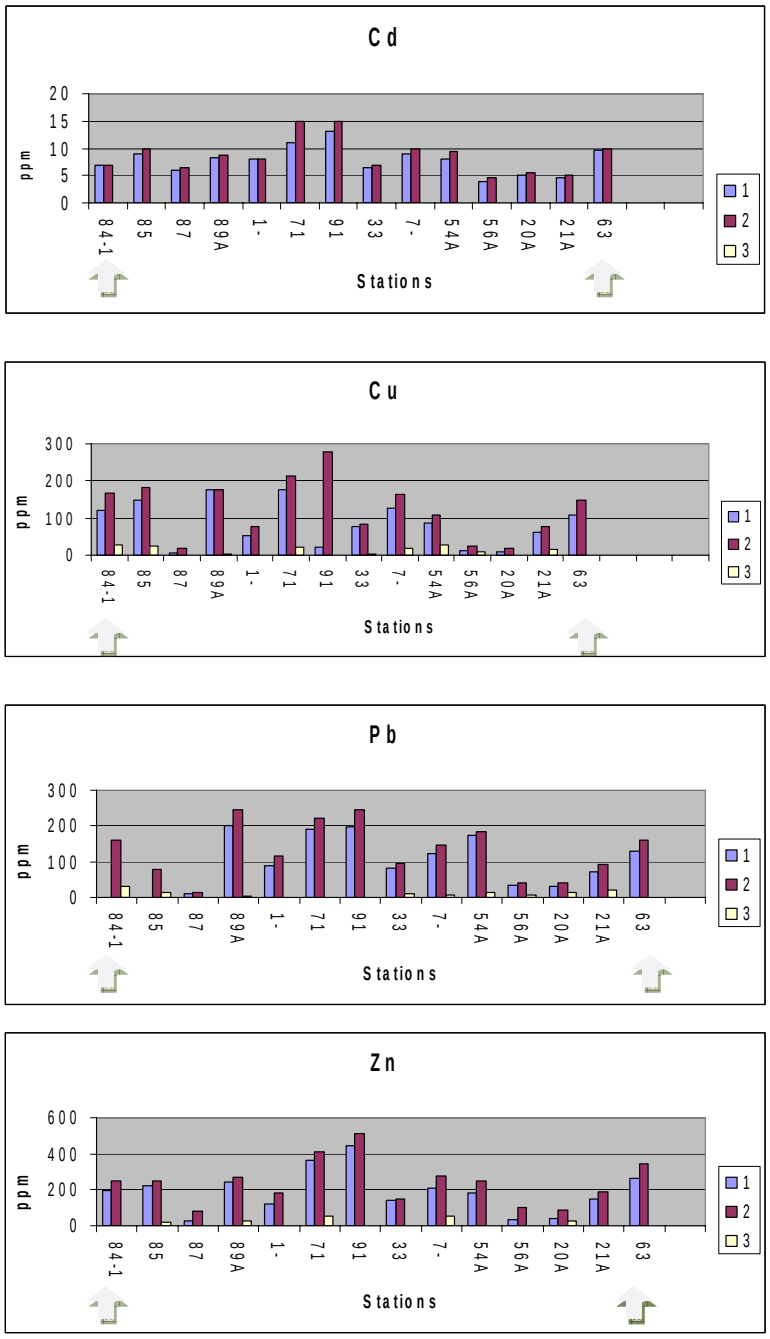

Figure 13: Extracted trace metal levels from clay fractions of the NYB apex

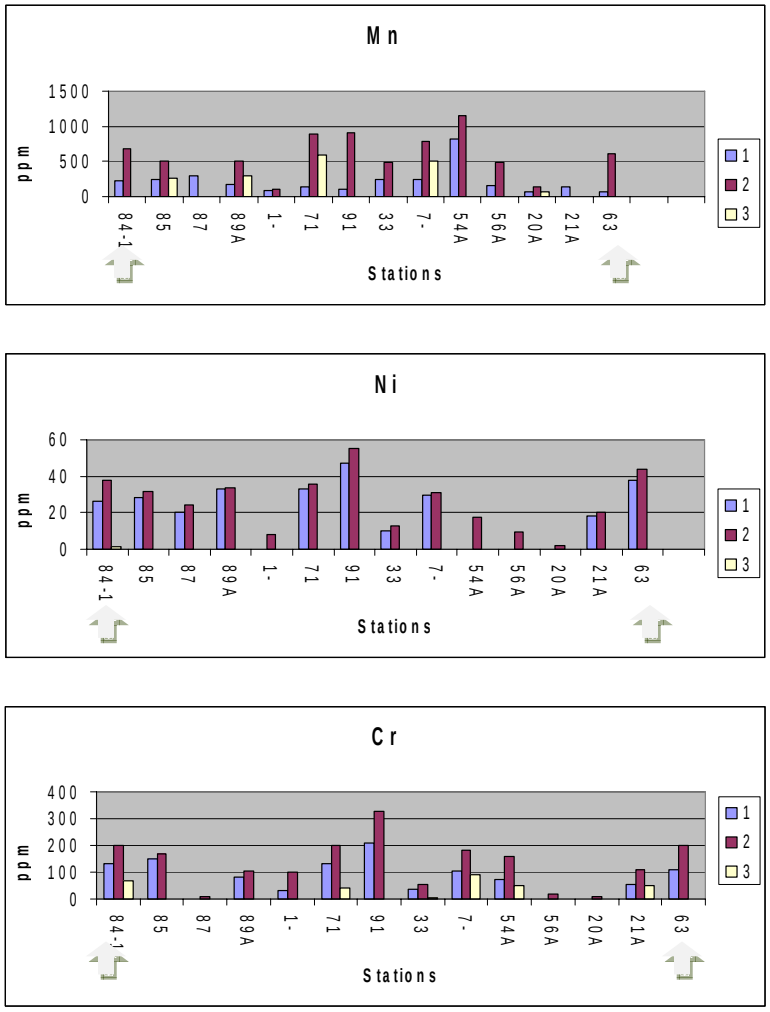

1) 50% HNO3 leach 2) $HF/HClO_4/HNO_3$ 3) $HF/HClO_4/HNO_3$ of residue 1

Figure 13: Extracted trace metal levels from clay fractions of the NYB apex (continued)

patches south of Long Beach) (10 ppm). The lowest concentration occurred at station 56A (south of Long Beach) (4.7 ppm). In general, the distribution of Cd in the apex of the NYB is relatively uniform throughout the sampling area (Figure 14).

4.3.1.2. Variability of Cu

Copper concentrations in clay fraction from the apex of the NYB are site dependent. Station 91 (north Christiansen Basin) again showed the highest value of 279 ppm and station 87 the lowest (17.5 ppm). The second highest Cu value occurred in north Christiansen Basin's mud at station 71 with a value of 213 ppm, and the third highest at station 89A (south of Christiansen Basin) with a value of 176 ppm. The copper level in MDS at station 87, and at sites 20A and 56A south of Long Beach did not vary significantly. Station 1-2 north of Christiansen Basin and site 21A south of Long Beach showed same level of Cu with mean value of 77 and 78 ppm, respectively.

4.3.1.3. Variability of Pb

Lead concentration in the NYB clay fraction varied significantly with sites. Station 89A (South of sewage sludge dumpsite) had the highest mean value of 247 ppm and stations 91 and 71 (north of sewage sludge area) following with means of 244 ppm and 220 ppm, respectively. Lead levels at these stations were not significantly different from each other. Station 87 at MDS showed the lowest concentration of 15 ppm. The second lowest Pb concentration occurred at station 56A south of Long Beach with a mean value of 42 ppm.

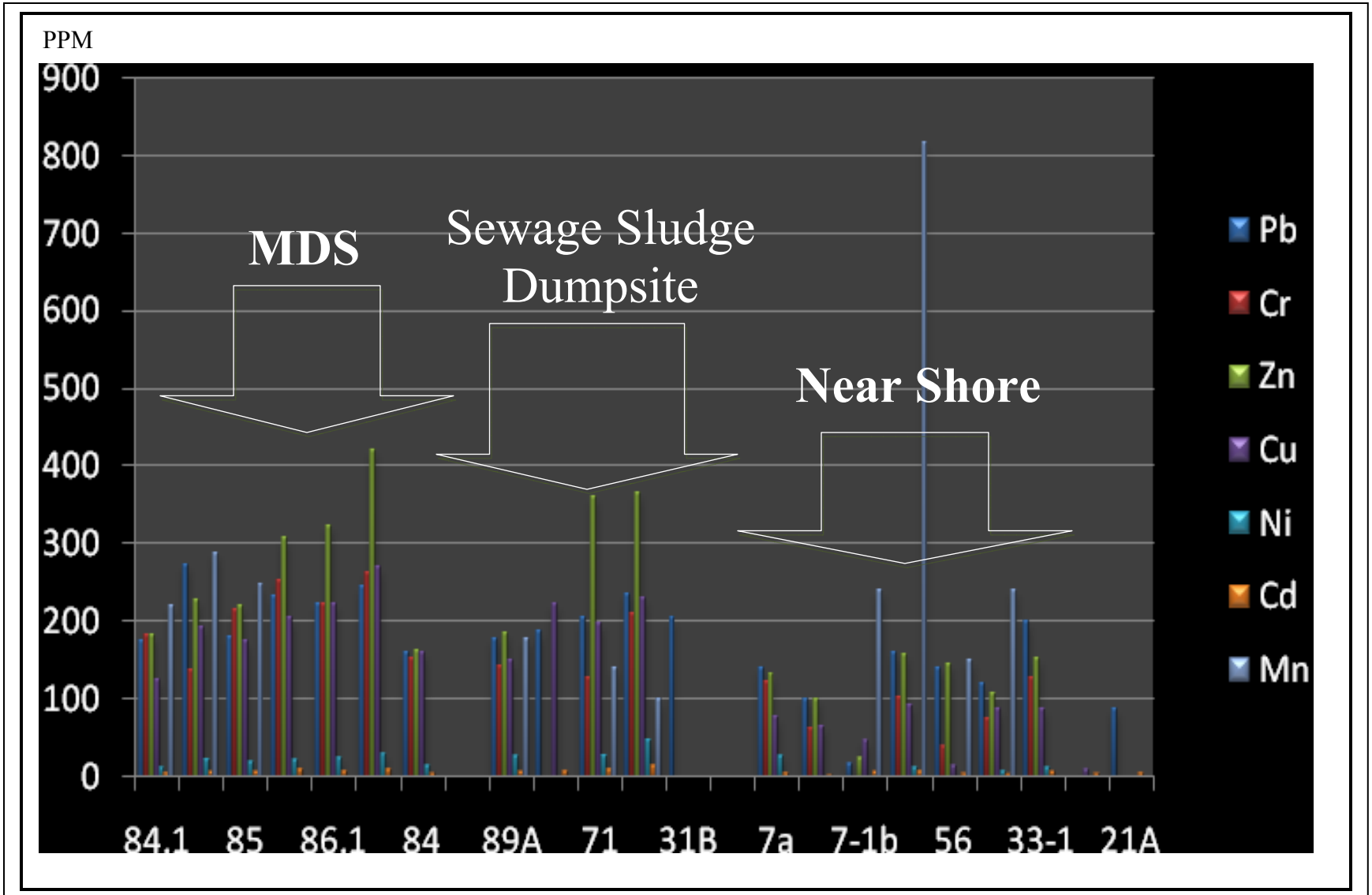

Figure 14: Trace metals variation in clay faction from the apex of the New York Bight. (MDS: Mud Dump Site)

4.3.1.4. Variability of Zn

Zinc concentrations in clay fraction from the NYB Apex varied significantly with site. All the sites showed more than 100 ppm Zn except station 20A south of Long Beach. The highest concentration occurred again in sewage sludge north of Christiansen Basin at station 91 with a mean value of 512 ppm. The second highest concentration also occurred in Christiansen Basin muds north of sewage sludge area at station 71 (411 ppm), and the lowest Zn levels occurred at station 20A south of Long beach with a mean value of 86 ppm. Clay fraction from MDS at stations 84-1 and 85 and from south of Long Beach at station 54A showed the same levels of Zn (248 ppm) (Figure 13).

4.3.1.5. Variability of Mn

Manganese was not uniformly distributed throughout the sampling area. The maximum concentration occurred in near shore mud-patches at station 54A south of Long beach (1145 ppm) with stations 91 and 71 having the second and third highest values (912 and 892 ppm, respectively). The lowest Mn concentration occurred at station 1-2 (108 ppm). Mn concentrations like all other metals except Cd varied significantly with sites (Figure 14).

4.3.1.6. Variability of Ni

Nickel content in clay fraction from the apex of the New York Bight was site dependent. The maximum value occurred in sewage sludge at station 91 with a value of 55 ppm and the minimum occurred south of Long Beach at station 20A with a value of 2 ppm. The second highest concentration occurred south of dump sites in Cholera Bank muds at station 63 with a mean of 44 ppm, and the third highest occurred in MDS clay faction at station 84-1 (38 ppm).

4.3.1.7. Variability of Cr

Cr like other metals was not uniformly distributed among the New York Bight sediment samples (Figure 14). The maximum Cr level occurred at station 91 north of sewage sludge area with a mean of 328 ppm and the minimum occurred at station 20A south of Long Beach with a mean of 8 ppm. The second highest level of Cr occurred north of sewage sludge dumpsite at station 71 (198ppm).

Generally, metal concentrations also varied considerably between the various metals analyzed of which Mn is the highest one followed by Zn, Cr, Cu, Pb, Ni and Cd (Figure 13 & Appendix C). The highest concentrations of trace metals except Mn occurred in sewage sludge north of Christiansen Basin at station 91. With increasing trace metal concentrations (ppm = mg/kg, dry sediment) were Mn (1145 ppm) > Zn (512 ppm) > Cr (328 ppm) > Cu (279 ppm) > Pb (ppm) > Ni (55 ppm) > Cd (15 ppm). The mean trace metal concentrations in the apex of New York Bight were Mn (606.58 ppm) > Zn (238.82 ppm) > Pb (131.65 ppm) = Cr (131.65 ppm) > Cu (123.78 ppm) > Cd 30.45 ppm > Ni 26 ppm.

4.3.2. Grain-Size Depencies of Trace Metal Concentrations Extracted by 50% HNO_3

4.3.2.1. Mud Dump Site (MDS)

Trace metal analysis of sediments from the MDS showed that all the selected trace metals were concentrated in clay fraction. The concentration levels of each metal decreased with increasing sediment particle size. Some of these trace metals did not occur in other size fractions other than clays (Appendix D, section D.3.).

The maximum Pb content occurred in clay fraction at station 87 (272 ppm) followed by the second highest at station 86-2 with a mean value of 245 ppm. The minimum lead level

occurred at station 84 (159 ppm). The Pb content decreased with increasing particle size. The lowest concentration of Pb occurred in medium sand.

Cr concentrations showed the same distribution as Pb. Station 86-2 showed the maximum concentration (263 ppm) with station 86 having the second highest value (253 ppm). Cr was not detected in fine and medium sand. Most of Cr was concentrated in clay fractions.

Zn content in sediments from MDS varied significantly with site but again as shown in Appendix D, most of Zn occurred in clay fractions. Zn levels decreased dramatically with particle size. Station 86-2 again showed maximum Zn concentration (420 ppm) with station 86-1 and 86 having the second and the third highest values of 322 and 308 ppm, respectively. The lowest concentration of Zn occurred at station 84-1 with a mean value of 125 ppm.

Copper showed the same distribution as other selected trace metals. High Cu levels were detected in clay fraction throughout the sampling area. Maximum concentration occurred at station 86.2 (269 ppm) followed by second highest at station 86-1 (223 ppm). Clay fraction from DMS at station 84 showed the lowest Cu concentration with a mean value of 160 ppm.

Nickel, in clay fraction showed low concentration when compared with Pb, Cu and Zn levels. Ni was not present in any of other sediment fractions other that clays. The highest concentrations occurred again at the site 86-2 (30 ppm) and the minimum Ni level was found at the station 84-1 with a mean value of 12 ppm.

Cadmium was uniformly distributed in clay fraction of the dredge spoil sediments. Unlike other trace elements Cd showed the lowest values. Its maximum concentration occurred in clay fraction at the station 86 (10.4 ppm) followed by the second highest at station 86-2 with a mean value of 10 ppm. The lowest concentration of Cd occurred at station 84 (4 ppm).

4.3.2.2. Sewage Sludge Dumpsite

Trace metal concentrations from the Christiaensen Basin varied from one trace element to another. Even though the concentrations varied among trace metals, the maximum level of these elements was associated with clay fraction. Trace metal concentration in sewage sludge clay varied significantly with particle size whatever its location (Appendix D).

Lead concentration from the Christiansen Basin clays did not vary significantly. High Pb levels occurred in sediments from north Christiansen Basin when compared to Pb levels in sediments of south Christiansen Basin. Station 91 had the highest mean value of 235 ppm with station 71 and 31B following with mean values of 206 and 204 ppm, respectively. Pb concentrations in clay fractions from these sites were not significantly different from each other. The lowest concentration occurred at station 89A south of the Christiansen Basin with a mean value of 177 ppm. Pb also was associated with very fine sand and fine sand, however its levels were lower than those retained by clay fraction of the same sample.

The levels of chromium from sewage sludge dumpsite were highly concentrated in clay fraction. Maximum Cr occurred again at station 91 with a mean value of 209 ppm. Cr was also detected in very fine and fine sand of the same sediment sample, but the Cr value were dramatically lower than those levels extracted from clay fractions (Appendix D).

Zinc like other selected trace metals showed maximum concentration in clay size particles from north Christiansen Basin. Maximum Zn was retained by clay size particles from station 91 (366 ppm) with stations 71 and 89A having the second and the third highest values of 359 and 185 ppm, respectively. Zinc was also associated with very fine, fine and medium sand, however its concentration was much lower compared to values retained by clay size particles (Appendix D).

Copper like other element was mostly retained by clay mineral surfaces. Cu again showed higher concentration in samples from north Christiansen Basin. The highest occurred again in clay faction from station 91 (230 ppm), the second highest value was associated with clay particles from station 89 south of Christiansen Basin.

Nickel concentrations in sewage sludge sediments were lower than those of Pb, Cu, Zn and Cr. When present, most Ni was concentrated in clay particles. Maximum level again occurred at station 91 north of Christiansen Basin with a mean value of 47.5 ppm. The second highest occurred at station 71 (28 ppm) and the lowest at station 89A (26 ppm). Ni was not detected in other particle size fraction except at station 91, where Ni was as low as 2 ppm in very fine sand.

Cadmium levels did not vary significantly within Christiansen Basin, but its concentration was the lowest among other trace metals studied. Cd unlike other metals was not detected in other particle size fractions. Maximum Cd again occurred in clay particles north of Christiansen Basin at station 91 (13.3 ppm). The second Cr level was found at site 71 with a value of 10.6 ppm. The minimum Cd concentration occurred at station 89A south of Christiansen Basin with a value of 6 ppm (Appendix D).

4.3.2.3. Near shore Mud-Patches

Analysis of near shore sediments showed that maximum trace metal concentrations were associated with clay size particles. As evident (Appendix D), the concentration of selected metals varied significantly with particle size. Lead concentration in near shore sediments was site dependent. Most of the lead was associated with clay fractions. For example, station 33-1 south of Jones Inlet had the highest mean value of 199 ppm with station 54A south of Long Beach and 7a and 56 following with means of 160 and 140 ppm, respectively. Pb content of these

three stations was not significantly different from each other. Station 7-1b showed the lowest concentration of 17 ppm. Pb also was extracted from other particle size fractions. For instance, station 7a showed a dramatic change of Pb level among various particle sizes. Maximum Pb occurred in clay particles (140 ppm) followed by very fine sand, fine sand and medium sand with mean of 33, 21, and 16 ppm, respectively. In general, the results showed that more than 50% Pb was associated with clay mineral surfaces.

Chromium was not uniformly distributed in clay of near shore sediments (Appendix D). Station 33-1 again showed the maximum concentration (127 ppm) with stations 7a and 54A having the second and the third highest values of 123 and 103 ppm, respectively. The lowest Cr concentration occurred at station 56 with a mean value of 39 ppm. Cr, unlike Pb, was not detected in other particle size fraction of the near shore sediments. With an exception at station 54A south of Long Beach, where 31 ppm Cr was retained by very-fine sand particles.

Not only did Zn vary significantly with site, but its values were also distributed differently among particle sizes of the same sample. For example, maximum Zn was retained by clay fraction, followed by very fine sand, fine sand and medium sand (Appendix D). The highest Zn concentration occurred at station 156 south of Long Beach with a mean value of 156 ppm. The second highest concentration occurred at station 33-1 south of Jones Inlet (151 ppm). The lowest Zn level (24 ppm) was associated with clay particles from trough mud-patches at station 7-1b. More than 50% Zn values like Pb, more than 50% Zn was concentrated in clay fraction from near shore sediments.

Copper concentrations did not vary significantly in clays of the near shore sediments, but it values varied among particle sizes. More than 50% Cu was enriched in clay sediments. Station 54A south of Long Beach showed highest Cu value of 91 ppm. The second highest level

occurred south of Jones Inlet at stations 33 and 33-1 with a value of 88 ppm, and 87 ppm, respectively. The minimum Cu content was associated by clay fraction collected from south of Long Beach Island at station 20A (10 ppm).

Nickel concentration unlike other elements was not detected in all samples. For instance, Ni was not detected in sediment samples from stations 20A and 56. Maximum Ni value occurred at station 7a (27 ppm) followed by the second highest (12 ppm) in both sediment samples from sites 54A and 33-1.

Cadmium was uniformly distributed among clays of the near shore sediment samples. Cd like Ni was detected only in clays. It values however, did not exceed 10 ppm in near shore sediments. For instance, maximum Cd occurred at station 54A (7 ppm). The second highest occurred at station 7-1b with a mean value of 6.6 ppm, and the third highest at station 33-1 (6 ppm). The minimum concentration was associated with sediment from site 7b (2.5 ppm) (Appendix D).

In general (see results), sediment trace metal concentrations within New York Bight environment are function of particle size, location, type of metal considered, trace metals input, and perhaps other parameters such as pH, Eh and hydrodynamics of the Bight.

4.3.3. Variability of trace metal concentrations in core AC 97-1 and AC 97- 9, summer 1997

Trace metal concentrations in core AC 97-1 sediments from sewage sludge and in core AC 97-9 sediments from mud dump site (MDS) are shown in Appendix D.

Core AC97-1: Lower concentrations of Pb, Zn, Cu, and Cr were found in different core intervals. Metal levels within the core ranged form 1.7 to 4.3 ppm Pb, from 8 to 12 ppm Cu, from 3.2 to 10 ppm Zn and from 1.6 to 8.6 Cr (Figure 15a & 15b). Ni and Cd were not detected throughout the core sections. The highest levels of selected metals were detected at depth

between 0-2cm (Figure 14a & 14b). Core AC 97-1, which is located within the preexisting sewage sludge dumpsite, shows low trace metal levels. Granulometrically, the core shows absence of clay fraction and dominance of clear fine to coarse-grained sand. This study showed that clay fraction plays an important role in the storage of trace metals; thereby the absence of clay fractions may explain low levels of metals in core AC97-1 of summer 1997. The dramatic decrease in trace metal concentrations can be also due to cessation of trace metal input at the sewage sludge dumping site.

By contrast, core AC 97-9 within DMS showed high levels of Pb, Cu, Cr, Zn, Cd and Ni at different depth intervals. The concentration levels for each metal did not vary dramatically with depth (Figure 16a & 16b). Levels of metals detected in core sections ranged from 54 to 174 ppm Pb, from, 12.3 to 17.3 ppm Cd, from 14 to 78 ppm Cu, from 70 to 230 ppm Zn, from 3.7 to 26 ppm Ni and from 3.1 to 32 ppm Cr. The core AC97-9, which is located within the Mud Dump Site (MDS), shows higher level of heavy metals than those extracted from core AC 97-1. The highest concentration occurred at 76-78 cm interval for Pb, at 5-6cm and 36-37cm intervals for Cu, at 78-88cm interval for Zn and Ni and at 5-6cm interval for Cr. Fluctuation of trace metal concentrations can be explained by variation in trace metal input during different periods of waste dumping. In addition to high level of trace metals, the granulometry of AC 97-9 as opposed to core AC97-1 is dominated by fine grained materials throughout the core intervals. The presence of this fine-grained materials (clays) play an important role in storing high level of metals, which in turns preserved the contaminant history in this studied area.

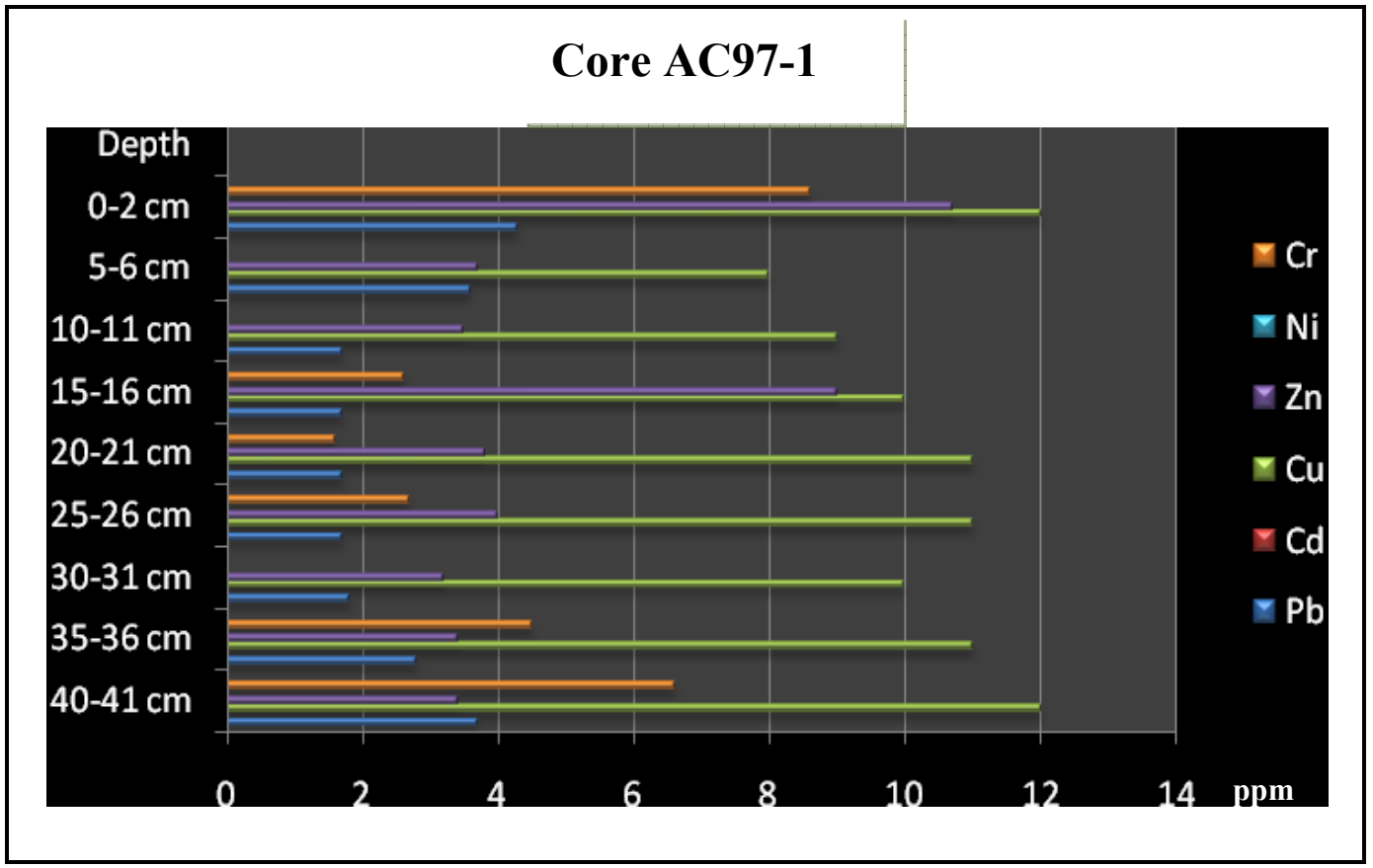

Figure 15a: Graphic representation of trace metal concentrations in core AC 97-1.

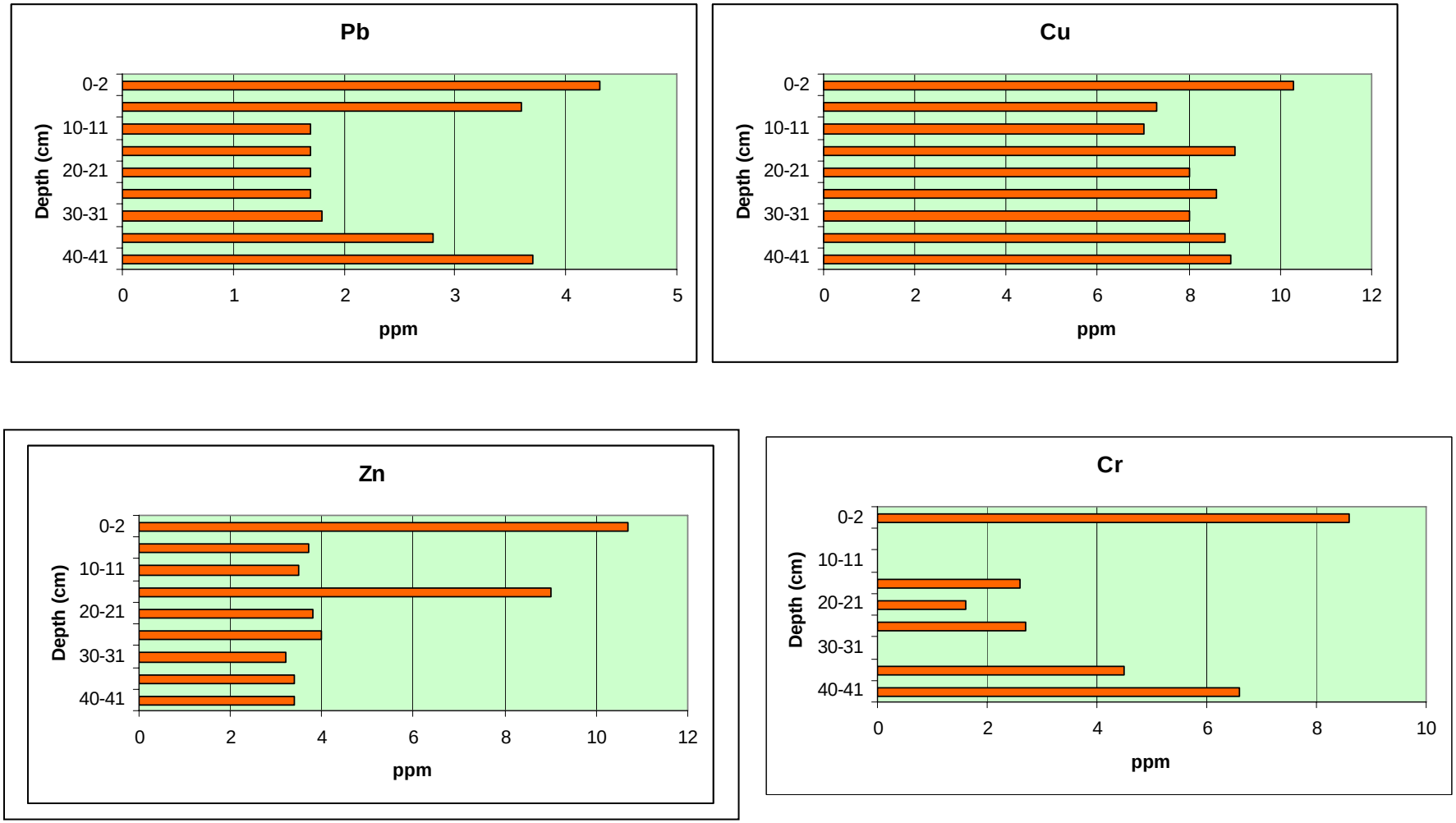

Figure 15b: Graphic representation of trace metal distribution in core AC 97-1.

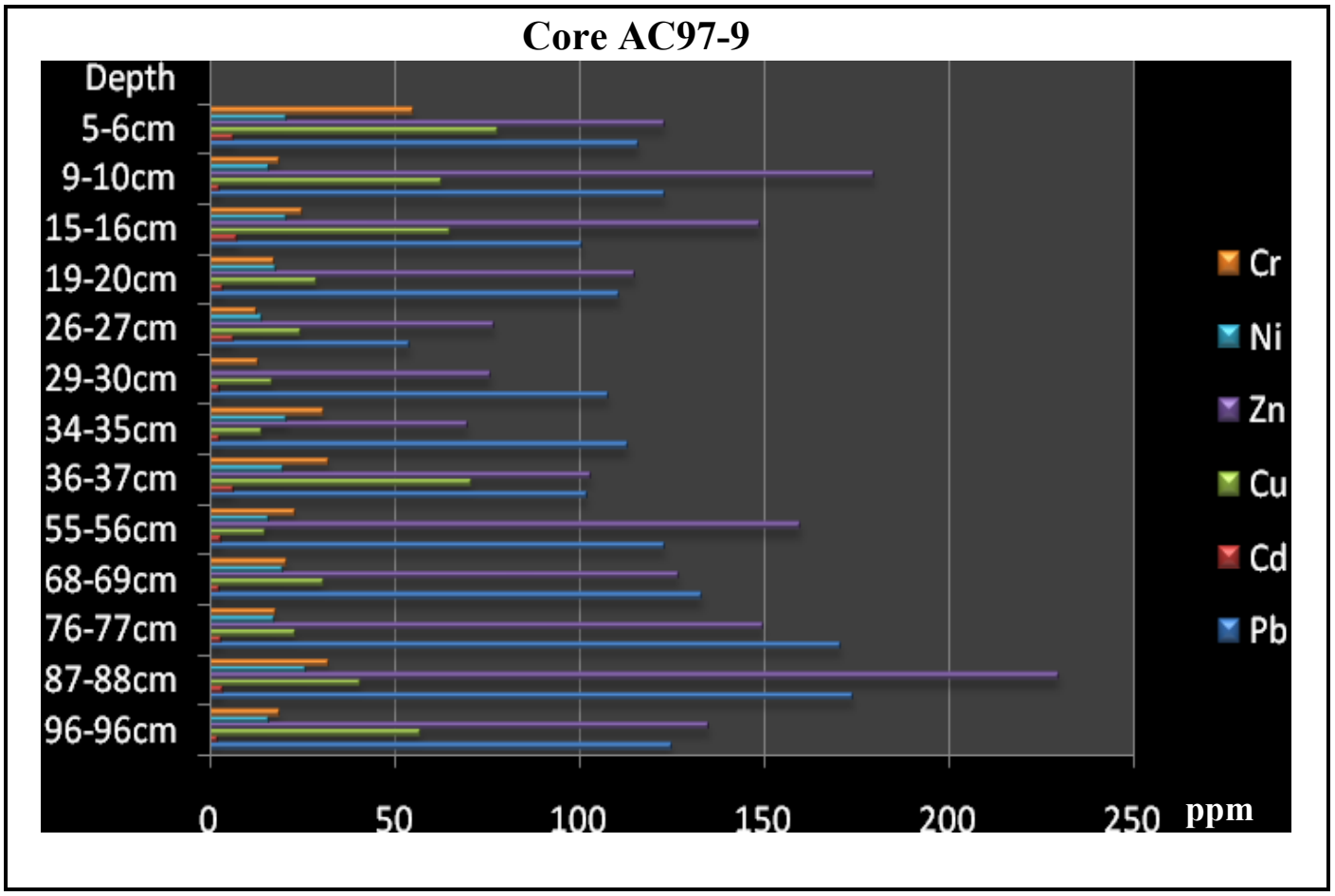

Figure 16a: Graphic representation of trace metal concentrations in core AC 97-9.

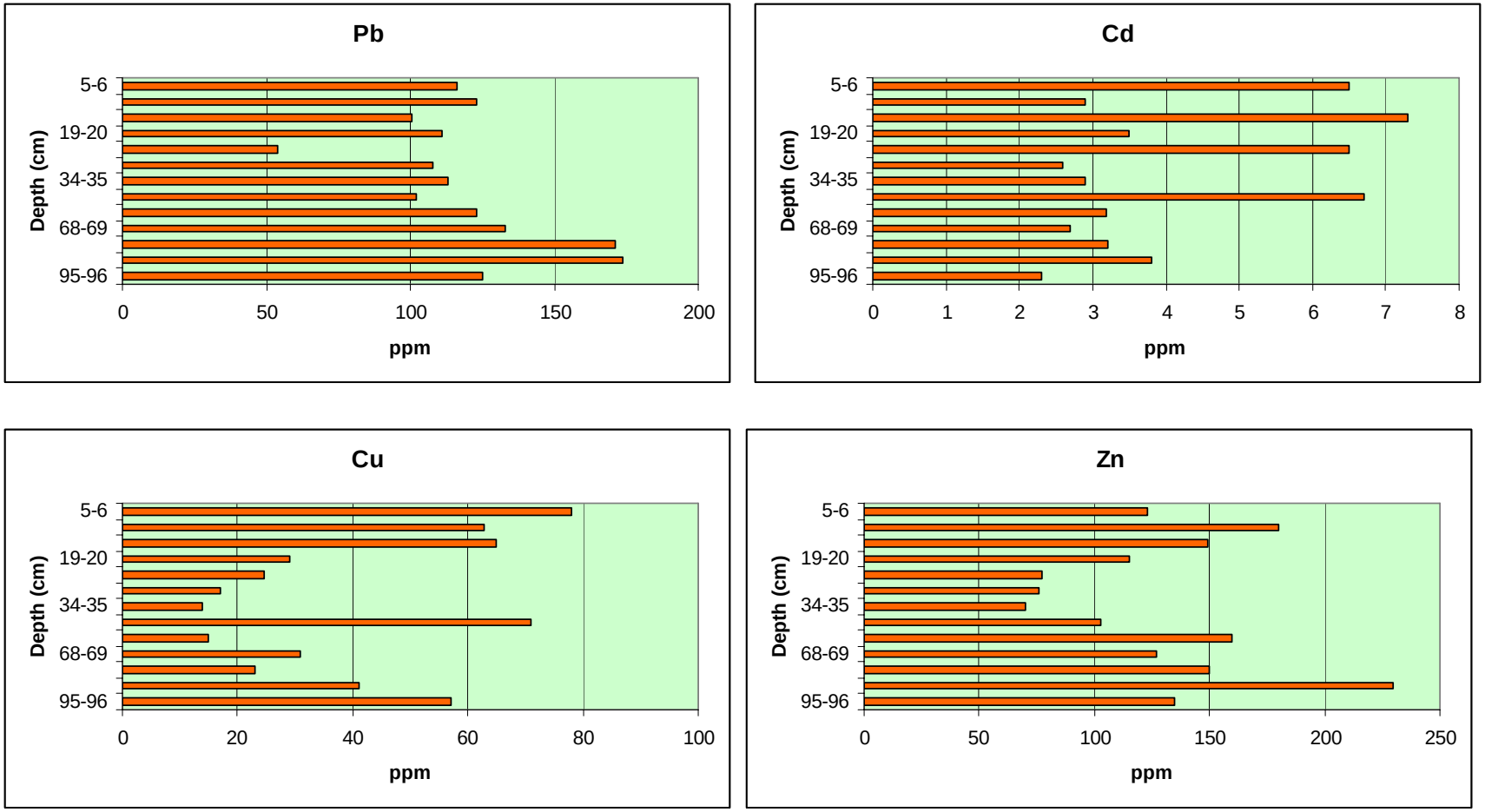

Figure 16b: Graphic representation of trace metal distribution in core AC 97-9.

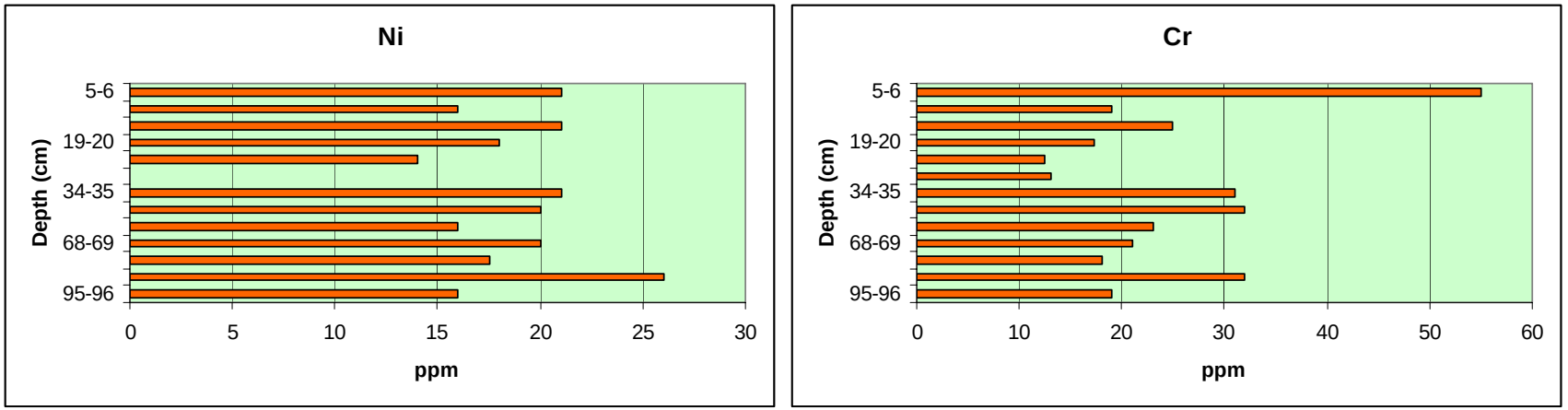

Figure 16b: Graphic representation shows trace metal distribution (ppm) in core AC 97-9 (continued).

4.3.4. Background Area (Controls)

Heavy metals concentrations in sediments from stations 158 and 53A (modern shelf sand), Hudson Shelf valley, and Holocene lagoonal clays from the near shore troughs south of Atlantic Beach were selected to present New York Bight Apex background values (Harris, 1976) . These sites were chosen as background , because 1) station 158 and station 53A located 20 miles southeast of the dumping region and south of Jones Beach, 2) sample from the Hudson Shelf valley, 110 miles from Ambrose Light, presumably seaward of any influence of the dumpsites in the bight apex. These stations were apparently unaffected by the dumping and 3) Holocene lagoonal green clays located 0.98 mile south of Atlantic Beach are younger than the freshwater peat stratigraphically below them which has been radiocarbon dated at 7,658 ± 83 yrs (Harris, 1982). These clays represent natural levels of metal concentrations in uncontaminated sediments prior to atmospheric nuclear weapon test in the early 1950's. They, thereby provide useful background data for metal contamination of the New York Bight fine-grained sediment. "Normal" trace metal concentrations in sediment uncontaminated by wastes are tabulated in Table 7.

Table 7: Comparison of background trace metal concentrations in sediments from the New York Bight

Location		Pb	Zn	Cu	Ni	Cr	Mn	Cd
Hudson Shelf Valley								
	(a)	18	35	8.8	9	8.4	45	ND
	(b)	14	20	6.7	8.2	6.4	-	-
	(C)	-	39	-	-	25	-	-
Southeast of dumping area								
	(a)							
1) 158		11.5	13	3.2	3	7.5	30	ND
2) 53A		10	9	2.8	2.5	5	34	ND
		(10.75)	(11)	(3)	(2.75)	(6.25)	(32)	ND
	(c)	0.12	4.9	-	-	8	34	-
Holocene								
Lagoonal clay	**(a)**	4	7	2	1.5	1.8	0.74	ND
	(c)	3.1	9	-	-	1.5	0.57	-

(a) This study **(b)** Carmody (1972**)** **(c)** Harris (1982) ND**:** not determined, average values in parentheses, -: not detected

4.4. Statistical Analysis of Trace Metals from the Apex of the NYB

Statistical Test for Normal Distribution

Graphically, a normal distribution curve is bell-shaped and symmetrical around the ordinate erected at the mean, which lies at the center of the distribution. The normal distribution plays a central role in statistical theory and practice. The test for normal distribution is helpful in that it determines which statistical procedure, parametric or non-parametric, can be applied in analyzing the data. If the statistical result yields normal distribution, then the parametric tests based on assumption about the distribution are used. A nonparametric or distribution-free test is used if a data set yields non-normal distribution. The statistical software JMP v.5.1.2 from the SAS Institute (2002), use the Shapiro-Wilk test (W) to test the data for normal distribution. The W value given by JMP test ranges from 0 to 1, with W = 1 indicating the normal distribution and the applicability of a classic parametric procedures. An important parameter of the normal curve is that we need to know only the mean (μ), which defines the location of the distribution on the x-axis and standard deviation (σ), which defines the dispersion or spread of the distribution to compute the entire distribution. The standard normal distribution occurs when $\mu = 0$ and $\sigma = 1$. However, in this study, the statistical analysis tests drawn from the plots (Figure 16) show a non normal distribution for all trace metals studied. As evident (Figure 16), the histograms with fitted line, Quantile plots, outlier box plot and the S-shaped normal Quantile plots all showed a skewed distribution.

Caption: Figure 17 shows both, histograms normally fitted and Quantile plots for each trace metal. The single vertical line within the box represents the median of the data. The center of the diamond displays the mean, and the width of the diamond indicates a 95% confidence interval for the mean. The parameters for the normal fitting and Quantile plots are μ (the mean), σ (standard deviation) and W (Shapiro-Wilk test). The solid straight line in each plot is a function of μ and σ of the trace metals data. These solid straight lines in normal Quantile plot is surrounded by solid curved lines, which stands for confidence interval (95%) limits for the distribution. When the trace metal is normally distributed the points will from a straight-line. Deviation from the line indicates non-normality.

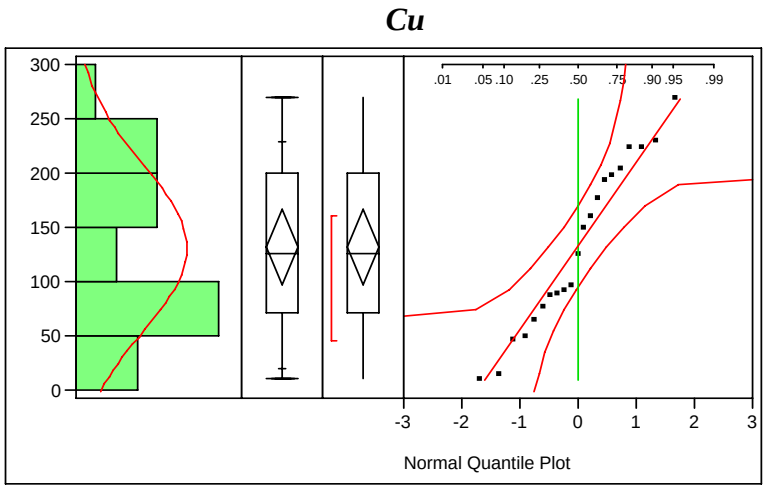

Normal (132.048, 76.975) Fitted Normal

Parameter Estimates

Type	Parameter	Estimate	Lower 95%	Upper 95%
Location	Mu	132.0476	97.00903	167.0862
Dispersion	Sigma	76.9750	58.89041	111.1572

Shapiro-Wilk W Test

W	Prob<W
0.950916	0.3545

Figure 17: Statistical Test for Cu Normal Distribution: The Quantile and Outlier Box Plots, Histograms and S-Shaped Normal Quantile plots.

Zn

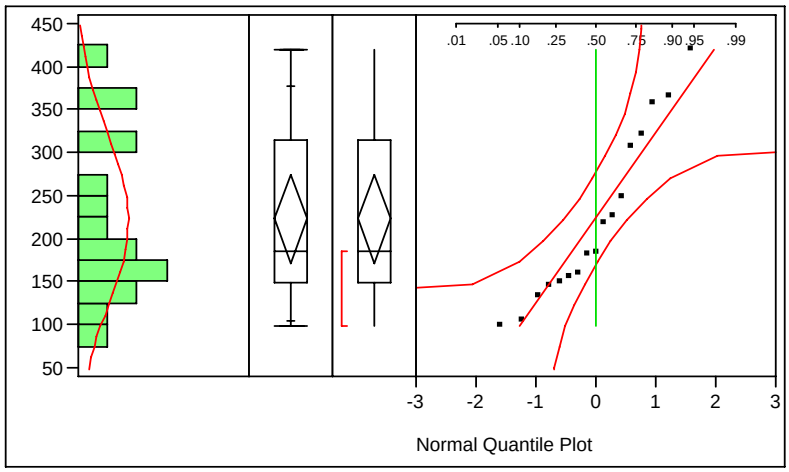

Normal (222.882, 98.5621) Fitted Normal

Parameter Estimates

Type	Parameter	Estimate	Lower 95%	Upper 95%
Location	Mu	222.8824	172.2064	273.5583
Dispersion	Sigma	98.5621	73.4061	150.0045

Shapiro-Wilk W Test

W	Prob<W
0.917311	0.1330

Figure 17: Statistical Test for Zn Normal Distribution: The Quantile and Outlier Box Plots, Histograms and S-Shaped Normal Quantile plots.

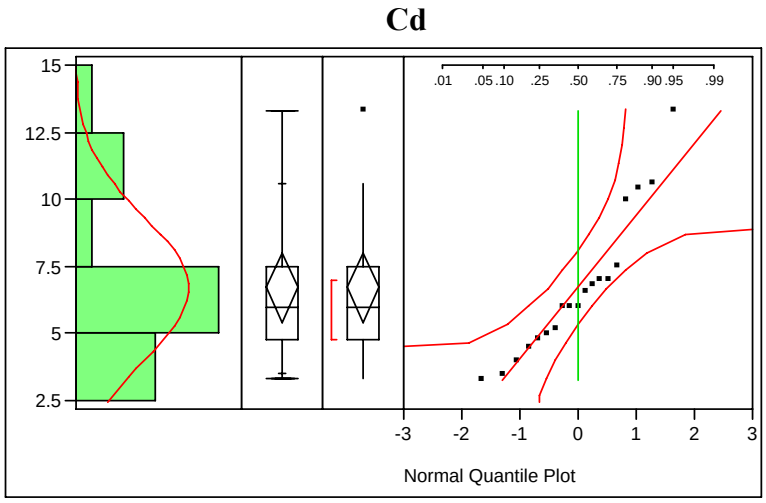

Normal (6.71053, 2.67018) Fitted Normal

Parameter Estimates

Type	Parameter	Estimate	Lower 95%	Upper 95%
Location	Mu	6.710526	5.423539	7.997514
Dispersion	Sigma	2.670184	2.017625	3.948734

Shapiro-Wilk W Test

W	Prob<W
0.909662	0.0730

Figure 17: Statistical Test for Cd Normal Distribution: The Quantile and Outlier Box Plots, Histograms and S-Shaped Normal Quantile plots.

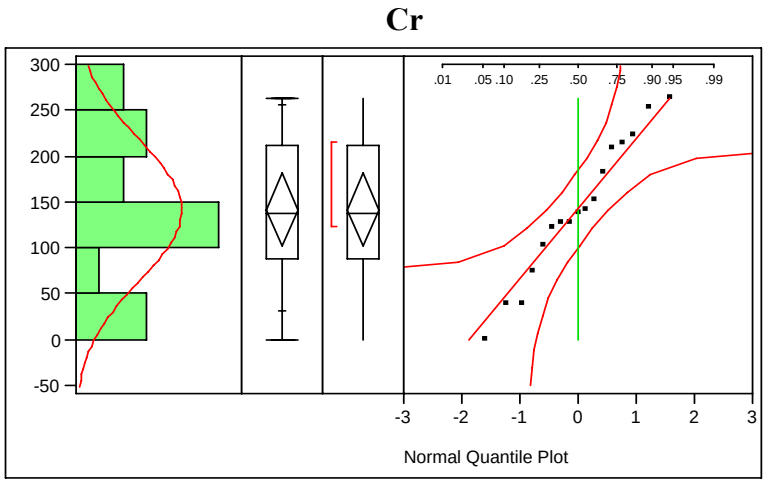

Normal (141.765, 76.4342) Fitted Normal

Parameter Estimates

Type	Parameter	Estimate	Lower 95%	Upper 95%
Location	Mu	141.7647	102.4659	181.0636
Dispersion	Sigma	76.4342	56.9259	116.3275

Shapiro-Wilk W Test

W	Prob<W
0.966624	0.7570

Figure 17: Statistical Test for Cr Normal Distribution: The Quantile and Outlier Box Plots, Histograms and S-Shaped Normal Quantile plots.

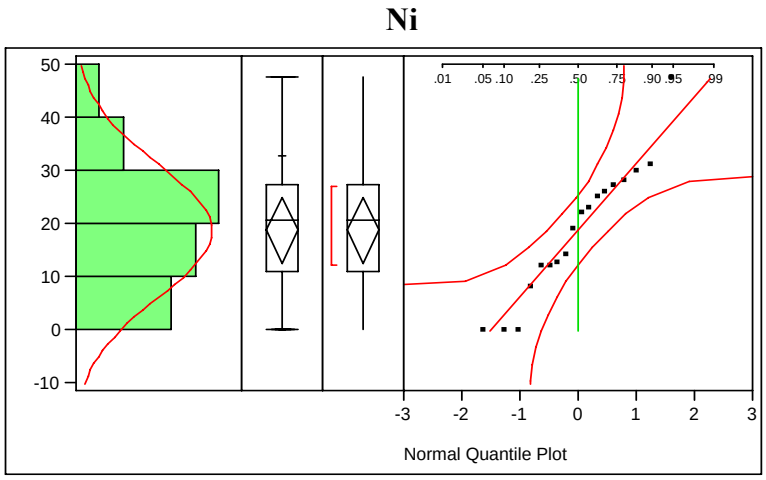

Normal (18.7222, 12.6028) Fitted Normal

Parameter Estimates

Type	Parameter	Estimate	Lower 95%	Upper 95%
Location	Mu	18.72222	12.45501	24.98944
Dispersion	Sigma	12.60278	9.45697	18.89338

Shapiro-Wilk W Test

W	Prob<W
0.948146	0.3967

Figure 17: Statistical Test for Ni Normal Distribution: The Quantile and Outlier Box Plots, Histograms and S-Shaped Normal Quantile plots.

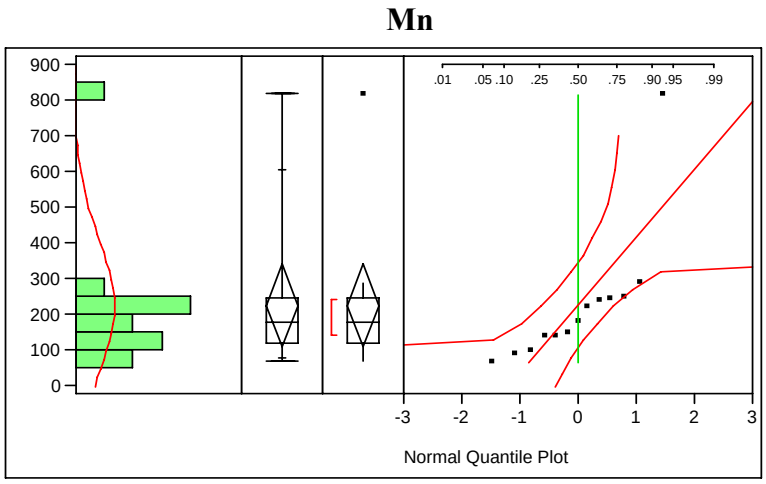

Normal (224.462, 190.765) Fitted Normal

Parameter Estimates

Type	Parameter	Estimate	Lower 95%	Upper 95%
Location	Mu	224.4615	109.1834	339.7396
Dispersion	Sigma	190.7650	136.7949	314.9024

Shapiro-Wilk W Test

W	Prob<W
0.656736	0.0002

Figure 17: Statistical Test for Mn Normal Distribution: The Quantile and Outlier Box Plots, Histograms and S-Shaped Normal Quantile plots.

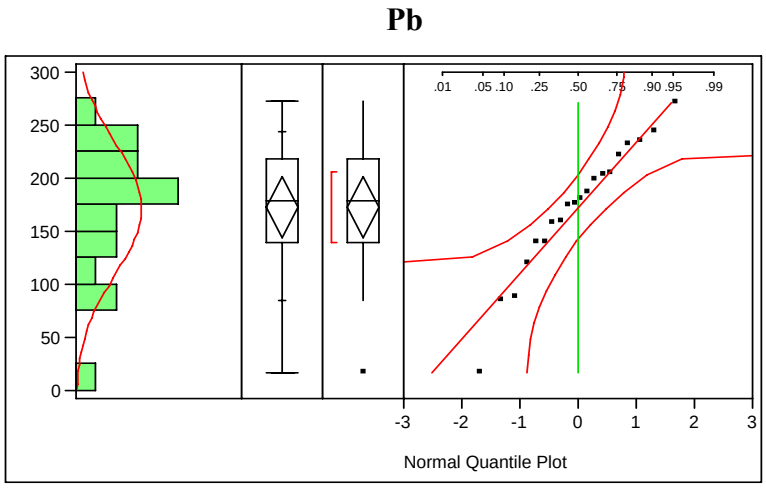

Normal (172.2, 61.7129) Fitted Normal

Parameter Estimates

Type	Parameter	Estimate	Lower 95%	Upper 95%
Location	Mu	172.2000	143.3175	201.0825
Dispersion	Sigma	61.7129	46.9321	90.1361

Shapiro-Wilk W Test

W	Prob<W
0.960656	0.5570

Figure 17: Statistical Test for Pb Normal Distribution: The Quantile and Outlier Box Plots, Histograms and S-Shaped Normal Quantile plots.

One-Way Analysis of Variance (ANOVA)

A central point is that One-Way Analysis of Variance (ANOVA)-literally a technique that analyzes or tests variances-provides us with test for the significance of the difference among the means. The sampling stations tested are grouped into three locations: Mud Dump Site (MDS), Sewage Sludge Dumpsite and near shore.

The results of analysis of variance and means of One-Way Anova by locations are shown in (Appendix E)**.** The trace metal is the continuous y variable, and locations are the nominal x variable. The horizontal line across the middle indicates the mean response of ANOVA by stations for all stations.

Mud Dump Site (MDS)

The spatial distribution of trace metals in MDS sediments are shown in Figure 18. Results of analysis of variance and means of One-Way Anova show significant difference between Pb, Cr, Cu, and Zn means, therefore spatial variation in these trace metals. The mean responses of One-Way Anova by station for all stations at MDS were 212.2858 ppm Pb, 203.8571ppm Cr, 192.8571ppm Cu and 262.7143ppm Zn (Appendix E).

Results of analysis of variance and means comparisons show no significant differences between Ni means, therefore no spatial variation in dredge spoil Ni (Figure 18). Except station 86.2, in general Ni was uniformly distributed in dredge spoil clay fraction. The mean of response of ANOVA by station for all stations at MDS was 20.71429 ppm (Appendix E). Results of analysis of variance and means comparisons show no significant difference between Cd means, therefore no spatial variation in Cd (Figure 18). The mean of response of ANOVA by station for all stations at MDS was 7.057143 ppm (Appendix E).

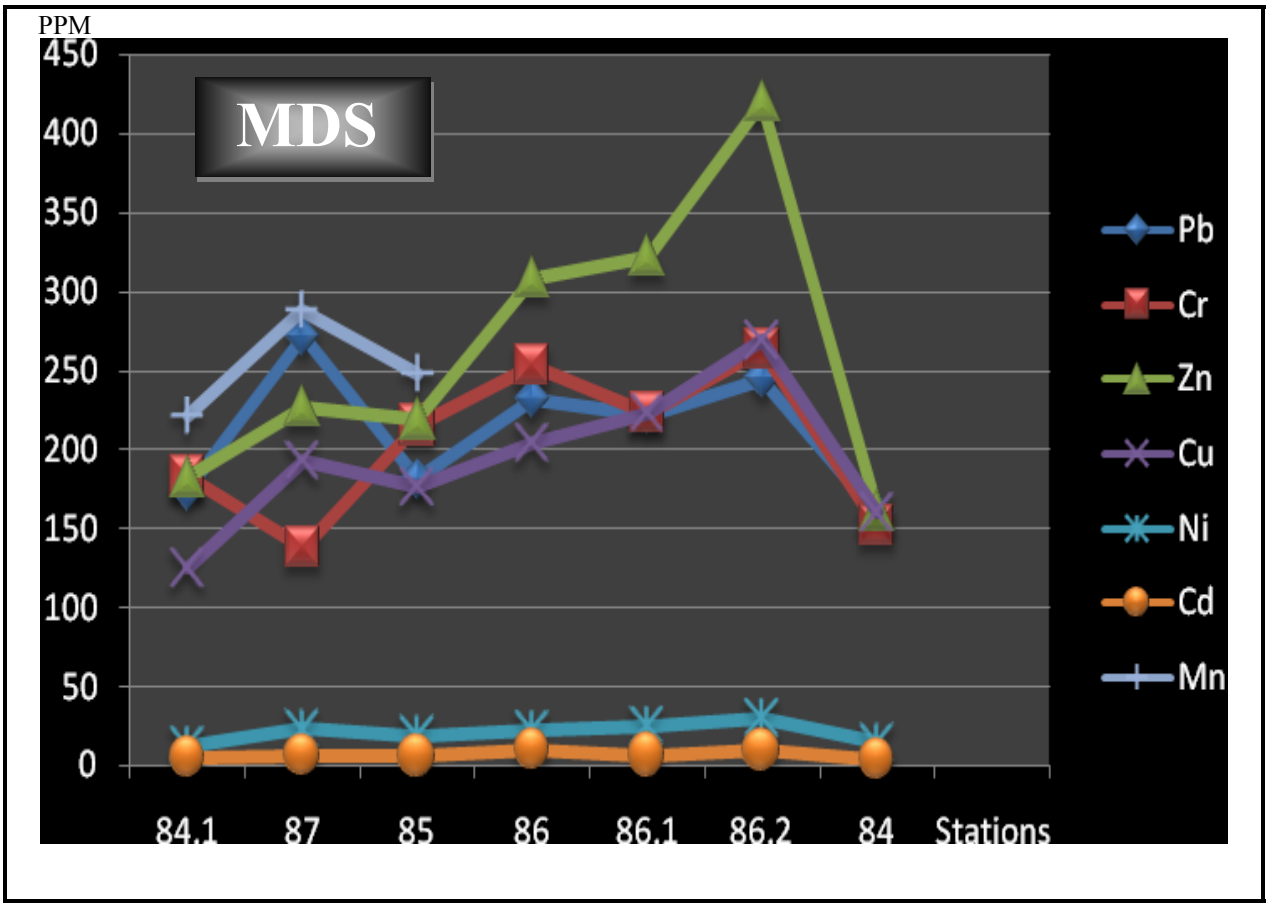

Figure 18: Variability of trace metals in clay fractions from MDS.

Nonparametric Correlations of Trace Metals

The statistical analysis shows a non-Normalcy for trace metals distribution (See section 4.4.) therefore, the non-parametric or distribution free procedure tests were applied. Unlike the normal distribution, which is based on assumptions, the non-normal distribution is free of assumptions and it is easy to carry out and understand. Furthermore, as it implied by the lack of underlying assumptions, the nonparametric procedures are applicable under a wide range of conditions. Many non-parametric techniques are in terms of the ranks or order rather than numerical values of the observation. An important parameter used to measure the degree of association between each is Pearson Correlation Coefficient "r". A correlation coefficient with a

value >+0.7 or <-0.7 represents a reasonably high degree of association. If there is an exact linear relationship between the two variables, the correlation is 1.000 or -1.000, depending on whether the variables are positively or negatively related. If there is no linear relationship, the correlation tends toward zero.

The correlation tests used in this study are: Pairwise correlation, Spearman's ρ (Rho) correlation and Kendall τ_b (Tau-b). The measures of association (correlation) between trace metals are shown in Appendix E. Table 8 shows well correlated trace metals in clay fractions from MDS. This strong association indicates that the geochemical behavior of these metals is similar at the MDS setting.

Table 8: Well correlated trace metals from MDS

Pairwise		Spearman's Rho		Kendall Tau-b	
Zn/Cu	0.9383	Zn/Cu	0.9643	Zn/Cu	0.9048
Cr/Zn	0.8132	Cr/Zn	0.7500	Ni/Cu	0.9048
Ni/Pb	0.7975	Ni/Pb	0.7857	Ni/Zn	0.8095
Ni/Cu	0.9746	Ni/Cu	0.9643	Cd/Zn	0.8095
Ni/Zn	0.9156	Ni/Zn	0.9286	Mn//Pb	1.000
Cd/Cu	0.7659	Cd/Cu	0.8571	Mn/Cu	1.000
Cd/Zn	0.8938	Cd/Zn	0.8929	Mn/Zn	1.000
Cd/Cr	0.7881	Cd/Cr	0.7500	Mn/Cd	1.000
Cd/Ni	0.7768	Cd/Ni	0.7500		
Mn/Pb	0.9370	Mn/Pb	1.000		
Mn/Cu	0.9239	Mn/Cu	1.000		
Mn/Zn	0.8926	Mn/Zn	1.000		
Mn/Ni	0.9644	Mn/Ni	1.000		
Mn/Cd	0.9938	Mn/Cd	1.000		

Sewage Sludge Dumpsite

The spatial distribution of trace metals in sewage sludge dumping site is shown in Figure 19.

Oneway Analysis of Variance (ANOVA)

Results of analysis of variance, means for Oneway ANOVA by station and means comparisons show no major significant difference between Pb means, thereby no spatial

variation in Pb (Figure 19). The mean of Oneway ANOVA by station for all stations in sewage sludge dumpsite was 201.8 ppm, which is slightly lower than the mean Pb in clay fractions from MDS (Appendix E).

Results of means for Oneway ANOVA by station show significant difference between Cu means, thereby spatial variation in Cu. The mean of Oneway ANOVA by station for all stations was 169.8 ppm (Appendix E) which is lower than the mean Cu in dredge spoil clays.
The mean of Oneway ANOVA by station for all stations was 204 ppm. Means for Oneway ANOVA by station show considerable difference between Zn means, thereby considerable spatial variation in Zn (Appendix E).

Results of means for Oneway ANOVA by station and means comparison show difference between Cr means, thereby spatial variation of Cr in clay fraction from sewage sludge dumpsite. The mean of Oneway ANOVA by station for all stations was 159.333 ppm which is lower than the Cd mean in clays of MDS (Appendix E). In general, except for station 91, Ni was uniformly distributed in sewage sludge dumpsite (Figure 19). The analysis of variance, means for Oneway ANOVA by station and means comparisons shows no significant difference between Ni means, thereby no spatial variation in Ni. The mean of response of Oneway ANOVA for all stations from sewage sludge dumpsite was 33.833 ppm, which is slightly higher than the Ni mean in clays from MDS (Figure 19).

The mean of response for Oneway ANOVA for all stations was 9.35 ppm which is slightly higher than Cd mean in dredge spoil clays. Means for Oneway ANOVA by station show no significant difference between Cd means in clay fractions from of sewage sludge dumpsite (Appendix E).

Mn concentrations were not uniformly distributed in sewage sludge area. Analysis of variance, means for Oneway ANOVA by station and means comparisons show significant difference between Mn means, therefore spatial variation in Mn (Figure 19). The mean of response of Oneway ANOVA for all stations was 126.25 ppm which is much lower than Mn mean in MDS sediments (252.333 ppm) (Appendix E).

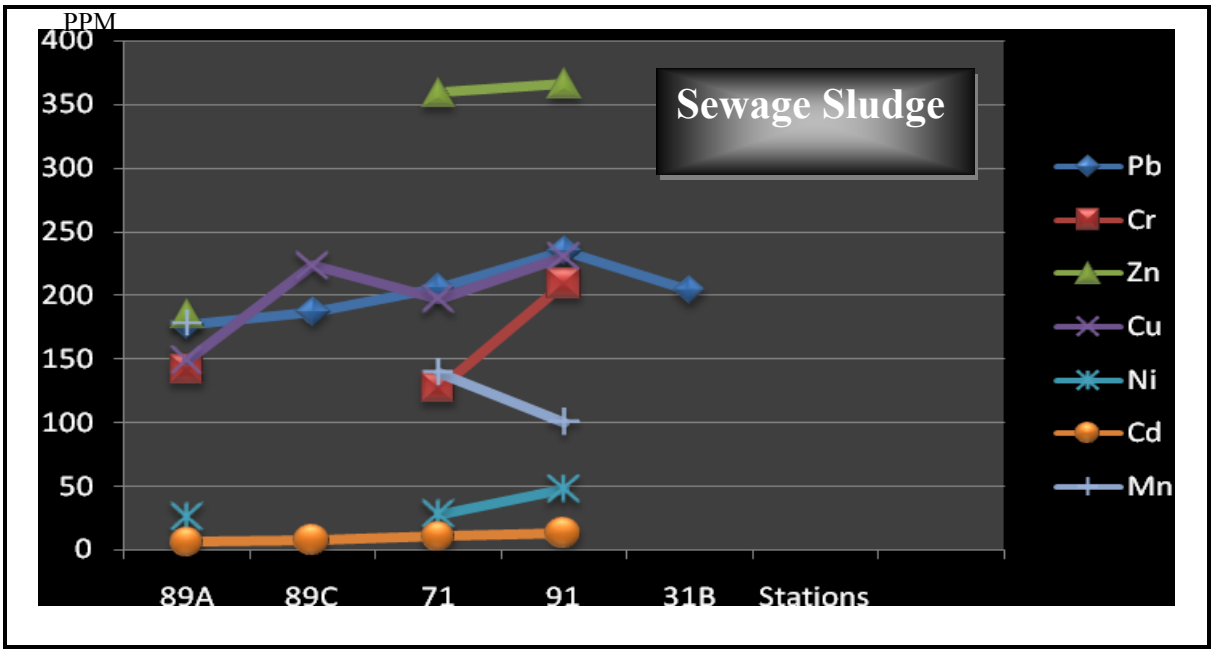

Figure 19: Variability of trace metals in clay fractions from sewage sludge dumpsite.

Nonparametric Correlations of Sewage Sludge Trace Metals

The selected trace metals (Pb, Cu, Ni, Zn, Mn, Cd and Cr) were further statistically correlated, using the Pairwise correlation, Spearman's Rho and Kendall Tau-b correlations (Appendix E). Table 9 shows the best degree of association between pairs of trace metals, which indicates that the divalent metals geochemically behave the same in the sewage sludge area of the NYB.

Table 9: Well correlated trace metals from sewage sludge dumpsite

Pairwise		Spearman's Rho		Kendall Tau-b	
Cr/Pb	0.7673	Cu/Pb	0.800	Cr/Zn	1.000
Cr/Zn	0.9705	Cr/Zn	1.000	Ni/Pb	1.000
Ni/Pb	0.9050	Ni/Pb	1.000	Ni/Cu	1.000
Ni/Cu	0.8547	Ni/Cu	1.000	Cd/Pb	1.000
Ni/Cr	0.9672	Cd/Pb	1.000	Cd/Ni	1.000
Cd/Pb	0.9904	Cd/Cu	0.8000	Mn/Pb	-1.000
Cd/Ni	0.8318	Cd/Ni	1.000	Mn/Ni	-1.000
Mn/Pb	-1.000	Mn/Pb	-1.000	Mn/Cd	-1.000
Mn/Cd	-0.9889	Mn/Cd	-1.000		
Mn/Ni	-0.9050	Mn/Ni	-1.000		
Mn/Cr	-0.7673				

Near shore Mud-Patches

The spatial distribution of trace metals in near shore muds is shown in Figure 20 The analysis of variance, means of Oneway ANOVA by station and means comparisons (difference in means) indicate a significant difference between the means of Pb, thereby a spatial variation in Pb (Figure 20). The mean of response of Oneway ANOVA by station for all stations was (120.5 ppm) (Appendix E).

Cu is not uniformly distributed in near shore mud patches (Figure 20). The analysis of variance, means of Oneway ANOVA by station and means comparisons (difference between means) indicate a significant difference between the means, thereby a significant spatial variation in Cu. The mean of response of Oneway ANOVA for all stations was 59.75 ppm (Appendix E).

Zn concentrations in near shore mud patches varied with site. ANOVA by station and means comparisons (difference between means) indicate a significant difference in near shore mud Zn concentrations, thereby a significant spatial variation in Zn. The mean of response of Oneway ANOVA by station for all stations in near shore mud patches was 116.2857 ppm (Appendix E).

The analysis of Oneway ANOVA by station and mean comparisons (difference in means) indicate a significant difference between the means, thereby a spatial variation in Cd. The mean of response of Oneway ANOVA by station for all stations was 4.8 ppm (Appendix E).

Cr showed same distribution pattern as other metals. ANOVA by station and means comparisons indicate as significant difference in Cr concentrations by area, thereby a spatial variation in Cr. The mean of response for Oneway ANOVA for all stations was 75.28571 ppm (Appendix E).

Ni showed similar distribution except station 7a where Ni is slightly higher (Figure 20). ANOVA by station and means comparisons indicate no significant difference between the means, Thereby no spatial variation in Ni. The mean of response of Oneway ANOVA by station for all stations was 11.9 ppm Ni (Appendix E).

The analysis of variance, means of Oneway ANOVA by station and mean comparison (difference in means) indicate a significant difference between Mn means, thereby a spatial variation in Mn (Figure 20). The mean of response of Oneway ANOVA for all stations was 300.8 ppm Mn.

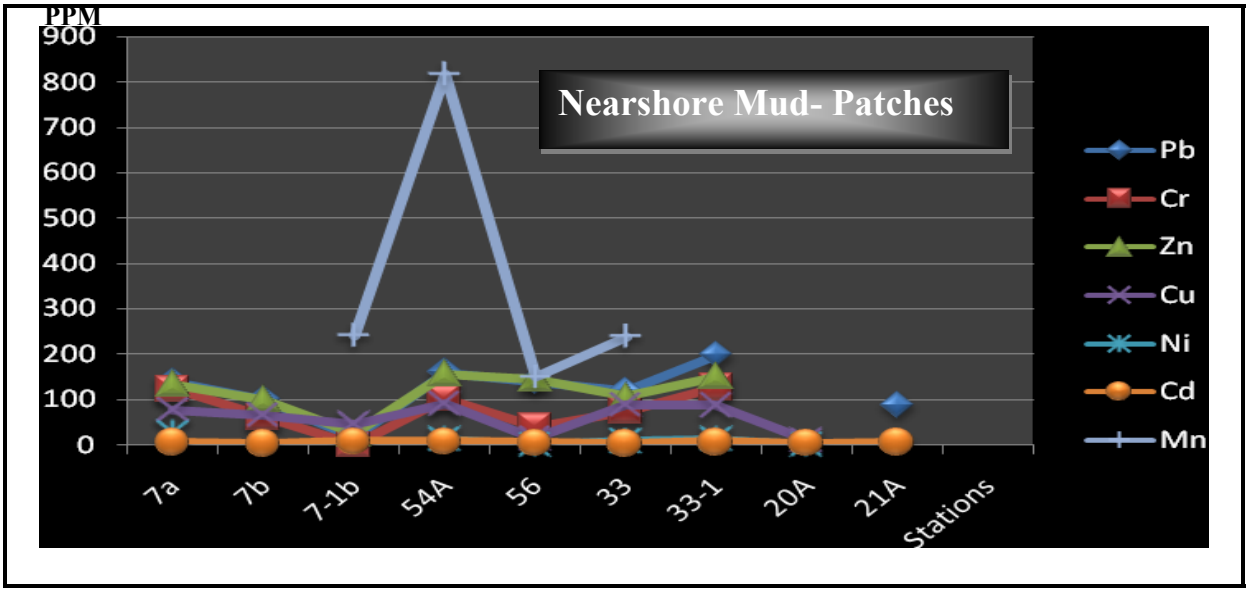

Figure 20: Variability of trace metals in clay fraction from near shore mud patches.

Metal-Metal Relationships in New York Bight Clay Fraction

All the trace metals in clay fractions from the apex of the NYB were subjected to multivariate correlations. Table 10 summarizes the strength of the linear relationship between each pair of trace metals in New York Bight clay fractions.

Table 10: Multivariate correlation of trace metals from the apex of the NYB

	Cu(ppm)	Zn(ppm)	Cd(ppm)	Cr(ppm)	Ni(ppm)	Mn(PPM)	Pb(ppm)
Cu(ppm)	1.0000	0.8163	0.7397	0.7891	0.8995	-0.2801	0.8076
Zn(ppm)	0.8163	1.0000	0.9407	0.5521	0.8541	-0.3861	0.7017
Cd(ppm)	0.7397	0.9407	1.0000	0.4921	0.8844	-0.1730	0.6467
Cr(ppm)	0.7891	0.5521	0.4921	1.0000	0.6783	-0.1975	0.5397
Ni(ppm)	0.8995	0.8541	0.8844	0.6783	1.0000	-0.3002	0.7156
Mn(PPM)	-0.2801	-0.3861	-0.1730	-0.1975	-0.3002	1.0000	-0.1809
Pb(ppm)	0.8076	0.7017	0.6467	0.5397	0.7156	-0.1809	1.0000

The value 1.000 in red color shows an exact linear relationship between the variables. The well correlated pairs of trace metals are shown in blue color. To help visualize the correlations, a scatter plot for each pair of trace metals is displayed in Figure 21. If each pair of trace metals was normally distributed, the density ellipse would enclose 99% data. In this case the ellipse collapses diagonally which means the geochemical behavior of the two metals is the same. If the ellipse was fairly round and was not diagonally oriented, the trace metals would show no correlation, which indicates the distortion of the geochemical behavior the two variables.

When trace metals of New York Bight are grouped and correlated together, they give strength and better picture of how these metals are related. Mn was not correlated to none of the trace metals (Table 11). Over all, trace metals did not show a strong degree of association based on Pairwise, Kendall Tau b and Spearman's Rho correlations. However, the trace metals that show a strong degree of association are shown in Table 11. The weak relationship between trace

metals in the NYB environment may indicate different trace metal sources or different chemical reactivities between clay and trace metals.

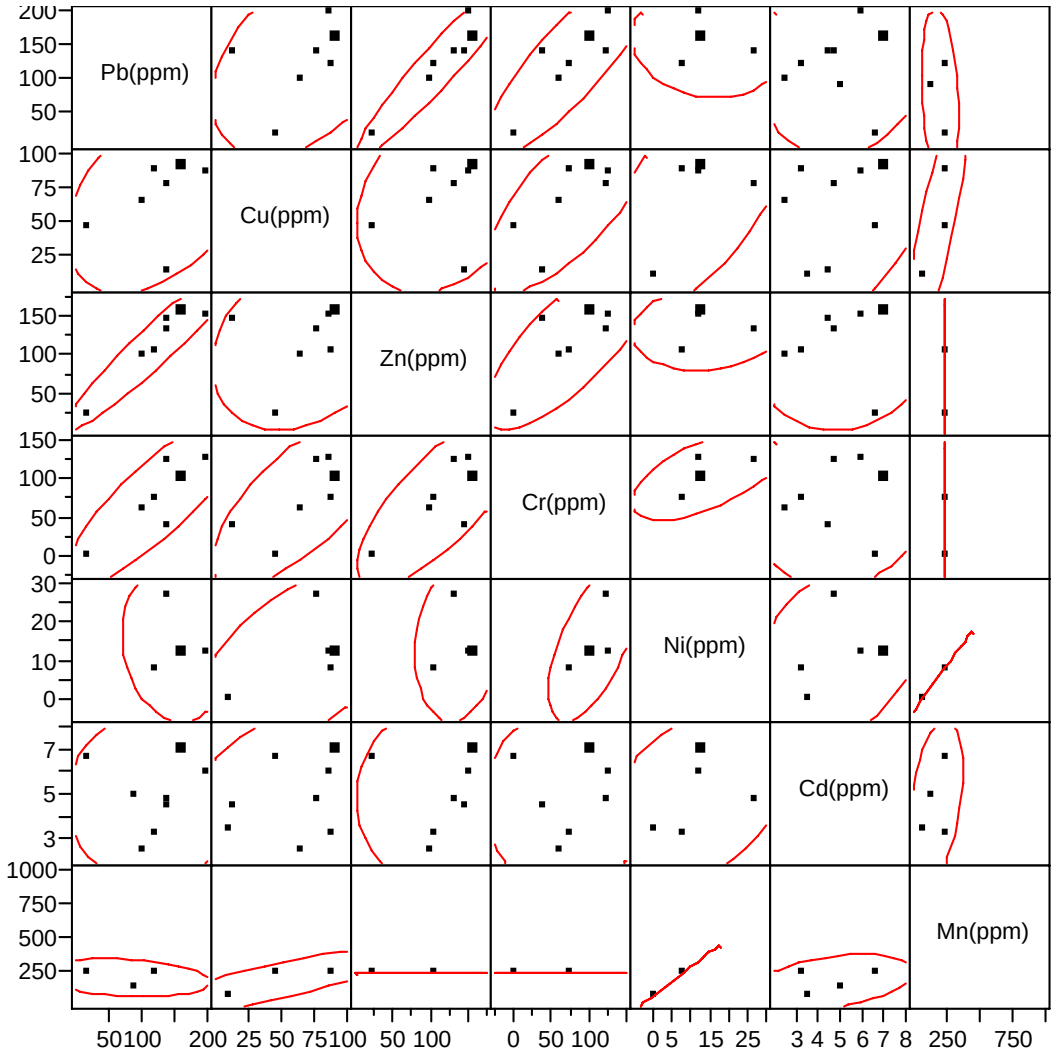

Figure 21: Bivariate scatter plot of trace metals in clay fractions from the apex of the NYB.

Table 11: Well correlated pairs of trace metals from the apex of the NYB

Pairwise		Spearman's Rho		Kendall Tau-b	
Zn/Cu	0.8671	Cd/Zn	0.7542	Zn/Cu	0.7941
Cd/Cu	0.7016	Cr/Cu	0.8454		
Cd/Zn	0.8400	Cr/Zn	0.7043		
Cr/Cu	0.8485	Ni/Zn	0.7373		
Ni/Cu	0.7149	Ni/Cd	0.7317		
Ni/Zn	0.7189	Pb/Cu	0.7428		
Ni/Cd	0.8016	Pb/Zn	0.7664		
Pb/Cu	0.7151	Pb/Cd	0.7381		
Pb/Cr	0.8017	Pb/Cr	0.7802		

CHAPTER 5

Discussion

5.1. Sediment Particle Size

The sediments samples of summer 1976 from the study area consist predominantly of sand followed by clay-silt fractions. Gravel size particles are mostly absent in all samples. When they are present, the grains consist of anthropogenic debris. The clay-silt fractions are not distributed uniformly among the New York Bight sediments. The highest concentrations of clay fraction occurred in low energy environment north and south of the Christiansen Basin. Clay-silt fractions were also present in MDS samples and near shore mud-patches. The distribution of sediments in this aqueous environment is a function of location, topography or bathymetry of the sampling area. For instance, the samples from near shore (south of Long Beach, south of Jones Inlet, south of Atlantic Beach) are characterized by coarse sand, medium sand, and small amount of very coarse sand and clay-silt fractions. The samples located within the Christiansen Basin, and samples from MDS and Cholera Bank are finer material, which consisting mostly of fine sand, very fine sand and clay-silt fractions. The most abundant sediment for the majority of the samples is fine sand, medium sand and very fine sand. The average mean sediments size is 2.33 Phi which represent fine sand. The standard deviation also shows that the samples are fine sand and medium sand. The majority of samples are moderately well sorted, moderately sorted and well sorted. Negative skewness characterizing most of the samples indicates predominance of sand over clay-silt fraction. Some of the sediments are characterized by positive skewness, which mean there is excess of clay-silt fraction. Negative skewness indicates that the depositional environment of these New York Bight sediments is predominantly high energy; where clay-silt

fraction can be easily removed. In contrast, positive skewness is characterized by low energy, where silt and clay can be deposited. This indicates that the New York Bight environment is characterized by both high and low energy, where sediments are greatly influenced by currents and storms. The cumulative-distribution curves for the sample studied shows that the dominant population in the NYB system is suspension. The suspension due to currents and storms is therefore the main sediment transport and therefore, contribute to the accumulation of clay-silt fraction in low energy environment. The suspension population in NYB environment is well developed for all the curves, which indicate again that the depositional environment is predominantly suspension due to storms. For instance, the cumulative-frequency distribution of the particle sediments from the site 91, 89A, 63, 71, 63-1 and 86 shows well developed suspension population, which indicate that the distribution of finer materials resulted from the deposition carried in suspension. Generally, the past dumping, the anthropogenic debris has changed the morphology of the Bight, and the natural granulometry, mineralogy and textural properties of its sediments.

Surficial sediments, sediment transport and large-scale morphologic features within the New York Bight have been previously mapped and discussed by numerous authors (Duane et al., 1972; Swift et al., 1972; Swift et al., 1973; Schlee, 1973; Williams and Duane, 1974; Mc Kinney et al., 1974; Schlee and Sanko, 1975; Harris, 1976; Swift et al., 1976; Williams, 1976; Swift and Freeland, 1978; Figueiredo et al., 1981; Swift et al., 1981; Vincent et al., 1981; Parker et., 1982; McBride et al., 1991; Rine et al., 1991; Trowbridge, 1995; Dalrymple and Hoogendoorm, 1997; Goff et al., 1999 and Butman et al., 2003).

In the New York area, massive discharges in the surf zones of the Long Island and New Jersey coasts move toward the New York harbor mouth; these discharges have built Sandy

hook and Rockaway spits within subhistoric to historic times (Swift et al., 1971). Sediment transport in the New York Bight is dominated by storm events when wave activities close to the bed, associated with the mean currents, produce the conditions under which bedload and suspended Load transport can occur. As consequence, the surficial sand sheet of the shelf floor bears a ridge and swale topography of sand ridges up to 10 m high and 2-4m apart (Swift et al., 1971). Sand ridges are created in the near-shore ridges zone, most probably by storm generated, southward-directed along shore currents (Swift and Field, 1981; Figueiredo et al., 1981; Towbridge, 1995). A detailed study of sand ridges morphology on the US Atlantic shelf can be found in (e.g., Swift et al., 1972; Duane at al., 1972; McKinney et al., 1974; Swift et al., 1978; Swift et al., 1981; Figueiredo et al., 1981; Stubblefield et al., 1984a; McBride and Moslow, 1991 and Goff et al., 1999).

Data from near-bottom currents in the New York Bight (Vincent et al., 1981) suggests that, suspended fine-sediment transport rates are higher in magnitude than the bedload transport but suspended transport is not though to dominate the total transport. Medium sands which form the surficial sediment of the New York Bights shelf are seldom moved by suspended transport except in shallow water (< 10m) or during intense storms. Vincent et al.data (1981) show that down valley transport events, which occur less frequently than up-valley events, are associated with coastal set-up and southwestward currents along the shelf, but also occur during quiet periods when there is little other transport event in the area. The NYB acts as a sink for the general net southwestward transport for sediment along the shelf. Sediment transport on any continental shelves is dominated by resuspension during energetic wave events (Butman et al., Lyne et al., 1978, Drake and Cacchione, 1985). Once resuspended, clay-silt associated with toxic elements can be transported by currents within the New York Bight to occupy low energy

settings. Conditions are optimum during winter-spring for sediments resuspension as a result of energetic events (Drake, 1984). During the stratified conditions of summer as a result of reduced waves and currents action, fine materials settle down forming mud patches along Long Island shoreline (Harris, 1982). Bathymetric depression usually characterized by reduced waves and currents action, such as Christiansen Basin and the area east of Cholera Bank favor the deposition of fine–grained materials.

Suspended sediments in the New York Bight system are exchanged between the Hudson estuary, the NYB Apex, Christainsen Basin and the Hudson Shelf Valley (Young et al., 1985). Previous studies noted that the Christiansen Basin shows sludge accumulation, which agree with high trace metal levels (this study).

In 1999-2000 when Butman et al measured the currents and sediment transport along the axis of the shelf valley and about 26 km on the adjacent shelves offshore of New Jersey and Long Island, New York. Currents and sediments transport were coherent over tens of kilometers during both-up valley and down-valley, and usually aligned with the axis of the shelf valley. Up valley transport coincided with times of winds from the northwest, low wave energy, and high current velocities (20-40 cm/s), and sea-level set down at the coast. Downvalley (off-shore transport was associated with energetic waves, wind from the east, moderate currents velocities (5-10 cm/s), and sea level setup at Sandy Hook, New Jersey. Butman et al (2003) concluded that the process observed (upvalley transport) during the winter of 1999-2000 would dominate transport throughout a typical year.

Waste disposal is the most critical environment issue in the New York Bight with regular dumping of sewage sludge, dredge spoil, chemical waste and construction rubble. Many of contaminants became adsorbed by mineral surfaces and transported with these mineral solids.

Knowledge of the transport paths and speed transport of the contaminated sediments is therefore important if environmental policy makers are to asses the ultimate destination of such contaminated materials. The fact that clay-silt fraction concentrate most of trace elements (this study), can be used to trace the dispersion pattern and the mobility of dumped waste and even possibly to locate the potential sources of trace metals and perhaps other aqueous species in the NYB system. Insights gained from this study are therefore essential to environmental managers.

5.2. Trace Metal Extraction from Different Particle Fractions

The laboratory extraction procedure was used to approximate, however crudely, the severest conceivably naturally occurring biochemical conditions, without completely degrading the sediments. But several samples were totally dissolved by $HF/HClO_4/HNO_3$ to see whether any significant amounts of the heavy metals were still retained in the silicate structure. The extraction of trace metals by a single 50% HNO_3 leach helps establish the strength with which trace metal are bound to mineral surface. Significant level of trace metals were released by a single 50% HNO_3 leach. All Cd and Ni associated with clay fractions were released from mineral surfaces. The $HF/HClO_4/HNO_3$ digestion of several samples showed no remaining Cd and Ni in the clay fraction. This suggests that the mobility of labile Ni and Cd from clay surfaces is relatively the same and therefore, total dissolution of sample is not necessary for the decontamination of these fine-grained materials.

The mobility of Pb, Zn, Cu, Cr and Zn from mineral surfaces varied significantly. Not all trace metal levels were leached by 50% HNO_3. This suggests that these metals may behave differently under the same environmental conditions. For instance, 50% HNO_3 extracted most of Pb from solid surfaces. The total acid digestion of several samples showed that less that 26 % Pb was still bound to mineral surfaces. Like Pb, most of Zn levels were extracted by 50% HNO_3

leach. The total acid digestion suggests that the remaining Zn is probably strongly bounded to mineral structure. Even though Zn and Pb levels differ, these two elements behave similarly when mineral solids were chemically reacted with 50% HNO_3.

A single 50% HNO_3 leach was not efficient in extracting all Cr from mineral surfaces. This suggests that more Cr levels were still firmly bound to mineral solids. This was confirmed by the fact that more chromium was dissociated from mineral solids when samples were totally digested by a combination of $HF/HClO_4/HNO_3$. When concentration of Cr was low, the 50% HNO_3 leach was efficient of extracting all Cr levels. This may explain that Cr is weakly bound to mineral surface when its levels were low. In contrast, when Cr content was high, some of Cr was strongly bounded to mineral functional groups. This finding may explain that the mobility of Cr from mineral solids may depend on its concentrations. In general, more than 50% Cr was released by 50% HNO_3 in acid solution without degrading the mineral structure.

Copper like Zn, Cr and Pb was not totally released in solution by 50% HNO_3 leach. This suggests that some Cu remains bound to mineral solids. Therefore, the total digestion is necessary for the decontamination of these fine-grained sediments.

Manganese was poorly leached by 50% HNO_3. More than 50% Mn was still bound to mineral solids. This suggests that most of Mn is strongly bounded to mineral functional groups. The total digestion is recommended for the decontamination of these fine-grained sediments that may contain Mn oxides..

From these results we can say that labile metals, those extracted easily can be assumed readily available for marine life and therefore enter the food- chain. These labile metals leached by 50% HNO_3 can be considered environmentally active. By contrast those metals that were strongly or remain bounded to mineral solids are environmentally inactive and cause no harm for

marine life or other living organism residing in such aqueous environments. If the environmental conditions (parameters) were the same as those of 50% HNO_3, then more than 50% of trace metals would be released in the aqueous environments. If this is the case, then any conditions (chemical, biological, and physical or a combination of all) that mimic the 50% HNO_3 leach will initiate the disturbance of fine-grained sediments. This disturbance will then be marked as a Chemical Time Bomb (CTB). A CTB is a chain of event resulting in the delayed and sudden occurrence of harmful effects. This happens when contaminants such as trace metals or other pollutants stored in sediments are mobilized as a consequence of alteration of certain environmental conditions.

The trace metals investigated in this study, whether they were leached by 50% HNO_3 or released by totally acid digested showed that all the trace metals with no exception were concentrated in clay fraction regardless of their location. When trace metals were detected, they showed that their concentrations decreased dramatically with increasing particle size. For instance, Pb, Cu, Zn, and Cr showed the same distribution. Their concentrations, however, were distributed unevenly among different particle sizes. The highest trace metal concentrations occurred in clay fractions and the lowest occurred in medium sands. Some of the trace metals were completely absent in some of the sand-sized particles. In contrast, Ni and Cd were concentrated only in clay fraction. With an exception, Ni also occurred in very fine sand at station 91 where Ni was maximum. Ni was also detected in very fine sand at station 89A. Like Ni, Cd also was detected in very fine sand at station 89A. Not only trace metals varied as a function of particle size, but also varied considerably between them of which Cd was the lowest one followed by Ni.

Since Cd and Ni were the lowest concentration, this may explain that clay fractions were good enough for retaining all Cd and Ni at their chemically reactive sites. When Ni and Cd levels were high, some of these elements were retained by very fine sand. This suggests that all clay surfaces were probably occupied by other trace elements. Therefore, the remaining Cd and Ni were chemically attached to very fine sand. This also explains that very fine sand possesses reactive sites and capable of adsorbing some amount of these trace elements. Pb, Cu, Cr and Zn showed high concentrations in clay fractions, but occasionally these trace elements also were found to occur in sand sized particles. These trace elements tend to compete with each other for reactive sites located at mineral surfaces or within the minerals structure. When all the reactive sites are occupied by trace elements, the remaining level of metals was distributed among other sand-sized particles. These finding showed that, clay fractions are the main scavengers of trace metals and therefore, play an important role in their storage and mobility within the NYB environment.

5.3. Importance of Clays in the New York Bight Environment

Clay fractions are important in the New York Bight system. Even though the percentage of these fine-grained particles is low, they play a commanding role in the regulation of the aqueous species.

This study shows that most of trace metals analyzed from the apex of NYB were concentrated in clay fractions whatever their location. Because clay particles have high surface area and chemically reactive sites therefore, they are scavengers for trace metals. These aquatic clay particles constitute the most important reservoir or sink for metals and perhaps for other pollutants. It is important to understand the type of clays present and their chemical reactivity with trace metals. A general summary of clay mineral structures is given in Appendix F.

Typically clays are sub-microscopic crystallites and belong to the group of silicate minerals known as layer silicates. These layers silicate are composed of well-defined sheets of linked silica tetrahedral and hydroxide octahedral. It is the combination of these sheets into various types of layers that distinguishes the major groups and impart to them of their characteristic chemical and physical properties (Grim, 1968). Small particle sizes and unique crystal chemistry also give the clays a high surface-charge density to mass ratio (Grim, 1968). Their reactions with natural waters are therefore relatively rapid (Sposito, 1989; Stumm, 1992; Stumm et al., 1996; Langmuir, 1997). Whether clay minerals, in particular mixed-layer clay, can attain thermodynamic equilibrium in low-temperature environments has long been controversial issue (cf. May et al., 1986; Aja and Rosenberg, 1992). Clay minerals exhibit reactive functional groups. The most important functional groups are the hydroxyl group (OH) exposed on the outer periphery of a mineral and the siloxane surface formed by the basal planes of the tetrahedral sheet (50% layer silicates) or the basal planes of the tetrahedral sheets and hydroxyl plane of the octahedral sheet (2:1 layer silicates). The hydroxyl (OH) group is found on phyllosilicate, on amorphous silicate minerals, and on metal oxide, oxyhydroxide, and hydroxides. The two types of edge-surface hydroxyl groups, which are often distinguished by the names aluminol and silanol. Kaolinite has these properties. Smectite minerals have larger percentage of siloxane ditrigonal cavities when compared to hydroxyl groups. The hydroxyl sites are very reactive, in that there a proton from the adjacent solution may be accepted or removed from the mineral surface (Sposito, 1989; Stumm, 1992; Stumm et al., 1996; Langmuir, 1997). Because of these reactions, a mineral's net charge can change sign from positive to negative with increasing pH. Thus, these surface sites are pH dependents. In contrast, the reactivity of siloxane cavity depends on the nature of the electronic charge distribution in the layer silicate structure. These

surface functional groups-hydroxyl group and siloxane ditrigonal cavities can behave as Lewis acids or Lewis bases. Therefore they have the ability to adsorb ions (cations and anions), thereby form surface complexes. The hard soft acid base principle (HSAB) states that hard Lewis acids prefer to complex or react with hard Lewis bases and soft acids prefer to complex with or react with soft bases. Most cations are Lewis acids and most anions are Lewis bases. In this study the cations (Lewis acids) will complex with the reactive functional groups of clay minerals (Lewis bases). The reactivity of clay minerals with cations can either form an inner-sphere complex (stable unit) or an outer-sphere complex (not very stable). The surface reactivity of clay minerals thereby plays critical roles in regulating the transport of a variety of aqueous species of the New York Bight system.

The XRD analyses of the oriented specimens revealed the occurrence of clay minerals in <4μm fraction of all selected samples. Illite phase dominated all the samples in the NYB environment (Figure 12). The second and third major mineral phases were chlorite and kaolinite. By contrast, mixed layer illite/smectite phases were detected only in some samples, especially at sit 7-1-2 south of Long beach. These clays are chemically reactive with a significant unsatisfied surface charge, which in turns make them potential sorbents for dissolved species. The geochemical analysis and the XRD analysis have advanced our understanding of the importance of clay minerals and their behavior in the New York Bight system. It is the presence of illite, chlorite and kaolinite of the clay fractions that play a major role in sorption of trace metal dumped in the NYB marine environment. Therefore, the regulators or policy makers should have an understanding of 1) the mineralogy of clay fraction, 2) the interaction of clay and aqueous species, and 3) the hydrodynamics of the system. Understanding the reactivity of clays and trace metals and the processes that resuspend and distribute them are of great importance in tracking

the dispersion pattern and the fate of pollutants introduced into any aqueous environment like NYB system.

The geochemical analysis of sediment from the NYB environment showed that trace metal concentrations were unevenly distributed among the dump sites. The highest concentration of heavy metals during active dumping (summer 1976) was found in the dredge spoil sediments (Mud Dump Site). The range of concentrations in (ppm) found in this dumping site was: Pb (159-272), Cr (138-253), Zn (161-420), Cu (125-269), Ni (12-30), and Cd (4-10.4). The second highest concentration of heavy metal was found in sediments collected from sewage sludge dumpsite. The range of metal levels in selected samples from this site was: Pb (177-235), Cr (127-209), Zn (185-366), Cu (50-230), Ni (26-47.5), and Cd (6-13.3).

Considerable amount of heavy metals were found in near shore mud-patches and in sediments at Cholera Bank south of sewage sludge dump site. These near shore and Cholera Bank environments were not selected as sites for waste dumping. Therefore, the trace metal concentrations in these locations should be of the same level as their background values. However, geochemical analysis showed that considerable amount of trace metals were hosted by clay fraction of these environmental settings. The levels of trace metals in non-dumping areas were lower than those found in the vicinity of MDS and sewage sludge dumpsite. The geochemical analysis showed also that trace metal levels associated with clay fraction varied slightly within the Christiansen Basin. For example, the metal concentrations were slightly higher north of the Christiansen Basin than those found south of the basin. The highest concentration of trace metals in NYB can be explained by high input during active dumping. As results showed (see discussion), highest trace metals and highest clay mineral amounts both occurred at the dumping sites of sewage sludge and MDS. Whereas, lower level of trace metals

and lower clay minerals weight percentage occurred in near shore environment and south of dumping sites. NYB contaminated muds are both physically dredged and dumped at selected sites, and naturally reworked and distributed by currents within the estuary. This mechanical input of contaminated muds explains high trace metal levels at selected sites such as MDS. Geochemical and XRD data showed the same trends between trace metal levels and clay mineral percentage, therefore a strong relationship between NYB clay-trace metals. The presence of illite, chlorite and kaolinite in NYB are responsible of hosting considerable amount of trace metals, which further have been distributed to reside and contaminate other NYB sites such as, south of Long Beach and south of Jones Inlet, and south of dumping sites at Cholera Bank. During waste dumping, once the metals are chemically reacted with clays, they will take considerably longer time to be deposited than coarser materials, thus contaminated clay fractions will be subjected to a greater influence of the currents. This means that during dumping in NYB, waste materials did not reside in a fixed designed location, but instead, the waste has been dispersed and mobilized to occupy other sites within the NYB. Harris (1981) found higher concentration of trace metals associated with near shore mud patches which agrees with study. Harris concluded that these mud patches contained sludge solids derived from the Christiansen Basin and the sewage sludge dumpsite. However, little was known whether the heavy metals were uniformly distributed throughout the waste materials, or were concentrated in fraction of particular size. This study has demonstrated that clays are the dominant scavengers and carriers of trace metals in this mixing zone of the NYB system. The likely cause of the motion of sediment associated with trace metals is the slow bottom currents which move dense ocean water shoreward to replace, in part, the Hudson River water moving sea ward on the surface (Pearce, 1969). Sediment transport on continental shelves is dominated by resuspension during energetic

waves (Butman et al., 1979; Lyne et al., 1987; Drake; and Cacchione, 1985). Like other shelf areas, therefore, sediment transport in the New York Bight has been thought to be wave-dominated. The study of particle size analysis (this study) confirms that the suspension by currents is the main mechanism of sediment transport in the apex of the NYB. This research further demonstrated that clay minerals serve as a vehicle for the transport of trace metals from high potentials sources (MDS & Sewage Sludge Dumpsite). The ultimate repository of these materials (Clay-Trace Metal) will be low energy environment (low currents & waves). Studies conducted by Buchholtz ten Brink and others (1996) and Lanier and others (1999), demonstrated that a sandy, organic-rich, black silt in the thalweg of the Hudson Shelf valley is from the Sewage Dumpsite. Trace metal concentrations (e.g., Ag, Cu and Zn) measured in core and surface-gage samples taken in 1993-1996 indicate the presence of sewage in Hudson Shelf Valley (HSV) surface sediments nearly 100 km from the dumpsite (Buchholtz ten Brink and others, 1997). Measurements in core samples also show presence of sludge lenses in the upper 25 Km of the HSV. This finding suggests a migration of sewage sludge through the submerged river valley. The sandy silt to silty clay anthropogenic layer in the low bathymetric depression of the Hudson shelf valley is indicative of dispersal of waste material (Buchholtz ten Brink and others, 1996). The suspension and distribution of contaminated clay fractions has then altered other part of the NYB ecosystem. Buchholtz ten Brink (1998) concluded that metal and bacterial contaminants in NYB sediment samples indicate wide spread contamination on the broad, sandy shelf and in the muddy sediments of the Hudson Shelf valley. High Metal level occurs in muddy deposits near dump sites and in northern basin of the upper Hudson Shelf valley (Buchholtz ten Brink et al., 1998). Buchholtz ten Brink measured data agrees perfectly with is study, which shows the same sediment distribution and migration pattern in the area. This study also shows

that the anthropogenic finer sediments are migrating away from the dumpsites toward near shore settings such as Long Beach and Jones Beach. These pools of contaminants are on going sources of the pollutants to the New York Bight. Even though the pollution in New York Bight is an old one; it has left pools of contaminant within low bathymetric areas (e.g. Christiansen Basin, Cholera Bank and near shore mud troughs). For instance, during active dumping, many areas of the New York Bight had been closed to commercial shell fishing, swimming, recreation because of elevated levels of coliform bacteria and other pollutants. Therefore, federal regulatory agencies or policy makers should then focus on Low bathymetric basins. Since low bathymetric areas are known as the home (sink) of fine grained anthropogenic materials, therefore, these sites will constitute an ultimate and important pool or repository of any contaminant hosted by clays. These low bathymetric settings may be an important habitat for any organisms that reside there. Since NYB is an ecosystem that is still alive, thereby the removal of contaminated clay fractions or capping the surficial sediment may be a good idea in helping restoring this unique environment. Even though, we can never restore this extraordinary resource to it pristine condition, such information may be a necessary step in making a difference.

5.4. Enrichment Factors of Trace Metals in New York Bight Sediments

5.4.1. Enrichment Factors of Trace Metals in Clay Fraction

The marine environment of the NYB has historically been the region's primary disposal site. These past discharges have created reservoirs of contaminants within the system. Bottom sediments collected on summer 1976 gave us a good opportunity to determine trace metal levels once existed in this mixing zone. To assess the magnitude of trace metal contamination in New York Bight bottom sediments, the metal concentrations in the study area were compared to background levels in term of Enrichment Factor (EF). The EF is defined as the measured

sediment concentration divided by the background concentrations. Holocene lagoonal clays were used to determine the EF in clay fractions of the New York Bight apex surficial sediments. Similarly, modern sand 20 miles south of Jones beach served as control for sand-sized fraction in the study area. The underlying assumption in such an approach is that the lagoonal clays and clay-silt fractions are of same characteristics. Similarly modern sand (control) and sand sized fractions characteristics from the study are also the same.

Concentration ranges and EF of Pb, Cd, Cr, Cu, Mn, Ni, Zn and "normal" trace metal concentrations in clay fractions from the apex of the New York Bight along with control level are given in Table 12. As evident (Table 12), trace metal concentrations in clay fractions from the apex of the NYB were higher than their corresponding background values (Holocene lagoonal clays). Table 12 shows that Mn displays the largest enrichment factors compared to its background levels (Holocene lagoonal clays). The largest EF (1101 ppm) occurred at station 54A in near shore muds. The second highest concentration of Mn occurred in clay fraction from MDS where it was enriched by 389 X compared to it background level (0.74 ppm). This suggests high input of Mn at these sites. Cr displayed the second largest enrichment factors in the NYB clay fractions. The maximum enrichment factors for Cr was 146X compared to its corresponding background value. This EF (146 ppm) occurred again in clay fractions from MDS at station 86.2. The second highest enrichment factors for Cr were in Christiansen Basin muds with a value of 116 X (station 31B) compared to Holocene lagoonal clays (0.74 ppm). As the result of enrichment factors indicate, either higher potential source of Cr at these sites or greater

Table 12: Minimum and maximum Enrichment Factors (EF)of trace metals in clay fractions from New York Bight Apex relative to the Holocene lagoonal clays

Location	Metal (ppm) Pb	Cd	Cr	Cu	Mn	Ni	Zn
Background area (Holocene lagoonal clays)	4	ND	1.8	2	0.47	1.5	7
Dredge Spoil	39.7-68	(4-10.4)	76-146	62.5-134.5	240-389	8-20	23-60
Christiansen Basin (North of Sewage Sludge)	44-58.7	(6-13.3)	70.5-116	25-115	135-323	17-31	26-52
Cholera Bank (South of Sewage Sludge)	21	(8.5)	21.6	48	85	20.6	35.7
Near shore Mud-patches	4-49.7	(2.5-7)	21.6-68	5-45.5	90-1101	5-8	15-22

ND: not detected, average values in parentheses.

ability of clay fraction of adsorbing higher Cr levels. This also indicates that Christiansen Basin setting serves as the sink for Cr, perhaps for other aqueous elements. Ni like Cr had similar background values of 1.8 ppm and 1.5 ppm, respectively. However, Ni displayed lower enrichment factors compared to Cr enrichment factors (Table 12). The highest enrichment factor for Ni was 31.6 X (station 91) north of sewage sludge dumpsite in the vicinity of Christiansen Basin. Since Ni and Cr have similar background levels (Table 12), this may indicate that, either there was a higher potential source of Cr or Cr was preferably adsorbed by clay mineral surfaces as compared to Ni. In either case, the Christiansen Basin served as residing site for the clay-metals. The maximum enrichment factor for Cu was 134.5 X, which was also concentrated in clays from MDS at station 86.2. The second highest enrichment factors for Cu occurred in the Christiansen Basin with a value of 115 X compared to it background value (Holocene lagoonal clays). The observed large enrichment factor for Cu was probably due to its low background level (2 ppm). The enrichment factors for Pb was larger that it corresponding background value (4 ppm). The maximum EF for Pb was also associated by clay fraction from MDS at station 87 (EF = 68 ppm), followed by second highest EF (58.7 ppm) which occurred in the vicinity of Christiansen Basin north of sewage sludge dumpsite. Zn background value (7 ppm) was twice as much as Pb background level (4 ppm). The enrichment factors for these two metals were almost the same (Table 12). The maximum enrichment factor for Zn (60 ppm) occurred in dredge spoil muds at station 86.2; followed by the second highest EF (52 ppm) was adsorbed by clay fraction north of sewage sludge in the vicinity of Christiansen Basin. The observed differences between Pb and Zn EF levels resulted from the differences in their background levels. As was discussed earlier, the mean Zn value was higher than the Pb mean value in the clay particles of the NYB. However, the EFs of Zn were lower than EF of Pb, this is due

probably to a larger background level of Zn (7 ppm) or Zn was greatly retained by clay fractions. Cd was not detected in Holocene lagoonal clays, therefore, no comparison of Cd concentrations in the New York Bight were made relative to Cd background values. However, Cd just like other trace metals showed higher concentration in clay fractions from the Christiansen Basin and MDS.

In general, the EFs indicate that all trace metal concentrations in the study area were higher than the Holocene lagoonal clay values (background levels). Except for Mn, the largest EF for all trace metals occurred in MDS, followed by Christiansen Basin, Cholera Bank and near shore mud-patches. These larger EFs indicate larger input of trace metals in the New York Bight environment since 1954, and a greater ability of clay fraction in the storage of trace metals studied. The past ocean wastes dumping has heavily contaminated the New York Bight sediments, especially fine-grained materials. Over time these contaminated materials have been dispersed to reside in low depression environment, including near shore depressions. In this study, near shore mud-patches which generally high energy environment also showed high EF compared to background levels. This indeed confirms that these near shore fine-grained materials were probably derived from heavily contaminated sources. Since finer materials were found near shore, this explains the existence of low energy occasions that favor deposition of polluted fine-grained materials. This study also confirms resuspension and redistribution of fine-grained materials within the NYB system. As was discussed above, that the ultimate repository of the suspended material associated with trace metal were low energy environments such as, Christiansen Basin, south of sewage sludge area at Cholera Bank and along near shore. Clay fractions associated with trace metals from the apex of New York Bight, therefore, may contribute a good deal in the contamination of the YNB biological system including humans.

5.4.2. Comparative Maximum Enrichment Factors of Trace Metals in Different Size Fractions

The enrichment factors (EF) help clarifies the distribution of trace metals among the different size fractions in the apex of the New York Bight. Once this clarified one can introduce the desired size fraction of maximum EF to decontaminate or at least reduce the trace metal levels in any polluted aqueous environment. Table 13 shows the enrichment factors of trace metals in various size fractions from New York Bight apex.

Table 13 reveals that most of trace metals were enriched in clay fractions of the apex of NYB environment compared to their corresponding background levels. The maximum enrichment can be explained by both, the highest influxes input of trace metals during active waste dumping and by the sorptive properties of clay minerals (see discussion above). Another important outcome of this study is the enrichment factors of trace metals in sand size fractions, which did not exceed their corresponding background values. The association of trace metals with sand sized particles could be explained by, 1) sand sized- particle may be coated by organics, oxides or clays, 2) exposed of negatively charged mineral surfaces due to broken bonds, and 3) the sand-sized particles may be floccules of clays. If one of these is true, then the excess (not retained by clays) of trace metals will be associated with reactive functional groups of sand surfaces. These facts were not demonstrated in this study, but in general, EF decreased dramatically with increasing sand size particles. Therefore, we can learn that during waste dumping most of trace metal influxes were enriched in clay fraction (clay minerals) rather than sand fractions. The metals retained by these minerals surface may be easily extracted by benthos, preferably in fauna. If this is the case then, within time the in fauna will concentrate the trace metals and this may from strong complexes with generally soft functional groups on

biomolecules (Sposito, 1989; Moral and Herring, 1993). This study showed that clays are the most polluted fraction and sand is the least contaminated sediment fraction in the NYB environment. This further demonstrates the importance of sand and clay fractions. Because of these findings, government agencies should either, 1) use clean sand to dilute or cap the preexisting contaminated materials or 2) removal of contaminated fine grained materials for further decontamination. The question that remains will be the cost of removal and decontamination, and what will be the ultimate disposal of the treated materials.

Table 13: Comparative maximum Enrichment Factors (EF) of trace metals in New York Bight Apex relative to control areas

		Pb		Cr		Cu	Ni	Zn
MDS								
	1)[a]	68		146		138.5	20	60
	2)[b]	6.8		7.5		19	ND	6.8
	3)[b]	4.8		4.3		17.7	ND	6
	4)[b]	1.5		ND		-	ND	1.9
Christiansen Basin (North of sewage sludge)								
	1)[a]	58.7		116		115	31.6	62
	2)[b]	9.3		6		30	6.5	10.5
	3)[b]	7.9		5		23	0.7	8
	4)[b]	-		ND		-	ND	1.9
Cholera Bank (South of sewage sludge)								
	1)[a]	21		21.6		48	20.6	35.7
	2)[b]	2.8		ND		15	ND	9
	3)[b]	2		ND		10	ND	-
	4)[b]	-		ND		-	ND	-
Near shore mud-patches								
	1)[a]	49.7	68	45.5	8	22.3		
	2)[b]	10.5	4.9	18	ND	8.4		
	3)[b]	4.4	ND	2	ND	4		
	4)[b]	1.6	ND	-	ND	3		

1) clay & silt 2) very fine sand 3) fine sand 4) medium sand

[a] relative to the Holocene lagoonal clay. [b] relative to modern shelf sand

ND: not detected - : not determined

5.5. Variability of Trace Metals Concentrations and Granulometry of Selected samples from the Apex of the NYB

5.5.1. Variability of trace metal levels in surficial sediment of summer 1976 and summer 1997

To determine the variation of trace metal concentration between summer, 1976 and summer, 1997, the order of magnitude (increase or decrease) has been calculated using the background values and the EFs for each trace metal selected. The underlying assumption in such approach is that the sampling techniques and grain size of the 1976 and 1997 sediment samples were the same. The sample grab locations used for trace metal concentrations and granulometry variation purposes were carefully selected from sewage sludge dumpsite and mud dump sites (MDS). The age of surficial sediments in the New York Bight is not known; therefore no comparison of trace metal levels can be made between selected sediment grabs. Sediment younger than 1965, defined as recent as revealed by the presence of ^{137}Cs, are presented by layers no more than 50 cm thick that deposited at rate as high as 5-10 mm/yr (McHugh, 2004). Recent sedimentation in the NYB system is mostly the result of anthropogenic dredge material dumping (Massa et al., 1996) and sediment reworking during storm events (Moore et al., 2001). The radionuclide analysis of core AC97-1 shows no detection of ^{137}Cs and ^{7}Be (McHugh, 2004), which suggests also that the most recent surficial sediment distributed in the NYB, is recycled anthropogenic materials from the preexisting dump sites.

The variation change in trace metal concentrations of summer, 1997 surficial sediments relative to summer, and 1976 surficial sediments is given in Table 14 and Figure 22. Trace metals concentrations has varied dramatically in 1997 Sewage sludge dumping sites than those in the comparable 1976 sewage sludge samples. As evident (Figure 22 and Table 14), Cd and Ni were not detected in 1997 sewage sludge sediment samples. This suggests that after the closure

of the sewage sludge dump sites in 1987, the input of Cd and Ni has also come to an end in sediment samples from the sewage sludge area. Thus, the sewage sludge materials dumped were the potential source of Ni and Cd in sewage sludge sediment samples. The second highest trace element that decreased in sewage sludge surficial sediments was Pb, followed by Zn, Cu and Cr with a magnitude that ranges from lowest to highest, 15.6-57.3 ppm, 18.5-37 ppm, 19-22 ppm and 15-24.6 ppm, respectively. In general, (Table14 and Figure 22), after the cessation of sewage sludge dumping in 1987, the surficial sediments became less polluted, which confirm that the sewage sludge was the main source of trace metals in the sewage sludge dump site prior to its closure. Even though there was a dramatic variation in trace metal levels after the closure of the sewage sludge dumpsite, some trace metals were still enriched at this site relative to their background levels, however, the EFs in sediments from the preexisting sewage sludge dumpsite were very low compared to the EFs in 1976 sediment samples (Table 14). The levels of trace metals in 1976 sewage sludge samples were then at their highest peak. These sediments analyzed in this study were collected during full waste dumping from the apex of the NYB. The last legal sewage sludge dumping in this sampling area was in December 1987. The core AC 97-1 from preexisting sewage sludge dumpsite was collected during a period of non-dumping. The core was about 41 cm thick. This means no sewage sludge was recovered at this site, thereby; low EFs of trace metals in surficial sediment of 1997 can be derived from low potential sources other than sewage sludge materials, probably from the non-point source pollution.

The surficial sediments of core AC 97- 9 from MDS showed only a slight decrease in trace metal levels than those of sewage sludge sediments (Figure 22). For instance, all trace metals selected in this study did not vary more than a magnitude of 10 as compared to those of core AC 97-1. The observed variation in trace metal concentrations from sewage sludge surficial

sediment of summer 1997 could be explained by the cessation of sewage sludge dumping in December 1987, and thus reduction of trace metal input in this area. By contrast, the slight variation in trace metal levels in MDS surficial sediments just prior to it closure in December 1997 was still undergoing some significant environmental stress. This finding suggests that anthropogenic materials dumped at MDS are probably being surficially reworked and redeposited locally by storms, which did not dramatically affect the sediment trace metal levels.

Table 14: Decrease in trace metal concentrations in summer, 1997 surficial sediment samples relative to surficial sediment samples of summer 1976.

Dumping Sites		Pb	Cd	Cu	Zn	Ni	Cr
Sewage Sludge							
	89	*46.75* **(45.6)**	7.6	*111.5* **(21)**	*26* **(18.5)**	*17.3* **(100)**	*79* **(16.8)**
1976:	91	*58.75* **(57.3)**	13.3	*115* **(22)**	*52* **(37)**	*31.6* **(100)**	*116* **(24.6)**
	71	*51.5* **(50)**	10.6	*98.5* **(19)**	*51* **(36)**	*18.6* **(100)**	*0.5* **(15)**
1997:	AC97-1	*1.025*	*ND*	*5.15*	*1.4*	*ND*	*4.7*
Mud Dump Site							
	87	*68* **(2.4)**	10	*96.5* **(3.2)**	*32* **(1.9)**	*15* **(1.2)**	*77* **(6.3)**
1976:	85	*45* **(1.6)**	6	*87.5* **(3)**	*31* **(1.9)**	*12.6* **(1)**	*119* **(9.8)**
	84	*44* **(1.6)**	4	*62.5* **(2)**	*26* **(1.5)**	*8* **(1.58^{+})**	*101.6* **(8.3)**
1997:	AC97-7	*28*	*6*	*30*	*16.7*	*12.6*	*12*

Note: Bold numbers in parentheses are trace metal decrease in summer, 1997 sediment relative to summer, 1976 sediment samples. Italized numbers are EFs of trace metals relative to their background concentrations: Pb (4 ppm), Cu (2 ppm), Zn (7 ppm), Ni (1.5 ppm), Cd (not detected) and Cr (1.8 ppm).
ND: Not detected, ($^{+}$): Increase of trace metal concentration

Figure 22: Variation between summer 1976 and summer 1997 trace metal concentrations in NYB dump sites.

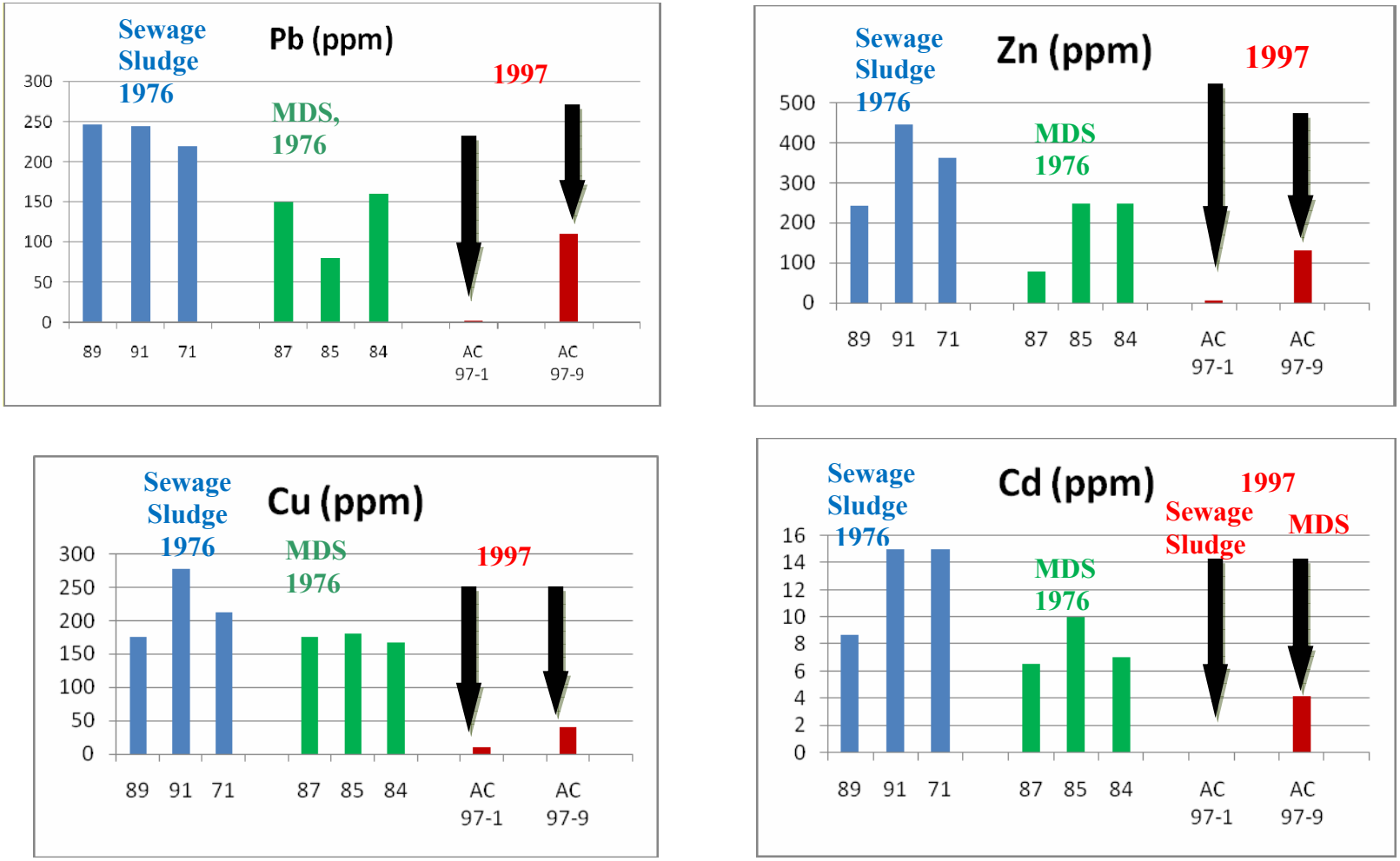

Figure 22: Variation of trace metals concentration between summer 1976 and summer 1997 at selected sample sites (continued).

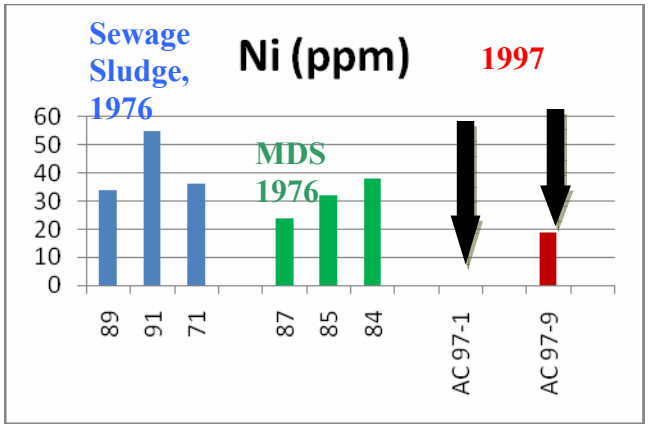

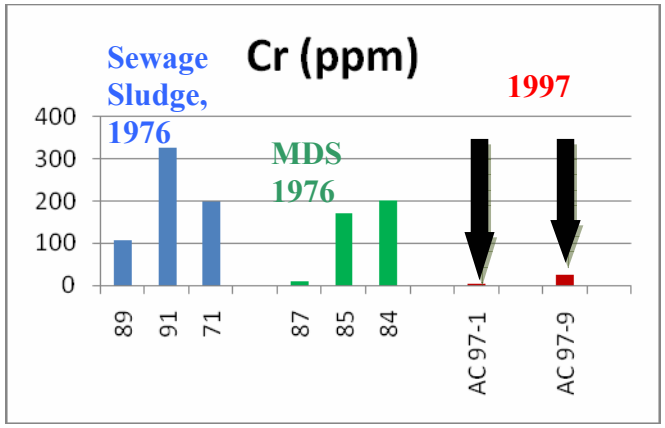

5.5.2. Sediment grain-size variation between selected samples of summer 1997 vs. 1976

NYB setting is characterized by sediment starvation and erosion (Swift et al., 1972; Austin et al., 1998; McHugh et al., 2004), therefore the NYB surficial sediments defined as recent (younger than 1965), are being resuspended and scattered by storms. The result of granulometric analyses shows certain degree of textural variations between 1976 and 1997 sediment samples (Table 15). For instance, sediment grabs from sites 89, 91 and 71 of summer 1976 shows higher percentage of clay fraction, very fine sand and fine sand relative to 1997 surficial sediment sample. By contrast, 1997 sediment sample shows higher percentage of medium sand, coarse sand, very coarse sand and gravels relative to 1976 sediment samples. As evident (Table 15), the dominance of coarse material in core AC97-1 may have been deposited in sewage sludge area by episodic storm events. The core AC97-1 (41 cm thick) in preexisting sewage sludge dumpsite was collected by McHugh in summer of 1997 during a period of non-dumping. Core sediments from the same sludge dumping area were also sampled and analyzed by Schwab in 1996 and shows that the sludge material is covered by 50 cm layer of clean fine to medium sand, which confirm sediment textural variation of core AC97-1 (this study). The presence of sand waves in this study area of the sewage sludge further suggests that this is an area of active sediment transport which dilutes and caps the dump sludge materials (Schwab et al, 1990). The cessation of dumping in 1987 has hence changed the granulometry of sediments (this study and Schwab, 1996) and shown a dramatic variation in trace metal concentrations sediments from a former sewage sludge dumpsite (this study). These findings indicate that the preexisting sewage sludge dumpsite is an area that is now less polluted and covered by 41 cm thick layer of clean sand. Since the Hudson Shelf Valley is sediment starved (McHugh et.,

2004), most of surficial sediment are recycled material derived from the preexisting anthropogenic dumped materials (Massa et al., 1996).

The result of sediment grain-size analysis shows variation in textural properties between summer 1997 and summer 1976 sediment sample (Table 15). These variations can be explained by the presence of storms that resuspend, redistribute and recycle the sediment particle and therefore a change in sediment texture. Site AC97-9 shows a decrease in the percentage of fine sand, very fine sand and clay fraction relative to site 85, 87 and 84 of summer 1976 MDS samples. The core AC 97-9 from MDS was about 96 cm thick and consisted mostly of medium sand (bout 60%), which is distributed as lenses throughout the core. These sand lenses injection could have been caused by occasional storms (currents) within the sampling area (McHugh, personal communication). The geochemical analysis showed that the clay fraction of summer 1997 MDS was heavily contaminated relative to sewage sludge sediment samples. The decreasing of low clay fraction still played an important role in the storage of trace metals.

In general, geochemical and sediment particle analysis of sediment samples of summer 1997 and summer 1976 showed the following: 1) a dramatic variation in sediment textural properties between sewage sludge sediment samples of summer 1997 and 1976, 2) a dramatic decrease in trace metal concentrations in 1997 sediment samples relative to 1976, 3) a small variation of trace metal concentrations in 1997 relative to 1976 MDS sediments samples, and 4) 1997 sediment samples from sewage sludge area are much less polluted than sediment samples from MDS. This suggests that sewage sludge dumpsite has been naturally capped by clean sand and recovered from high pollutants after it closure in 1987. By contrast, the MDS, just prior to its closure in September 1997, still have metal concentrations sufficiently high to cause toxic effects in test organisms.

Table 15: Variation of granulometry in selected NYB sediment grabs: Summer 1976 vs. summer 1997

Sewage Sludge Sites				
	Summer 1997		**Summer 1976**	
	AC97-1	**89**	**91**	**71**
Percent:				
Gravels	19.36	0	0	0
Very Coarse sand	4.63	1.075	0.49	0.21
Coarse sand	21.41	8.30	1.40	0.98
Medium sand	52.35	35.70	2.07	5.20
Fine sand	3.14	29.08	65.87	52.77
Very fine sand	0.05	9.45	19.75	37.87
Clay	0.08	16.39	10.42	2.98
Mud Dump Sites				
	Summer 1997		**Summer 1976**	
	AC97-9	**87**	**85**	**84**
Percent:				
Gravels	4.27	0	0	0
Very Coarse sand	4.52	2.06	0	2.15
Coarse sand	5.15	13.61	0.2	11.46
Medium sand	58.99	18.87	3.27	17.97
Fine sand	19.83	27.61	27.10	29.10
Very fine sand	2.83	18.94	22.51	30.91
Clay-silt	3.87	18.89	46.90	8.40

5.6. Trace Metal Concentrations in New York Bight Apex Sediments Compared to Sediment Quality Guidelines

Over the years, a number of methodologies have been developed to estimate environmental threshold level for chemicals that may have an adverse effect on biota. For instance, sediment concentrations of heavy metals which exceed designated threshold have been proven to be hazardous to biota. Hence, contamination of sediments by toxic heavy metals has been an issue of prime concern in many areas of the United States or probably all over the world. To assess potential effect for future benthos studies, New York Bight trace metal levels during active dumping in 1976 (this study) were compared to the U.S.E.P.A. adopted effect-based

sediment quality guidelines discussed by Long and Morgan (1991) and Long et al. (1995). Trace metals from this study were also compared to Canadian Environmental Protection Authority (EPA) standard values (EPA, 1976). Sediment quality guidelines establish certain "regulatory or screening level of concern" for sediment toxicity based on certain measurements: 1) concentration of toxic chemicals, 2) toxicity environmental samples, and 3) evidence of modified residence of biota, especially the in fauna (Long and Chapman, 1985).

U.S.E.P.A. adopted two threshold levels for trace metals, so-called, ERL and ERM. E – RL stands for Effect – Range Low, indicating metal levels at which adverse biological effect begin to be seen. E – RM stands for Effects – Range Median, concentrations above which adverse biological effects are probable. Therefore, any value between the two threshold levels indicates a "possible-effect range". Total concentration of substances present in the environment (New York Bight, this study) may not represent the actual exposure level for biota. The bioavailability of chemical in this aqueous environment depends on the intrinsic properties of the chemical substances, the type of the substance or medium in which it is present, and on (variation in) environmental factors. A lower bioavailability generally implies a lower toxicity for the inhabiting biota. Although trace metal concentration alone do not provide an indication of biological damage, ERL and ERM values are necessary steps to determine the degree of pollutants. The Guidelines limits for metals in sediments are shown in Table 16.

Table 16: Guidelines for metals in sediments (ppm)

Metals	ERL [1]	ERM [1]	Canadian EPA [2]
Cd	1.2	9.6	2
Cr	81	370	-
Cu	34	270	8
Ni	20.9	1.6	-
Pb	46.7	218	22
Zn	150	410	40

[1] USEPA Adopted ERL and ERM Concentrations for Sediment Trace Metals (Long and Morgan, 1991; Long et al., 1995)
[2] Canadian Environmental Protection Authority Guidelines (EPA, 1976)

Figure 23 shows the distribution pattern of trace metals with reference to guideline levels. As evident (Figure 23), all trace metals concentrations exceeded the Canadian Protection Authority (EPA) standards values, except at station 7-1b where Pb concentration was lower than EPA standard value. Cd and Cu are the only two metals that were higher than USEPA ERL values at all sites. Pb concentrations in this study were also higher that USEPA ERL levels, except at site 7-1b where Pb is lower than ERL value. Ni, Cu and Zn levels in the study area did not exceed the USEPA EMR standard values. However, Cd and Pb are the two metals that exceeded their EMR values at certain sites of the study area. For instance, Pb exceeded EMR values only at four sites (86, 86.2, 87, and 91). Cd was higher than its EMR values only at three sites (86, 71, 91). Since Cd and Pb exceed their guideline EMR values, they can be considered the most pervasive contaminants in the study area. No Canadian EPA guideline values were given for Ni and Cr.

In general, in 1976, during full dumping, NYB system showed remarkable differences in the degree of metal pollution (this study). Most of trace metal concentrations fall between the adopted ERL and ERM of the U.S.E.P.A standard values, which indicate a possible effect on biota. Concentration of contaminants (Ag, Cu, Pb, Zn and organic carbon) measured in cores and surficial sediments taken in 1993-1996 indicate that their levels are sufficiently high to cause toxic effect on biota (Butchholtz ten Brink, 1997). Thereby, the environmental system needs close monitoring so that the safe limits are not exceeded. Whereas, the trace metal concentrations during active dumping exceeded the Canadian Environmental Protection Authority Standard values. Therefore, the pollution of NYB which both a dynamic living ecosystem and center of human activity, would be an environment issue of prime concern, if the Canadian guidelines should be adopted. The adopted ERL and ERM of the USEPA standard

values are much higher than those of the Canadian guidelines. Since tarce metals in aqueous environment can be released from mineral surfaces, therefore the USEPA should adopt lower ERL and ERM values other than these discussed here.

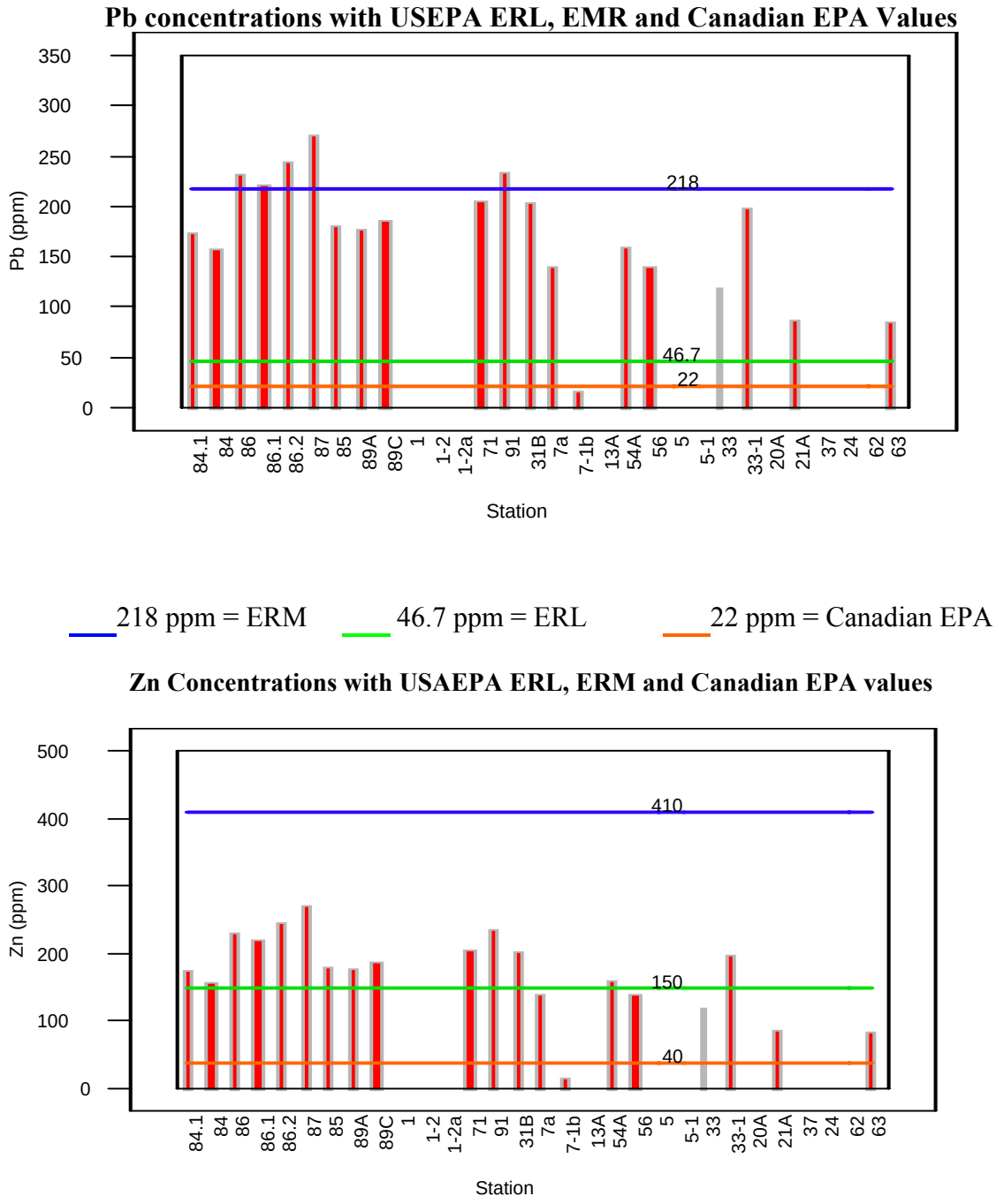

Figure 23: Metal concentrations in New York Bight surficial bottom sediments as compared to sediment quality guidelines.

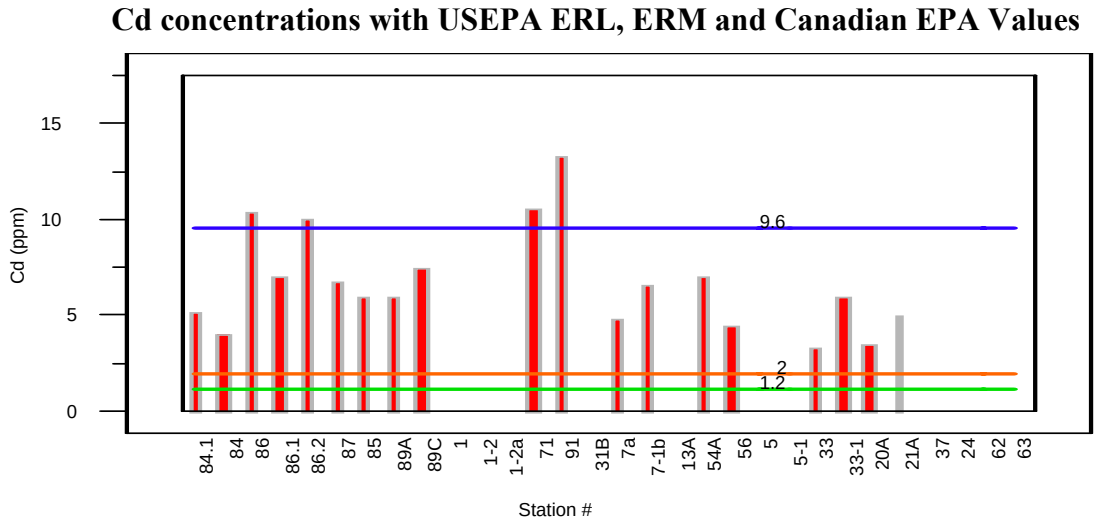

96 ppm = ERL 1.2 ppm = ERM 2 ppm = Canadian EPA

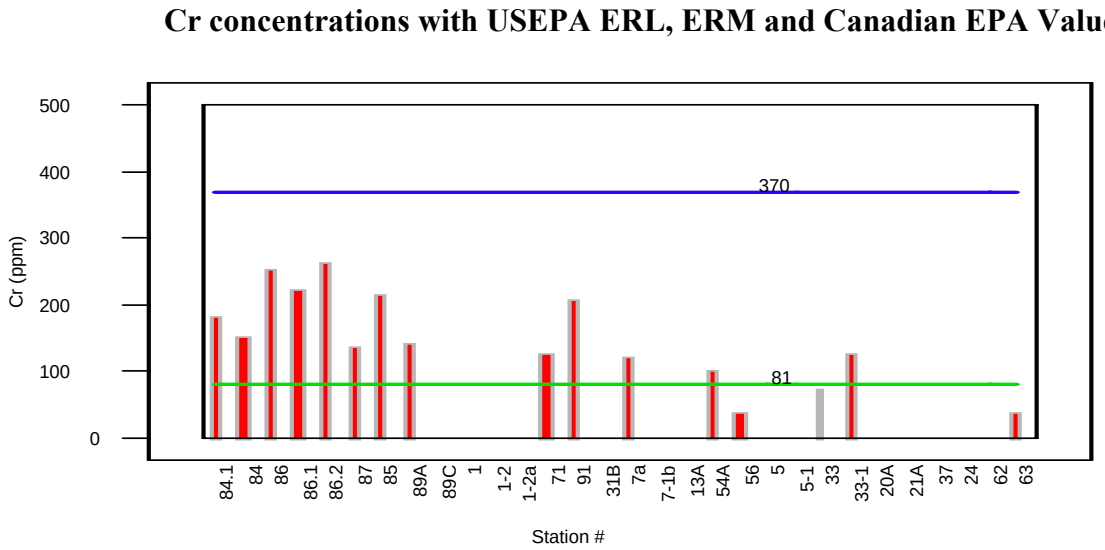

70 ppm = ERM 81ppm = ERL

Figure 23: Metal concentrations in New York Bight surficial bottom sediments as compared to sediment quality guidelines (continued).

Cu concentrations with USEPA ERL, ERM and Canadian EPA Values

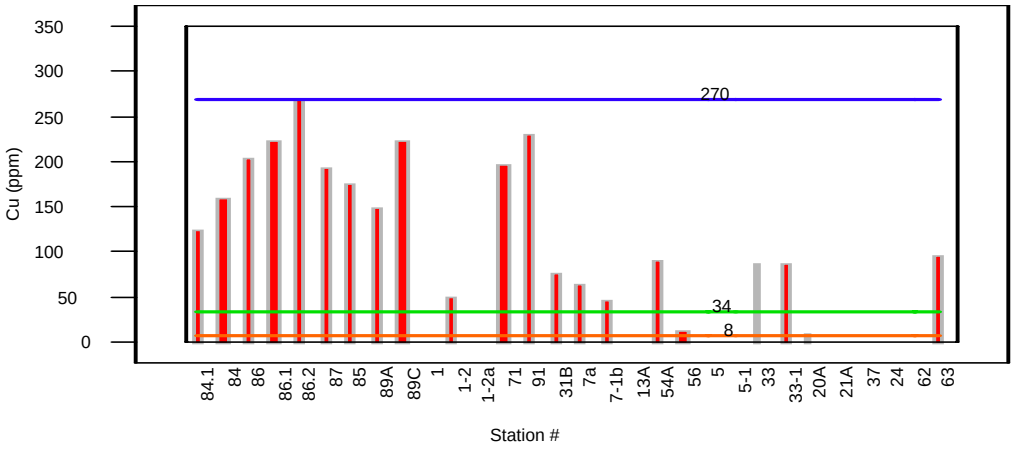

270 ppm = ERM 34 ppm = ERL 8 ppm = Canadian EPA

Ni concentrations with USEPA ERL, ERM and Canadian EPA Values

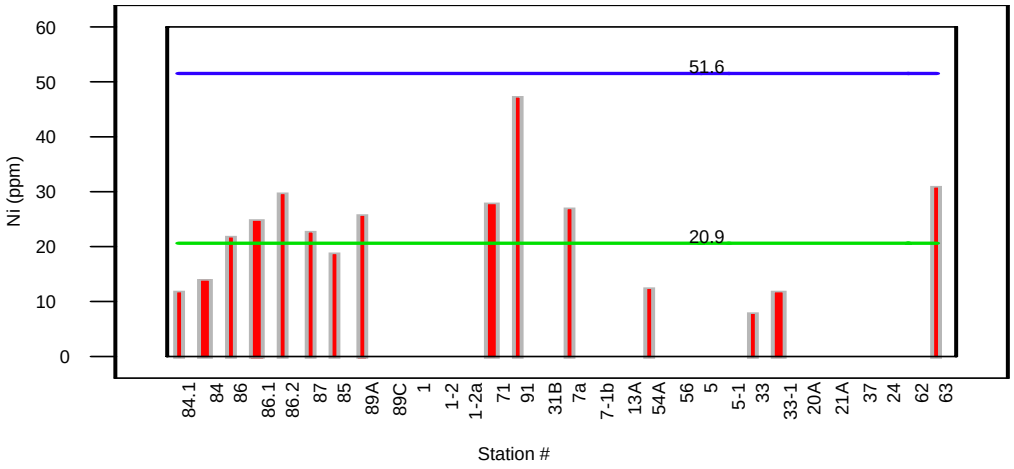

270 ppm = ERM 34 ppm = ERL

Figure 23: Metal concentrations in New York Bight surficial bottom sediments as compared to sediment quality guidelines (continued)

The discharge of contaminated wastes into the estuary from various sources have degraded the quality of the estuarine water and bottom sediments, resulting in the decline in fish population and diversity, and thus health advisories (Clark, 1990). The degradation of the ecosystem therefore, indicates that the values of trace metals that fall between ERL and ERM of the USEPA are of prime concern and the Canadian guideline values thereby should be adopted here instead of USEPA values. The government regulators need to do more work on sediment contamination, biota tissue and guideline standard values to address this and similar problems. The environmentalists or geochemists should adopt the same guideline standard values for each metal, which could be used universally.

5.7. Statistical Analysis

Results of analysis of variance and mean of Oneway ANOVA showed that the means of response of Oneway Anova by station for all stations were different, which indicates significant differences in trace metals, thereby significant spatial variation in trace metals (Appendix F).

Bivariate cluster analysis of trace metals from dredge spoil, sewage sludge and near shore muds are summarized in Table 17. The pairs of trace metals are well correlated in sewage sludge and MDS. However, trace metals of near shore muds were not well correlated compared to sewage sludge and MDS trace metals. This may indicate that trace metals may have been derived from different sources and distributed near shore environment.

The results of Pairwise, Spearman's Rho and Kendall Tau b also showed high degree of association between pairs of trace metals from the same location area. When all the pairs of trace metals from the study area are correlated, however, they do not show a strong degree of

Table 17: Well correlated pairs of trace metals from New York Bight Apex

Bivariate Analysis					
Dredge Spoil		**Sewage Sludge**		**Near shore Muds**	
Cu/Zn	0.93	Pb/Cr	0.76	Cu-Cr	0.72
Cd/Cu	0.76	Pb/Cd	0.99	Pb/Zn	0.95
Ni/Cu	0.97	Cu/Nin	0.85	Pb/Cr	0.84
Ni/Pb	0.79	Zn/Cr	0.97	Zn/Cr	0.76
Zn/Cr	0.86	Zn/Ni	0.87	Mn/Cu	0.83
Zn/Ni	0.91	Cr/Ni	0.96	Mn/Cr	-1.00
Cd/Ni	0.77	Cr/Mn	-0.76	Mn/Ni	1.00
Cd/Cr	0.78	Pb/Mn	-1.00		
Mn/Pb	0.93	Ni/Cd	0.83		
Mn/Cu	0.92	Ni/Mn	-0.90		
Mn/Zn	0.89	Cd/Mn	-0.98		
Mn/Ni	0.96				
Mn/Cd	0.99				

association. Trace metals derived from various sources have been distributed unevenly among sediments and geographical sites of the New York Night apex. A non-normal distribution of trace metals also suggests that the sediment nature, its mineralogy and its particle size influence their normal distributions. Previous studies (Grant, 1999) have tried to overcome this problem of nonnormal distribution of trace metals. Grant (1999) has related nonnormal distribution of trace metals to inhomogeneity of sediments. Several studies have been tried to overcome this problem of nonnormal distribution of trace metals, however, they did not solve the problem based on grain size only. In this study I have separated clay and silt fraction to solve this persistent problem. I have thought that trace metals would be evenly distributed in clay fraction, but this does not seem to solve the matter of normalcy. This study further suggests that an important factor that may influence the normal distribution is the selectivity sequence and the competitive adsorption of heavy metals with clay minerals. The adsorption of heavy metals has been studied and reported in the literature for silicate minerals (Swift and McLaren, 1991); for Fe- and Al-, and Mn oxides (Schwertmann and Taylor, 1989) and for humic substances (Stevenson and Fitch, 1986). According to McBride (1994), electronegativity is valuable factor that determines which trace metals chemisorbs with the highest preference, on this basis, the predicted order of metals

to form strong bonds would be Cu> Ni > Co > Pb > Cd > Zn > Mg > Sr. On the basis of radius and the ionization potential quantified by Misono softness parameter, the metal cations form covalent bonds in the following sequence: Pb > Cd > Co > Ni > Zn (Sposito, 1989). According to Schwertmann and Taylor (1989), the selectivity sequence of metal cations adsorption by goethite is Cu > Pb > Zn > Cd > Co > Ni > Mn, while hematite gave the following sequence Pb > Cu > Zn > Cd > Co > Ni > Mn. In this study no conclusion can be made on the selectivity sequence of trace metals. This research showed that there is no linear relationship between clay fractions and trace metal levels. Therefore, further research would necessary to study the selectivity sequence and competitive adsorption of trace metals by NYB clays to overcome this problem of normalcy.

In general, the divalent metals have similar geochemical behavior. Their behavior, however, have been affected by, sediment particle size, mineralogy, pH, Eh, competitive adsorption of trace metals by clay mineral surfaces and perhaps by hyrodynamics of the New York Bight environment. A combination of all this may explain both, a non normal distribution and low degree of correlation between pairs of trace metals studied.

CHAPTER 6

Conclusion

This research was conducted in the apex of the New York Bight, New York-New Jersey metropolitan area and included series of sediment samples. First series of sediment samples were collected during active waste dumping in summer of 1976, which includes sediment sampling from Mud Dump Site (MDS), Sewage sludge area, and near shore mud-patches. The second series, which includes core AC97-1 that was collected in summer of 1997 from sewage sludge dumpsite and core AC97-9 from MDS just prior to it closure by Clinton administration in September 1997. The first series of sediment samples collected in 1976 offered the opportunity to study the variability, distribution and behavior of trace metals in New York Bight marine environments. The second series collected in 1997 provided the opportunity to study both, trace metal concentrations and sediment textural variations. This study indicates the following conclusions:

1- Past and current municipal and industrial discharges have created reservoirs of trace metals within the New York Bight environment.
2- During full dumping, the sediments from the apex of the NYB contained high concentration of trace metals of which Zn the highest followed by Pb, Cr, Cu, Ni, and Cd.
3- The highest concentrations of trace metals occurred at MDS followed by sewage sludge dumpsite and considerable amounts were found in near shore mud patches and south of dumpsites.

4- Pb, Zn, Cu, Ni and Cd show generally similar distribution patterns. However, they are highest at dumping sites and slightly lower south of dumping sites and near shore mud patches.

5- Anthropogenic dredged sediment and waste material dumped in the apex of the NYB are the major source of trace metals and perhaps other enviro-toxic pollutants.

6- All trace metal concentrations were higher than their corresponding background levels, which indicate high trace metal inputs during dumping.

7- In summer of 1976, Pb, Zn, Cu, Ni and Cr in the NYB section of New York-New Jersey estuary, with respect to biological system including human, was at dangerous levels. Most of the sediments had metal concentrations that fell between USEPA ERL and ERM values.

8- In summer 1976, sediment samples with high level of trace metals were also found near shore, south of Jones Beach and Atlantic Beach, therefore there was a major issue in coastal water use, such as swimming and fishing.

9- The trace metal levels were not uniformly distributed among NYB sediment fractions.

10- All trace metals were heavily enriched in clay fraction regardless of their location in the study area.

11- Clay fractions were the most contaminated and therefore constitute an important repository for trace metals in the NYB marine environment.

12- Contaminated clay fractions have been suspended and distributed within NYB system to occupy low bathymetric areas, such as Christiansen Basin and Cholera Bank, and near shore troughs, which pose risks to both human and ecosystem health.

13- The clay fractions are important vehicle in the transport of these heavy metals; their dispersion has polluted other areas of the New York Bight ecosystem. They, thereby, play an important role in the mobility and dispersion of trace metals and perhaps other aqueous species in the NYB environment.

14- XRD analyses of the clay fractions showed the presence of illite, chlorite and kaolinite. Illite is the dominant phase in the clay fractions from the NYB samples. The second and third major mineral phases are chlorite and kaolinite. Mixed-layer illite/smectite levels were very low to absent. The highest level of illite/smectite occurred at site 7-1-2 south of Long Beach. The concentration of all clays were in the vicinity of dump sites (MDS) and sewage sludge, which showed the same trends as trace metal concentrations. The clay minerals occur in small particle sizes and therefore have remarkably large surface areas, thus high surface reactivities for their weights. One common property of all clays is that, their surfaces contain functional groups which interact with metal ions. This process, called *sorption,* has a strong influence on the mobility and uptake of metals in aqueous environment such as NYB.

15- Clay minerals (e.g., illite, chlorite and kaolinite) associated with trace metals can be considered both as a sink and as pollutants in the NYB, therefore these clays may play an important role in the cycle of NYB trace metals.

16- Core AC97-1, which is located within the preexisting sewage sludge dump-site, showed surprisingly low trace metal concentrations and low percentage of clay fractions. The core AC97-1 did not exceed 50 cm in length, which means that no sewage sludge was recovered at this site. After the closure of sewage sludge dumpsite in December 1987, storm events have naturally buried the preexisting sewage sludge area with a layer of

clean sand. Thus, a dramatic change in trace metal levels and sediment textural properties at the sampling sites.

17- Core AC97-9, which is located within MDS showed high trace metal concentrations and considerable amount of clay-silt fractions. The MDS was formerly closed to any further ocean disposal in October of 1997. The core AC97-9 was collected in summer of 1997, which means that this site was still undergoing some environmental stress. Trace metal levels measured in this core are sufficiently high to cause effect in test organisms. properties.

18- The particle size analysis showed that the dominant sediment transport in the apex of the New York Bight system is suspension due to occasional storms.

19- Recent sedimentation in the NYB environment is mostly the result of anthropogenic dumping and sediment reworking during episodic storm events.

20- Since NYB is sediment starved, the preexisting contaminated anthropogenic sediments are occasionally being reworked and recycled. This indicates that the health of the New York Bight environmental system can never be restored to its pristine condition. However, the existence of pools of contaminants in low bathymetric areas should be left undisturbed. As a consequence of changing environmental conditions, toxic metals can be released from mineral surfaces (a process called desorption). This disturbance will be then marked as Chemical Time Bomb (CTB).

21- In general, trace metals studied are divalent and therefore, their geochemical behavior should be the same. However, their behavior has been distorted by numerous parameters such as, pH, and Eh and perhaps the Bight's hydrodynamics. Sediment particle size, it

mineralogy and selectivity sequence of heavy metals can also play an important role in influencing trace metal reactivities.

22- In general, Pairwise, Spearman's ρ (Rho) and Kendal τ_b (Tau -b) analysis show low degree of correlation between pairs of variables-Pb, Zn, Cu, Pb, Ni and Cd in the NY Bight, which suggest different behavior and sources of these trace metals. The statistical analysis tests also yield a non normal distribution for all trace metals studied, which may be due to clay-metal cations selectivity.

The New York Bight is extraordinary in many ways—its abundant resources, its beauty and many competing uses. The NYB a "bite" of the New York-New Jersey Harbor, which is the most populated region of the nation. It provides recreational opportunities including fishing, boating, and swimming to over 20 million residents, and yet it support a world class port for both passengers and cargo. It is also a repository for industrial and municipal effluents, while additional wastes are carried directly from land by regional currents. Harbor dredge spoils that are contaminated with heavy metals and organic pollutant also have been disposed of in this area. These materials have been dispersed and diluted over time; however, sediments have become contaminated as a result of such activities. When sediment becomes contaminated with heavy metals and other pollutants, they have the potential to adversely impact biological systems, including humans.

For all these reasons and more, those who work and play here should consider the Bight as resource worthy of protection. Although we can never restore this extraordinary resource to its pristine condition, we can make a difference-each of us can. Because pollution has degraded the marine life of the Bight, all the preexisting dump-sites in the New York Bight has been formerly closed to any further ocean disposal.

Results from this study help establish a sound scientific basis on which managers can consider resources when wastes are introduced to coastal marine environment. Since pollution in New York Bight environment occurs at much larger scale than any other urban centers, insights gained from this study may be of universal application.

Appendices

Appendix A

A 1.0. A Summary of History of Uses and Regulation of Ocean Disposal Sites in the New York Bight

A 2.0. a) Sources of Suspended Sediments Discharged into the Bight
b) Sources and Composition of Suspended Matter

A 3.0. Sediment Description

A 4.0. Summary of Sampling Techniques

A 5.0. AAS Techniques and Instrumental Parameters

Appendix A

A 1.0. A Summary of History of Uses and Regulation of Ocean Disposal Sites in the New York Bight.

WASTE DISPOSAL	HISTORY OF SITE USE AND REGULATION
1- ACID WASTE	-First used in 1984 -Interim site designation 1973 -EIS in 1980 -Final designation 1983 -No disposal since Sept. 1988 -Dedesignated in 1991
2- CELLAR DIRT	-In use since 1940 -Designated interim site 1973 -EIS in 1982 -Final designation 1983 -No disposal since Nov. 1989 -Redesignated 1994
3- DREDGED SPOIL	(1) Mud Dump Site (MDS) -Parts of MDS and vicinity in use since 1914 -Designated an interim site in 1973 -EIS in 1982 -Final designation in 1984 -Current status; preparation of Supplemental EIS (2) Inlet Sites -EIS in 1988 and sites designated in 1990 -Only small amounts disposed sporadically for beach nourishment (3) Deep water 106-Mile site -In use since 1961 -EPA first regulated in 1972 -EIS on 106-Mile site in 1980

Appendix A

A 1.0. A Summary of History of Uses and Regulation of Ocean Disposal Sites in the New York Bight (Continued)

WASTE DISPOSAL	HISTORY OF SITE AND REGULATION
4- INDUSTRIAL WASTE	(1) Deep water 106-Mile Site - In use since 1961 - EPA first regulation 1972 - EIS on 106-Mile Site in 1980 (2) Deep water Industrial Waste Disposal Site (within 106-Mile Site) -Designated site 1984 -Last disposal 1987 - Dedesignated in 1994
	(1) 12-Mile site -In use since 1924 -Designated an interim site in 1973 -EIS in 1978 -Final designation 1979 -Phase out began in 1986 and ended in 1989. -Redesignated in 1990
5- SEWAGE SLUDGE	
	(2) Deep water 106-Mile Site -In use since 1961 -EIS on 106-Mile site in 1980
	(3) Deepwater Municipal Sludge Dump Site (within 10-Mile site) -Designated site in 1984 -Disposal began 1986 -No disposal since June1992

(Adapted from Massa 1996 (modified))

Appendix A

A 2.0. a) Sources of Suspended Sediments Discharged into the Bight

Sources and input	x 10 tones/year
Direct Bight (68%)	
Dredged (54%)	4.7
Sludge (2.1%)	0.18
Cellar Dirt (6.8%)	0.60
Total barged (62.9%)	5.51
Atmospheric (5%)	0.45
Coastal zone 32%	
(98% of coastal zone input is through the Rockaway Sandy-Hook transect)	
Municipal wastewater (4%)	0.35
Industrial wastewater (0.2%)	0.02
Gauged runoff (16%)	1.4
Urban rain off (12%)	1.1
Total coastal zone	2.87
Total input	8.83

b) Sources and Composition of Suspended Matter

Source	Composition	
Rivers	80-90% minerals	10-20% Combustible organics
Estuaries	60-80% minerals and Biogenic shells	20-40% Combustible organics
Shelf	10-70% minerals and biogenic shells	30-90% Combustible organics

Appendix A

A 3.0. Sediment Descriptions

Location	Description
1)Mud Dump Site	
84	Gray muddy sand , with small shell fragments
84-1	Dark gray muddy sand, with small shell fragments
86	Dark gray sandy mud, with some fibrous plant debris
86-1	Dark gray sandy mud, with plant debris
86.2	Gray sandy mud with plant debris
87	Gray to green muddy sand, with small shell fragments and plant debris
85	Dark gray granular mud, with no shell fragments
85-1	Dark gray granular mud
2) Sewage sludge	
89A	Dark gray muddy sand, with plant debris and shell fragments
89C	Dark gray muddy sand, with shell fragments and plant debris
1	Brown sand , with few shell fragments
1-2	Light brown sand, with some shell fragments
71	Light gray silty sand, with plant debris and some shell fragments
91	Dark gray muddy sand, with few shell fragments and substantial amount of plant debris
3) Near shore mud-patches	
13	Clean light silty sand, with great amount of shell fragments
7-1	Clean light sand, with shell fragments and some plant debris
5	Clean sand, with substantial amount of shell fragments
5-1	Clean sand containing great amount of shell fragments
20A	Clean sand with presence of shell fragments
21	Light sand containing shell fragments
33	Green to gray muddy sand , with small shell fragments
33-1	Gray muddy sand containing shell fragments
37	Clean sand containing substantial amount of shell fragments
24	Light sand with the presence of some pieces of shells
4) Cholera bank	
62	Mixture of dark and light sand grains, with presence of plant debris and shell fragments
63	Sand containing plant and shell fragments

A 3.0. Sediment Descriptions (continued)

5) Sewage Sludge: Core 97-1 (0-45 cm)

Core depth (cm)	
0-2	Light sand, abundant shell fragment , mica, gain of quartz, pieces of coal up to 2 cm in diameter
5-6	Light sand, pieces of shells (same as 0-2), small pieces of coal, filament of plants
10-11	Light sand, fragment of shells up to 5 mm, pieces of coal up to 2 mm in size, clear to brown gains of quartz
15-16	Light sand, pieces of shells of less than 2mm , pieces of coal, White, clear to brown grains of quartz
20-21	Sand, presence of coal, pieces of slate up to 1cm long, Shell fragments present (1mm-1cm), clear to brown grains of quartz
25-26	Sand, coal, shell fragments (up to 1 cm in diameter), Clear to brown grains of quartz
30-31	Sand, shell fragment present, small pieces of coal (1mm), Brown to clear grains of quartz
35-36	Sand with presence of red brown concretions, presence of pieces and whole shells (1cm), pieces of coal up to 1 cm, Red brown concretion-easy to break (iron oxide as cement), angular to round pebble of quartz (>2mm)
40-41	Abundant shell fragments, presence of coal, iron oxide nodules, angular pebbles of quartz, presence of thick shells-up to 2mm thick

A 3.0. Sediment Descriptions (continued)

6) MDS: Core 97-9 (0-96cm)

Core depth (cm)	
5-6	Very muddy, shell fragments
9-10	Very sticky dark brown mud, brown wood, shell fragments up to 1 mm, pieces of mica (>1mm), clear gains of quartz, presence of coal
15-16	Very muddy, shell fragments
19-20	Dark brown mud (sticky), whole shell of clam (few mm to > 1 cm), lot of shells, some pieces of coal, pieces of mica
26-27	Dark brown mud, sand injection, whole and pieces of shells
29-30	Dark brown mud, whole shells (same as 19-20), presence of mica and coal, sand injection (beds of sand)
34-35	Light brown muddy sand, presence of coal, mica and pieces of white shells, filament of plants, white grains of quartz
36-37	Muddy sand, gains of quartz, mica, pieces of white shells
48-49	Very muddy and sticky, presence of quartz and mica
55-56	Very sticky mud , few pieces of shells, presence of coal, mica, clear grain of quartz in sand size fraction, plastic from liner
68-69	Very sticky mud, shell fragments, gains of quartz, no coal , no wood, few mica flakes, gravelly beds of sand
76-77	Sandy mud and sticky, pieces of shell, brown wood, no coal, clear grains of quartz
87-88	Very muddy, brown wood, very small white shell fragments,
95-96	Very muddy, presence of a lot of brown wood fragments (> 1cm), smooth pebbles, presence of coal and flakes of mica

Appendix A

A 4.0. Summary of Sampling Techniques

In this study, two series of sediment samples were analyzed. The first series of sediments were collected by Harris (1976). Bottom sediments were obtained with a Smith-McIntyre grab sampler. The upper 4 cm of sediment in the sampler was sampled over 3/8 of the surface area of the sampler with a plastic spoon, placed in a precleaned polyethylene jars (free of trace metals), and over 3/8 of the sampler surface area with stainless steel spoon, place in plasticizer-free NASCO Whirl-pack bags (TOC and TCH) and kept frozen until analysis. Plastic tubes about 4.4 cm in diameter were inserted to the depth of the grab in that area from which the surface sediment subsamples had been removed. Cored samples for trace metals, and TOC and TCH were extruded into polyethylene jars and Whirl-pack bags, respectively and kept frozen until analysis. All necessary precautions were taken so as to eliminate contamination, arrest bacterial action and preserve the integrity of the organic matter.

The second series of New York Bight sediments were sampled by McHugh (1997). The samples were kept refrigerated at Columbia University- Lamont Doherty Research Laboratories. The samples were collected aboard the New Jersey Marine Sciences Consortium Research Vessel, R/V Wallford. The R/V wallford was designated as an oceanographic research vessel under supervisions of 46 U.S.C2101 (18) by U.S Coast Guard. The ship is well equipped with the necessary navigational, laboratory, and mechanical facilities to support geological, biological, chemical, and physical oceanography research. Sample stations were established near and across the Mud-Dump Site and in the vicinity of the Sewage Sludge Site based on the detailed Sidescan-Sonar images and Sean Beam bathymetry obtained from the United States

Geological Survey (USGS). The Sampling locations were determined by using LORAN-C and Global Positioning System (GPS) or Differential (D-GPS).

A 5.0. AAS Techniques

The chemical compositions of the aqeous extracts were determined using a Perkin-Elmer atomic spectrophotometry (Model 3300) at Brooklyn College. The concentration of Pb, Cu, Zn, Ni, Cd, Cr and Mn in the extracts was measured at the following wavelengths 283.3, 324.8, 213.9, 232.0, 228.8, 357.9 and 279.5 nm, respectively.

The basic principle behind atomic absorption analysis is that the absorption of electromagnetic radiation (absorbance) at a specific wavelength characteristic of element being analyzed is directly proportional to the number of ground-state atoms of that element present in the light path. The incident light beam is attenuated by atomic vapor absorption according to Beer's law (A = kC). Beer's law states that A is directly proportional to the concentration of absorbing atom. Thus, if A is plotted against C the result shows a straight line of slope k that passes through the origin. This graph is known as "calibration curve". Each chemical element is posses a specific number of electrons. The most stable orbital configuration of an atom is known as ground-state. If energy is applied to an atom, the energy will be absorbed and the electrons occupying the outer shell of the atom will be promoted to what known as the exited state. To obtain a good results in the AAS, a beam of electromagnetic radiation characteristic of the resonant ground-state wavelength of the element being analyzed need to be passed through the optimum flame region (maximum number of ground state atoms) in order to maximize absorption. Concentrations of each element were calculated from calibration curves relating absorbance to concentration. This requires that the relationship between absorbance and concentration be linear, or as close to linear as possible.

When performing the analysis, optimizing of the instrument (with regard to sensitivity and range linearity) is achieved for each element separately. The matrix of the calibration standards are matched to that of the sample digests. The calibration standards are optimized both before and following each 10-sample batch so as to reflect changing flame conditions.

Detection limits of trace elements by AAS analysis

Element		Pb	Cu	Zn	Ni	Cd	Cr	Mn
Limits	Dry sediment (ppm)	2	1	1	2	0.5	1	2
	Solution (ppm)	0.02	0.01	0.01	0.01	0.005	0.01	0.02

Instrumental settings used for the method

Parameters	Pb	Cu	Zn	Ni	Cd	Cr	Mn	Fe
Wavelength (nm)	283.3	324.8	213.9	232.0	228.8	357.9	279.5	248.3
Slit Width (nm)	0.70	0.70	0.70	0.20	0.70	0.70	0.20	0.20
Lamp Current (mA)	10	15	15	25	4	25	20	30
Flame Type	A-A	A-A	A-A	A-A	A-A	A-A	A-A	A-A
Oxidant flow (L/min)	10.0	10.0	10.0	10.0	10.0	10.0	10.0	10.0
Fuel flow (L/min)	2.0	2.0	2.0	2.0	2.0	3.8	2.0	2.0
Read Time (Sec.)	3.0	3.0	3.0	3.0	3.0	3.0	3.0	3.0
Background correction	on	on	on	on	on	on	on	on

A-A = Air-Acetylene

Precision and Accuracy of the Analysis

The accuracy of the analytical methods utilized was referenced to the Standard Reference Material, NBS Estuarine sediment 1646a (U.S. National Bureau of Standards). The material for this SRM was dredged from the Chesapeake Bay by the Virginia Institute of Marine Sciences, Gloucester point, VA. The material was freeze-dried at Hanover Foods, Inc., Lancaster, PA, and transferred to the U.S. Geological Survey (USGS) in Denver, CO. The material was lightly deagglomerated and sieved through a 1 mm screen to remove coarse materials. The < 1 mm was

then ball milled to pass a (75 μm) 200 mesh and then blended in a single batch using a $10ft^3$ blender. The material was radiated sterilized at COBE laboratories, Lakewood, CO, and then bottled.

0.500 mg of the NBS SRM were digested and analyzed using the same procedures as was used for the sediment samples.

Appendix B

Appendix B

B 1.0. Sediment Particle Size
MDS

Site 84

Particle size (mm)	Particle size (Phi units)	Weight of sieved fraction (grams)	Cumulative weight of sieved fraction (grams)	Weight percent	Cumulative weight percent	Size class
>2	-1	0.000	0.000	0.00	0.00	Gravels
2-1	0	2.128	2.128	2.15	2.15	Very coarse sand
1-0.5	+1	11.338	13.466	11.46	13.60	Coarse sand
0.5-0.25	+2	17.785	31.251	17.97	31.58	Medium sand
0.25-0.125	+3	28.800	60.051	29.10	60.67	Fine sand
0.125-0.0625	+4	30.600	90.651	30.91	91.58	Very fine sand
<0.0625	+5	8.320	98.971	8.40	100.00	Silt and clay

Total weight before sieving: 99.50 grams
Total weight of sieved fraction: 98.971 grams
Percent of dry weight: 99.47%

Site 86

Particle size (mm)	Particle size (Phi units)	Weight of sieved fraction (grams)	Cumulative weight of sieved fraction (grams)	Weight percent	Cumulative weight percent	Size class
>2	-1	0.000	0.000	0.00	0.00	Gravels
2-1	0	0.000	0.000	0.00	0.00	Very coarse sand
1-0.5	+1	0.189	0.189	0.20	0.20	Coarse sand
0.5-0.25	+2	2.957	3.146	3.27	3.48	Medium sand
0.25-0.125	+3	24.464	27.61	27.10	30.58	Fine sand
0.125-0.0625	+4	20.323	47.933	22.51	53.09	Very fine sand
<0.0625	+5	42.346	90.279	46.90	100.00	Silt and clay

Total weight before sieving: 91.00 grams
Total weight of sieved fraction: 90.279 grams
Percent of dry weight: 99.20%

Site 87

Particle size (mm)	Particle size (Phi units)	Weight of sieved fraction (grams)	Cumulative weight of sieved fraction (grams)	Weight percent	Cumulative weight percent	Size class
>2	-1	0.000	0.000	0.00	0.00	Gravels
2-1	0	2.313	2.313	2.06	2.06	Very coarse sand
1-0.5	+1	15.291	17.604	13.61	15.68	Coarse sand
0.5-0.25	+2	21.196	38.800	18.87	34.55	Medium sand
0.25-0.125	+3	31.011	69.811	27.61	62.16	Fine sand
0.125-0.0625	+4	21.270	91.081	18.94	81.10	Very fine sand
<0.0625	+5	21.219	112.300	18.89	100.00	Silt and clay

Total weight before sieving: 113.00 grams
Total weight of sieved fraction: 112.3 grams
Percent of dry weight: 99.38 %

B 1.0. Sediments Particle Size (continued)

Sewage Sludge

Site 89A

Particle size (mm)	Particle size (Phi units)	Weight of sieved fraction (grams)	Cumulative weight of sieved fraction (grams)	Weight percent	Cumulative weight percent	Size class
>2	-1	0.000	0.000	0.00	0.00	Gravels
2-1	0	1.384	1.384	1.075	1.075	Very coarse sand
1-0.5	+1	10.681	12.065	8.30	9.37	Coarse sand
0.5-0.25	+2	45.966	58.031	35.70	45.08	Medium sand
0.25-0.125	+3	37.432	95.463	29.08	74.15	Fine sand
0.125-0.0625	+4	12.165	107.628	9.45	83.60	Very fine sand
<0.0625	+5	21.104	128.732	16.39	100.00	Silt and clay

Total weight before sieving: 129.00 grams
Total weight of sieved fraction: 128.732.00 grams
Percent of dry weight: 99.79%

Site 91

Particle size (mm)	Particle size (Phi units)	Weight of sieved fraction (grams)	Cumulative weight of sieved fraction (grams)	Weight percent	Cumulative weight percent	Size class
>2	-1	0.000	0.000	0.00	0.00	Gravels
2-1	0	0.621	0.621	0.49	0.49	Very coarse sand
1-0.5	+1	1.774	2.395	1.40	1.89	Coarse sand
0.5-0.25	+2	2.625	5.02	2.07	3.96	Medium sand
0.25-0.125	+3	83.519	88.539	65.87	69.82	Fine sand
0.125-0.0625	+4	25.049	113.588	19.75	89.58	Very fine sand
<0.0625	+5	13.211	126.799	10.42	100.00	Silt and clay

Total weight before sieving: 127.00 grams
Total weight of sieved fraction: 126.799 grams
Percent of dry weight: 99.84%

Site 71

Particle size (mm)	Particle size (Phi units)	Weight of sieved fraction (grams)	Cumulative weight of sieved fraction (grams)	Weight percent	Cumulative weight percent	Size class
>2	-1	0.000	0.000	0.00	0.00	Gravels
2-1	0	0.223	0.223	0.21	0.21	Very coarse sand
1-0.5	+1	1.032	1.255	0.98	1.19	Coarse sand
0.5-0.25	+2	5.487	6.742	5.20	3.39	Medium sand
0.25-0.125	+3	55.698	62.440	52.77	59.16	Fine sand
0.125-0.0625	+4	39.971	102.411	37.87	97.03	Very fine sand
<0.0625	+5	3.136	105.547	2.97	100.00	Silt and clay

Total weight before sieving: 106.00 grams
Total weight of sieved fractions: 105.547 grams
Percent of dry weight: 99.57 %

B 1.0. Sediments Particle Size (continued)

Near Shore Mud-Patches

Site 54A

Particle size (mm)	Particle size (Phi units)	Weight of sieved fraction (grams)	Cumulative weight of sieved fraction (grams)	Weight percent	Cumulative weight percent	Size class
>2	-1	0.000	0.000	0.00	0.00	Gravels
2-1	0	34.766	34.766	17.09	17.09	Very coarse sand
1-0.5	+1	84.021	118.787	41.30	58.40	Coarse sand
0.5-0.25	+2	67.820	186.607	33.34	91.73	Medium sand
0.25-0.125	+3	13.753	200.32	6.74	98.50	Fine sand
0.125-0.0625	+4	2.919	203.239	1.43	99.91	Very fine sand
<0.0625	+5	0.180	203.419	0.088	100.00	Silt and clay

Total weight before sieving: 204.00 grams
Total weight of sieved fraction: 203.419 grams
Percent of dry weight: 99.71%

Site 56

Particle size (mm)	Particle size (Phi units)	Weight of sieved fraction (grams)	Cumulative weight of sieved fraction (grams)	Weight percent	Cumulative weight percent	Size class
>2	-1	0.000	0.000	0.00	0.00	Gravels
2-1	0	7.102	7.102	5.03	5.03	Very coarse sand
1-0.5	+1	61.792	68.894	43.72	48.75	Coarse sand
0.5-0.25	+2	58.764	127.658	41.58	90.45	Medium sand
0.25-0.125	+3	9.761	137.419	6.90	97.24	Fine sand
0.125-0.0625	+4	2.978	140.397	2.10	99.35	Very fine sand
<0.0625	+5	0.918	141.315	0.65	100.00	Silt and clay

Total weight before sieving: 142.00 grams
Total weight of sieved fraction: 141.315 grams
Percent of dry weight: 99.52%

Site 37A

Particle size (mm)	Particle size (Phi units)	Weight of sieved fraction (grams)	Cumulative weight of sieved fraction (grams)	Weight percent	Cumulative weight percent	Size class
>2	-1	0.000	0.000	0.00	0.00	Gravels
2-1	0	30.822	30.822	17.39	17.39	Very coarse sand
1-0.5	+1	81.085	111.907	45.74	63.12	Coarse sand
0.5-0.25	+2	49.151	161.058	27.72	90.85	Medium sand
0.25-0.125	+3	14.215	175.273	8.01	98.86	Fine sand
0.125-0.0625	+4	1.862	177.135	1.05	99.92	Very fine sand
<0.0625	+5	0.146	177.281	0.082	100.00	Silt and clay

Total weight before sieving: 178.00 grams
Total weight of sieved fraction: 177.281 grams
Percent of dry weight: 99.60%

Near shore Mud-Patches (continued)

Site 7-1

Particle size (mm)	Particle size (Phi units)	Weight of sieved fraction (grams)	Cumulative weight of sieved fraction (grams)	Weight percent	Cumulative weight percent	Size class
>2	-1	0.000	0.000	0.00	0.00	Gravels
2-1	0	7.947	7.947	5.60	5.60	Very coarse sand
1-0.5	+1	7.433	15.38	5.24	10.84	Coarse sand
0.5-0.25	+2	37.790	53.17	26.63	37.48	Medium sand
0.25-0.125	+3	53.751	106.921	37.89	75.36	Fine sand
0.125-0.0625	+4	31.005	137.926	21.85	97.21	Very fine sand
<0.0625	+5	3.952	141.878	2.78	100.00	Silt and clay

Total weight before sieving: 142.00 grams
Total weight of sieved fraction: 141.878 grams
Percent of dry weight: 99.91%

Site 5

Particle size (mm)	Particle size (Phi units)	Weight of sieved fraction (grams)	Cumulative weight of sieved fraction (grams)	Weight percent	Cumulative weight percent	Size class
>2	-1	0.000	0.000	0.00	0.00	Gravels
2-1	0	5.240	5.240	3.07	3.07	Very coarse sand
1-0.5	+1	11.594	16.834	6.80	9.87	Coarse sand
0.5-0.25	+2	41.602	58.436	24.40	34.28	Medium sand
0.25-0.125	+3	89.993	148.429	52.79	87.06	Fine sand
0.125-0.0625	+4	21.289	169.718	12.49	99.55	Very fine sand
<0.0625	+5	0.766	170.484	0.45	100.00	Silt and clay

Total weight before sieving: 171.00 grams
Total weight of sieved fraction: 170.484 grams
Percent of dry weight: 99.70%

Site 20A

Particle size (mm)	Particle size (Phi units)	Weight of sieved fraction (grams)	Cumulative weight of sieved fraction (grams)	Weight percent	Cumulative weight percent	Size class
>2	-1	0.000	0.000	0.00	0.00	Gravels
2-1	0	1.188	1.188	0.65	0.65	Very coarse sand
1-0.5	+1	8.245	9.433	4.48	5.13	Coarse sand
0.5-0.25	+2	24.781	34.214	13.47	18.60	Medium sand
0.25-0.125	+3	110.029	144.243	59.82	78.42	Fine sand
0.125-0.0625	+4	37.269	181.512	20.26	98.68	Very fine sand
<0.0625	+5	2.421	183.933	1.31	100.00	Silt and clay

Total weight before sieving: 184.00 grams
Total weight of sieved fraction: 183.933 grams
Percent of dry weight: 99.96%

Near Shore Mud-Patches (continued)

Site 37

Particle size (mm)	Particle size (Phi units)	Weight of sieved fraction (grams)	Cumulative weight of sieved fraction (grams)	Weight percent	Cumulative weight percent	Size class
>2	-1	0.000	0.000	0.00	0.00	Gravels
2-1	0	41.145	41.145	22.05	22.05	Very coarse sand
1-0.5	+1	90.036	131.181	48.26	70.32	Coarse sand
0.5-0.25	+2	45.244	176.425	24.25	94.57	Medium sand
0.25-0.125	+3	8.302	184.727	4.45	99.00	Fine sand
0.125-0.0625	+4	1.761	186.488	0.94	99.96	Very fine sand
<0.0625	+5	0.072	186.560	0.039	100.00	Silt and clay

Total weight before sieving: 187.00 grams
Total weight of sieved fraction: 186.56 grams
Percent of dry weight: 99.76%

Site 33-1

Particle size (mm)	Particle size (Phi units)	Weight of sieved fraction (grams)	Cumulative weight of sieved fraction (grams)	Weight percent	Cumulative weight percent	Size class
>2	-1	0.000	0.000	0.00	0.00	Gravels
2-1	0	8.499	8.499	5.83	4.83	Very coarse sand
1-0.5	+1	17.792	26.291	12.22	18.06	Coarse sand
0.5-0.25	+2	16.088	42.379	11.05	29.11	Medium sand
0.25-0.125	+3	74.636	117.015	51.26	80.37	Fine sand
0.125-0.0625	+4	23.813	140.828	16.35	96.72	Very fine sand
<0.0625	+5	4.770	145.598	3.28	100.00	Silt and clay

Total weight before sieving: 146.00 grams
Total weight of sieved fraction: 145.598 grams
Percent of dry weight: 99.72%

Site 20A

Particle size (mm)	Particle size (Phi units)	Weight of sieved fraction (grams)	Cumulative weight of sieved fraction (grams)	Weight percent	Cumulative weight percent	Size class
>2	-1	0.000	0.000	0.00	0.00	Gravels
2-1	0	0.342	0.342	0.18	0.18	Very coarse sand
1-0.5	+1	4.903	5.245	2.62	2.80	Coarse sand
0.5-0.25	+2	24.288	29.533	13.00	15.81	Medium sand
0.25-0.125	+3	100.280	129.813	53.70	69.50	Fine sand
0.125-0.0625	+4	53.566	183.379	28.68	98.18	Very fine sand
<0.0625	+5	3.405	186.784	1.82	100.00	Silt and clay

Total weight before sieving
Total weight of sieved fraction: 186.784 grams
Percent of dry weight: 99.88%

Near Shore Mud-Patches (continued)

Site 13

Particle size (mm)	Particle size (Phi units)	Weight of sieved fraction (grams)	Cumulative weight of sieved fraction (grams)	Weight percent	Cumulative weight percent	Size class
>2	-1	0.000	0.000	0.00	0.00	Gravels
2-1	0	0.321	0.321	0.19	0.19	Very coarse sand
1-0.5	+1	0.723	1.044	0.43	0.62	Coarse sand
0.5-0.25	+2	17.04	18.084	10.11	10.73	Medium sand
0.25-0.125	+3	91.03	109.114	54.00	64.76	Fine sand
0.125-0.0625	+4	54.52	163.634	32.36	97.13	Very fine sand
<0.0625	+5	4.839	168.473	2.87	100.00	Silt and clay

Total weight before sieving: 169.00 grams
Total weight of sieved fraction: 168.473 grams
Percent of dry weight: 99.86%

Site 21-A

Particle size (mm)	Particle size (Phi units)	Weight of sieved fraction (grams)	Cumulative weight of sieved fraction (grams)	Weight percent	Cumulative weight percent	Size class
>2	-1	0.000	0.000	0.00	0.00	Gravels
2-1	0	0.981	0.981	0.79	0.79	Very coarse sand
1-0.5	+1	3.557	4.538	2.89	3.68	Coarse sand
0.5-0.25	+2	30.773	35.311	25.00	28.65	Medium sand
0.25-0.125	+3	68.909	104.22	55.91	84.57	Fine sand
0.125-0.0625	+4	17.442	121.662	14.15	98.73	Very fine sand
<0.0625	+5	1.568	123.23	1.27	100.00	Silt and clay

Total weight before sieving: 123.489 grams
Total weight of sieved fraction: 123.23 grams
Percent of dry weight: 99.79%

Site 13-1

Particle size (mm)	Particle size (Phi units)	Weight of sieved fraction (grams)	Cumulative weight of sieved fraction (grams)	Weight percent	Cumulative weight percent	Size class
>2	-1	0.000	0.000	0.00	0.00	Gravels
2-1	0	0.620	0.620	0.32	0.32	Very coarse sand
1-0.5	+1	2.853	3.473	1.49	1.82	Coarse sand
0.5-0.25	+2	22.519	25.992	11.79	13.62	Medium sand
0.25-0.125	+3	117.142	143.134	61.37	75.00	Fine sand
0.125-0.0625	+4	45.489	188.623	23.83	98.81	Very fine sand
<0.0625	+5	2.259	190.882	1.18	100.00	Silt and clay

Total weight before sieving: 191.00 grams
Total weight of sieved fraction: 190.882
Percent of dry weight: 99.93%

Near Shore Mud-Patches (continued)

Site 37B-1

Particle size (mm)	Particle size (Phi units)	Weight of sieved fraction (grams)	Cumulative weight of sieved fraction (grams)	Weight percent	Cumulative weight percent	Size class
>2	-1	0.000	0.000	0.00	0.00	Gravels
2-1	0	17.826	17.826	9.04	9.04	Very coarse sand
1-0.5	+1	82.292	100.118	41.74	50.78	Coarse sand
0.5-0.25	+2	77.540	177.658	39.33	90.11	Medium sand
0.25-0.125	+3	17.185	194.843	8.71	98.83	Fine sand
0.125-0.0625	+4	1.983	196.826	1.00	99.84	Very fine sand
<0.0625	+5	0.316	197.142	0.16	100.00	Silt and clay

Total weight before sieving: 197.50 grams
Total weight of sieved fraction: 197.142 grams
Percent of dry weight: 99.82%

Site 5-1

Particle size (mm)	Particle size (Phi units)	Weight of sieved fraction (grams)	Cumulative weight of sieved fraction (grams)	Weight percent	Cumulative weight percent	Size class
>2	-1	0.064	0.064	0.037	0.037	Gravels
2-1	0	9.768	9.832	5.66	5.70	Very coarse sand
1-0.5	+1	9.528	19.36	5.52	11.21	Coarse sand
0.5-0.25	+2	13.252	32.612	7.68	18.89	Medium sand
0.25-0.125	+3	102.221	134.833	59.21	78.11	Fine sand
0.125-0.0625	+4	35.051	169.884	20.30	98.41	Very fine sand
<0.0625	+5	2.736	172.62	1.58	100.00	Silt and clay

Total weight before sieving: 173.00 grams
Total weight of sieved fraction: 172.62 grams
Percent of dry weight: 99.78%

Sediment Particle Size (Continued)

Cholera Bank

Site 62

Particle size (mm)	Particle size (Phi units)	Weight of sieved fraction (grams)	Cumulative weight of sieved fraction (grams)	Weight percent	Cumulative weight percent	Size class
>2	-1	0.000	0.000	0.00	0.00	Gravels
2-1	0	0.000	0.000	0.00	0.00	Very coarse sand
1-0.5	+1	0.098	0.098	0.063	0.063	Coarse sand
0.5-0.25	+2	0.934	1.032	0.60	0.67	Medium sand
0.25-0.125	+3	126.810	127.842	82.25	82.92	Fine sand
0.125-0.0625	+4	25.597	153.439	16.60	99.52	Very fine sand
<0.0625	+5	0.737	154.176	0.48	100.00	Silt and clay

Total weight before sieving: 154.5 grams
Total weight of sieved fraction: 154.176 grams
Percent of dry weight: 99.79%

Site 63

Particle size (mm)	Particle size (Phi units)	Weight of sieved fraction (grams)	Cumulative weight of sieved fractions (grams)	Weight percent	Cumulative weight percent	Size class
>2	-1	0.000	0.000	0.00	0.00	Gravels
2-1	0	0.000	0.000	0.00	0.00	Very coarse sand
1-0.5	+1	0.581	0.581	0.58	0.58	Coarse sand
0.5-0.25	+2	2.447	3.028	2.46	3.04	Medium sand
0.25-0.125	+3	66.246	69.274	66.48	73.14	Fine sand
0.125-0.0625	+4	29.205	98.479	29.30	98.83	Very fine sand
<0.0625	+5	1.168	99.647	1.17	100.00	Silt and clay

Total weight before sieving: 100.00 grams
Total weight of sieved fractions: 99.647 grams
Percent of dry weight: 99.647%

Site 63-1

Particle size (mm)	Particle size (Phi units)	Weight of sieved fraction (grams)	Cumulative weight of sieved fraction (grams)	Weight percent	Cumulative weight percent	Size class
>2	-1	0.000	0.000	0.00	0.00	Gravels
2-1	0	0.048	0.048	0.03	0.03	Very coarse sand
1-0.5	+1	0.827	0.875	0.51	0.54	Coarse sand
0.5-0.25	+2	3.514	4.389	2.19	2.73	Medium sand
0.25-0.125	+3	115.005	119.394	71.56	74.29	Fine sand
0.125-0.0625	+4	38.228	157.622	23.79	98.08	Very fine sand
<0.0625	+5	3.082	160.704	1.91	100.00	Silt and clay

Total weight before sieving: 161.00 grams
Total weight of sieved fraction: 160.704 gram**s**
Percent of dry weight: 99.81%

Appendix B

B 2.0. Frequency-Distribution Curves

Mud Dump Site

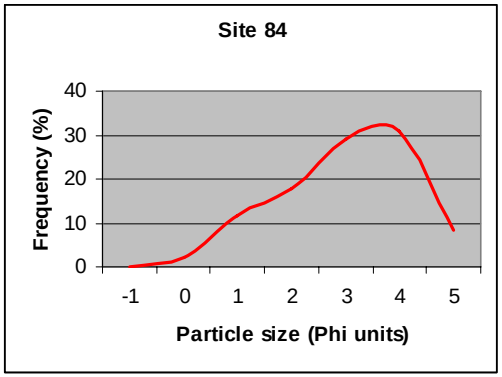

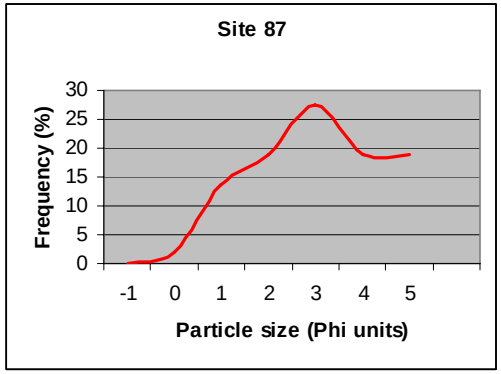

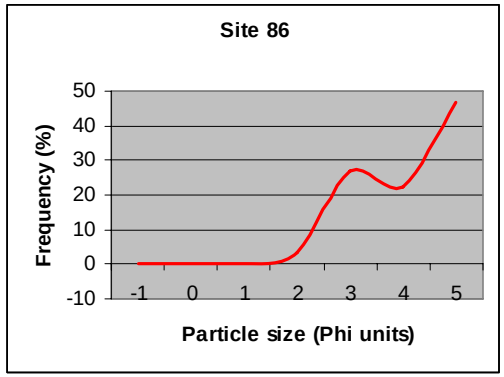

B 2.0. Frequency-Distribution Curves (continued)

Sewage Sludge Dumpsite

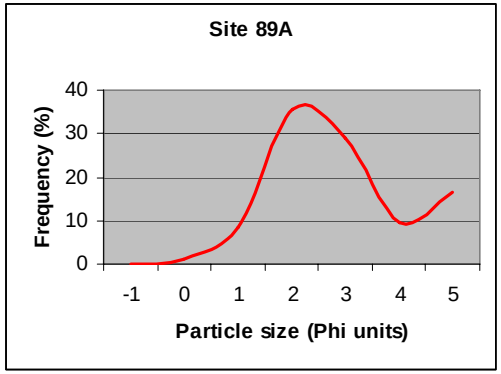

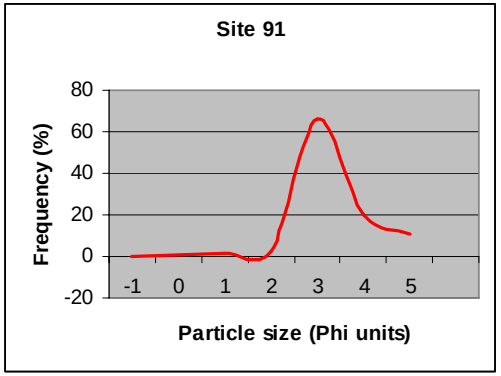

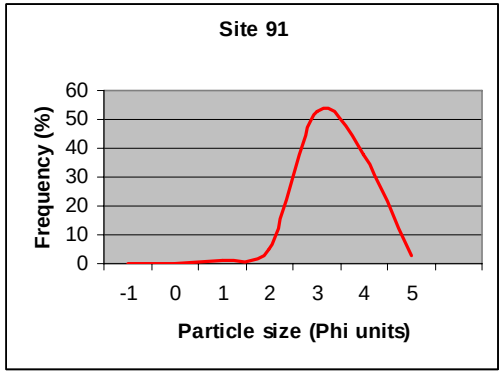

B 2.0. Frequency-Distribution Curves (continued)
Cholera Bank

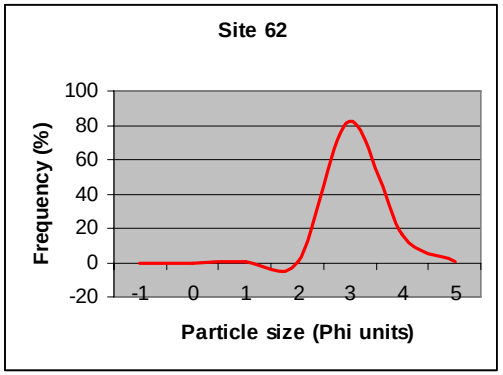

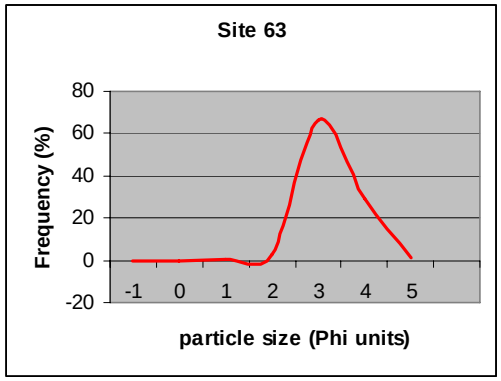

B 2.0 Frequency-Distribution Curves (continued)

Near shore mud-patches

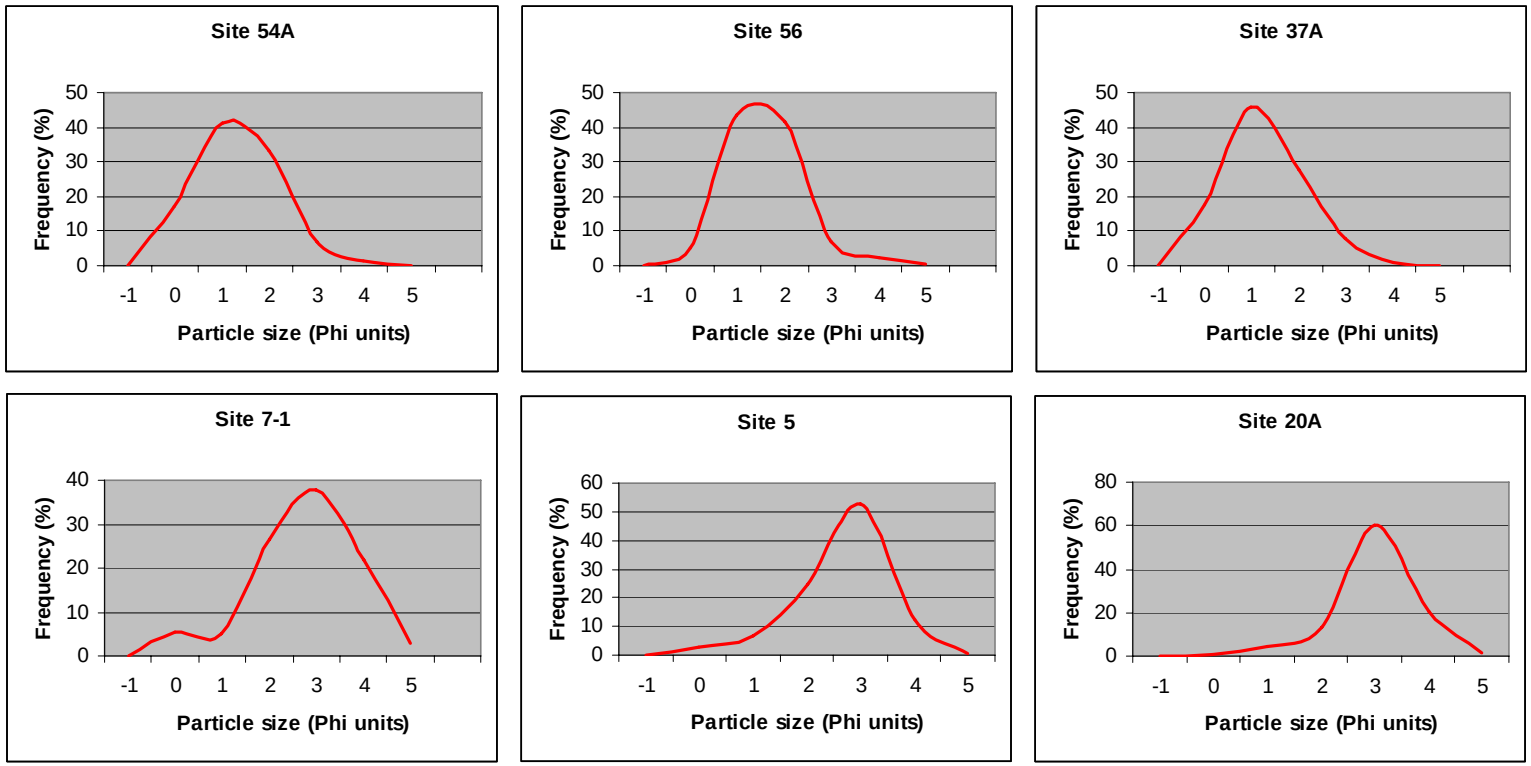

B 2.0. Frequency-Distribution Curves
Near shore mud-patches (continued)

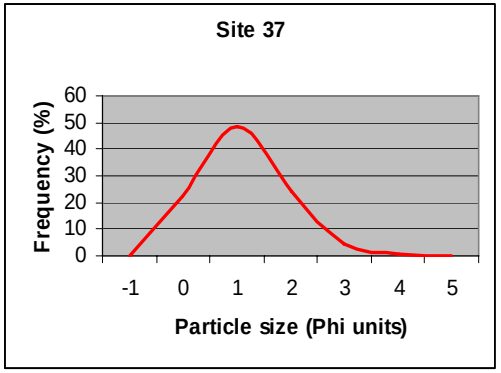

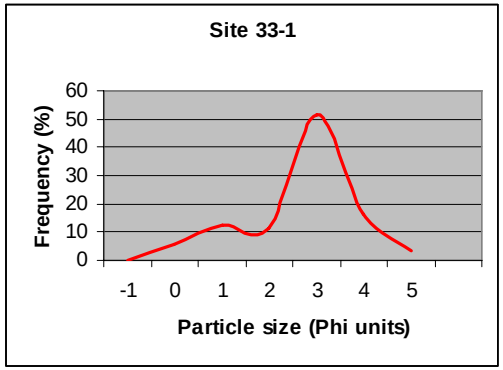

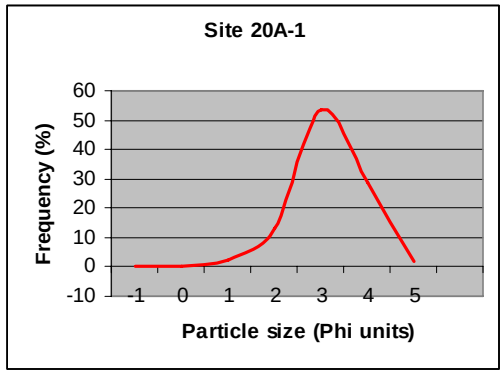

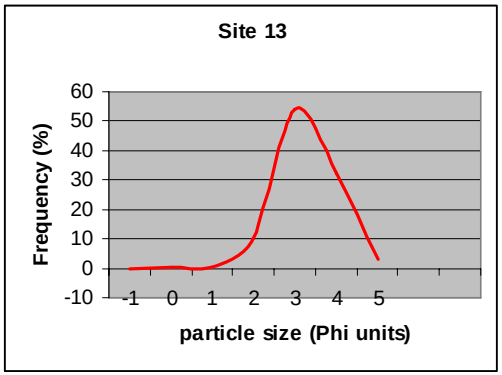

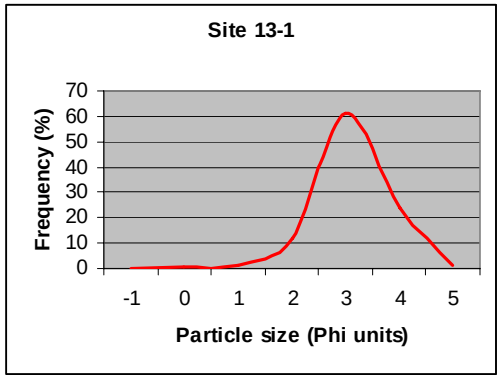

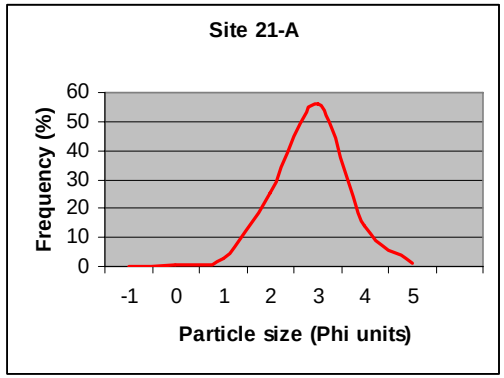

B 2.0. Frequency-Distribution Curves
Nearshore mud-patches (continued)

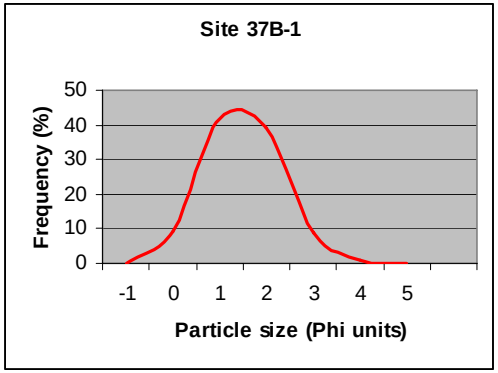

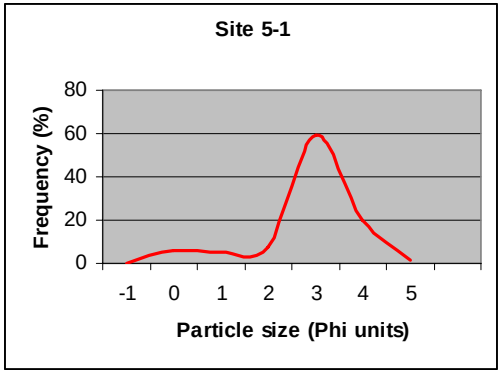

Appendix B

B 3.0. Arithmetic-Distribution Curves (continued)

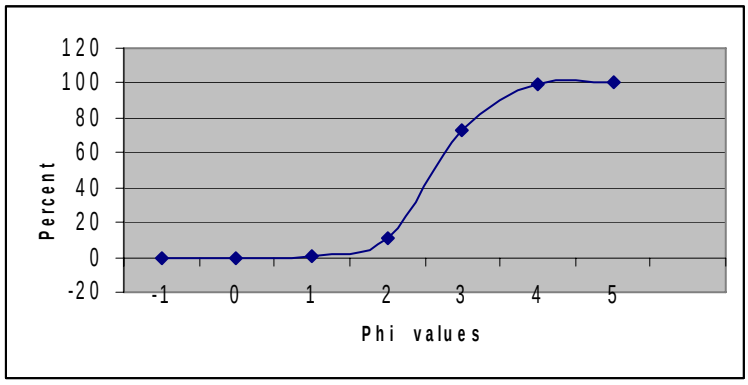

Arithmetic-distribution curve of sediment from the site 63

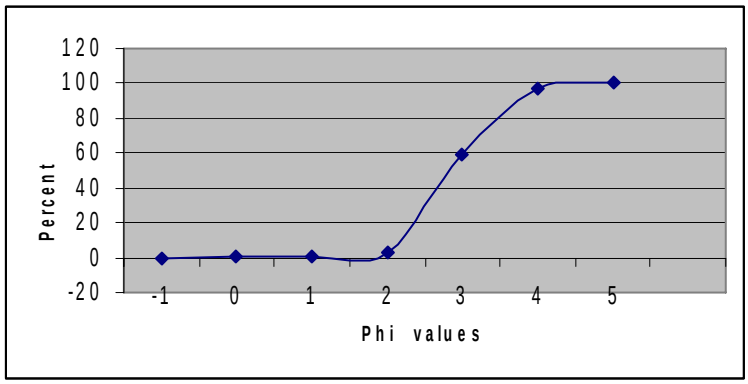

Arithmetic-distribution curve of sediment from the site 71

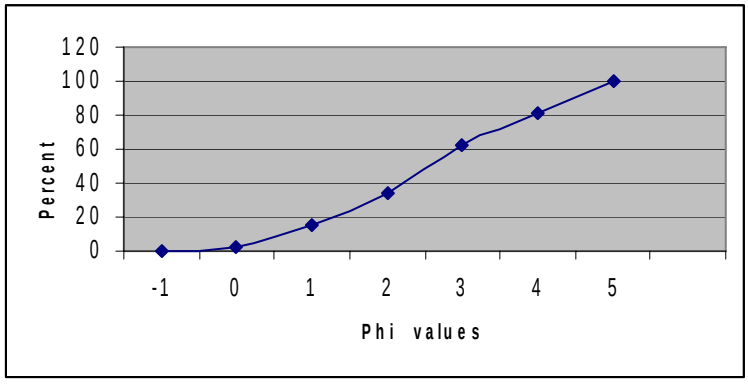

Arithmetic-distribution curve of sediment from the site 87

Appendix B

B 3.0. Arithmetic-Distribution Curves (continued)

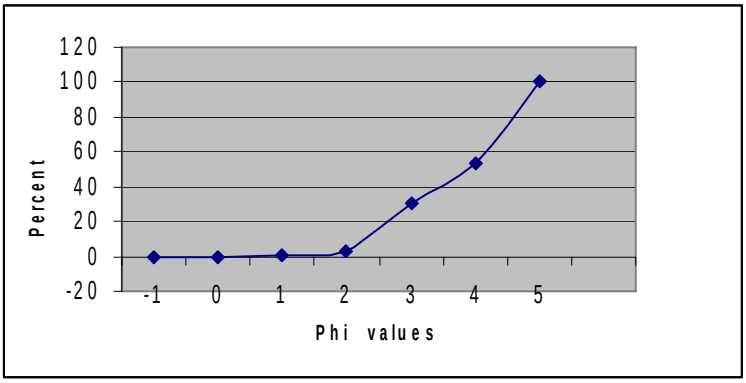

Arithmetic-distribution curve of sediment from the site 86

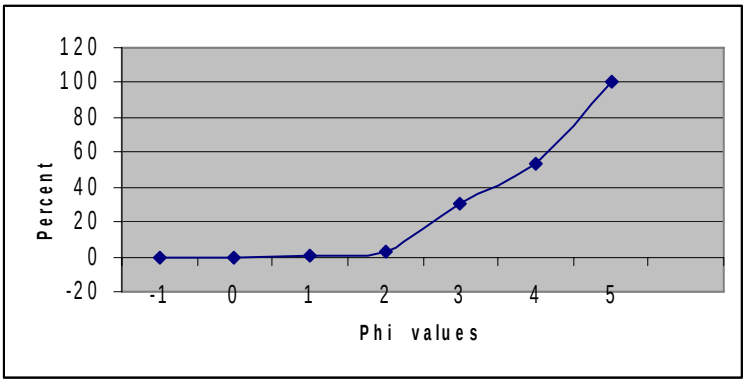

Arithmetic-distribution curve of sediment from the site 89A

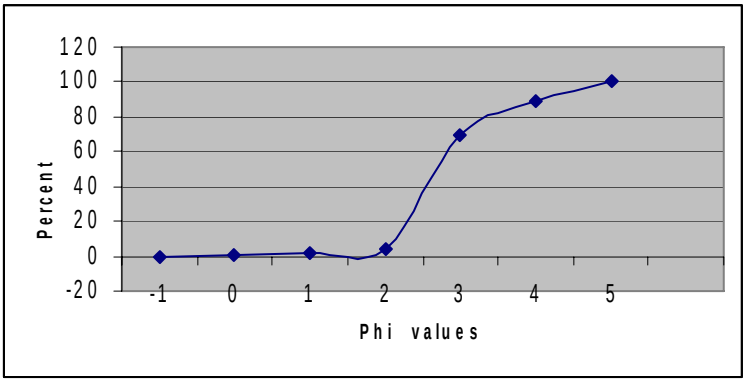

Arithmetic-distribution curve of sediment from the site 91

Appendix B

B 3.0. Arithmetic-Distribution Curves (continued)

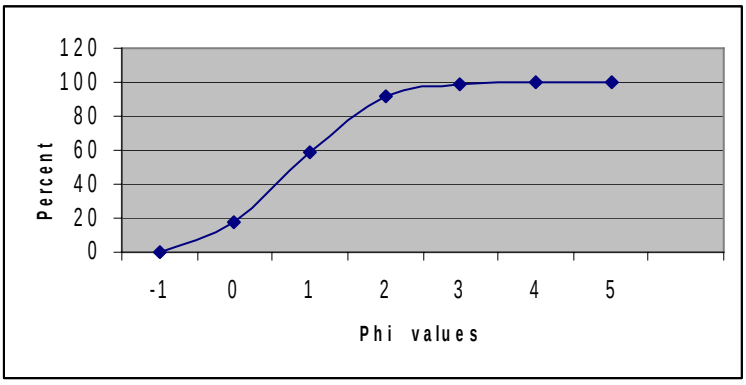

Arithmetic-distribution curve of sediment from the site 54A

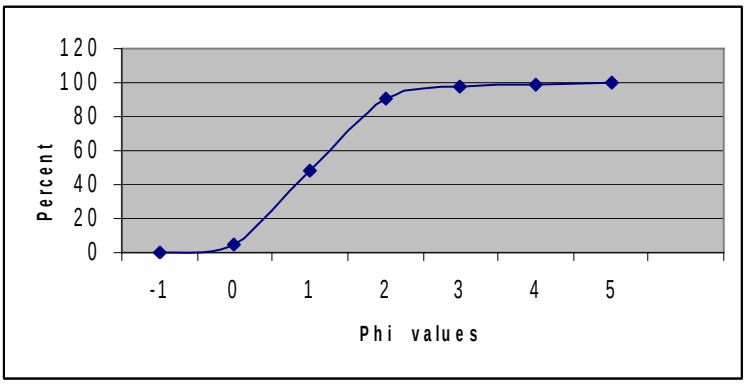

Arithmetic-distribution curve of sediment from the site 56

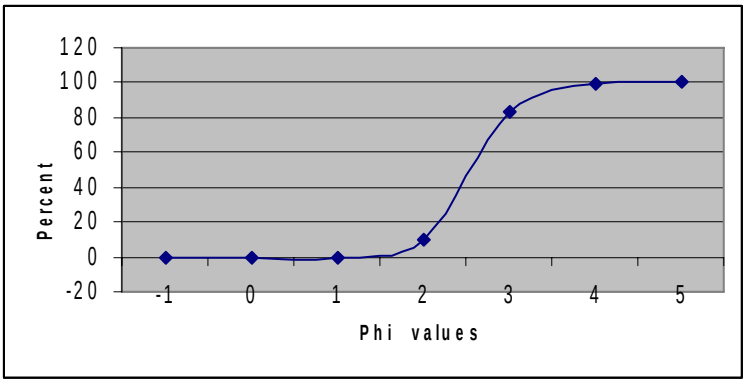

Arithmetic-distribution curve of sediment from the site 62

Appendix B

B 3.0. Arithmetic-Distribution Curves (continued)

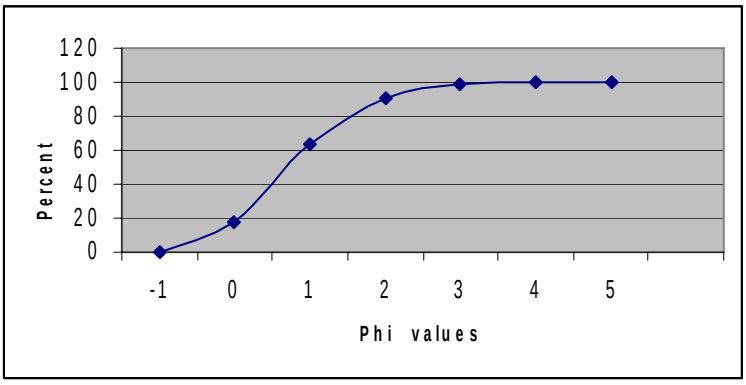

Arithmetic-distribution curve of sediment from the site 37A

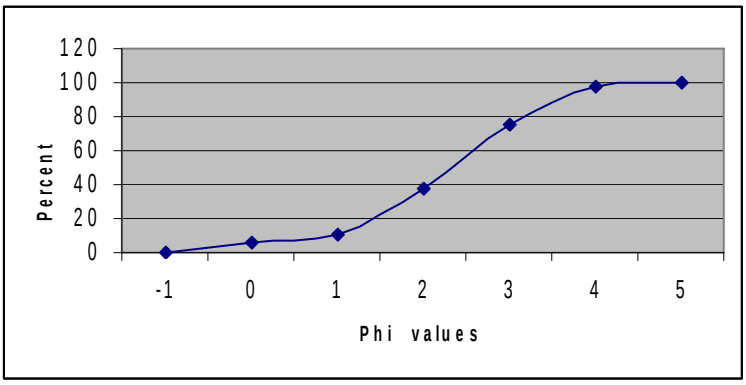

Arithmetic-distribution curve of sediment from the site 7-1

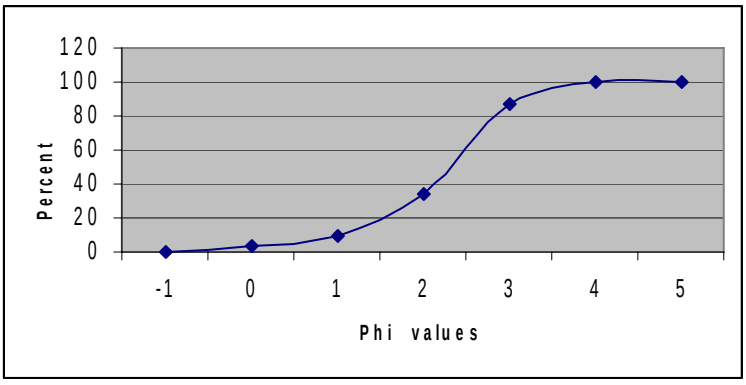

Arithmetic-distribution curve of sediment from the site 5

Appendix B

B 3.0. Arithmetic-Distribution Curves (continued)

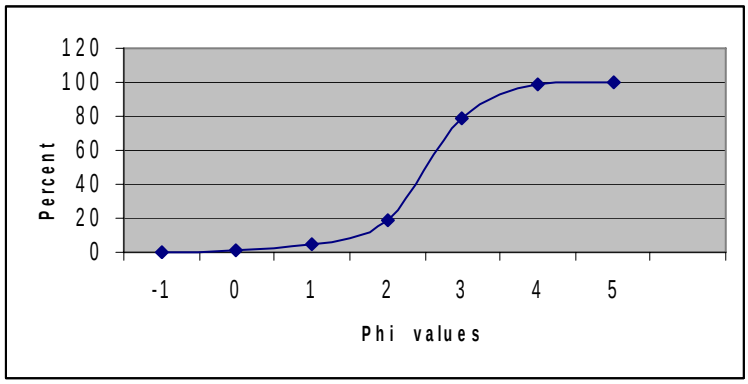

Arithmetic-distribution curve of sediment from the site 20A

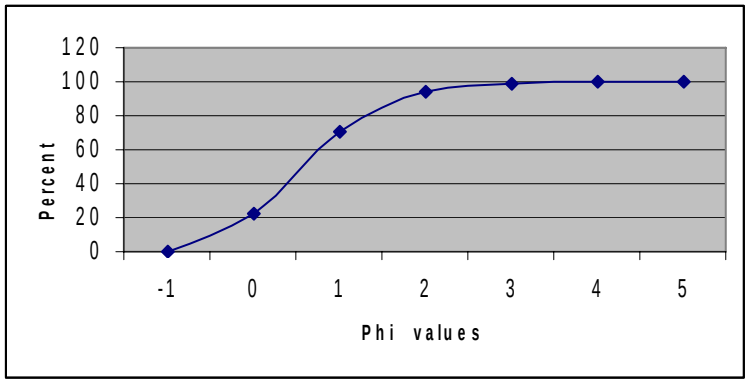

Arithmetic-distribution curve of sediment from the site 37

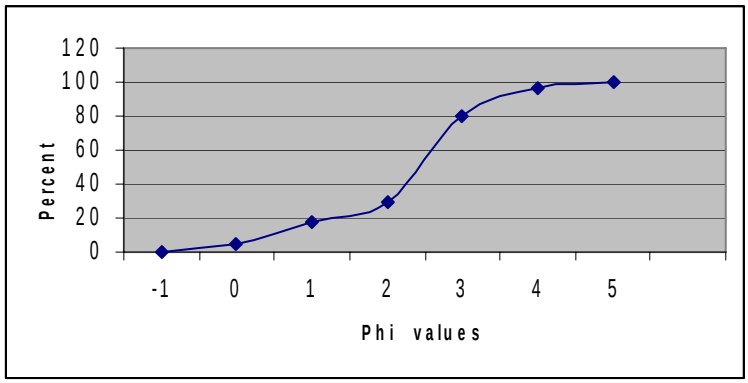

Arithmetic-distribution curve of sediment from the site 33-1

Appendix B

B 3.0. Arithmetic-Distribution Curves (continued)

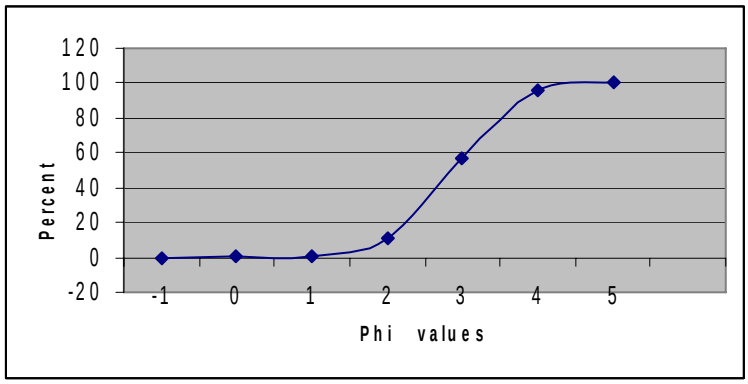

Arithmetic-distribution curve of sediment from the site 1-2

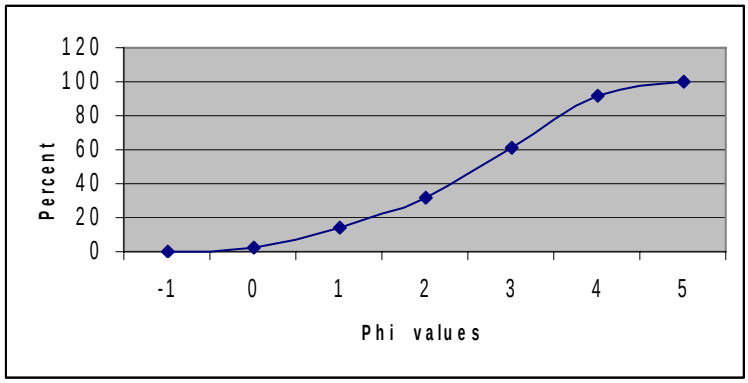

Arithmetic-distribution curve of sediment from the site 84

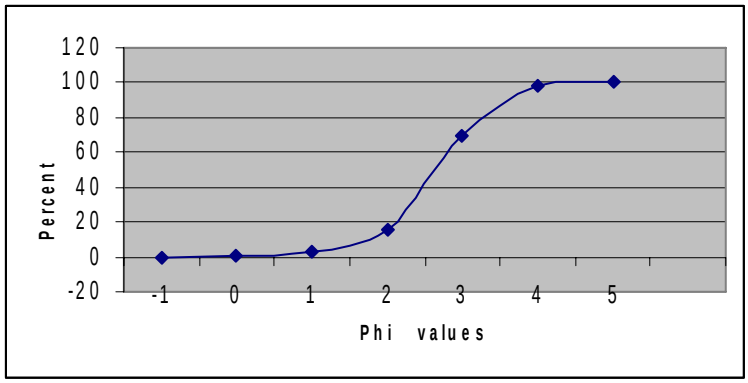

Arithmetic-distribution curve of sediment from the site 20A

Appendix B

B 3.0. Arithmetic-Distribution Curves (continued)

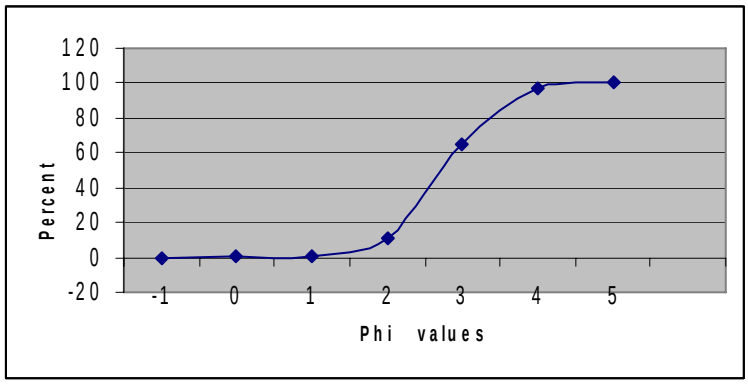

Arithmetic-distribution curve of sediment from the site 13

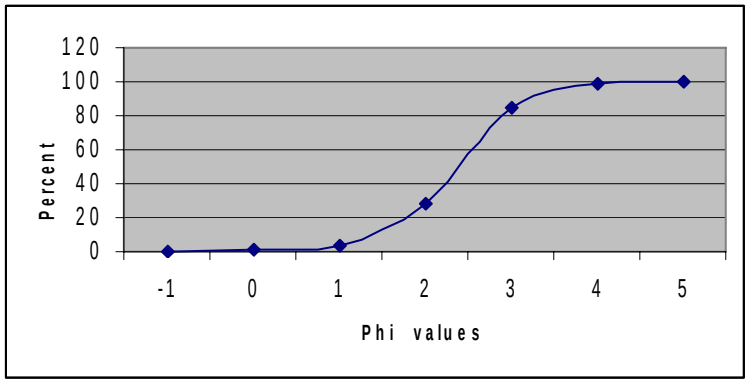

Arithmetic-distribution curve of sediment from the site 21-A

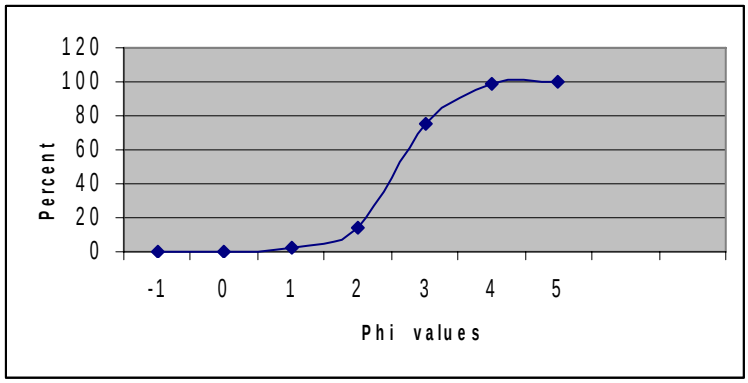

Arithmetic-distribution curve of sediment from the site 13-1

Appendix B

B 3.0. Arithmetic-Distribution Curves (continued)

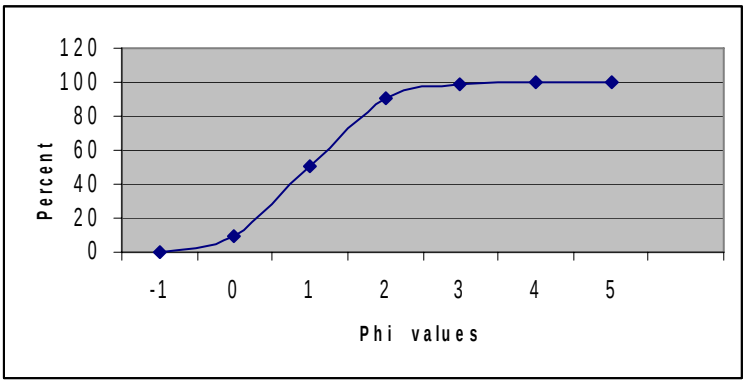

Arithmetic-distribution curve of sediment from the site 37B-1

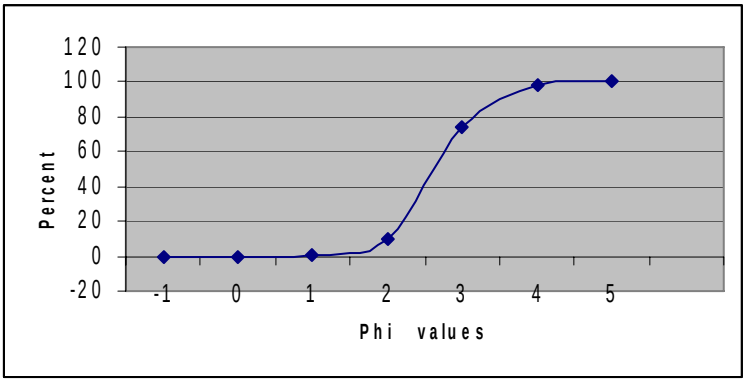

Arithmetic-distribution curve of sediment from the site 63

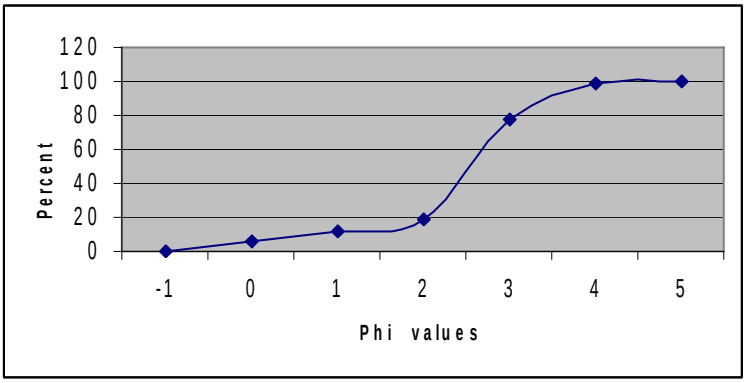

Arithmetic-distribution curve of sediment from the site 5-1

Appendix B

B 4.0. Cumulative-Distribution Curves

Mud Dump Site

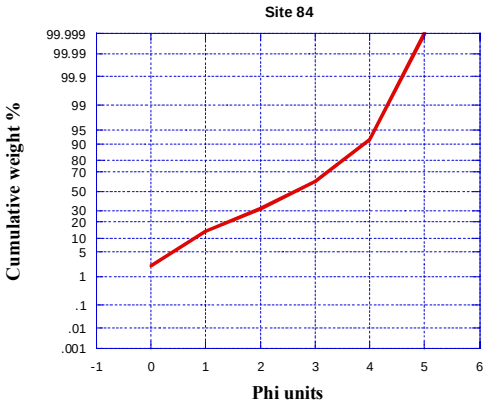

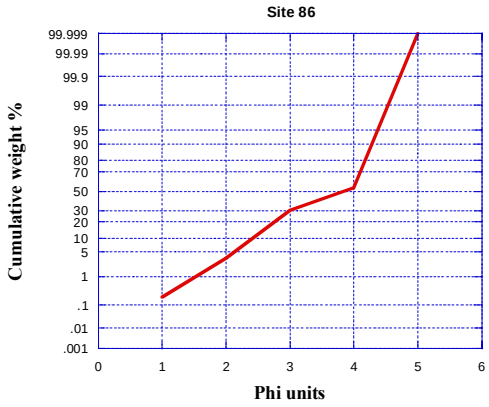

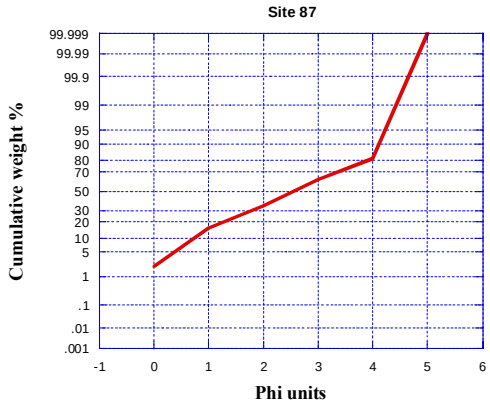

B 4.0. Cumulative-Distribution Curves (continued)

Sewage Sludge Dumpsite

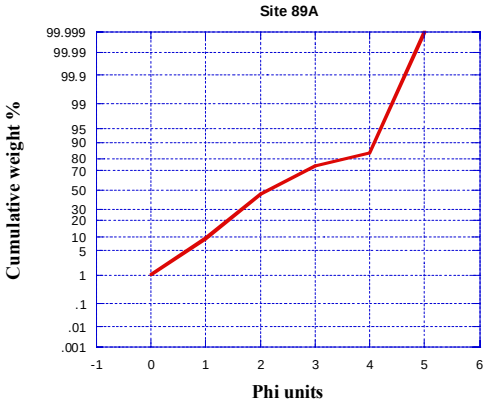

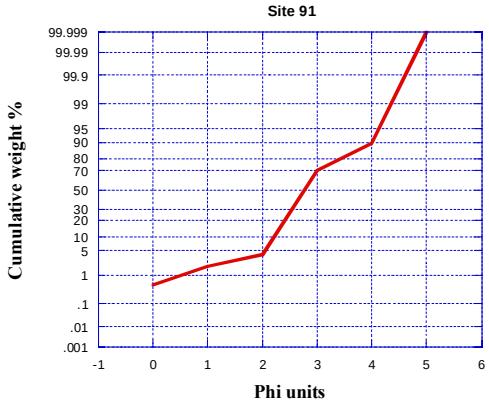

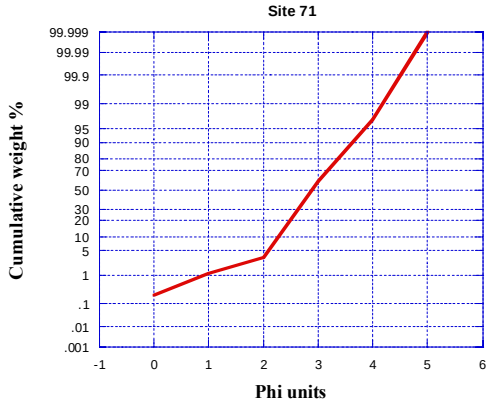

B 4.0. Cummulative-Distribution Curves (continued)

Nearshore mud-patches

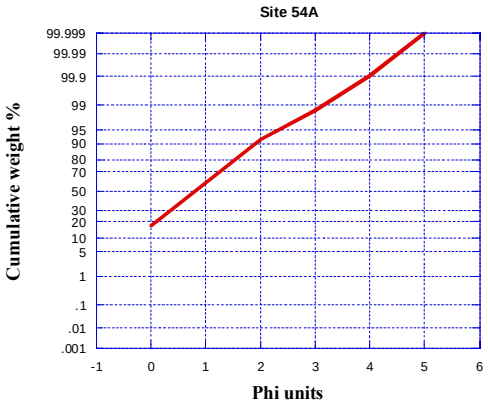

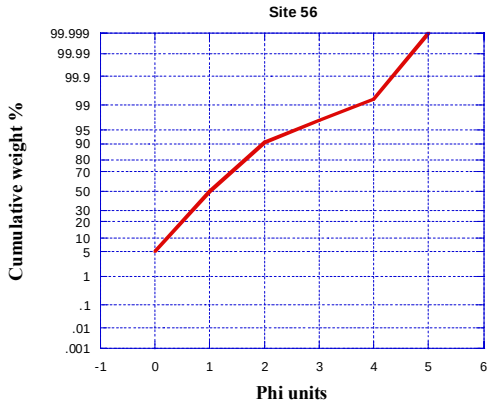

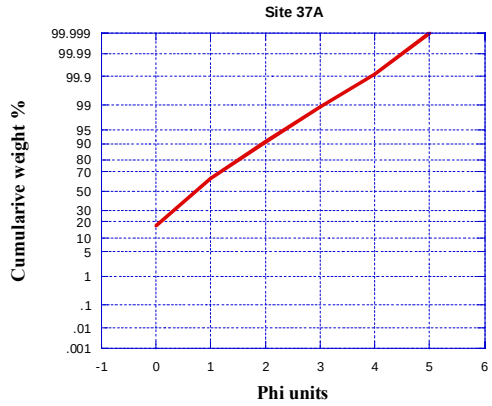

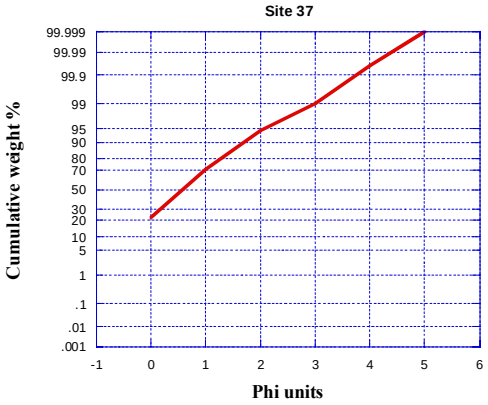

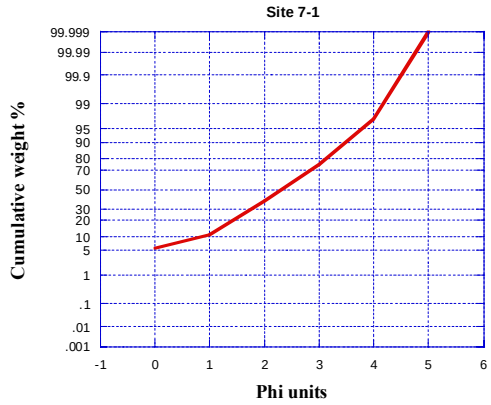

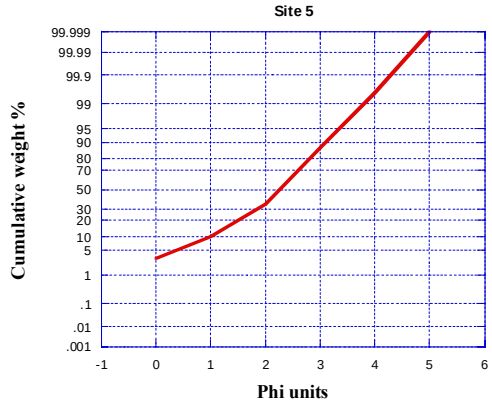

B 4.0. Cumulative-Distribution Curves

Nearshore mud-patches (continued)

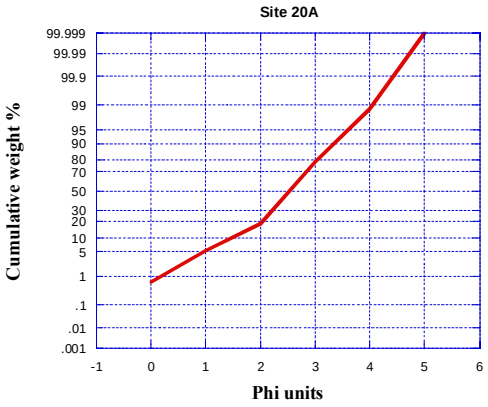

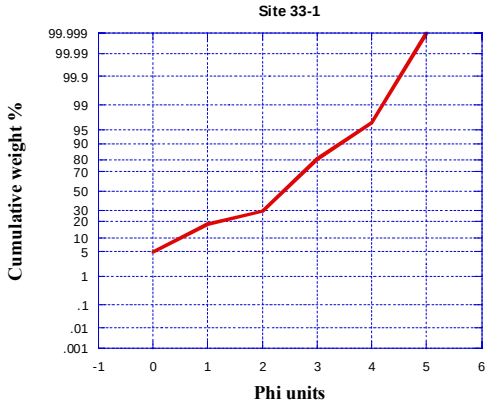

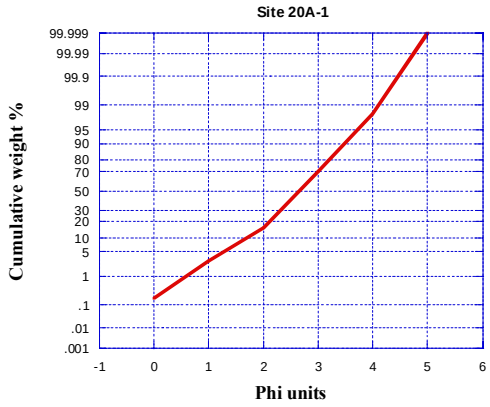

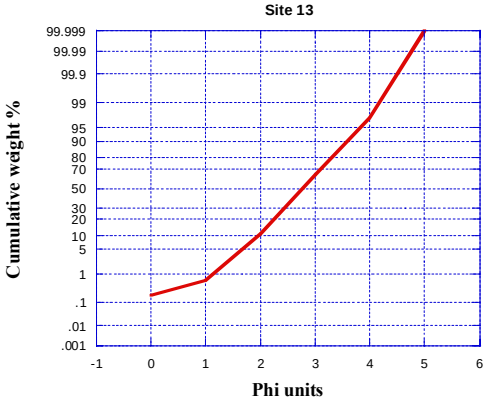

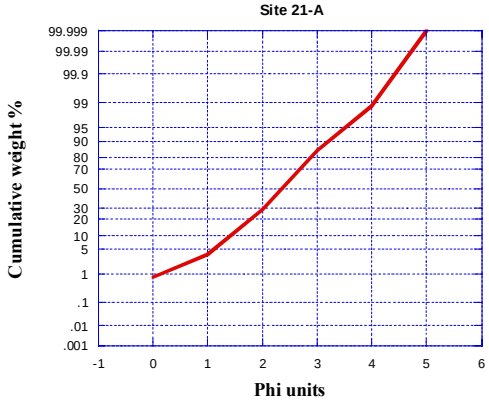

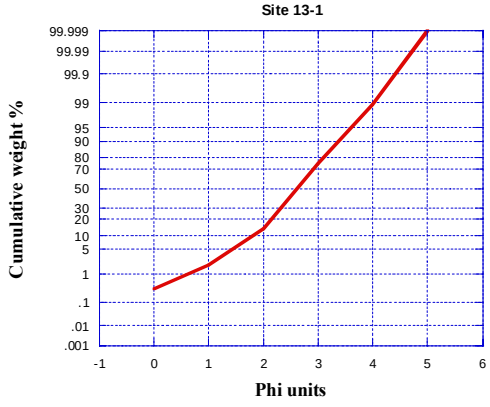

B 4.0. Cumulative-Distribution Curves

Nearshore mud-patches (continued)

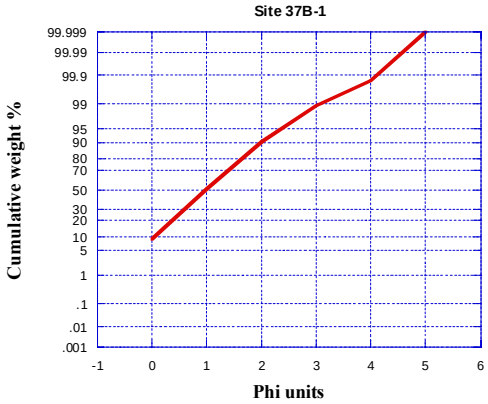

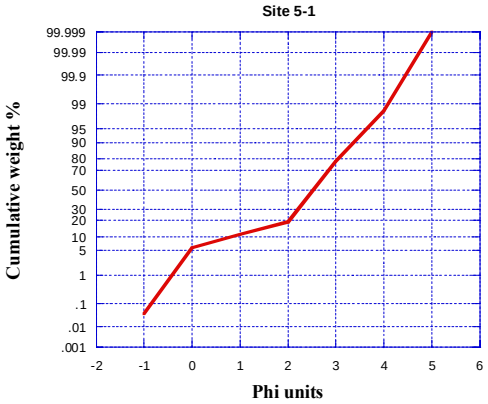

Appendix C

C 1.0. Experimental XRD patterns (oriented slides, <4μm size fraction) of the seventeen samples selected as being representative of New York Bight Apex. The solid red traces represent XRD patterns recorded in the Air Dried (AD) state. Peak positions are outlined as solid green hachures for illite&mica, solid blue for chlorite, solid red for kaolinite, solid purple for I/S and solid green olive for quartz.

C 2.0. Experimental XRD patterns (oriented slides, <4μm size fraction) of the seventeen samples selected as being representative of New York Bight Apex. The solid red traces represent XRD patterns recorded after Ethylene Glycol (EG) solvation. Peak positiosn are outlined as solid green hachures for illite&mica, solid blue for chlorite, solid red for kaolinite, solid purple for I/S and solid green olive for quartz.

C 3.0. Experimental XRD patterns (oriented slides, <4μm size fraction) of the seventeen samples selected as being representative of New York Bight Apex. The solid green traces represent XRD patterns recorded after Ethylene Glycol (EG) solvation and The solid red traces represent XRD patterns recorded in the Air Dried (AD) state. Peak positiosn are outlined as solid green hachures for illite&mica, solid blue for chlorite, solid red for kaolinite, solid purple for I/S and solid green olive for quartz.

Appendix C

C 1.0. Experimental XRD patterns (oriented Slides, <4μm size fraction) of the seventeen samples selected as being representative of New York Bight Apex. The solid red traces represent XRD patterns recorded in the Air Dried (AD) state. Peak position are outlined as solid green hachures for illite&mica, solid blue for chlorite, solid red for kaolinite, solid purple for I/S and solid green olive for quartz.

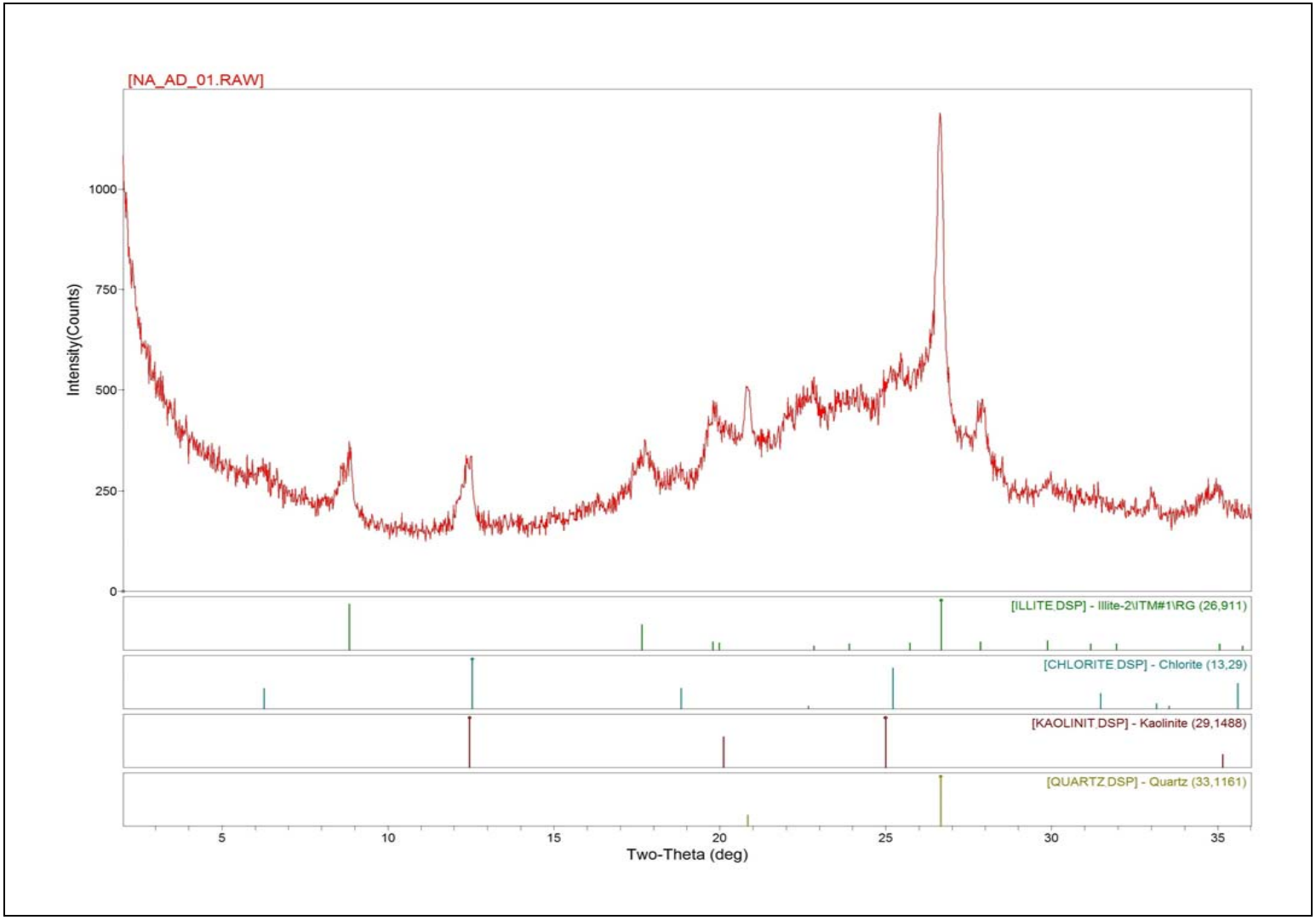

Site 1-1

Experimental XRD patterns (oriented slides, <4µm size fraction): The solid red traces represent XRD patterns recorded in the Air Dried (AD) state. Peaks Position are outlined as solid green hachures for illite&mica, solid blue for chlorite, solid red for kaolinite and solid green olive for quartz.

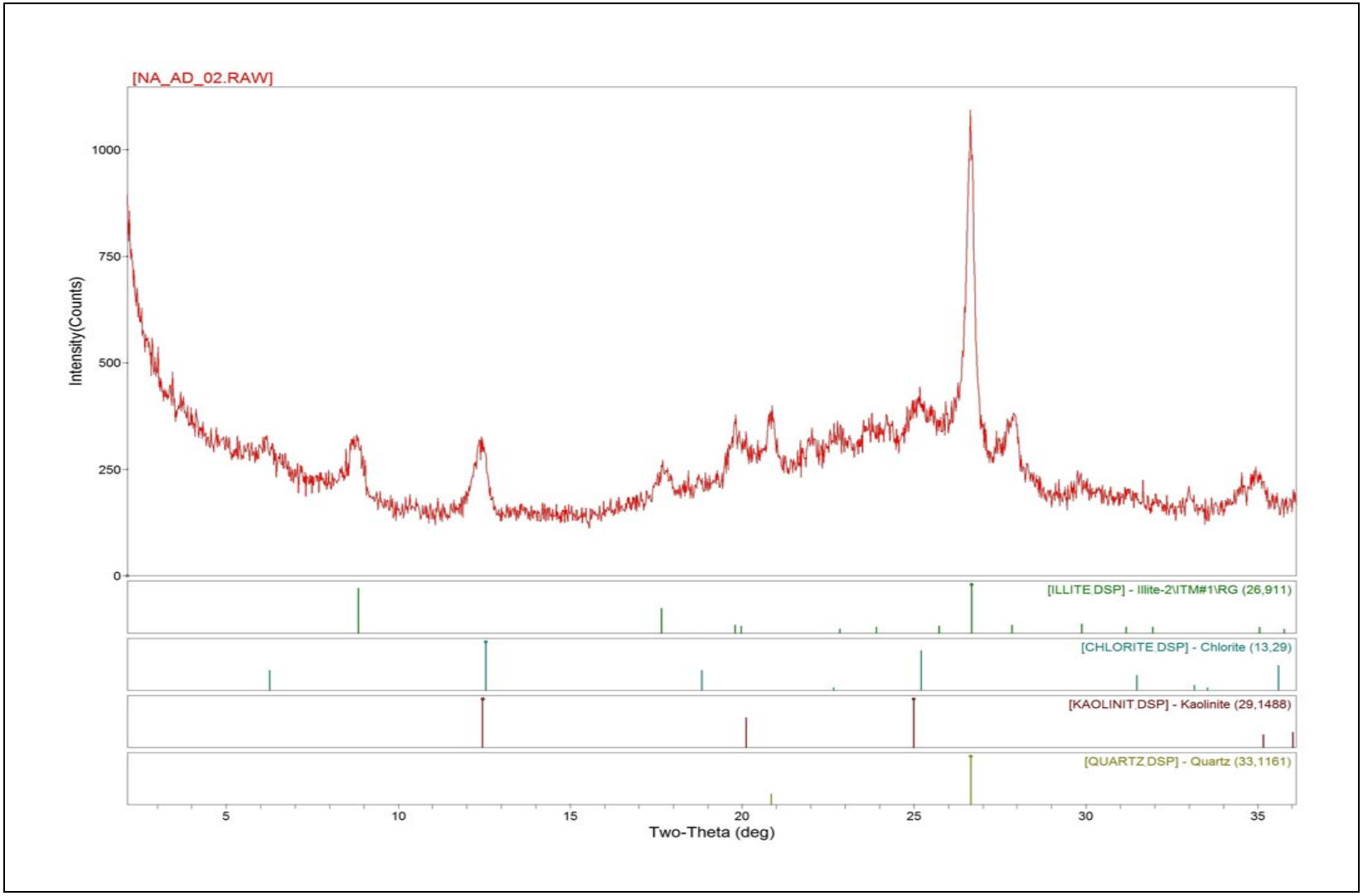

Site 1-2

Experimental XRD patterns (oriented slides, <4μm size fraction): The solid red traces represent XRD patterns recorded in the Air Dried (AD) state. Peak positions are outlined as solid green hachures for illite&mica, solid blue for chlorite, solid red for kaolinite and solid green olive for quartz.

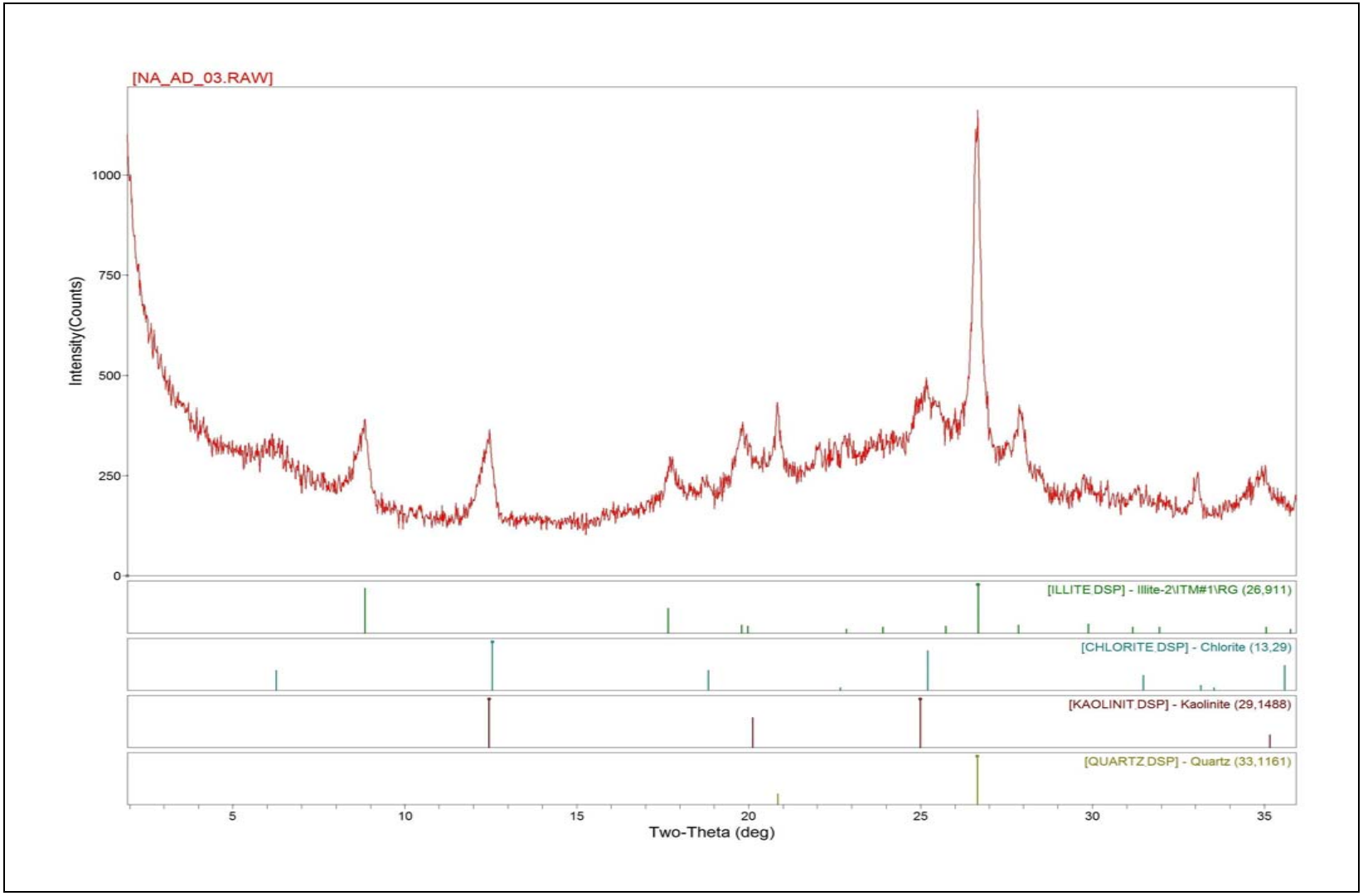

Site7-1

Experimental XRD patterns (oriented slides, <4μm size fraction): The solid red traces represent XRD patterns recorded in the Air Dried (AD) state. Peak positions are outlined as solid green hachures for illite&mica, solid blue for chlorite, solid red for kaolinite and solid green olive for quartz.

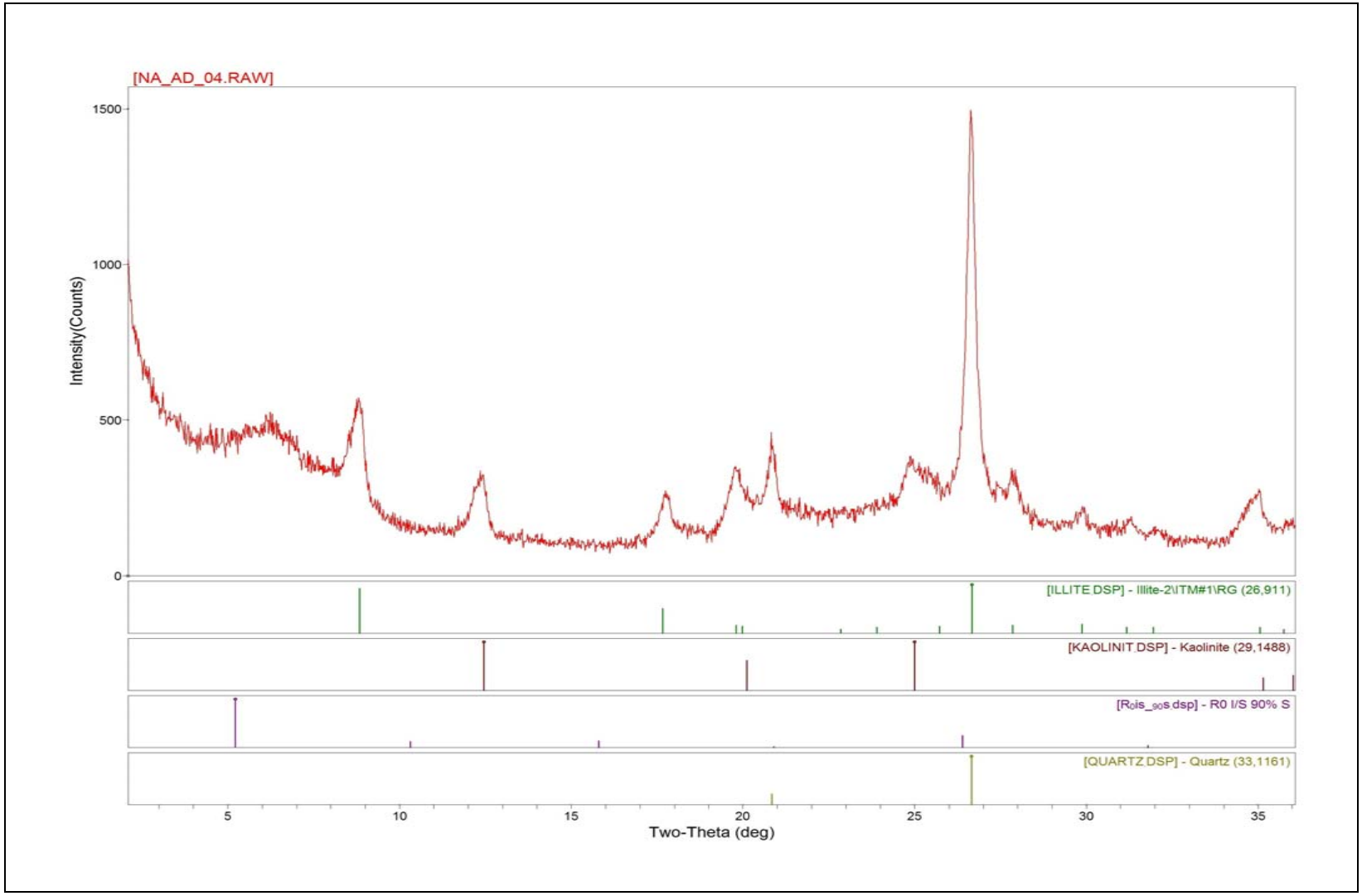

Site 7-1-2

Experimental XRD patterns (oriented slides, <4μm size fraction): The solid red traces represent XRD patterns recorded in the Air Dried (AD) state. Peak positions are outlined as solid green hachures for illite&mica, solid blue for chlorite, solid red for kaolinite, solid purple for I/S and solid green olive for quartz.

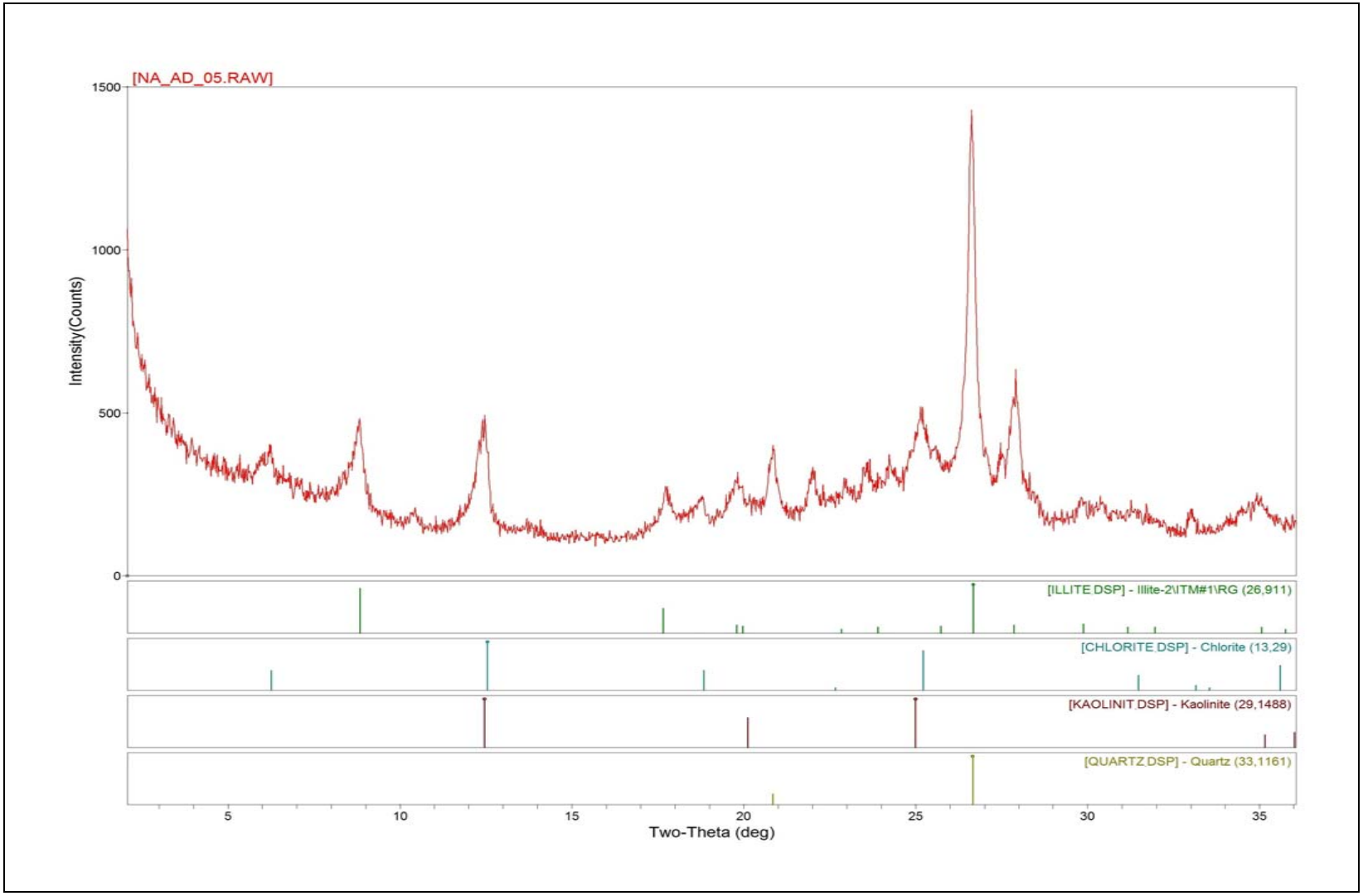

Site 33-1

Experimental XRD patterns (oriented slides, <4μm size fraction): The solid red traces represent XRD patterns recorded in the Air Dried (AD) state. Peak positions are outlined as solid green hachures for illite&mica, solid blue for chlorite, solid red for kaolinite and solid green olive for quartz.

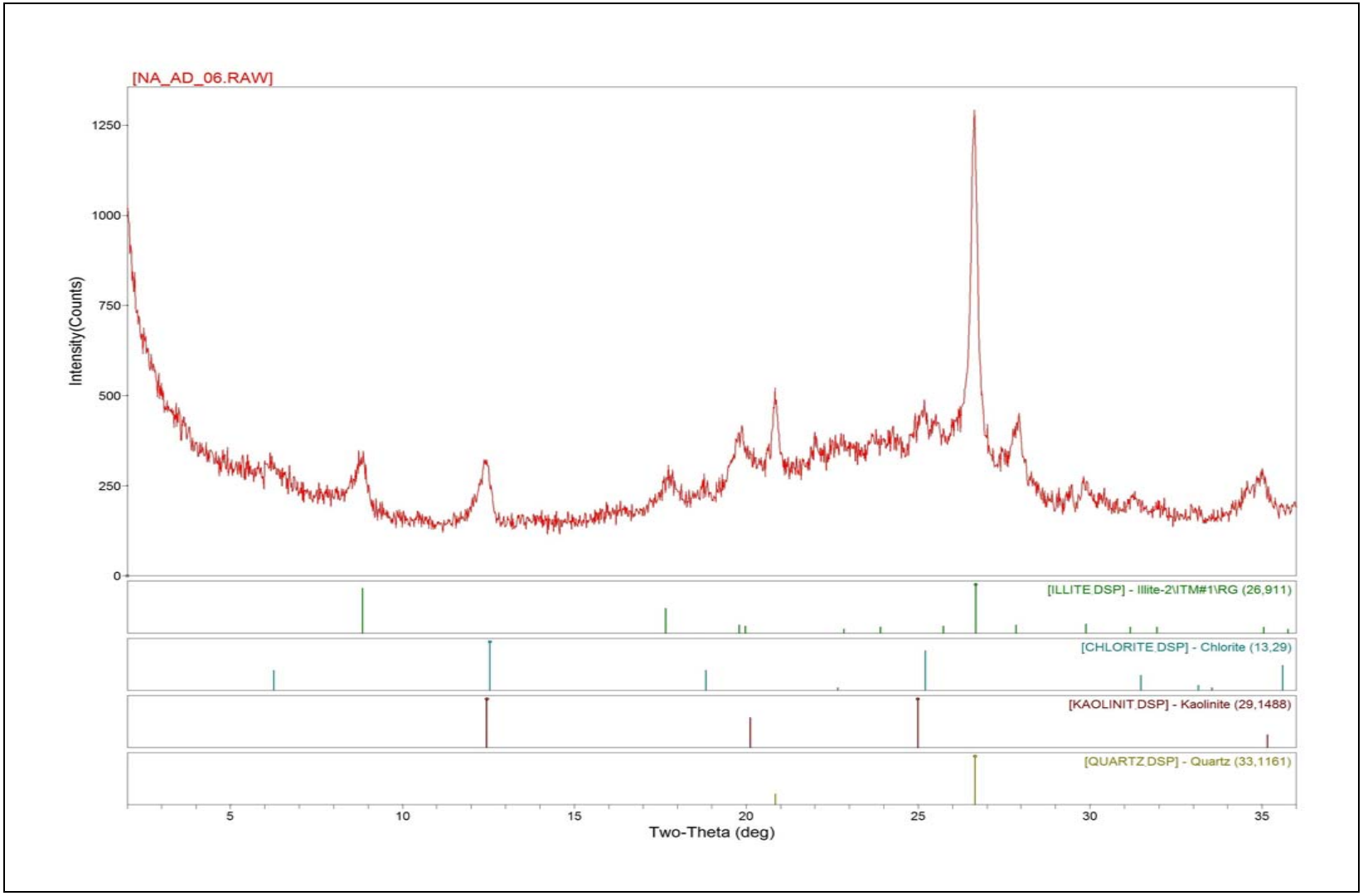

Site 55-1

Experimental XRD patterns (oriented sides, <4µm size fraction): The solid red traces represent XRD patterns recorded in the Air Dried (AD) state. Peak positions are outlined as solid green hachures for illite&mica, solid blue for chlorite, solid red for kaolinite and solid green olive for quartz.

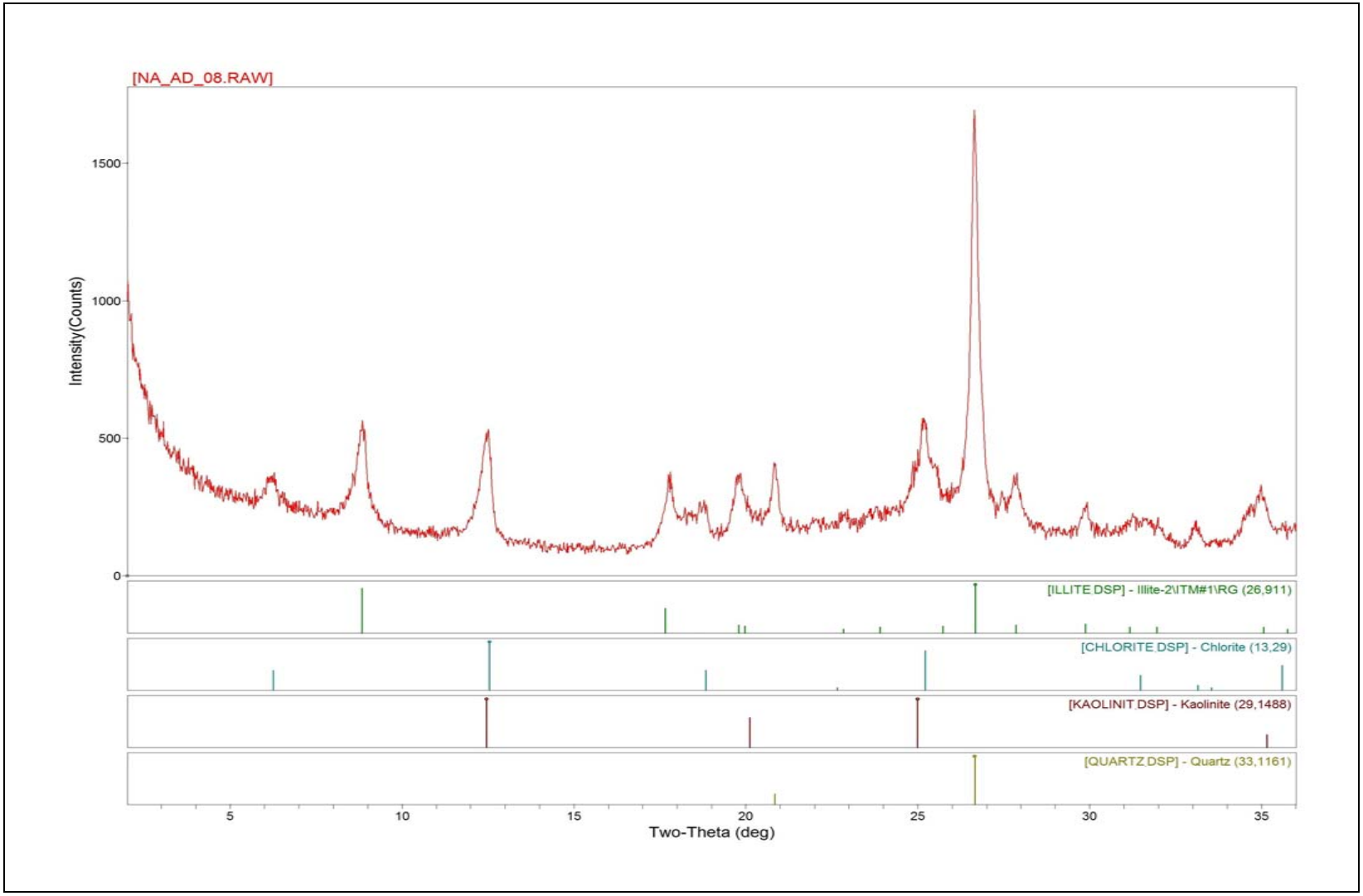

Site 56

XRD patterns (oriented slides, <4µm size fraction): The solid red traces represent XRD patterns recorded in the Air Dried (AD) state. Peak positions are outlined as solid green hachures for illite&mica, solid blue for chlorite, solid red for kaolinite and solid green olive for quartz.

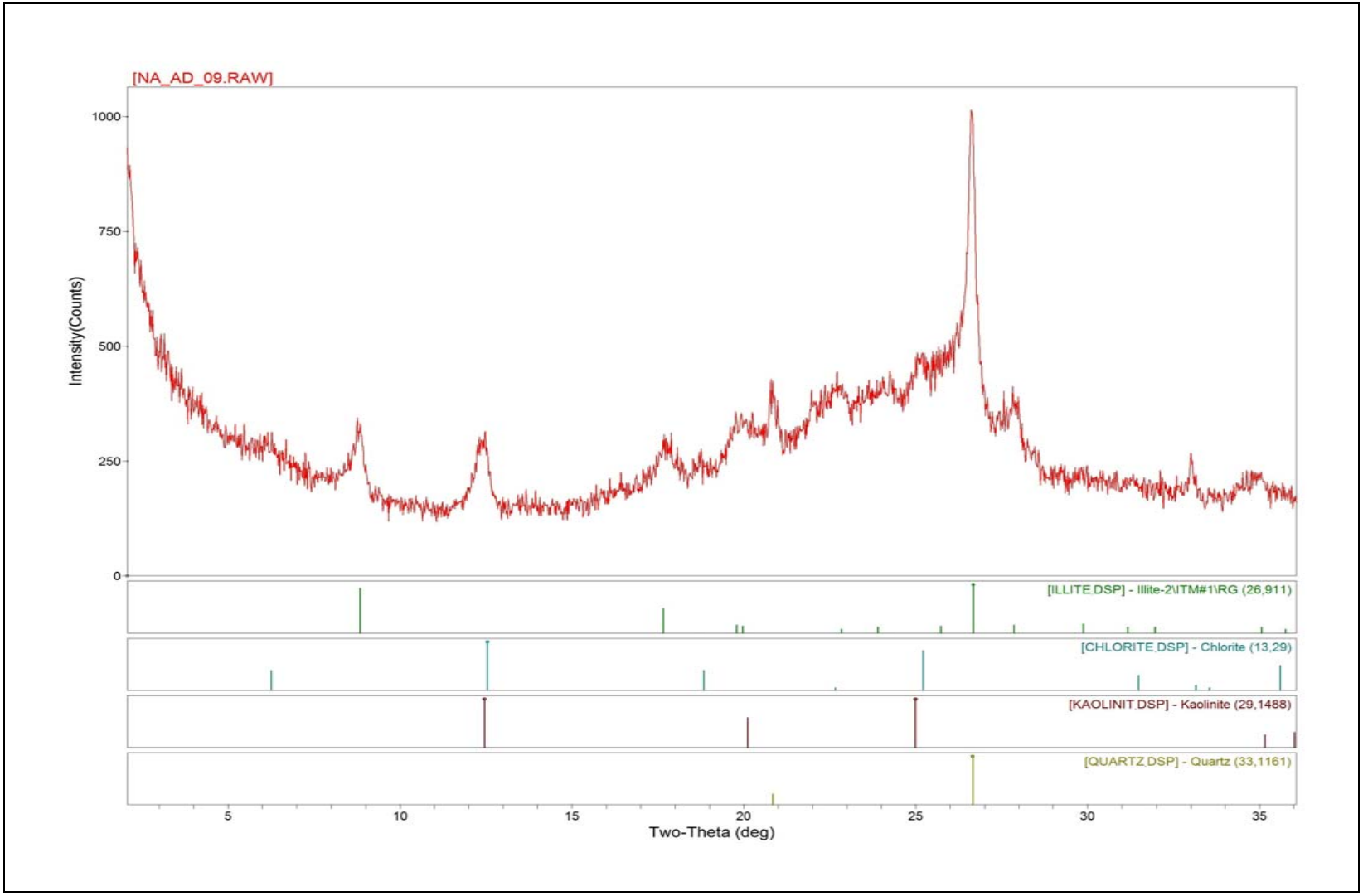

Site 63

XRD patterns (oriented slides, <4µm size fraction): The Solid red traces represent XRD patterns recorded in the Air Dried (AD) state. Peaks positions are outlined as solid green hachures for illite&mica, solid blue for chlorite, solid red for kaolinite and solid green olive for quartz.

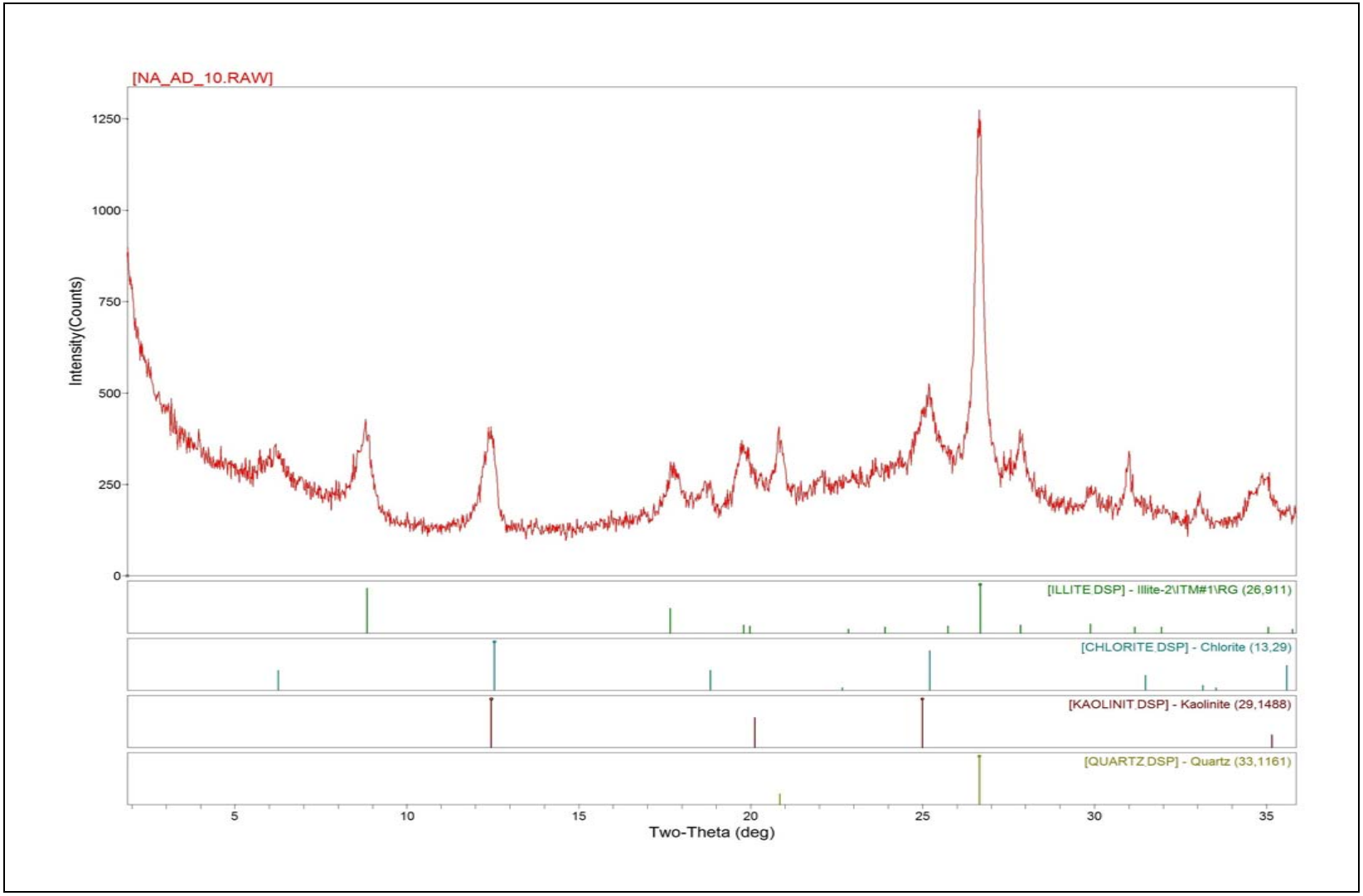

Site 84-1

XRD patterns (oriented slides, <4μm size fraction): The solid red traces represent XRD patterns recorded in the Air Dried (AD) state. Peak positions are outlined as solid green hachures for illite&mica, solid blue for chlorite, solid red for kaolinite and solid green olive for quartz.

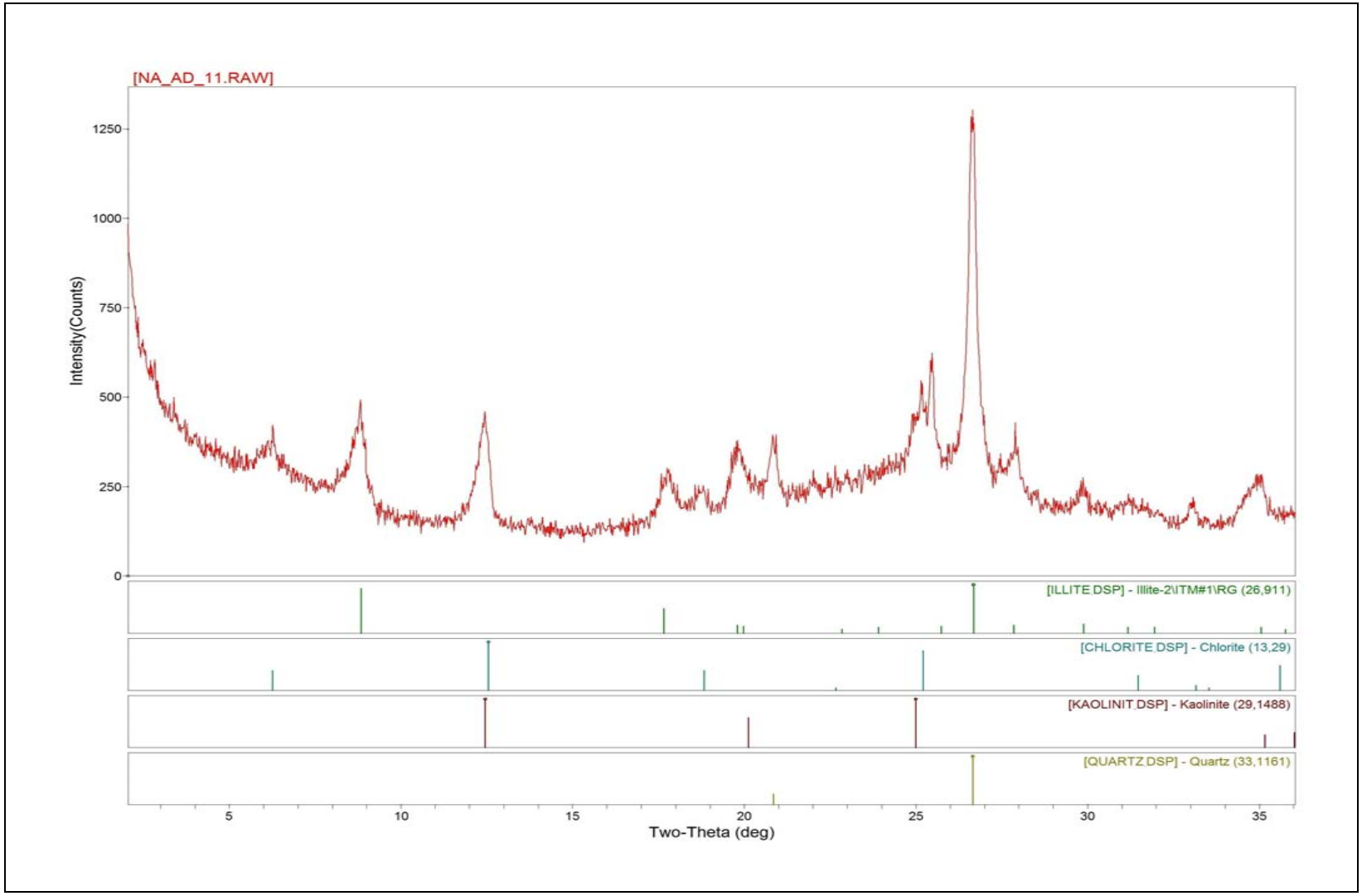

Site 85-1

XRD patterns (oriented slides, <4μm size fraction): The solid red traces represent XRD patterns recorded in the Air Dried (AD) state. Peak positions are outlined as solid green hachures for illite&mica, solid blue for chlorite, solid red for kaolinite and solid green olive for quartz.

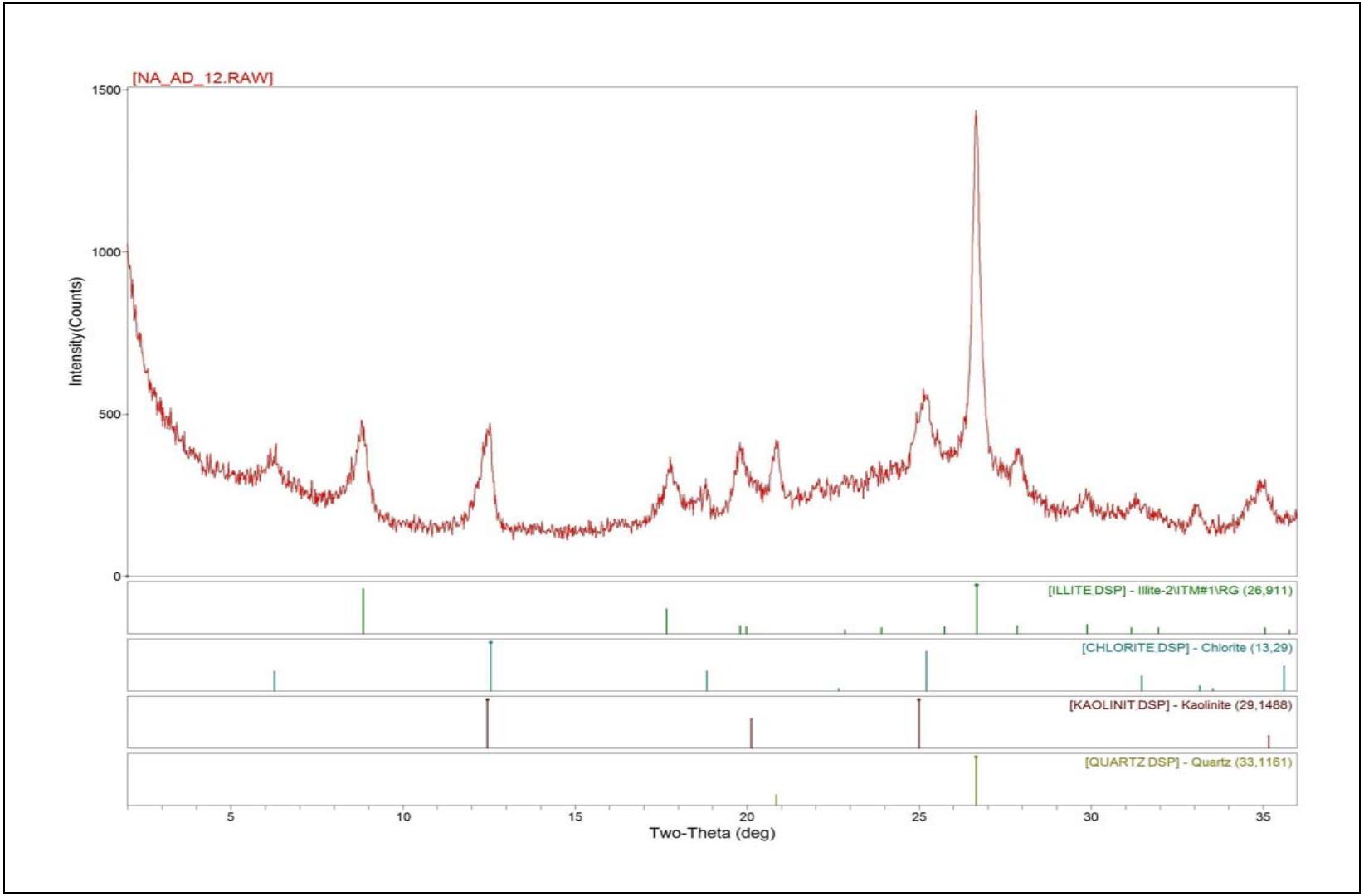

Site 86

XRD patterns (oriented slides, <4µm size fraction): The solid red traces represent XRD patterns recorded in the Air Dried (AD) state. Peak positions are outlined as solid green hachures for illite&mica, solid blue for chlorite, solid red for kaolinite and solid green olive for quartz.

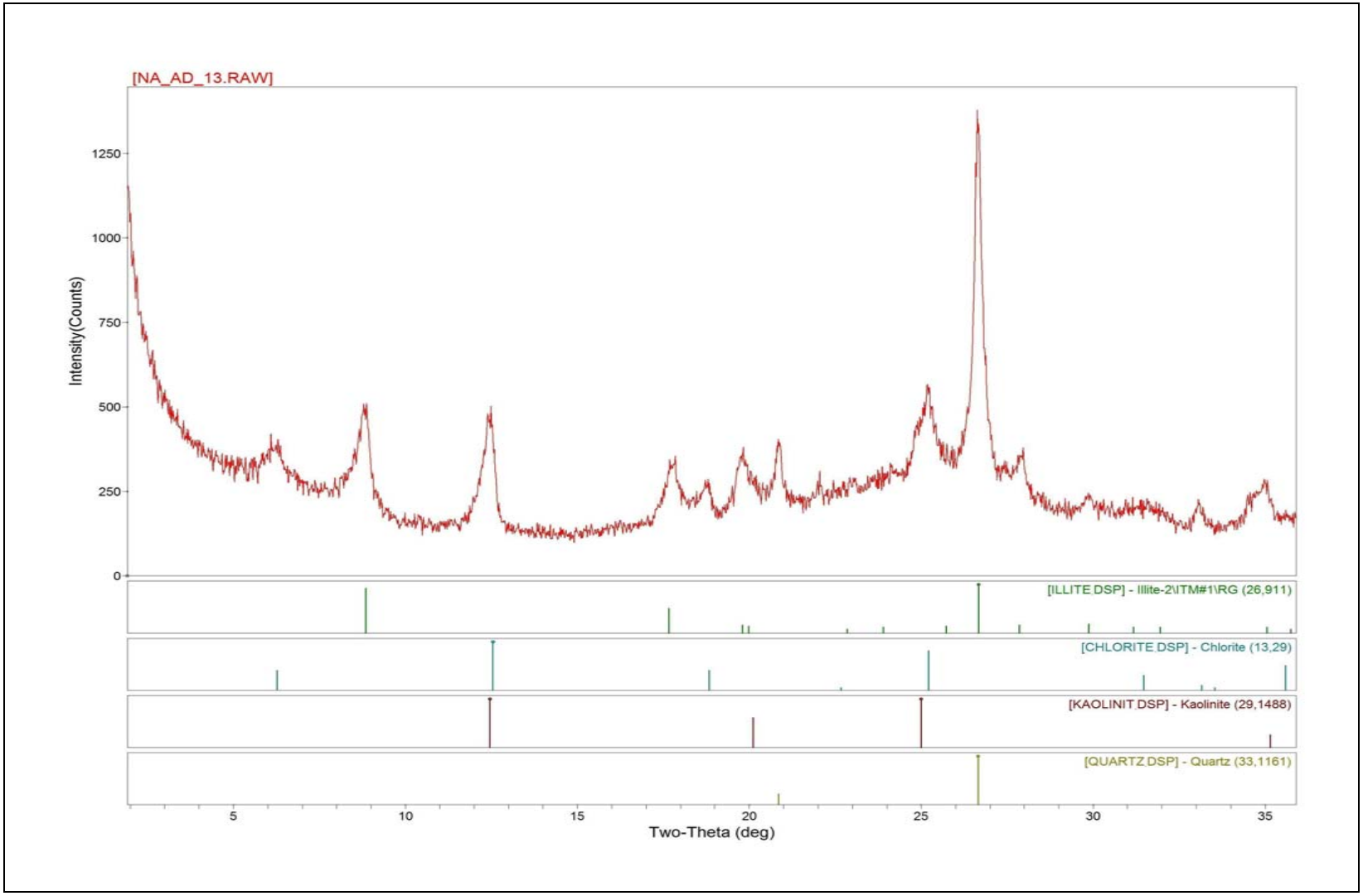

Site 86-1

XRD patterns (oriented slides, <4μm size fraction): The solid red traces represent XRD patterns recorded in the Air Dried (AD) state. Peak positions are outlined as solid green hachures for illite&mica, solid blue for chlorite, solid red for kaolinite and solid green olive for quartz.

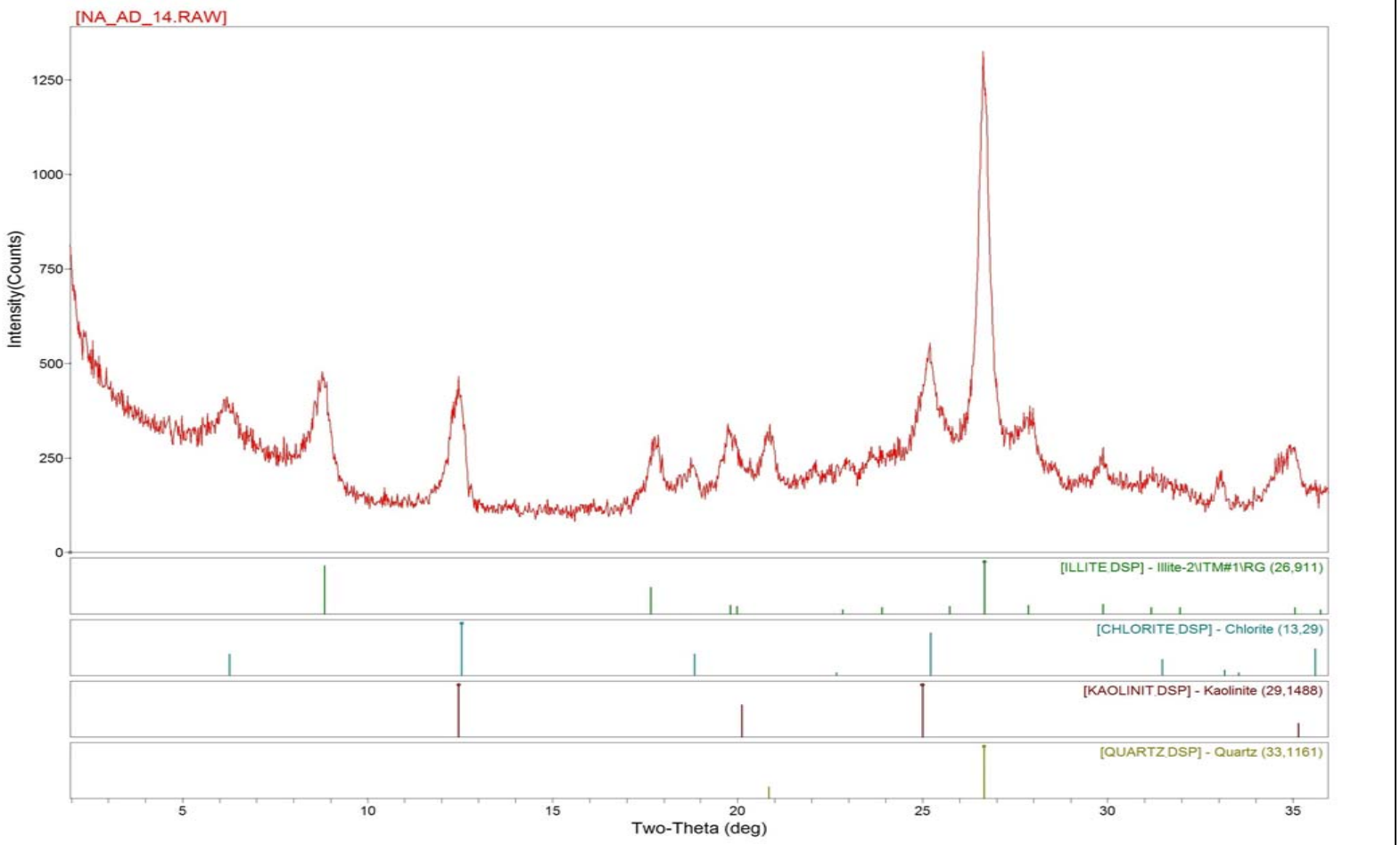

Site 87-1

XRD patterns (oriented slides, <4µm size fraction): The solid red traces represent XRD patterns recorded in the Air Dried (AD) state. Peak positions are outlined as solid green hachures for illite&mica, solid blue for chlorite, solid red for kaolinite and solid green olive for quartz.

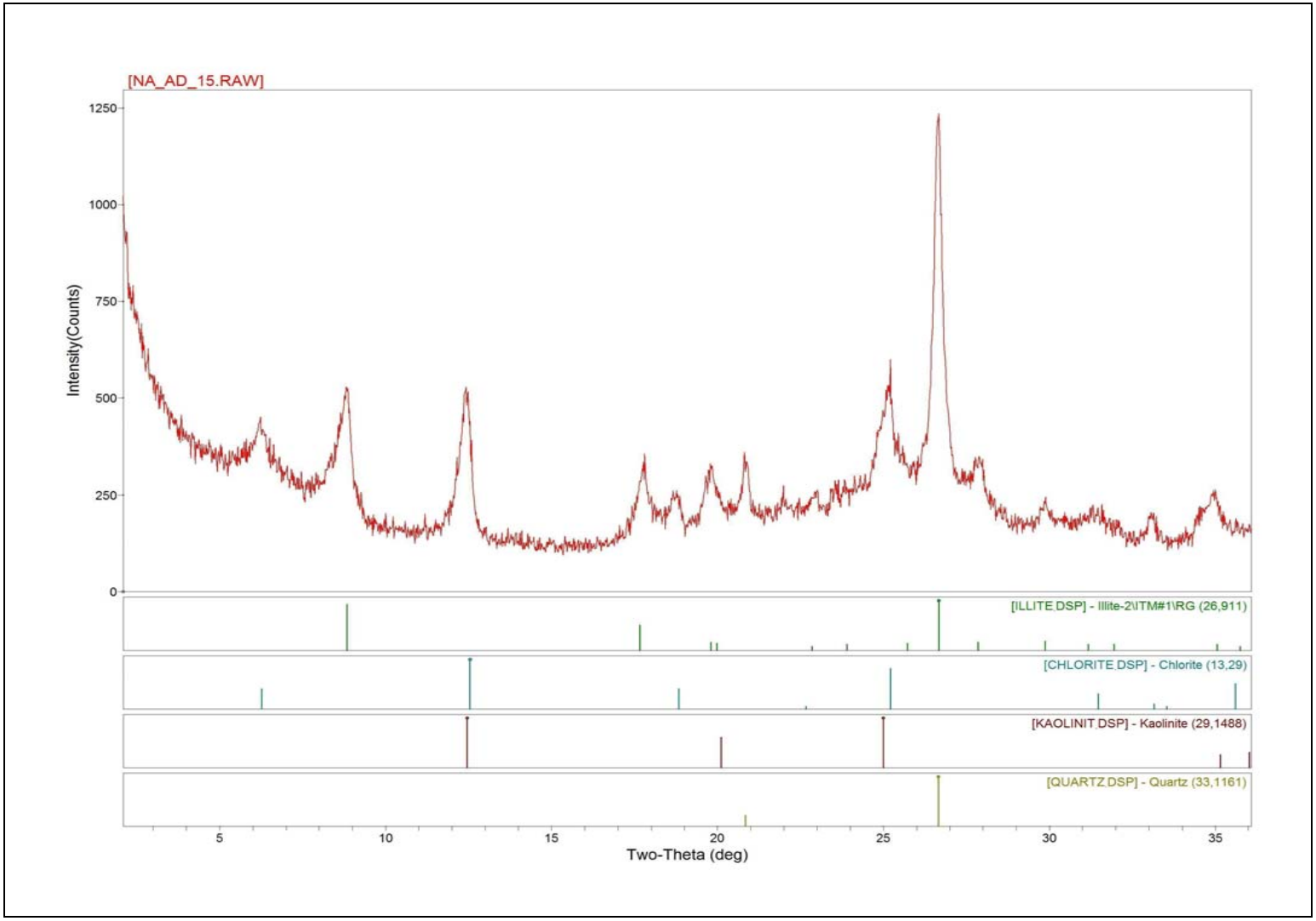

Site 88-1

XRD patterns (oriented slides, <4µm size fraction): The solid red traces represent XRD patterns recorded in the Air Dried (AD) state. Peak positions are outlined as solid green hachures for illite&mica, solid blue for chlorite, solid red for kaolinite and solid green olive for quartz.

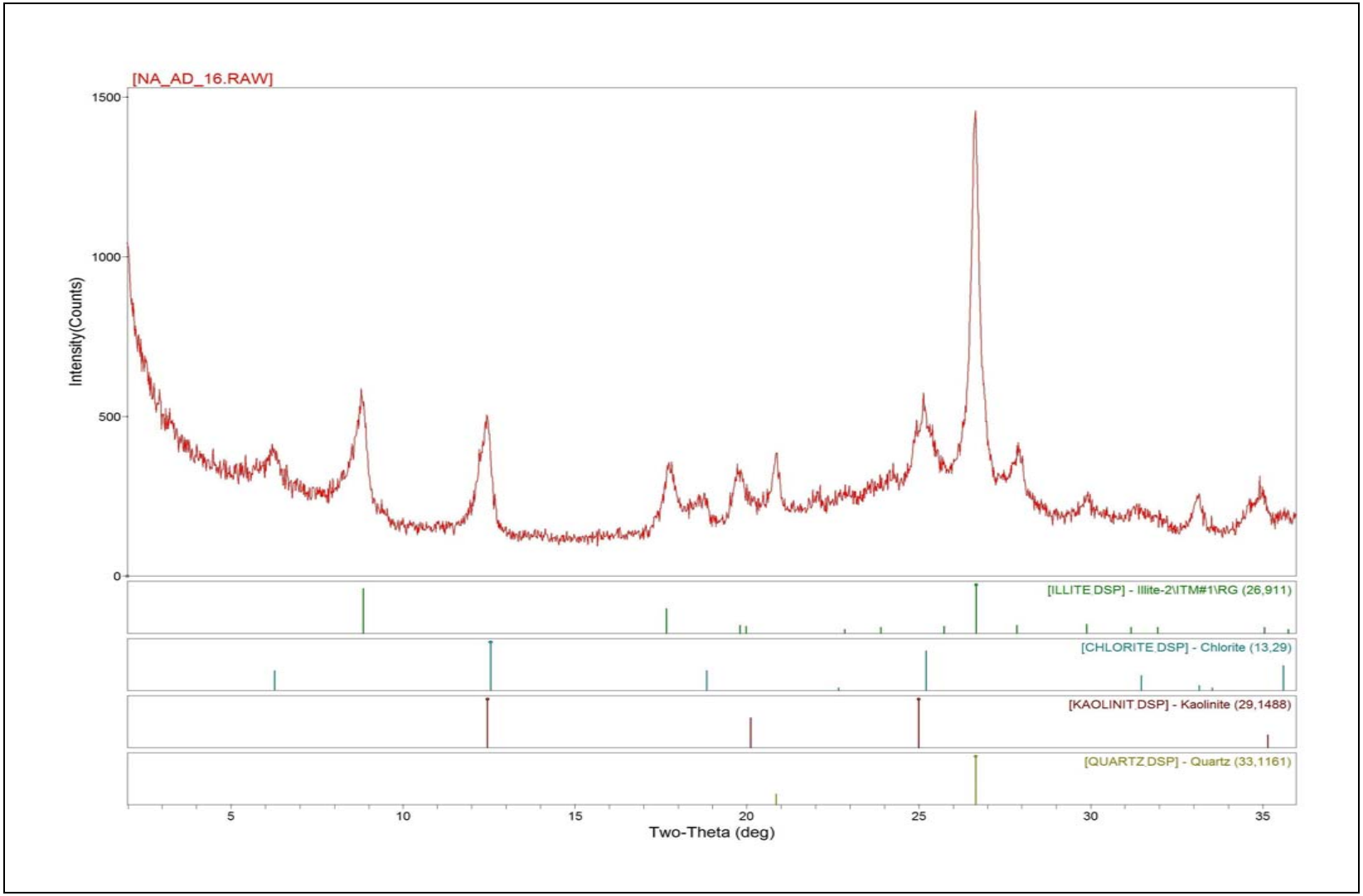

Site 89A

XRD patterns (oriented slides, <4µm size fraction): The solid red traces represent XRD patterns recorded in the Air Dried (AD) state. Peak positions are outlined as solid green hachures for illite&mica, solid blue for chlorite, solid red for kaolinite and solid green olive for quartz.

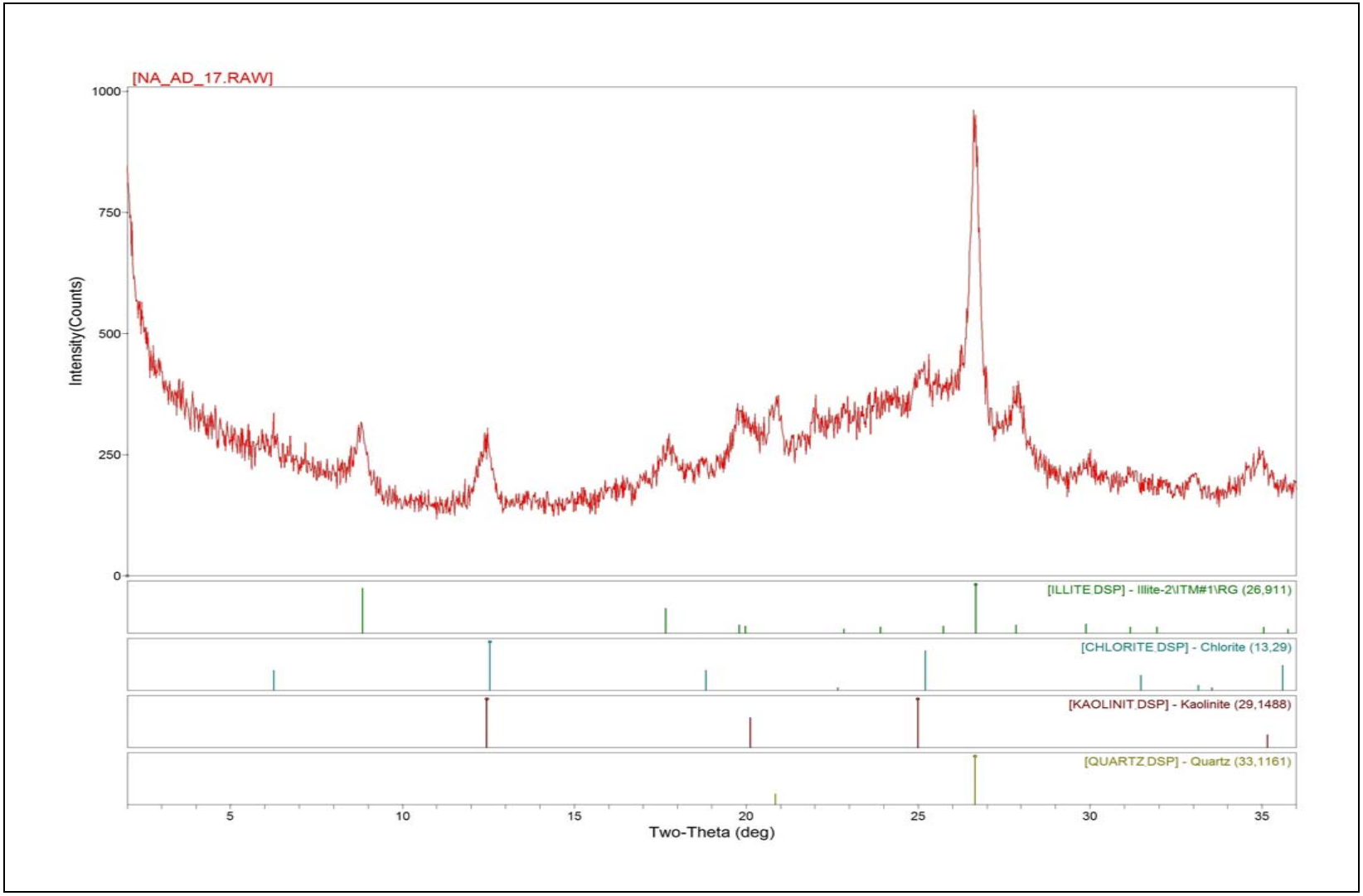

Site 91

XRD patterns (oriented slides, <4μm size fraction): The solid red traces represent XRD patterns recorded in the Air Dried (AD) state. Peak positions are outlined as solid green hachures for illite&mica, solid blue for chlorite, solid red for kaolinite and solid green olive for quartz.

Appendix C

C-2. Experimental XRD patterns (oriented slides, <4μm size fraction) of the seventeen samples selected as being representative of New York Bight Apex. The solid red traces represent XRD patterns recorded after Ethylene Glycol (EG) solvation. Peak position are outlined as solid green hachures for illite&mica, solid blue for chlorite, solid red for kaolinite, solid purple for I/S and solid green olive for quartz.

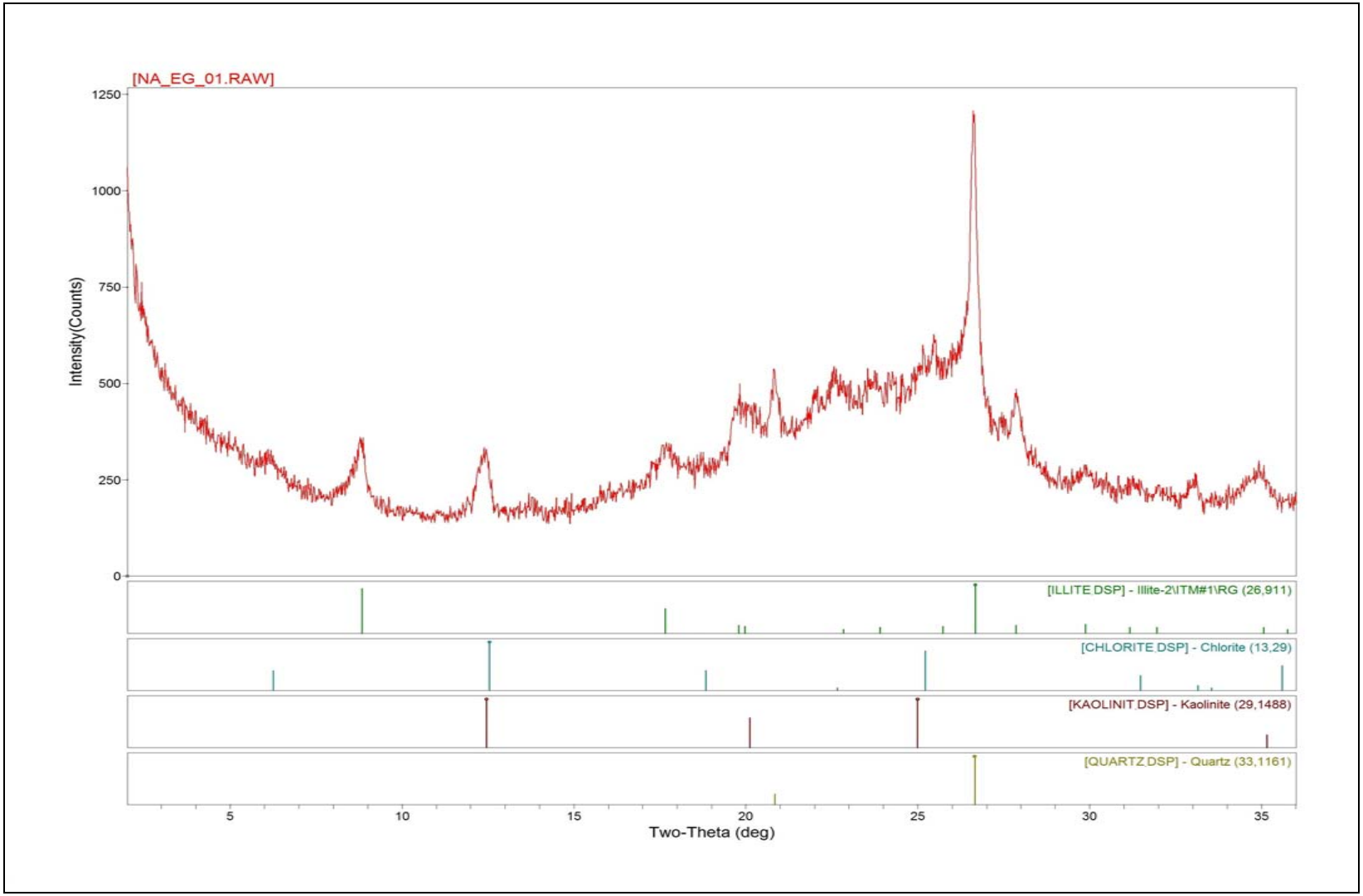

Site1-1

XRD patterns (oriented slides, <4μm size fraction): The solid red traces represent XRD patterns recorded after the Ethylene Glycol (EG) solvation. Peak positions are outlined as solid green hachures for illite&mica, solid blue for chlorite, solid red for kaolinite and solid green olive for quartz.

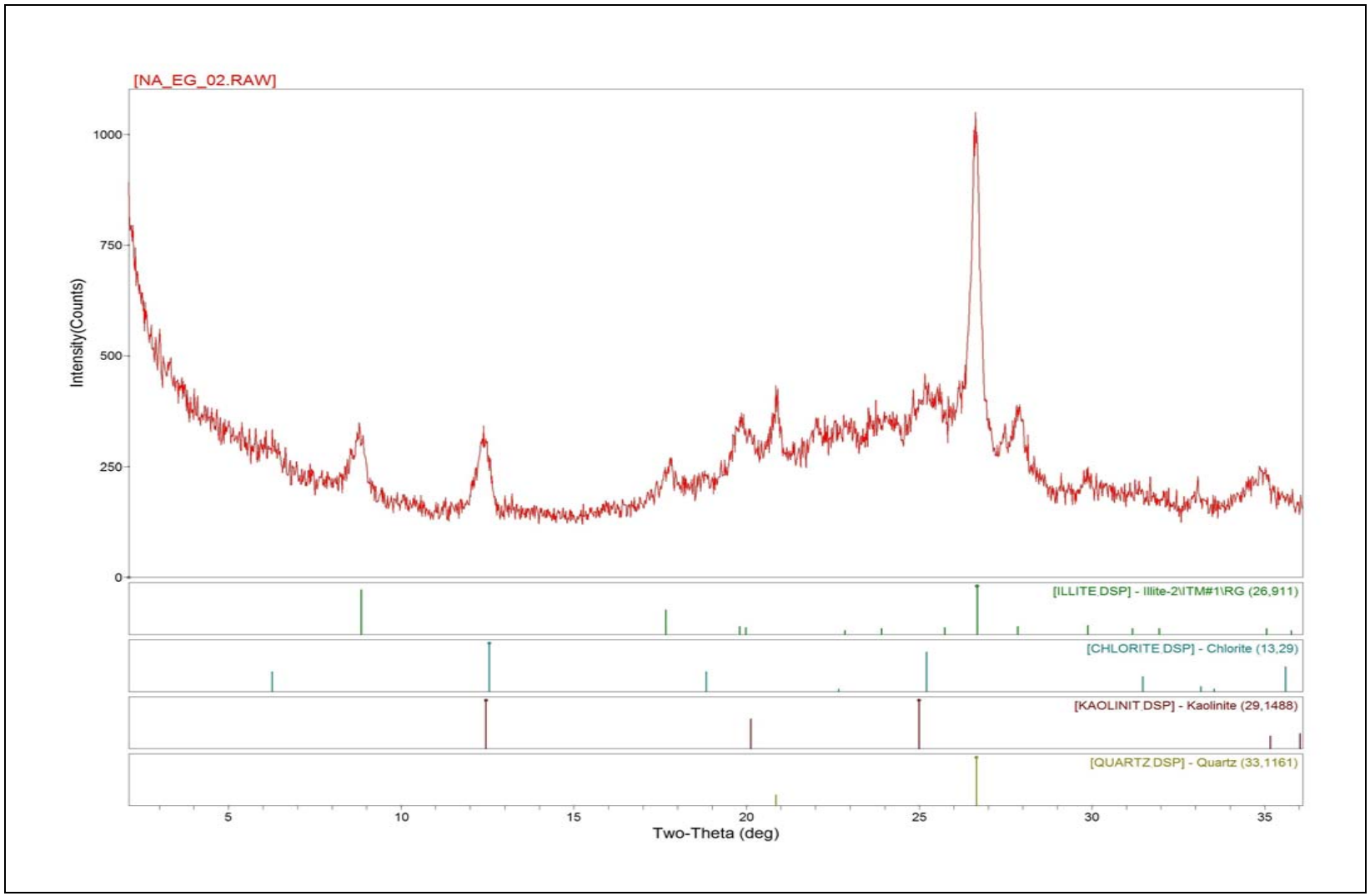

Site 1-2

XRD patterns (oriented slides, <4μm size fraction): The solid red traces represent XRD patterns recorded after the Ethylene Glycol (EG) solvation. Peak positions are outlined as solid green hachures for illite&mica, solid blue for chlorite, solid red for kaolinite and solid green olive for quartz.

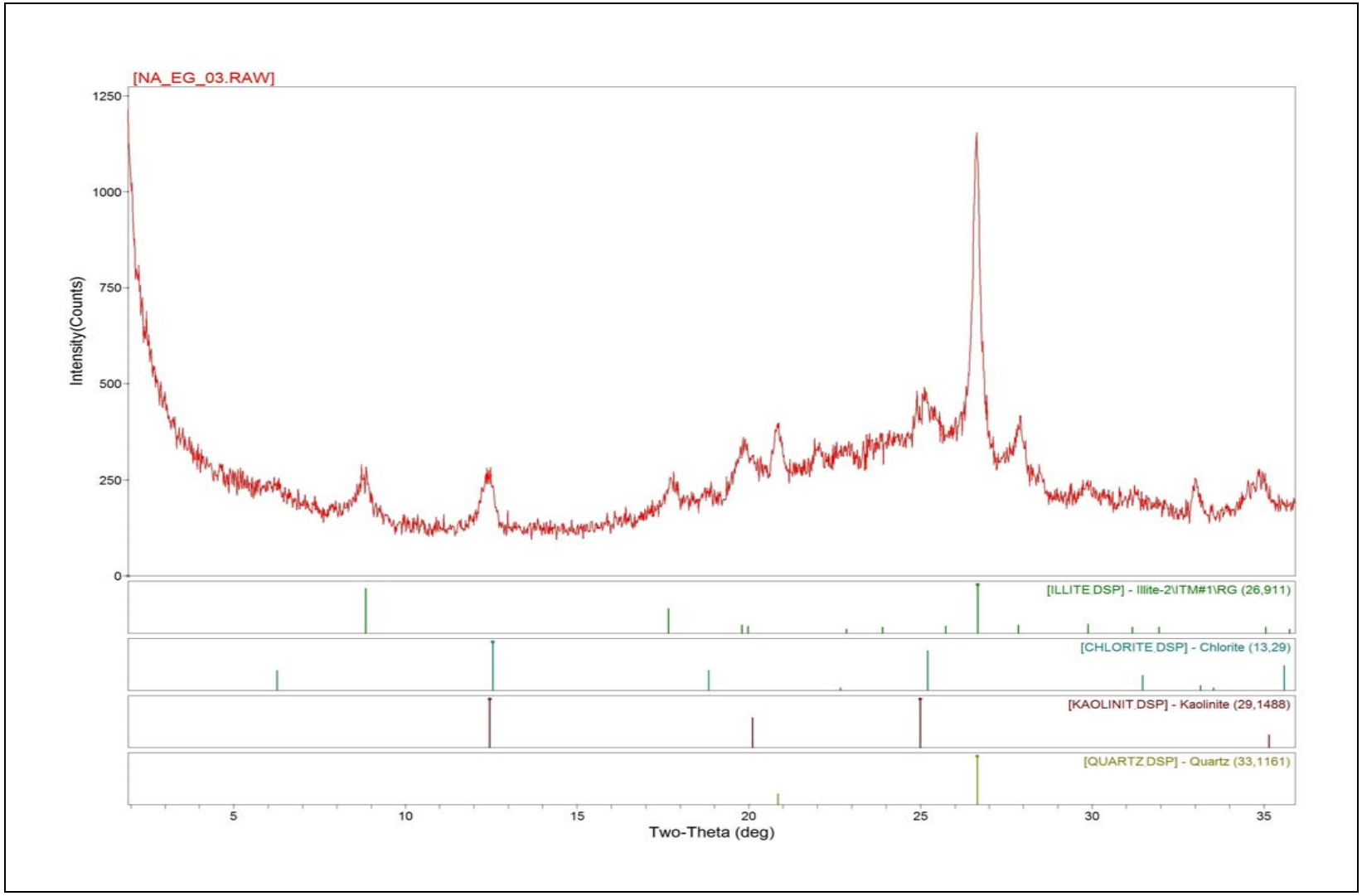

Site 7-1

XRD patterns (oriented slides, <4µm size fraction): The solid red traces represent XRD patterns recorded after the Ethylene Glycol (EG) solvation. Peak positions are outlined as solid green hachures for illite&mica, solid blue for chlorite, solid red for kaolinite and solid green olive for quartz.

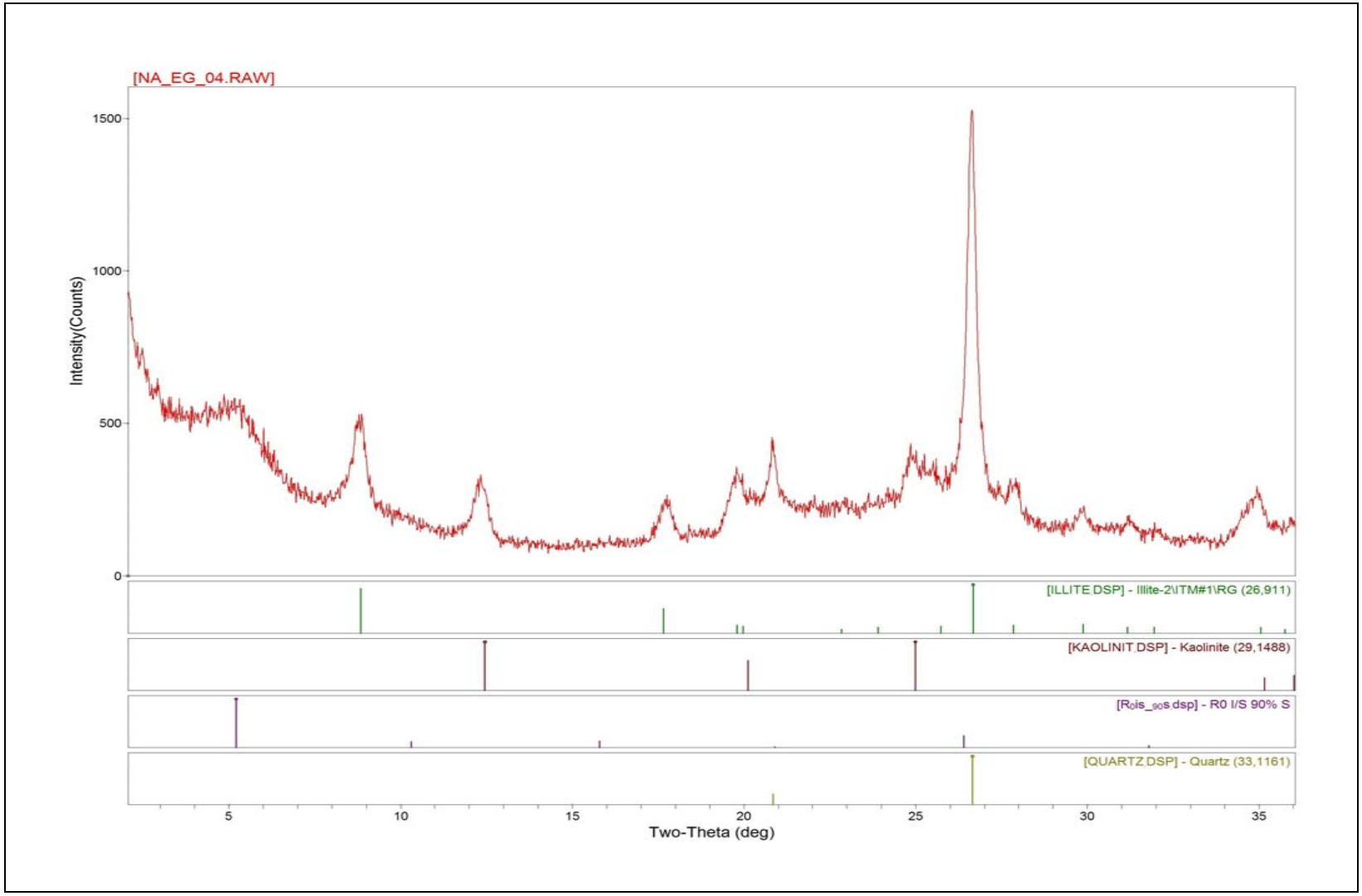

Site 7-1-2

XRD patterns (oriented slides, <4µm size fraction): The solid red traces represent XRD patterns recorded after the Ethylene Glycol (EG) solvation. Peak positions are outlined as solid green hachures for illite&mica, solid blue for chlorite, solid purple for I/S, solid red for kaolinite and solid green olive for quartz.

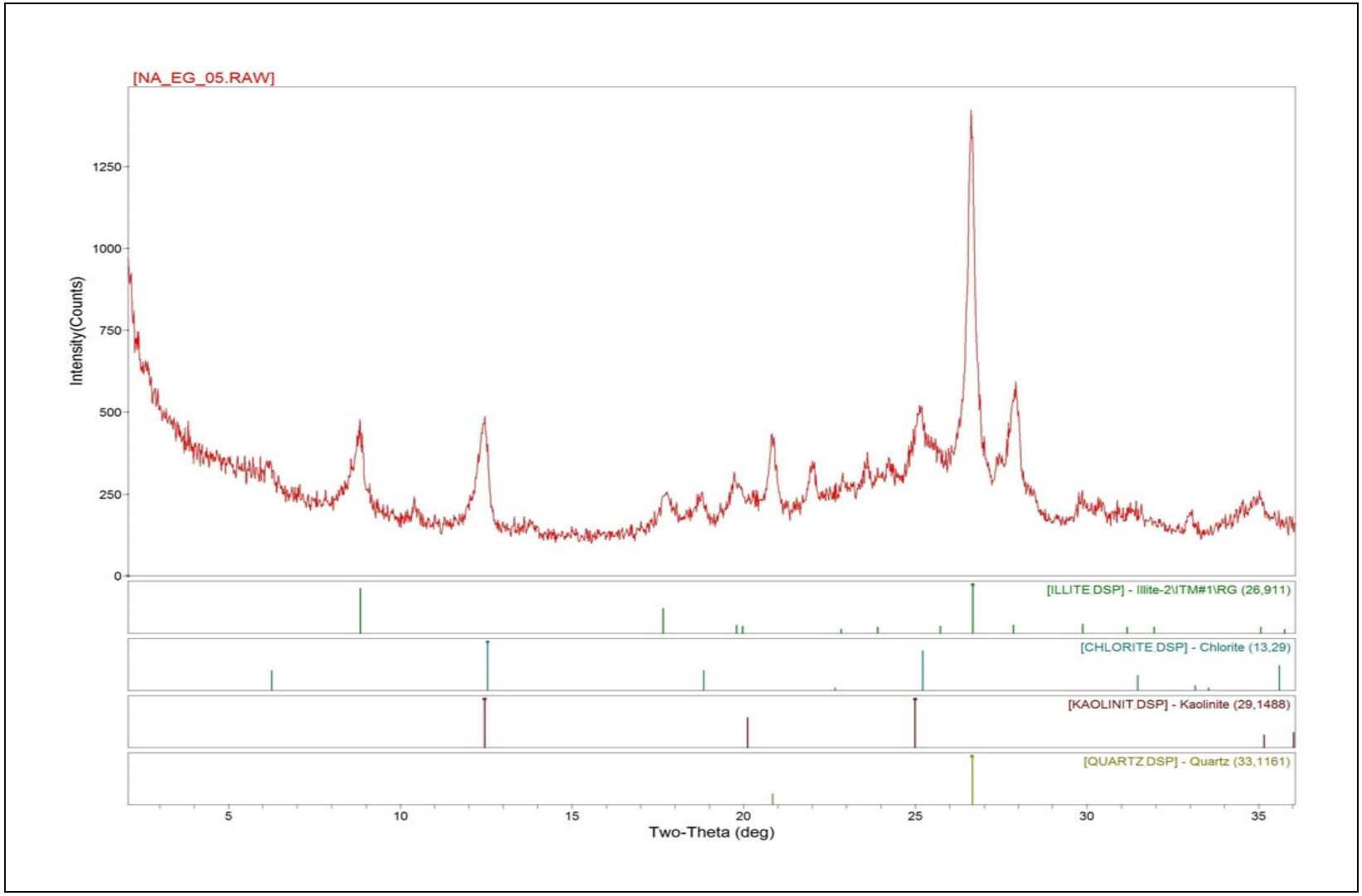

Site 33-1

XRD patterns (oriented slides, <4µm size fraction): The solid red traces represent XRD patterns recorded after the Ethylene Glycol (EG) solvation. Peak positions are outlined as solid green hachures for illite&mica, solid blue for chlorite, solid red for kaolinite and solid green olive for quartz.

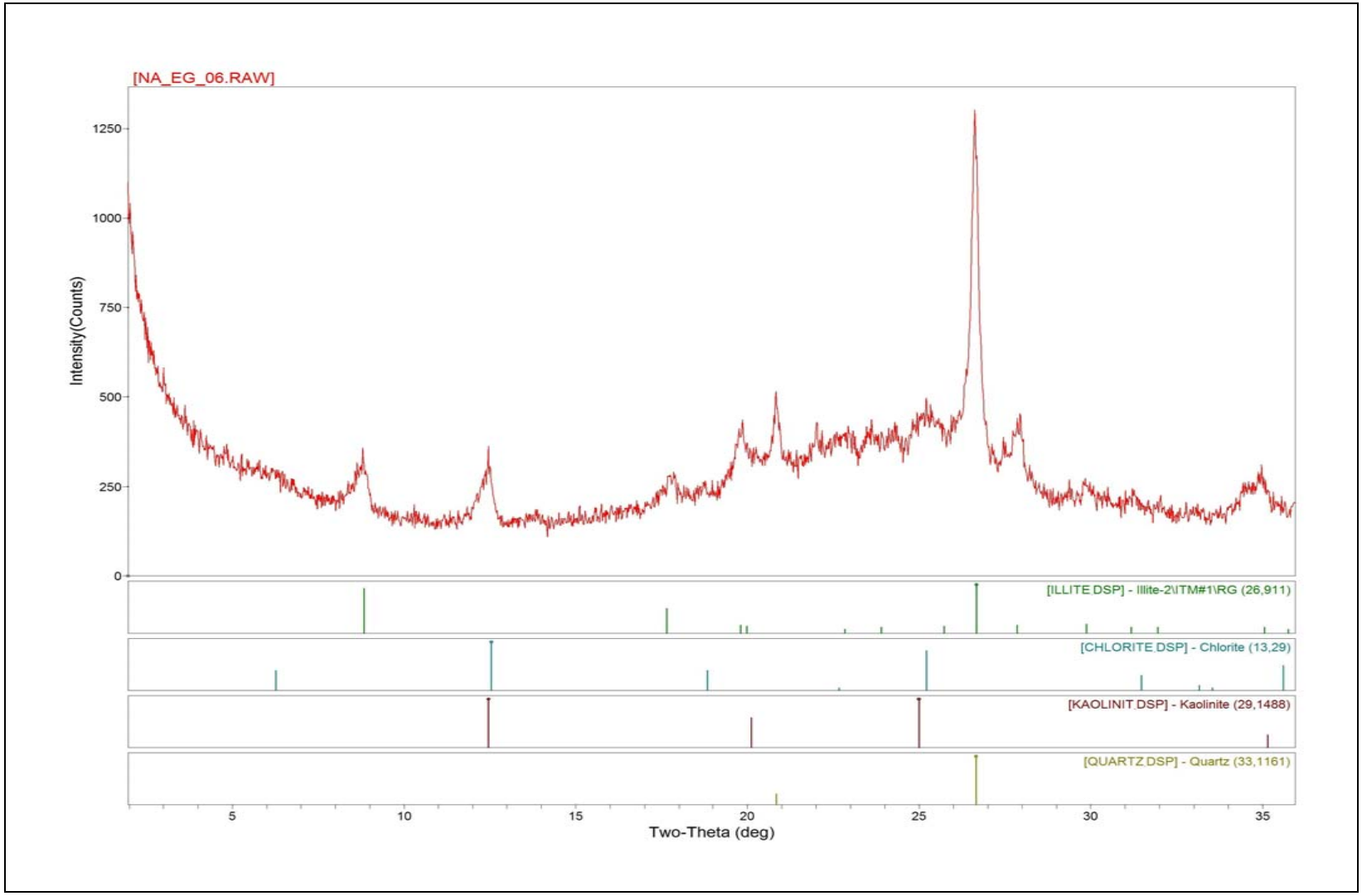

Site 54A

XRD patterns (oriented Slides, <4µm size fraction): The solid red traces represent XRD patterns recorded after the Ethylene Glycol (EG) solvation. Peak positions are outlined as solid green hachures for illite&mica, solid blue for chlorite, solid red for kaolinite and solid green olive for quartz.

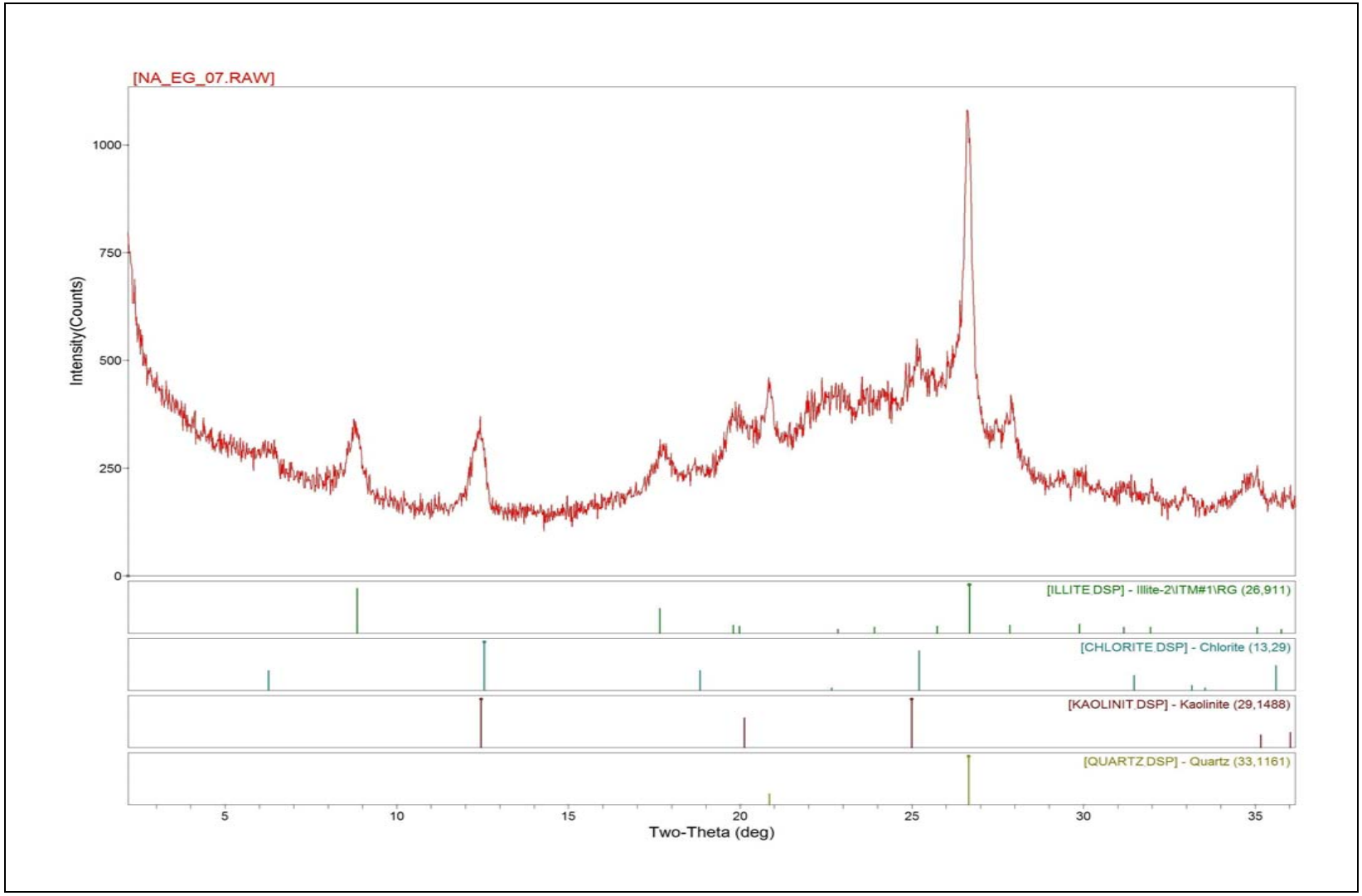

Site 55-1

XRD patterns (oriented Slides, <4µm size fraction): The solid red traces represent XRD patterns recorded after the Ethylene Glycol (EG) solvation. Peak positions are outlined as solid green hachures for illite&mica, solid blue for chlorite, solid red for kaolinite and solid green olive for quartz.

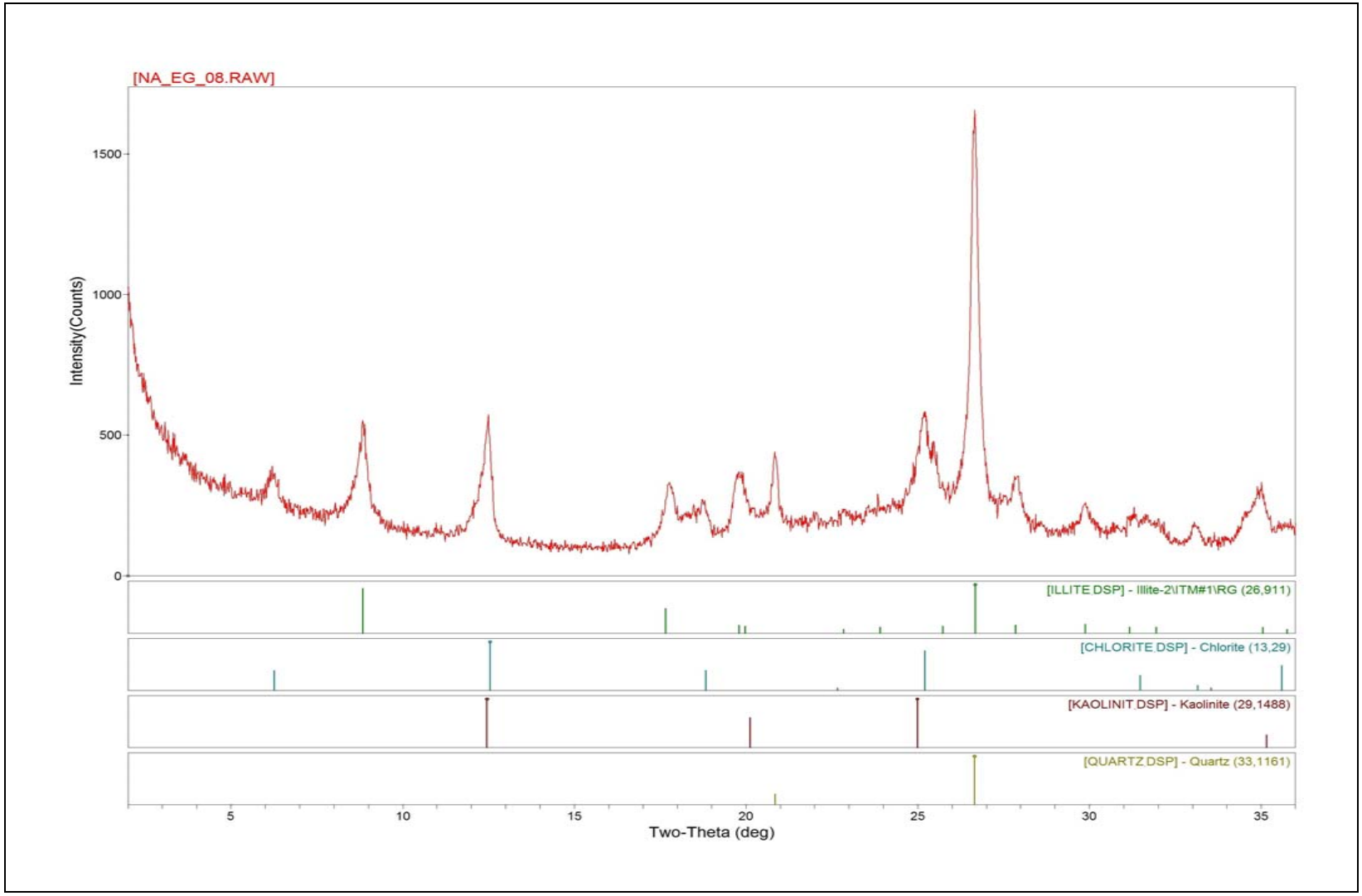

Site 56A

XRD patterns (oriented Slides, <4µm size fraction): The solid red traces represent XRD patterns recorded after the Ethylene Glycol (EG) solvation. Peak positions are outlined as solid green hachures for illite&mica, solid blue for chlorite, solid red for kaolinite and solid green olive for quartz.

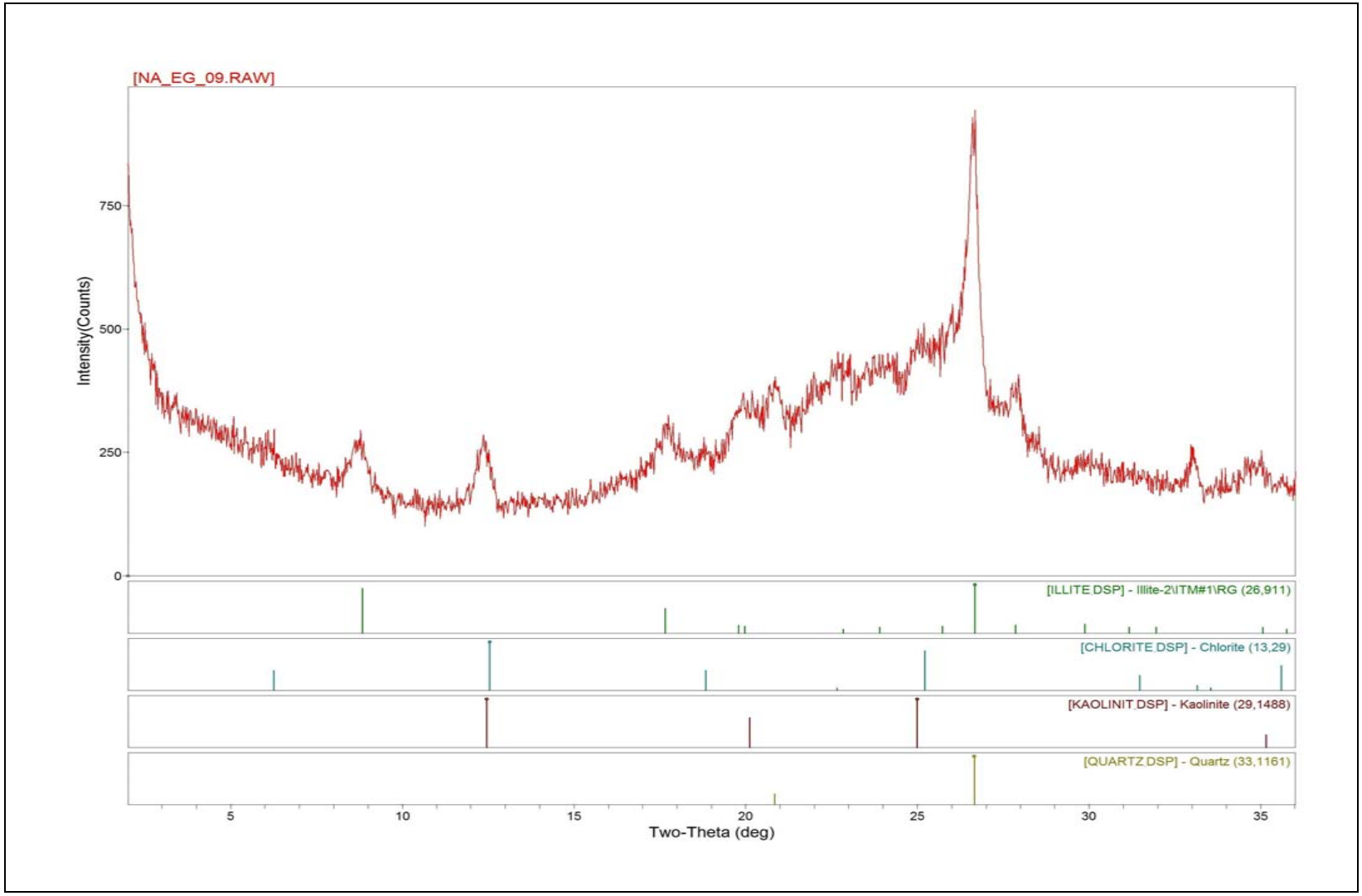

Site 63

XRD patterns (oriented Slides, <4µm size fraction): The solid red traces represent XRD patterns recorded after the Ethylene Glycol (EG) solvation. Peak positions are outlined as solid green hachures for illite&mica, solid blue for chlorite, solid red for kaolinite and solid green olive for quartz.

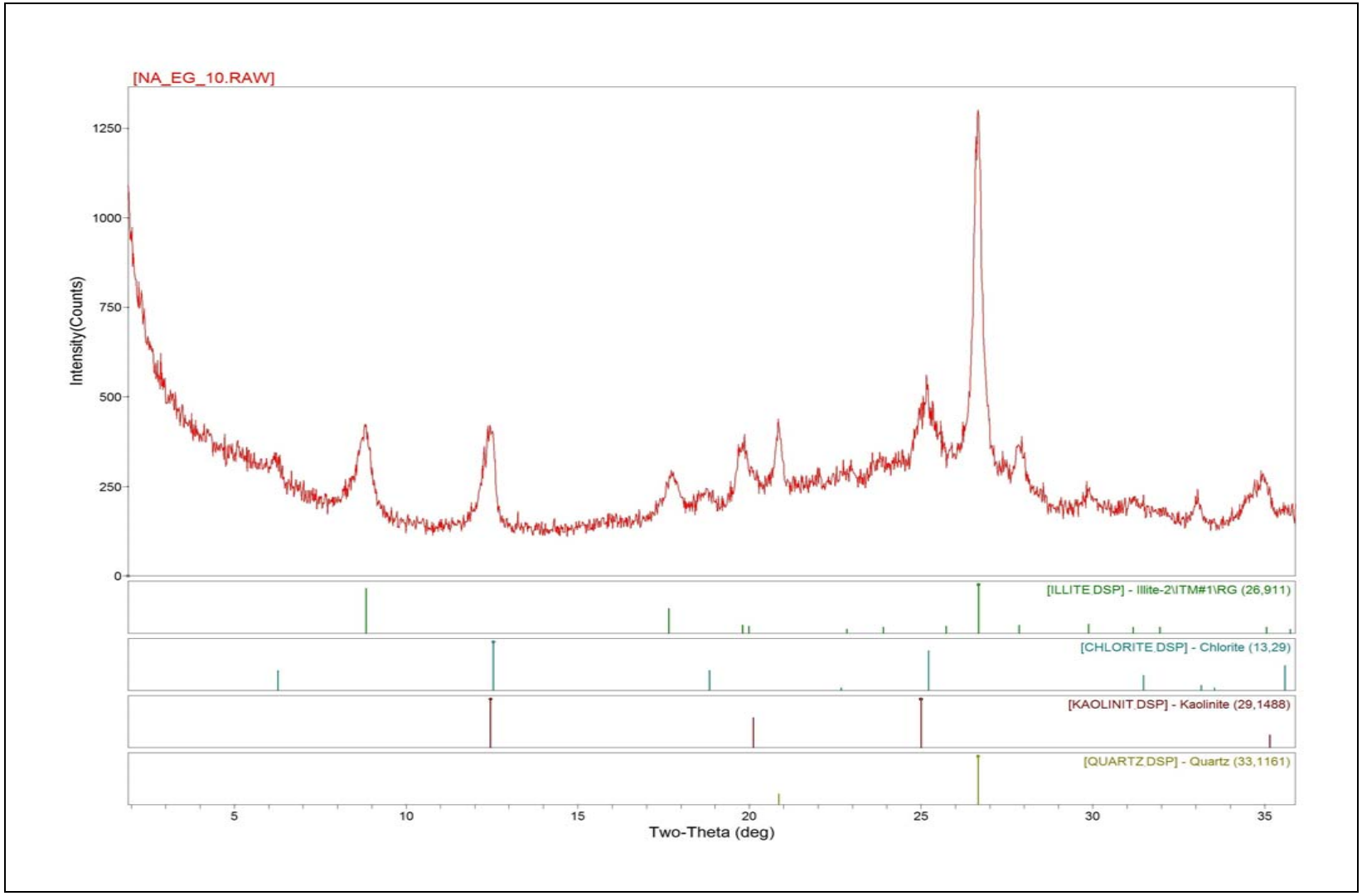

Site 84-1

XRD patterns (oriented Slides, <4µm size fraction): The solid red traces represent XRD patterns recorded after the Ethylene Glycol (EG) solvation. Peak positions are outlined as solid green hachures for illite&mica, solid blue for chlorite, solid red for kaolinite and solid green olive for quartz.

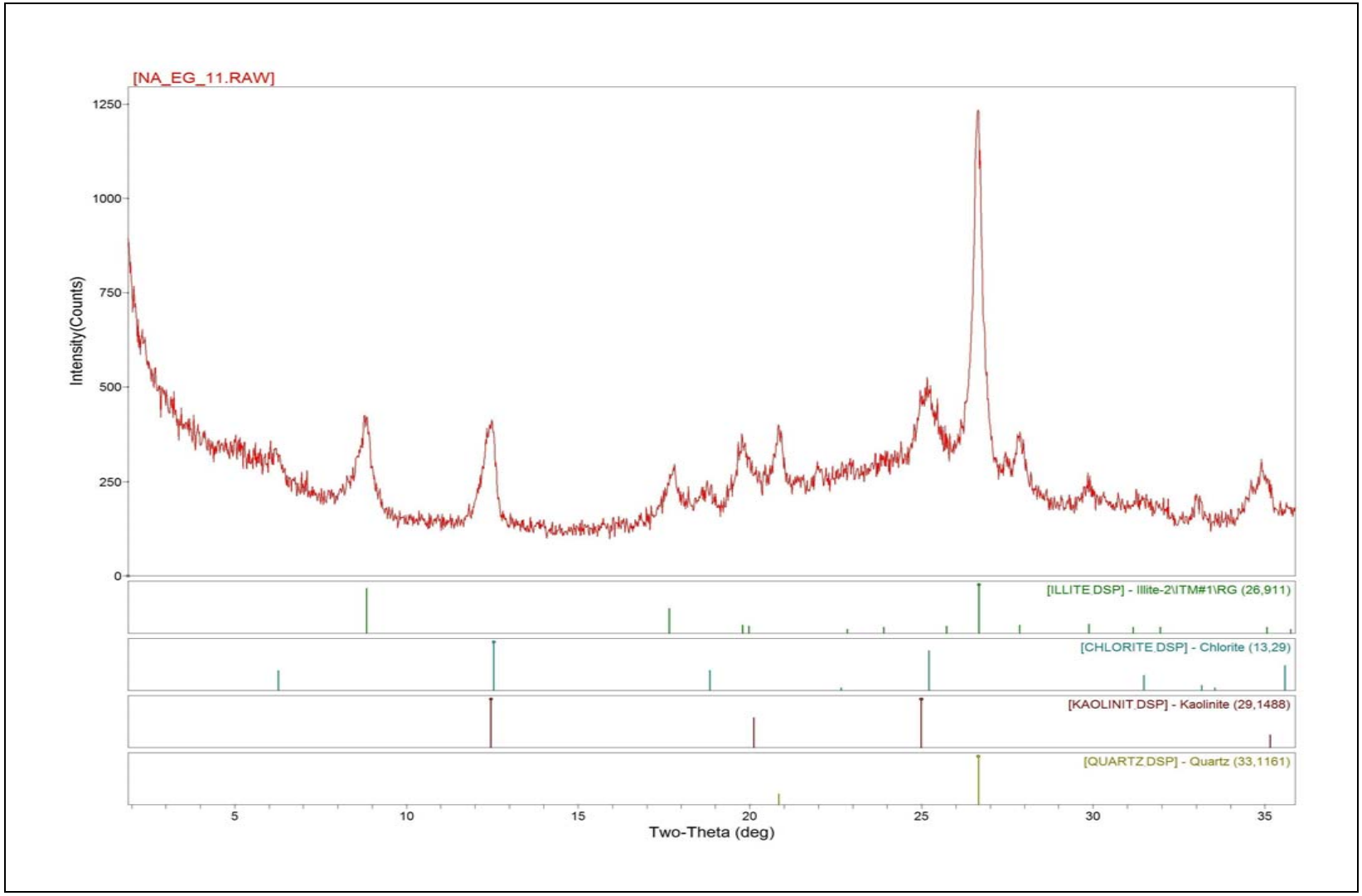

Site 85-1

XRD patterns (oriented Slides, <4µm size fraction): The solid red traces represent XRD patterns recorded after the Ethylene Glycol (EG) solvation. Peak positions are outlined as solid green hachures for illite&mica, solid blue for chlorite, solid red for kaolinite and solid green olive for quartz.

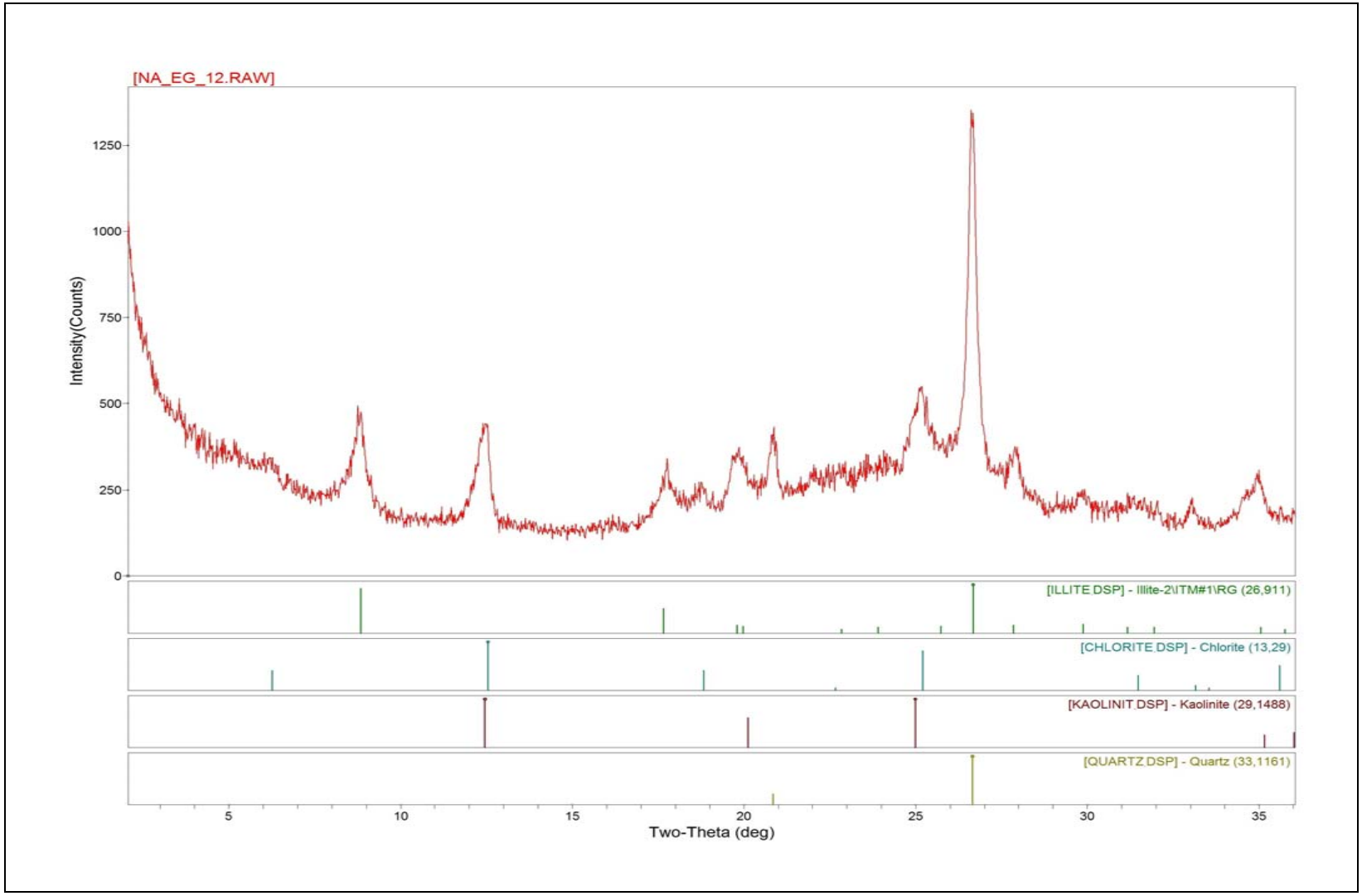

Site 86

XRD patterns (oriented Slides, <4µm size fraction): The solid red traces represent XRD patterns recorded after the Ethylene Glycol (EG) solvation. Peak positions are outlined as solid green hachures for illite&mica, solid blue for chlorite, solid red for kaolinite and solid green olive for quartz.

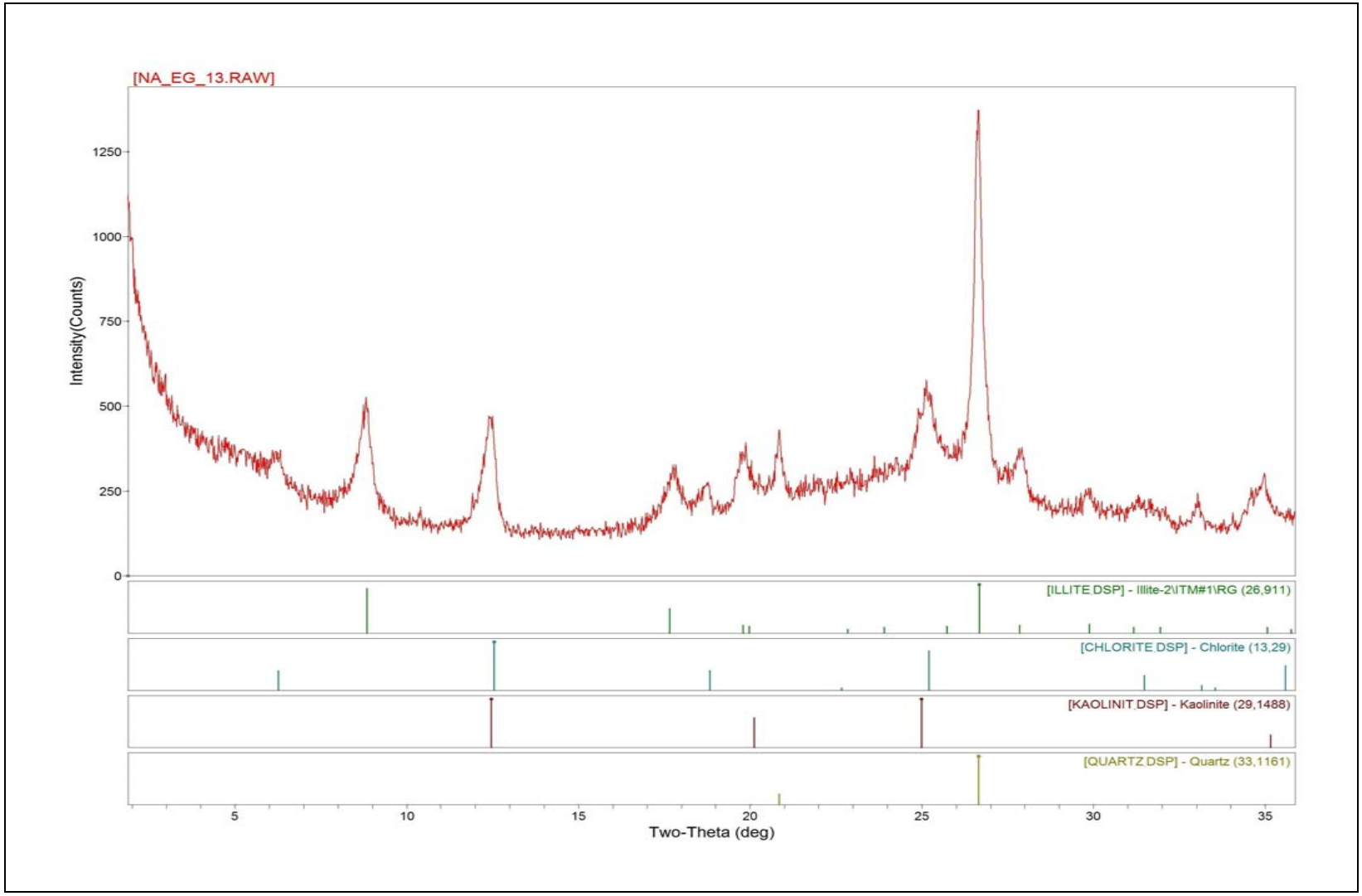

Site 86-1

XRD patterns (oriented Slides, <4µm size fraction): The solid red traces represent XRD patterns recorded after the Ethylene Glycol (EG) solvation. Peak positions are outlined as solid green hachures for illite&mica, solid blue for chlorite, solid red for kaolinite and solid green olive for quartz.

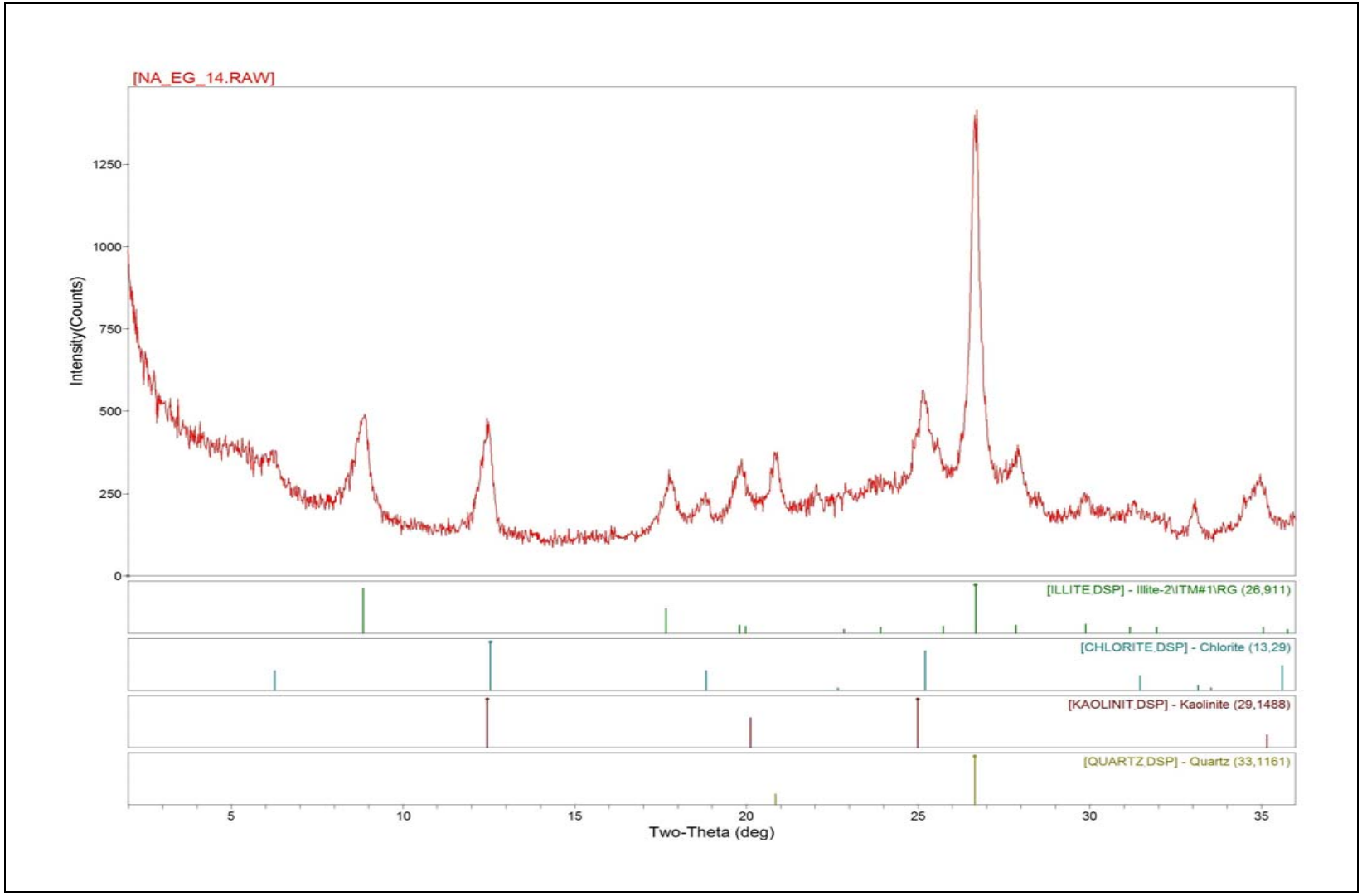

Site 87-1

XRD patterns (oriented Slides, <4µm size fraction): The solid red traces represent XRD patterns recorded after the Ethylene Glycol (EG) solvation. Peak positions are outlined as solid green hachures for illite&mica, solid blue for chlorite, solid red for kaolinite and solid green olive for quartz.

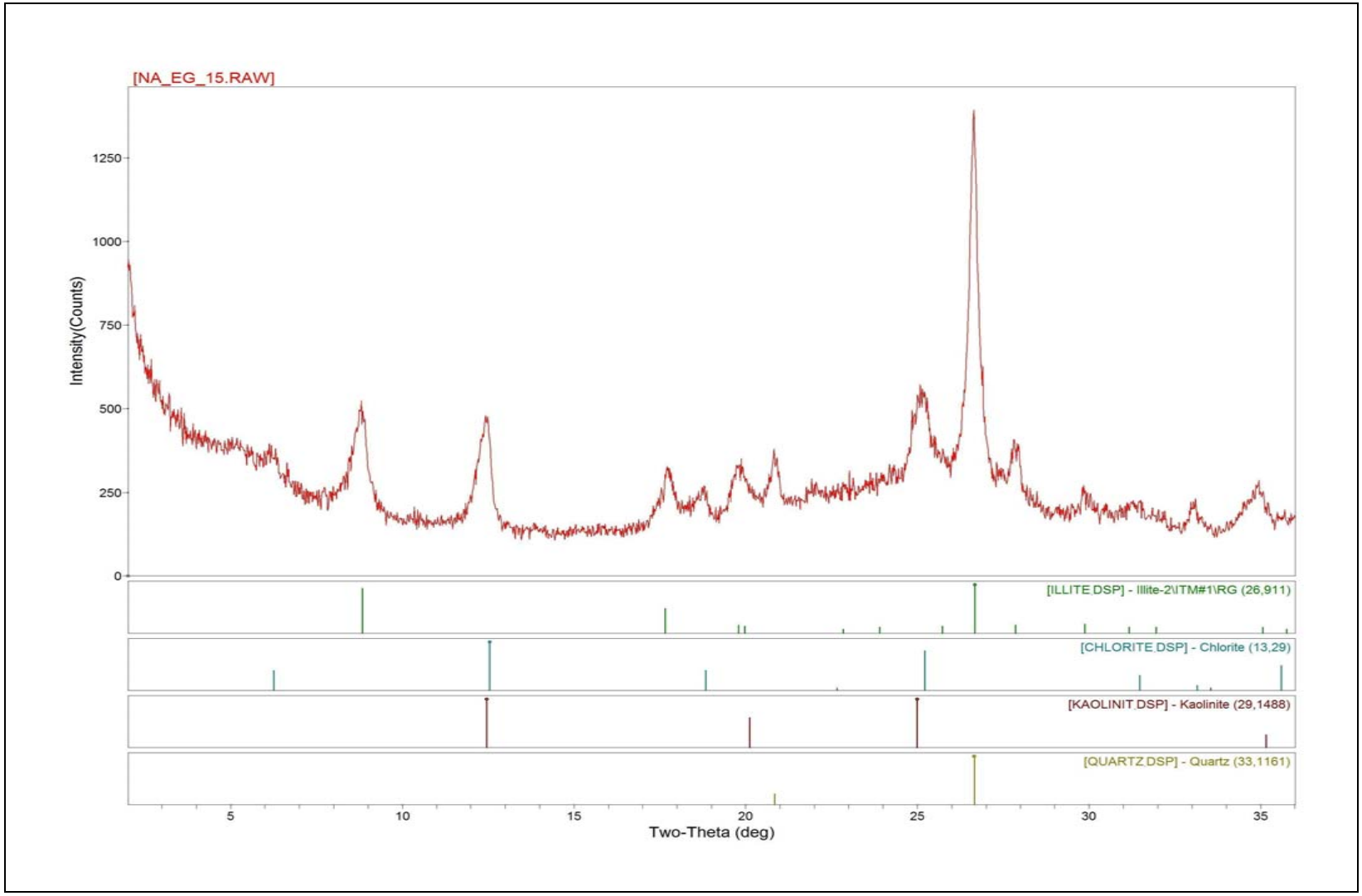

Site 88-1

XRD patterns (oriented Slides, <4µm size fraction): The solid red traces represent XRD patterns recorded after the Ethylene Glycol (EG) solvation. Peak positions are outlined as solid green hachures for illite&mica, solid blue for chlorite, solid red for kaolinite and solid green olive for quartz.

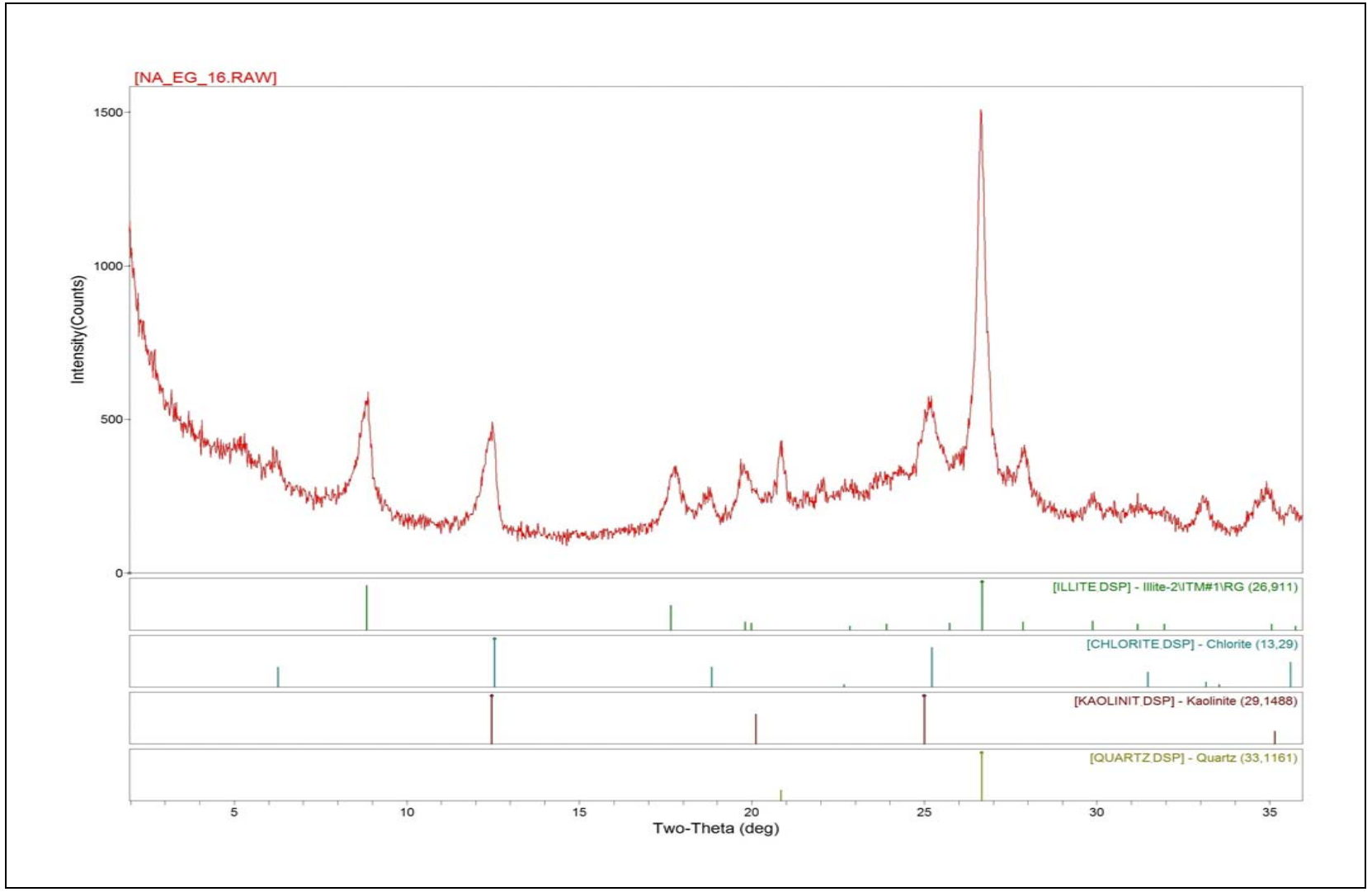

Site 89A

XRD patterns (oriented Slides, <4µm size fraction): The solid red traces represent XRD patterns recorded after the Ethylene Glycol (EG) solvation. Peak positions are outlined as solid green hachures for illite&mica, solid blue for chlorite, solid red for kaolinite and solid green olive for quartz.

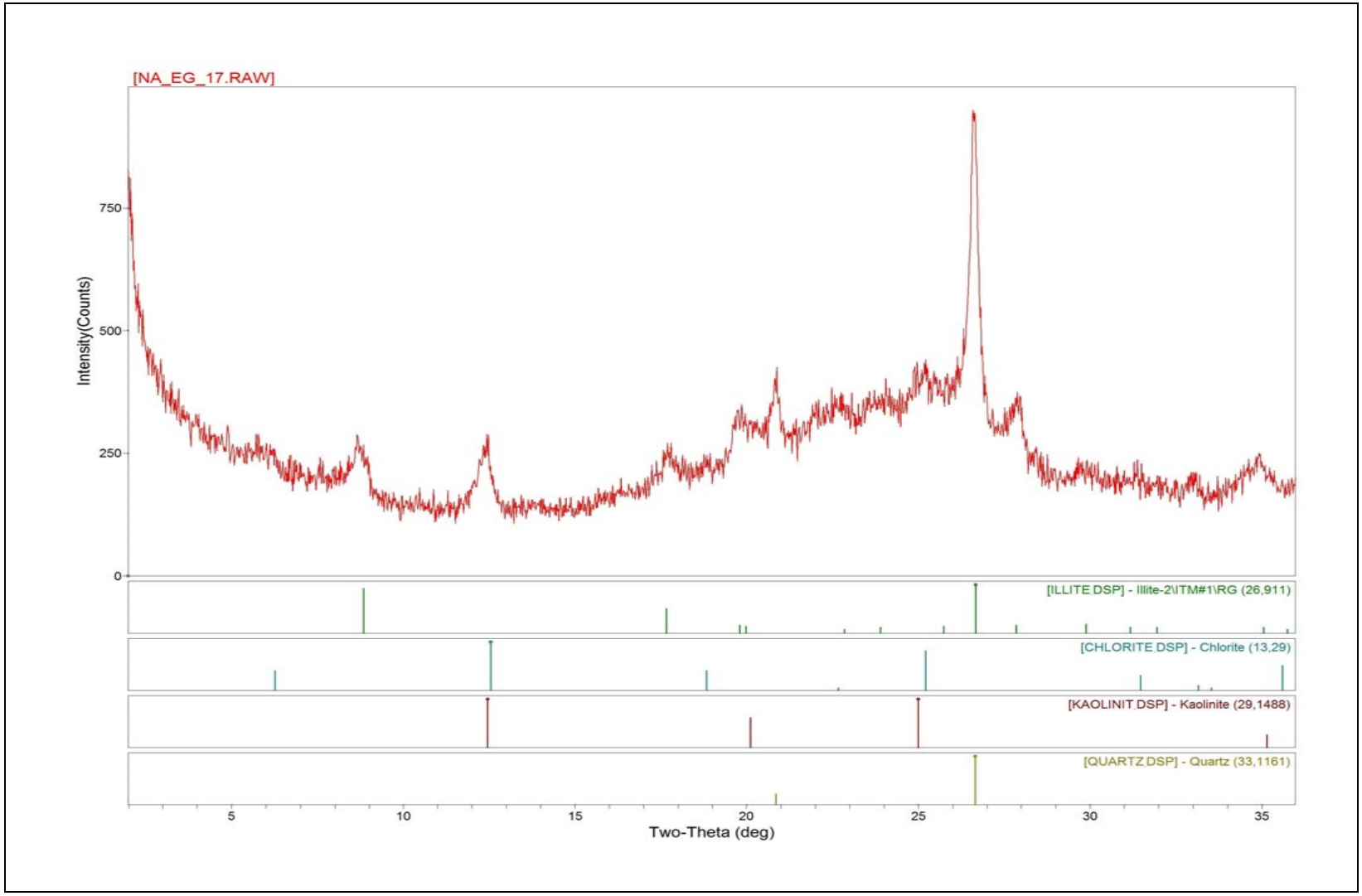

Site 91

XRD patterns (oriented Slides, <4µm size fraction): The solid red traces represent XRD patterns recorded after the Ethyelene Glycol (EG) solvation. Peak positions are outlined as solid green hachures for illite&mica, solid blue for chlorite, solid red for kaolinite and solid green olive for quartz.

C 3.0. Experimental XRD patterns (oriented slides, <4μm size fraction) of the seventeen samples selected as being representative of New York Bight Apex. The solid green traces represent XRD patterns recorded after Ethylene Glycol (EG) solvation and The solid red traces represent XRD patterns recorded in the Air Dried (AD) state. Peak positiosn are outlined as solid green hachures for illite&mica, solid blue for chlorite, solid red for kaolinite, solid purple for I/S and solid green olive for quartz.

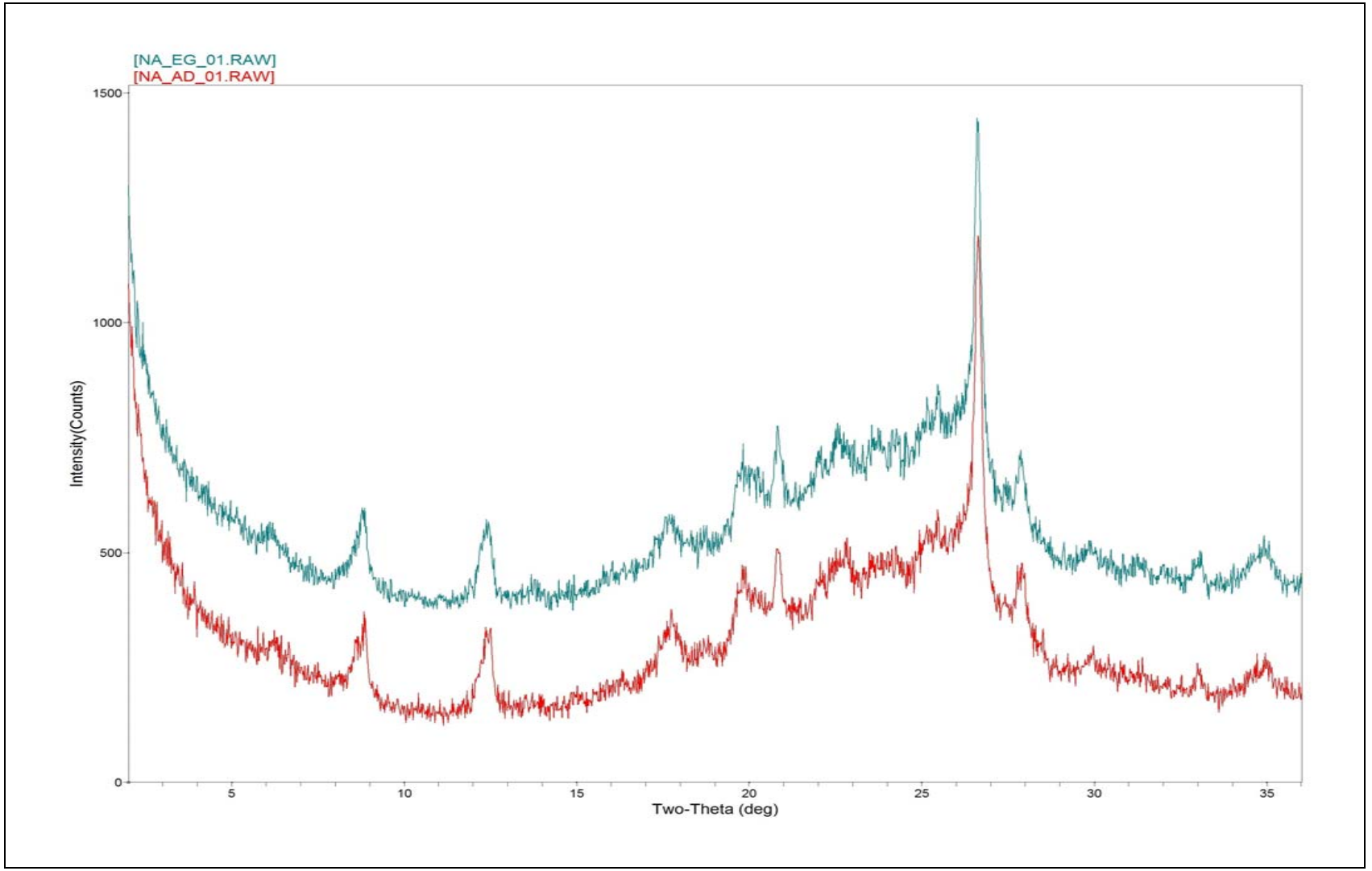

AD: Air Dried; EG: Ethylene Glycole

Site 1-1

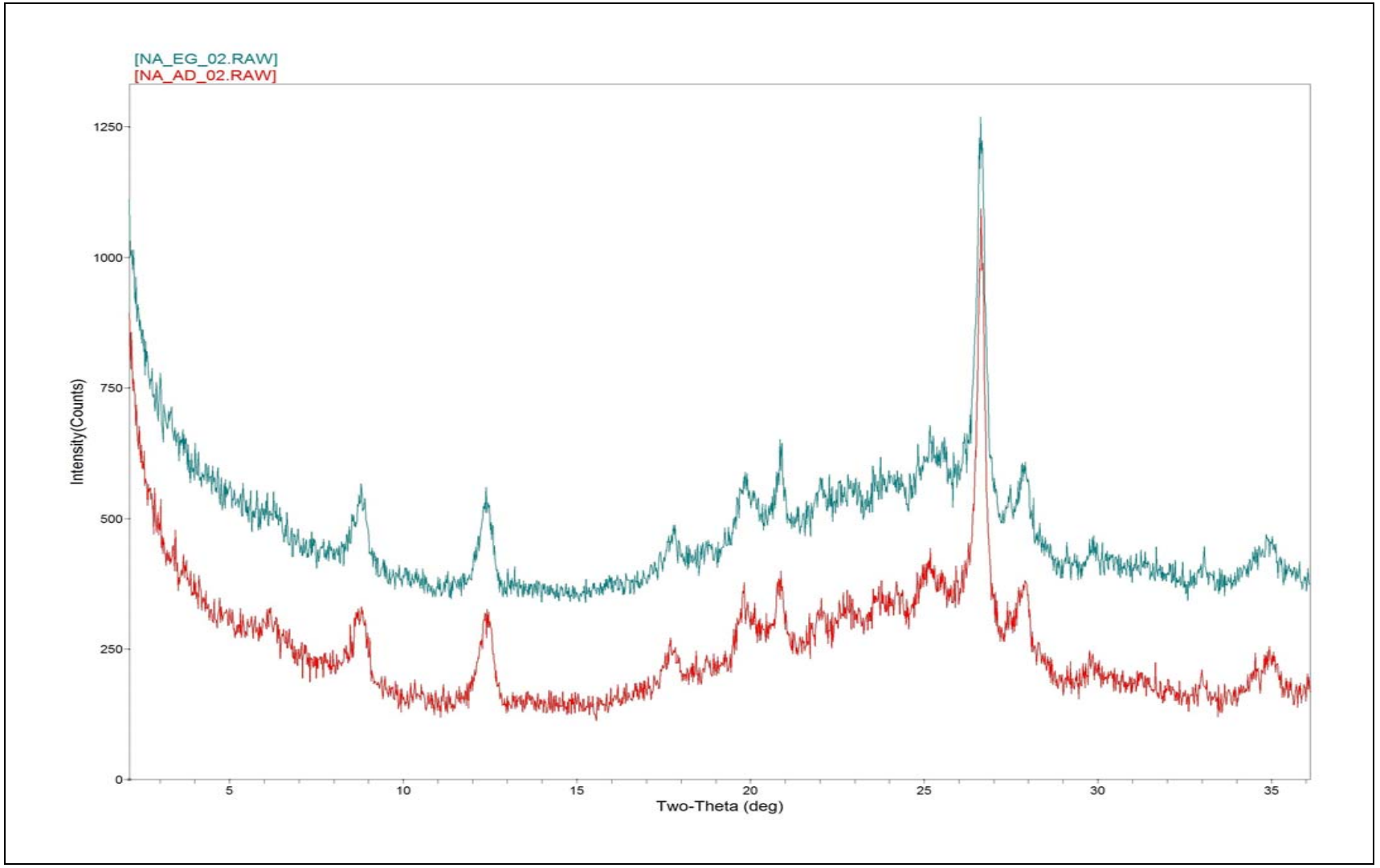

AD: Air Dried; **EG: Ethylene Glycole**

Site 1-2

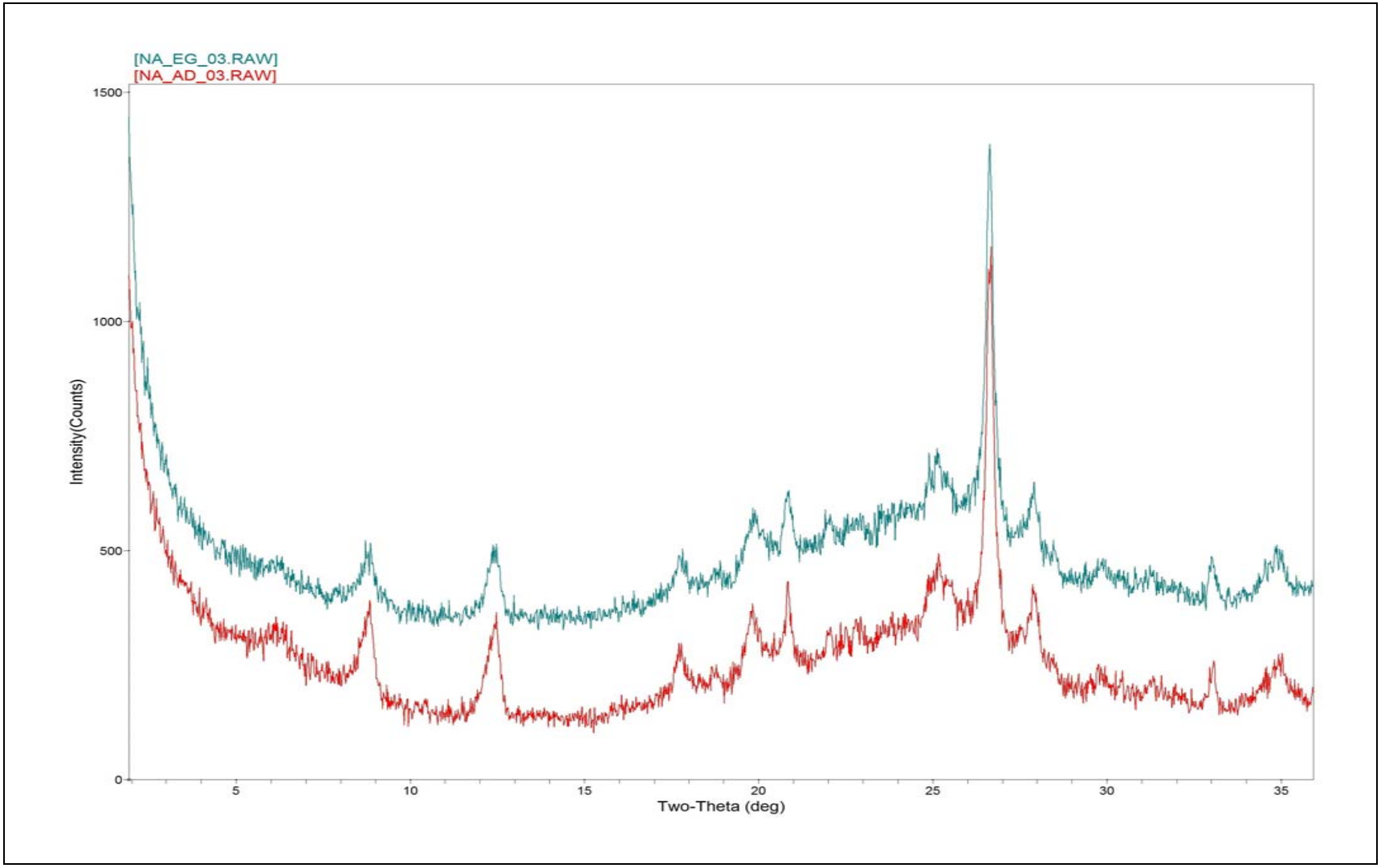

AD: Air Dried; EG: Ethylene Glycole

Site 7-1

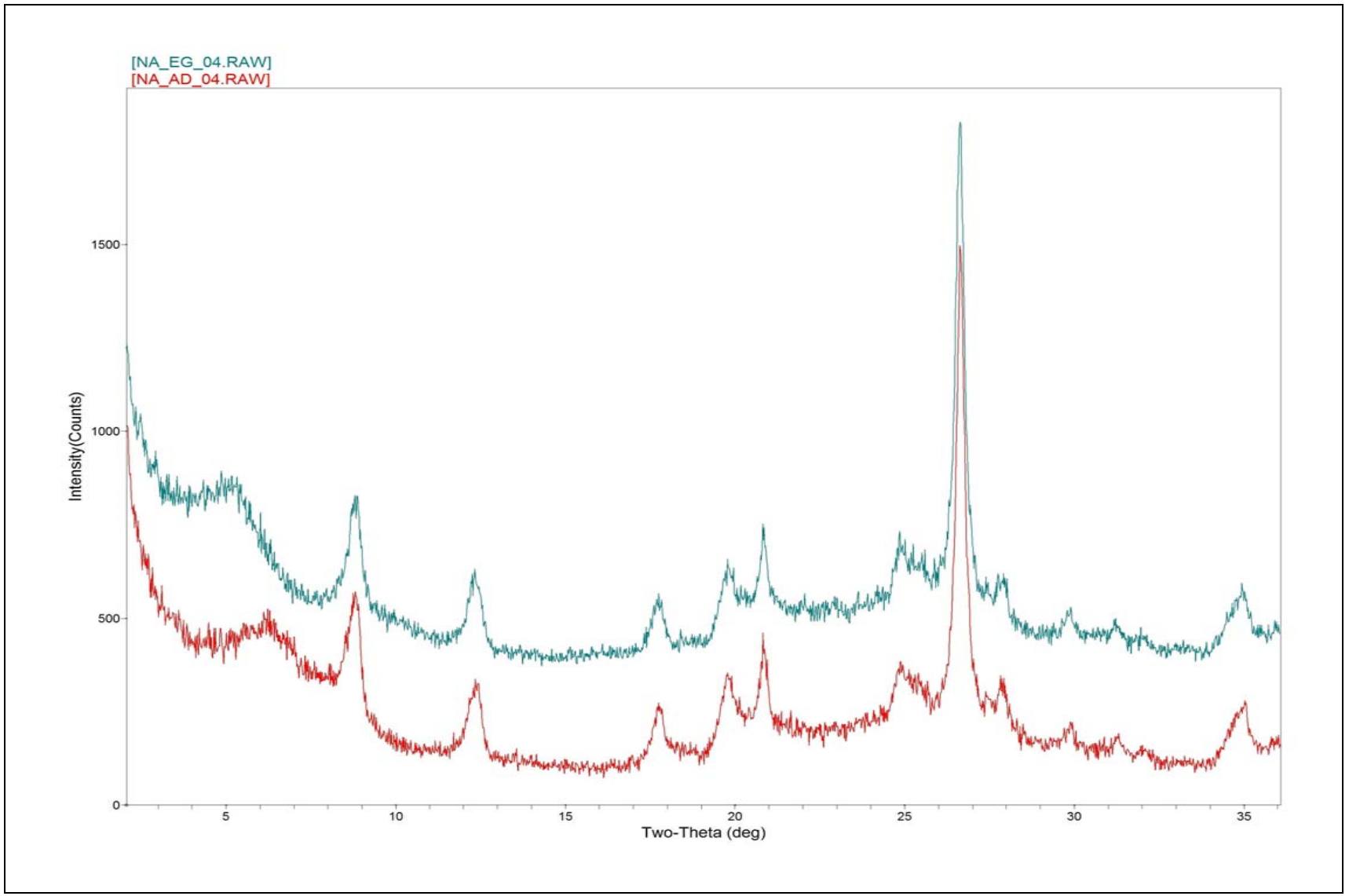

AD: Air Dried; EG: Ethylene Glycole

Site 7-1-2

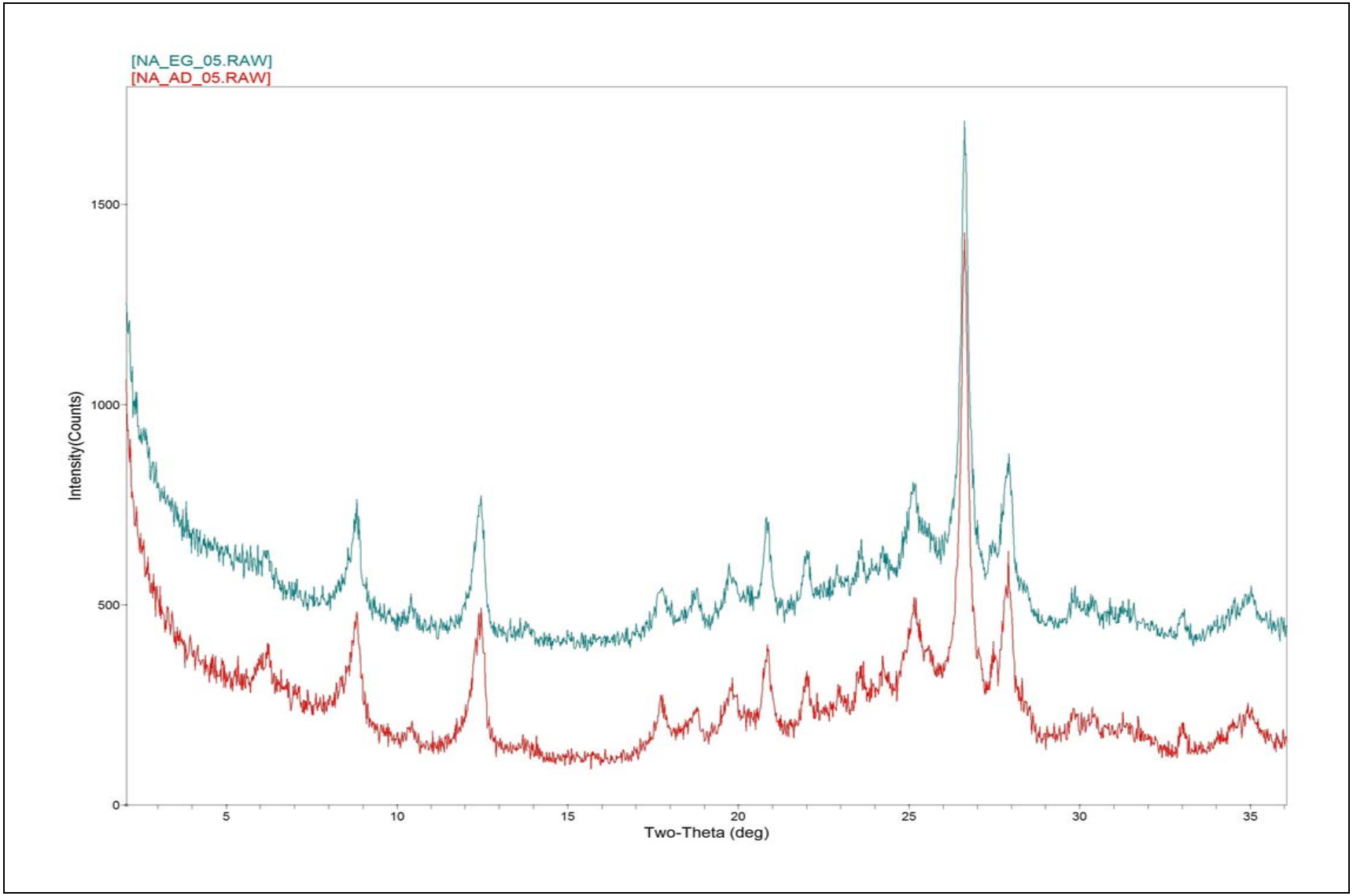

AD: Air Dried; EG: Ethylene Glycole

Site 33-1

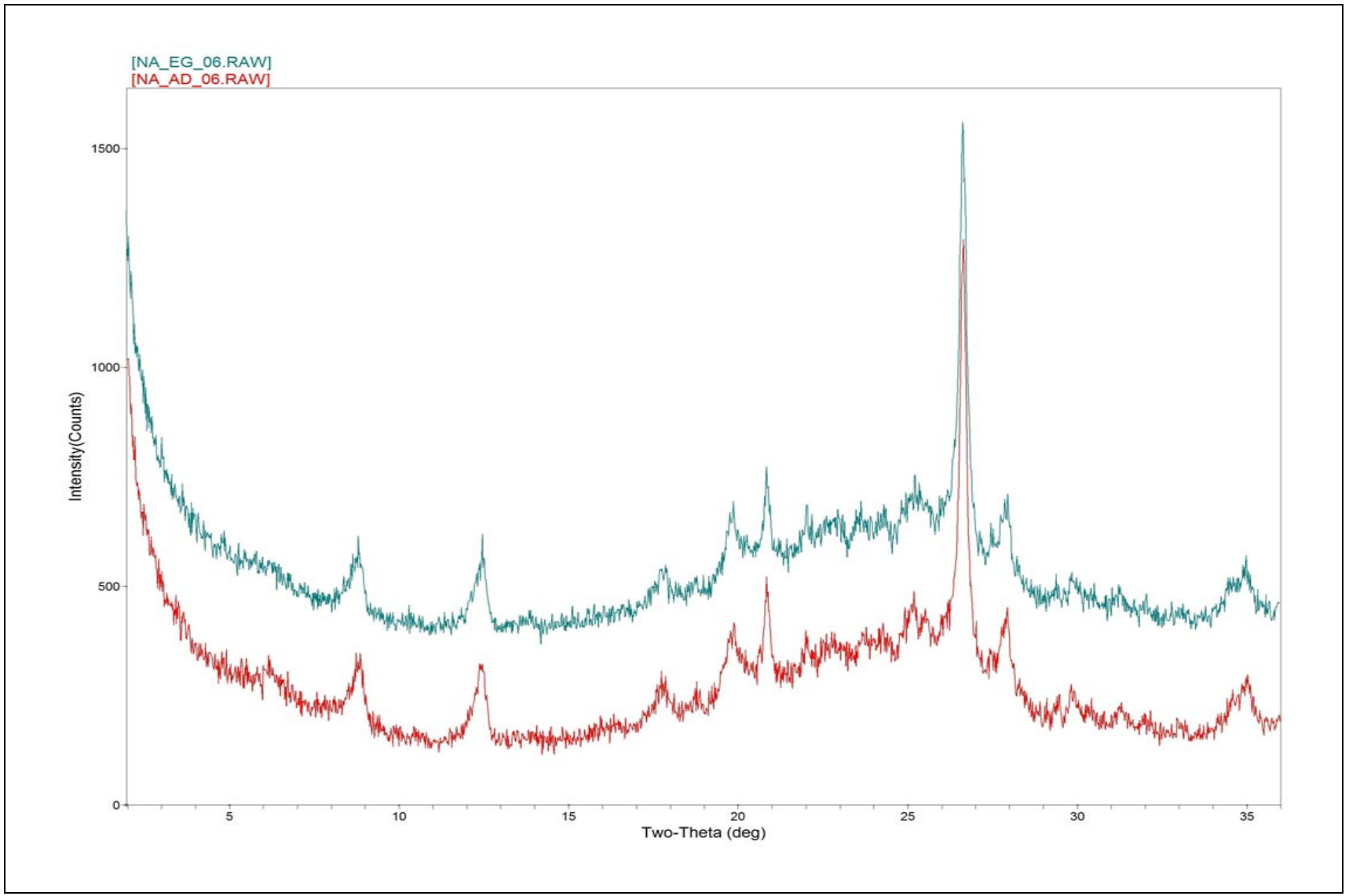

AD: Air Dried; EG: Ethylene Glycole

Site 54A

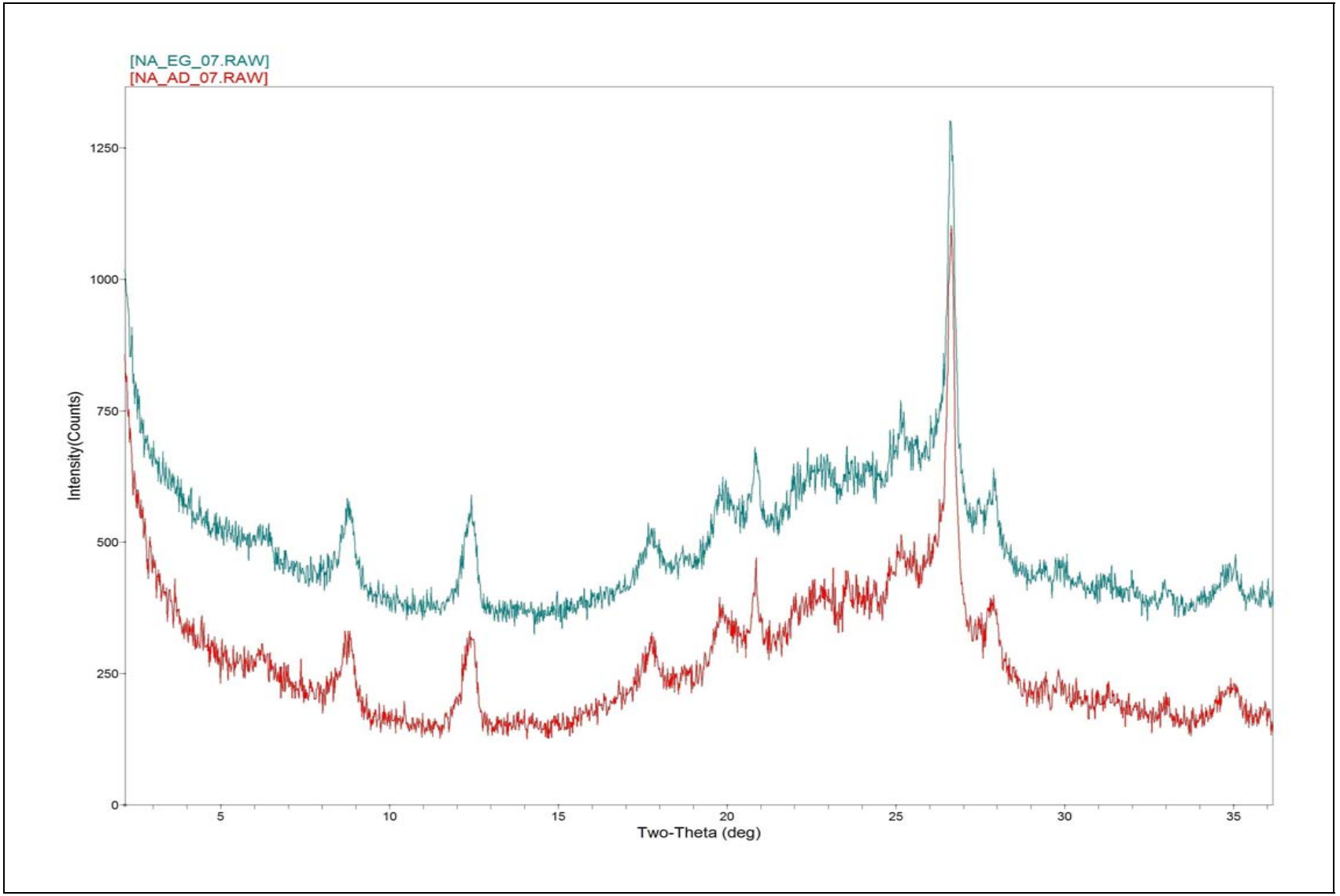

AD: Air Dried; EG: Ethylene Glycole

Site 55-1

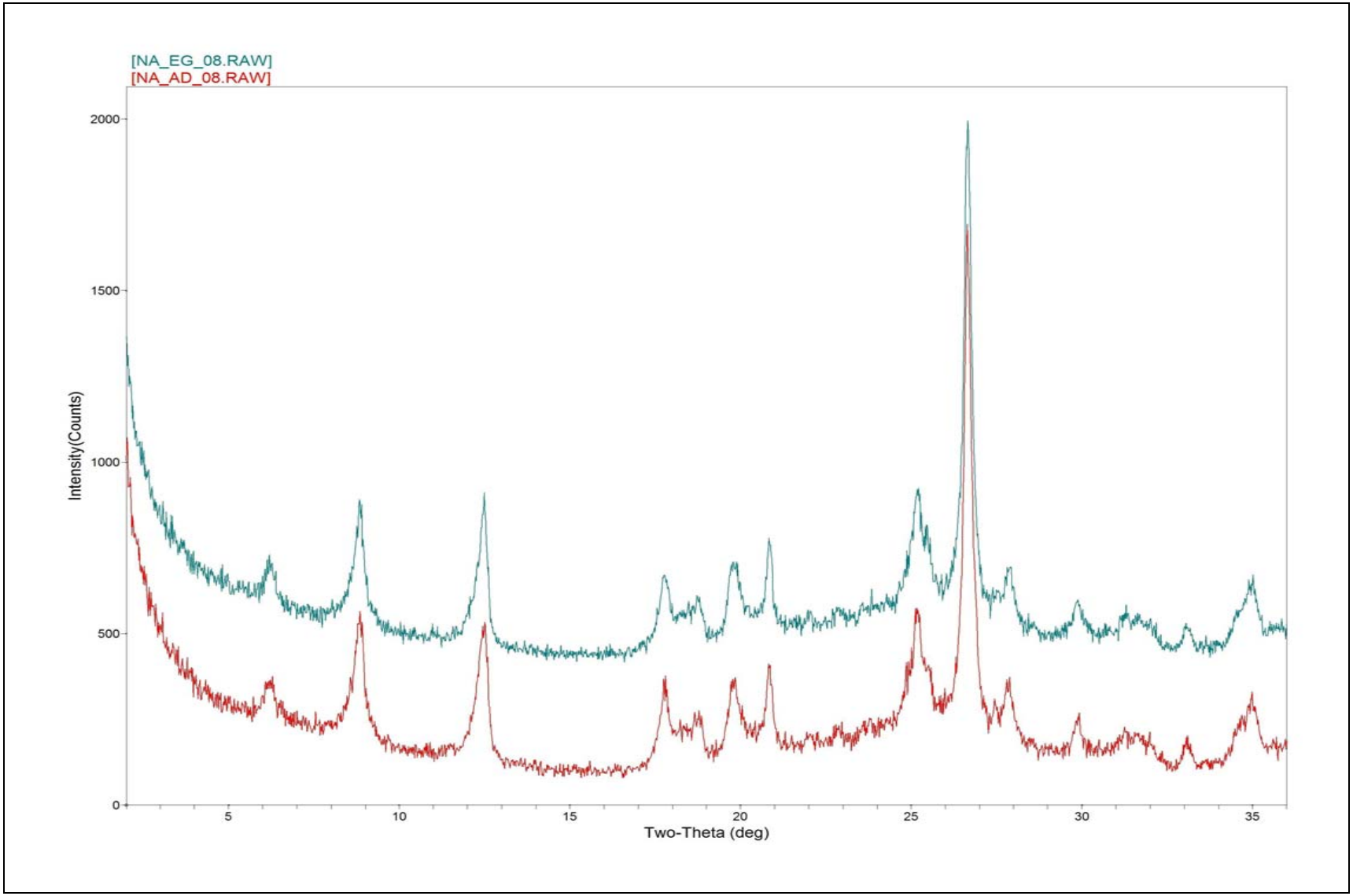

AD: Air Dried; EG: Ethylene Glycole

Site 56

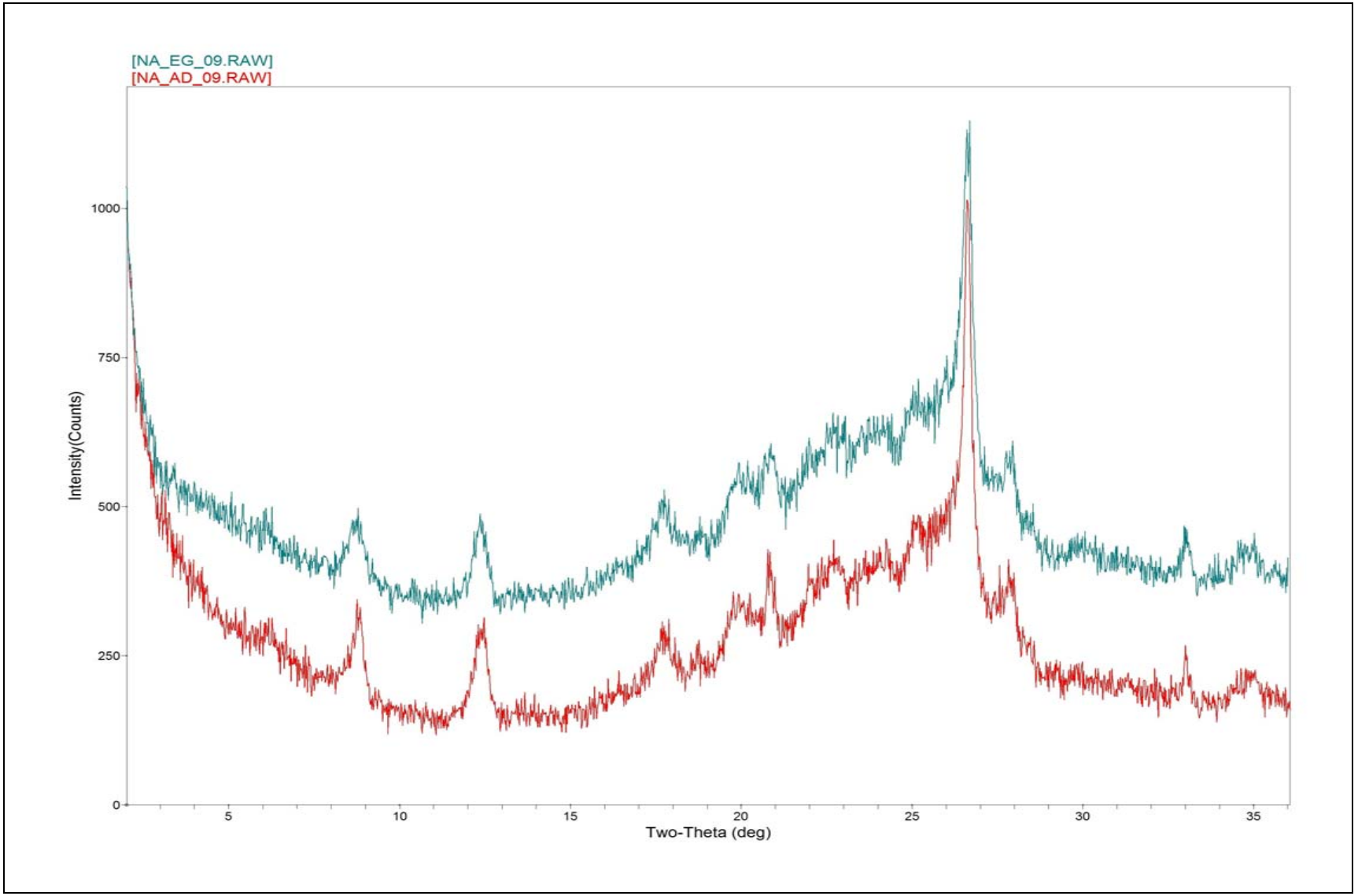

AD: Air Dried; EG: Ethylene Glycole

Site 63

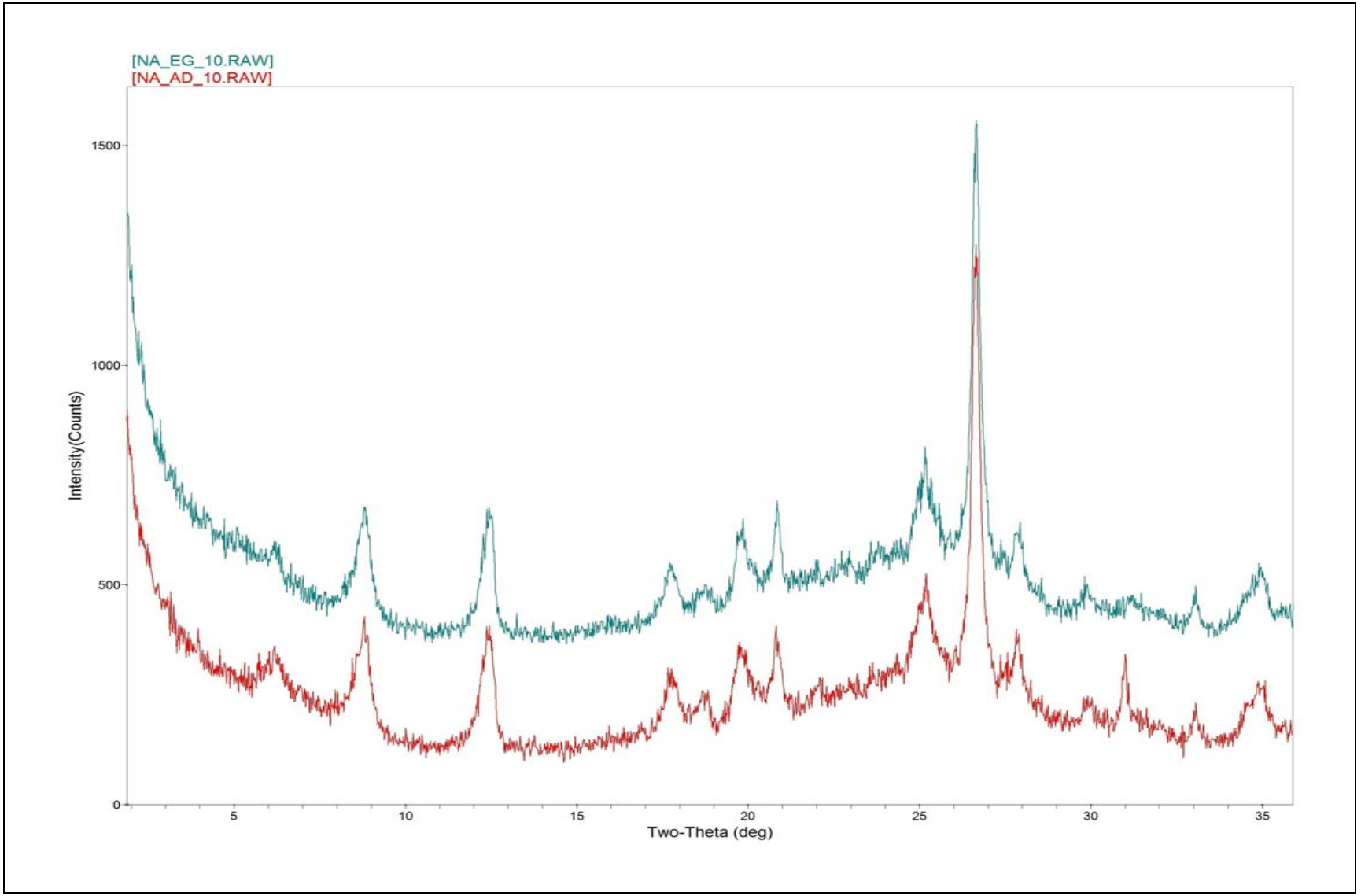

AD: Air Dried; EG: Ethylene Glycole

Site 84-1

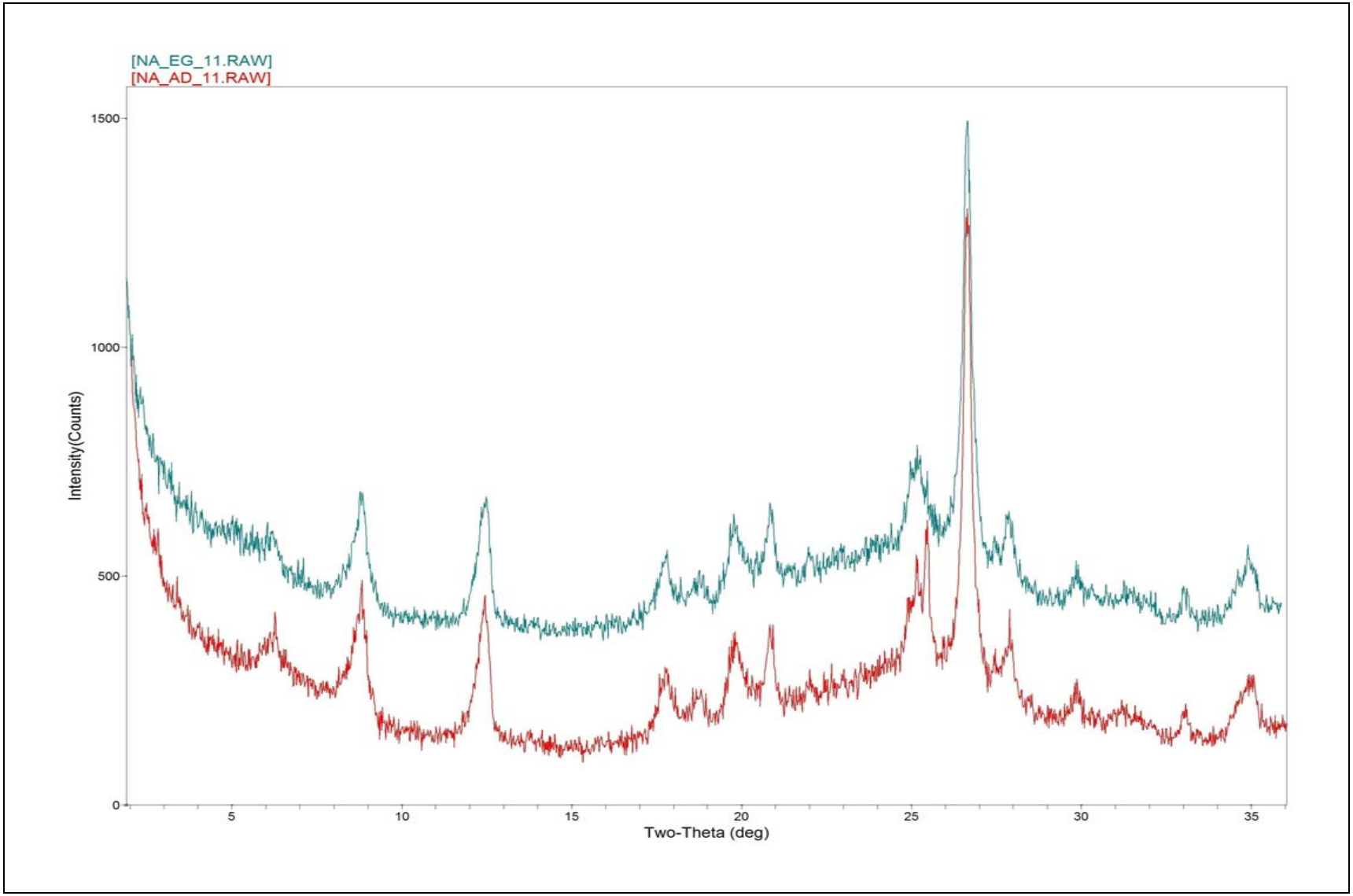

AD: Air Dried; EG: Ethylene Glycole

Site 85-1

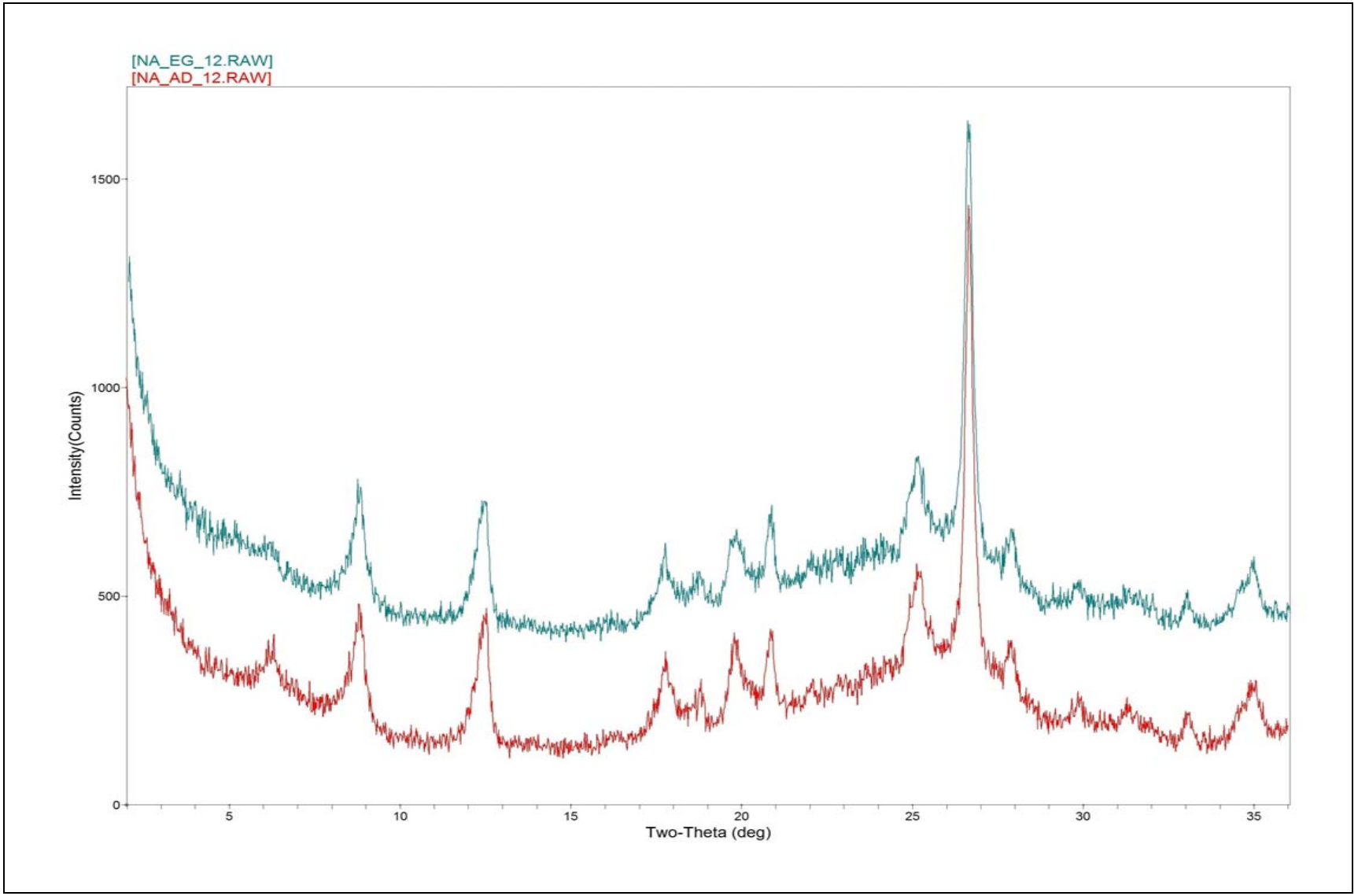

AD: Air Dried; EG: Ethylene Glycole

Site 86

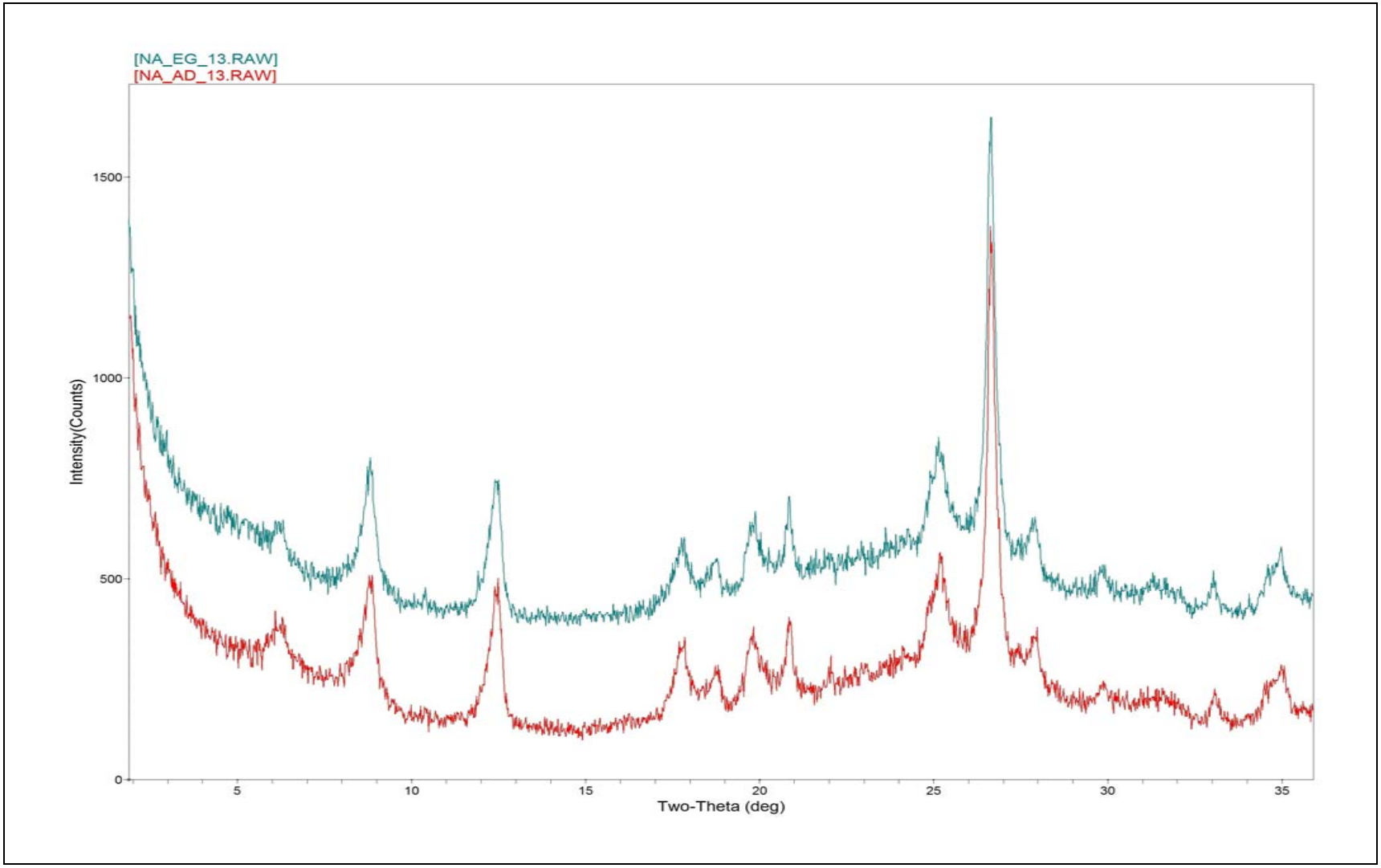

AD: Air Dried; EG: Ethylene Glycole

Site 86-1

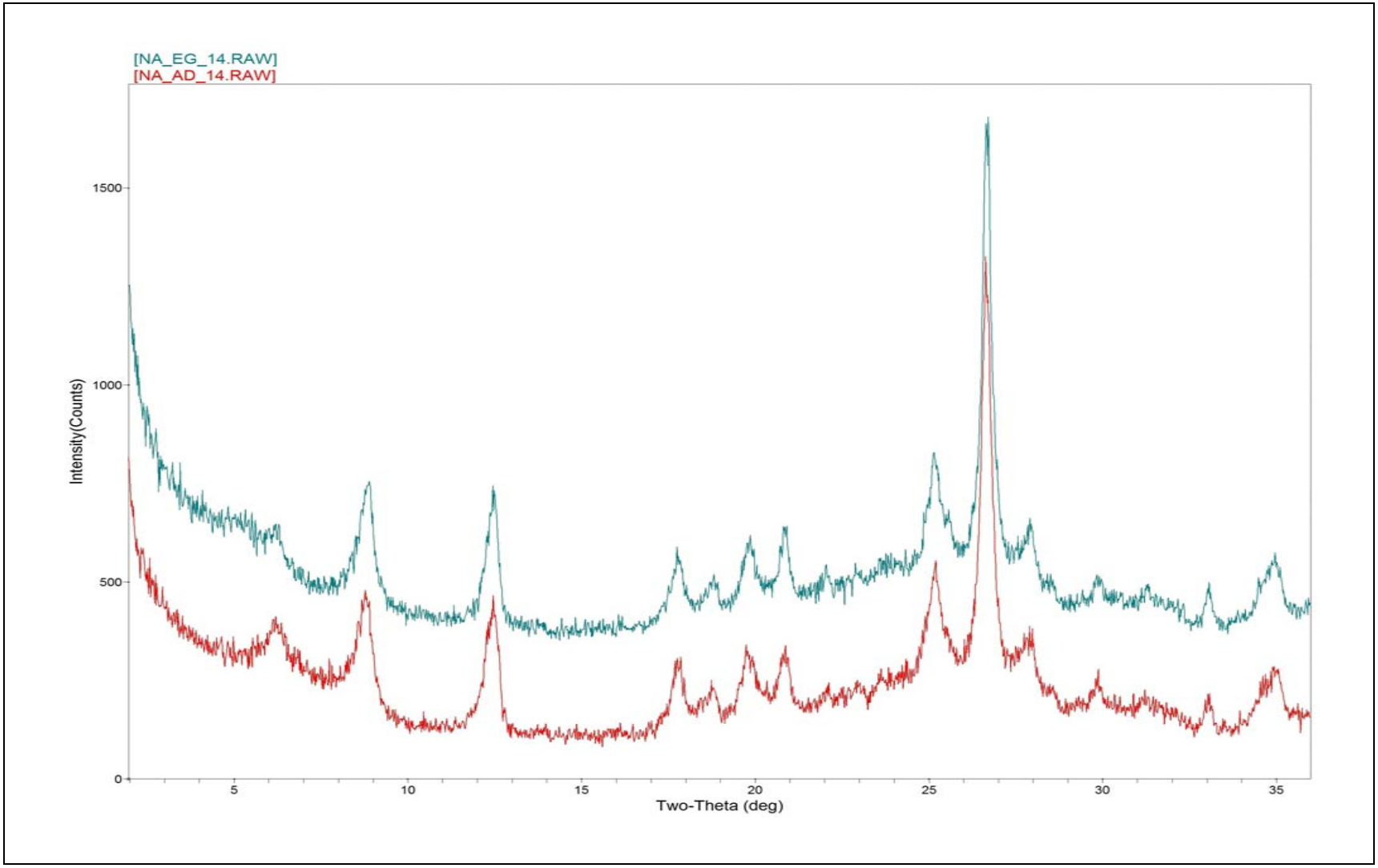

AD: Air Dried; EG: Ethylene Glycole

Site 87-1

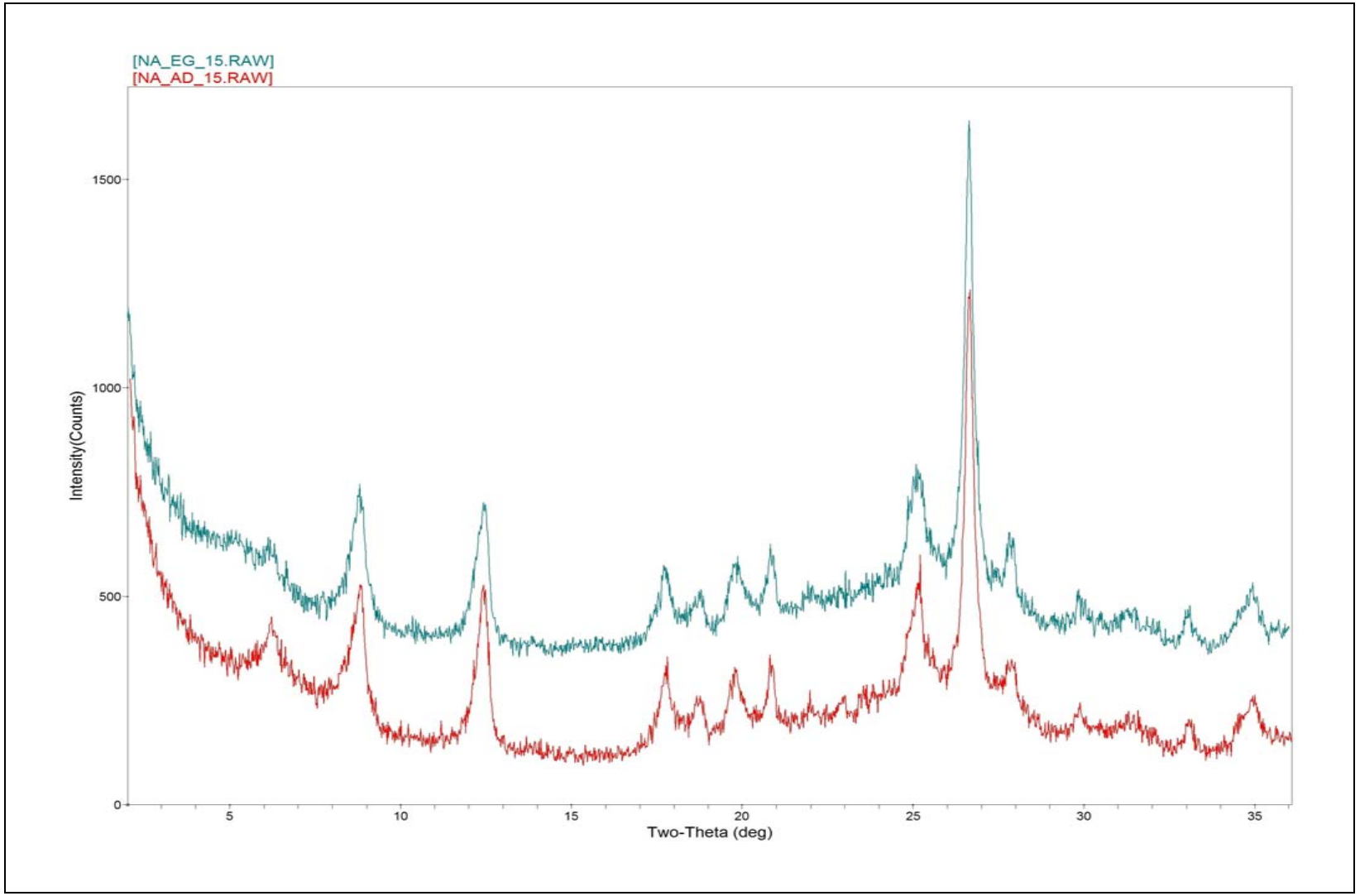

AD: Air Dried; EG: Ethylene Glycol

Site 88-1

Appendix D

D 1.0. Comparative Concentrations of Selected Trace Metals in Clay Fractions from the NYB

D 2.0. Effect of 50% HNO_3 and Total Acid Digestion on Trace Metal Concentration in Core AC 97-1 and AC97-9

D 3.0. Grain Size Depencies of Trace Metal Concentration Extracted by 50%HNO_3

Appendix D

D.1. Comparative Concentrations of Selected Trace Metals in Clay Fractions from the NYB (ppm = mg/kg, dry sediment)

a. Pb

Sample	(1)	(2)	(3)
84-1	NA	160 ± 1.2	29 ± 0.7
85	NA	80 ± 0.4	15 ± 1.2
87	10 ± 0.3	15 ± 1.3	NA
89A	200 ± 0.20	247 ± 3.6	5 ± 0.2
1-2	88 ± 2	115 ± 4.7	NA
71	190 ± 4.5	220 ± 12	NA
91	197 ± 2.0	244 ± 3.5	NA
33	82 ± 2.5	94 ± 2.3	10.8 ± 0.4
7-1	124 ± 1.6	148 ± 10.9	6.4 ± 0.1
54A	175 ± 2	185 ± 0.3	15 ± 1.5
56A	35 ± 0.8	42 ± 1.5	6 ± 0.1
20A	30 ± 1.9	40 ± 2.4	13 ± 0.7
21A	70 ± 1.0	93 ± 6.5	21 ± 1.2
63	129 ± 6	160 ± 3.3	NA

%RSD = 12.45

b. Cd

Sample	(1)	(2)	(3)
84-1	7 ± 0.7	7 ± 0.5	ND
85	9 ± 0.5	10 ± 0.6	ND
87	6 ± 0.6	6.5 ± 0.2	ND
89A	8.3 ± 0.2	8.7 ± 0.1	ND
1-2	8 ± 0.1	8 ± 0.4	ND
71	11 ± 0.4	15 ± 0.9	ND
91	13 ± 0.3	15 ± 0.3	ND
33	6.5 ± 0.4	7 ± 0.1	ND
7-1	9 ± 0.5	10 ± 0.7	ND
54A	8 ± 0.4	9.4 ± 0.3	ND
56A	4 ± 0.5	4.7 ± 0.6	ND
20A	5 ± 0.4	5.5 ± 0.2	ND
21A	4.7 ± 0.9	5 ± 1.0	ND
63	9.6 ± 0.4	10 ± 0.3	ND

%RSD = 5.41

c. Cr

Sample	(1)	(2)	(3)
84	130 ± 9.1	200 ± 0.6	70 ± 2.3
85	150 ± 3.9	170 ± 0.5	NA
87	ND	10.8 ± 1.4	ND
89A	84 ± 9.6	106 ± 0.1	NA
1-2	34 ± 3.0	100 ± 0.8	NA
71	130 ± 6.4	198 ± 1.2	39 ± 2.0
91	207 ± 5.7	328 ± 2.4	NA
33	38 ± 6.4	56 ± 1	5 ± 0.2
7-1	103 ± 2.0	182 ± 2	92 ± 1.5
54A	75 ± 2.1	158 ± 0.5	50 ± 4.8
56A	ND	16 ± 0.3	NA
20A	ND	8 ± 0.4	ND
21A	55 ± 5.0	108 ± 1.3	49 ± 2.8
63	110 ± 2.3	200 ± 0.5	NA

%RSD = 1.10

(1) 50% HNO_3 leach (2) $HF/HClO_4/HNO_3$ digestion (3) $HF/HClO_4/HNO_3$ digestion of residue (1)
ND: not detected, NA: not analyzed, RSD: relative standard deviation

D 1.0. Comparative Concentrations of Selected Trace Metals in Clay Fractions From the NYB (ppm = mg/kg, dry sediment) (continued)

d. Cu

Sample	(1)	(2)	(3)
84-1	122 ± 0.5	168 ± 0.5	28 ± 0.3
85	149 ± 0.9	181 ± 0.9	26 ± 0.9
87	7 ± 0.1	17.5 ± 1.0	NA
89A	175 ± 0.4	176 ± 2.3	3 ± 0.1
1-2	54 ± 0.4	77 ± 0.6	NA
71	175 ± 0.3	213 ± 1.3	22 ± 0.4
91	222 ± 1.0	279 ± 0.5	NA
33	78.6 ± 0.3	82.5 ± 0.3	4 ± 0.1
7-1	128 ± 0.1	164 ± 1.3	19 ± 0.2
54A	87 ± 0.7	107 ± 0.3	27 ± 0.1
56A	12.7 ± 0.2	24 ± 0.1	8.5 ± 0.3
20A	7.8 ± 0.2	18 ± 0.4	NA
21A	62 ± 0.2	78 ± 0.5	14 ± 0.2
63	108 ± 2.0	148 ± 2.4	NA

% RSD = 0.81

e. Mn

Sample	(1)	(2)	(3)
84-1	221 ± 13.7	686 ± 0.7	NA
85	248 ± 8.6	513 ± 9.4	268 ± 1.6
87	288 ± 5.7	NA	NA
89A	178 ± 2.3	499 ± 5.3	305 ± 1.9
1-2	90 ± 3.0	108 ± 0.3	NA
71	139 ± 1.7	892 ± 3.5	586 ± 2.2
91	100 ± 2.7	912 ± 6.1	NA
33	239 ± 2.2	497 ± 7.9	NA
7-1	241 ± 7.4	780 ± 8.4	503 ± 4.9
54A	817 ± 13.6	1145 ± 13.9	NA
56A	150 ± 4.7	493 ± 1.2	NA
20A	67 ± 0.9	138 ± 0.3	65 ± 0.9
21A	140 ± 5.1	NA	NA
63	71 ± 1.3	616 ± 0.9	NA

%RSD = 0.74

f. Ni

Sample	(1)	(2)	(3)
84-1	26 ± 5.0	38 ± 3.6	1.4
85	28 ± 1.3	32 ± 1.0	ND
87	20 ± 2.2	24 ± 3.4	ND
89A	33 ± 1.1	34 ± 2.8	ND
1-2	ND	8 ± 1.5	ND
71	33 ± 1.7	36 ± 3.8	ND
91	47 ± 3.3	55 ± 3.5	NA
33	10 ± 1.1	13 ± 4.9	ND
7-1	30 ± 1.8	31 ± 2.3	ND
54A	NA	17.7 ± 2.1	NA
56A	ND	9.5 ± 0.9	ND
20A	ND	2 ± 0.1	ND
21A	18.5 ± 1.9	20 ± 1.5	ND
63	37.5 ± 3.9	44 ± 3.1	ND

%RSD = 7.95

(1) 50% HNO_3 leach (2) $HF/HClO_4/HNO_3$ digestion (3) $HF/HClO_4/HNO_3$ digestion of residue (1)
ND: not detected, NA: not analyzed, RSD: relative standard deviation

D 1.0. Comparative Concentrations of Selected Trace Metals in Clay Fractions of the NYB (ppm = mg/kg, dry sediment) (continued)

g. Zn

Sample	(1)	(2)	(3)
84-1	195 ± 5.0	248 ± 0.6	NA
85	225 ± 1.3	248 ± 0.8	19 ± 0.4
87	29 ± 2.2	78.5 ± 0.9	NA
89A	244 ± 1.1	271 ± 0.9	29 ± 0.5
1-2	123 ± 2.7	183 ± 0.9	NA
71	364 ± 1.7	411 ± 1.8	52 ± 1.0
91	448 ± 3.3	512 ± 3	NA
33	143 ± 1.1	150 ± 1.2	NA
7-1	212 ± 1.8	275 ± 1.2	54 ± 0.4
54A	182 ± 0.2	248 ± 1.6	NA
56A	33 ± 0.05	100 ± 0.4	NA
20A	39 ± 0.16	86 ± 0.9	25 ± 0.4
21A	146 ± 1.6	189 ± 1.2	NA
63	260 ± 3.4	344 ± 0.7	NA

% RSD = 0.50

(1) 50% HNO_3 leach (2) $HF/HClO_4/HNO_3$ digestion (3) $HF/HClO_4/HNO_3$ digestion of residue (1)
ND: not detected, NA: not analyzed, RSD: relative standard deviation

D 2.0. Effect of 50% HNO_3 and Total Acid Digestion on Trace Metal Concentrations in Cores AC 97-1 and AC 97-9 (ppm = mg / kg, dry weight)

Station	Sample Interval (cm)	Pb		Cd		Cu		Zn		Ni		Cr	
		(1)	(2)	(1)	(2)	(1)	(2)	(1)	(2)	(1)	(2)	(1)	(2)
AC 97-1	0-2	4.1	4.3	ND	ND	10.3	12	10	10.7	ND	ND	8.0D	8.6
	5-6	3.1	3.6	ND	ND	7.3	8	3.3	3.7	ND	ND	ND	ND
	10-11	1.0	1.7	ND	ND	7	9	3.3	3.5	ND	ND	ND	ND
	15-16	1.1	1.7	ND	ND	9	10	8	9	ND	ND	2	2.6
	20-21	1.1	1.7	ND	ND	8	11	3.3	3.8	ND	ND	1.3	1.6
	25-26	1.2	1.7	ND	ND	8.6	11	3.6	4	ND	ND	2.5	2.7
	30-31	1.2	1.8	ND	ND	8	10	2.8	3.2	ND	ND	ND	ND
	35-36	2.3	2.8	ND	ND	8.8	11	3	3.4	ND	ND	4	4.5
	40-41	3.4	3.7	ND	ND	8.9	12	3.2	3.4	ND	ND	6.2	6.6
Station	**Sample Interval (cm)**	**(1)**	**(2)**	**(1)**	**(2)**	**(1)**	**(2)**	**(1)**	**(2)**	**(1)**	**(2)**	**(1)**	**(2)**
AC97-9	5-6	113	116	6	6.5	60	78	117	123	19	21	22	55
	9-10	119	123	2.6	2.9	61.5	62.8	175	180	12.7	16	18	19
	15-16	100	100.7	6.8	7.3	NA	65	NA	149	18	21	22	25
	19-20	106	111	3.2	3.5	18.3	29	111	115	16	18	16.2	17.3
	26-27	49	54	6	6.5	15.7	24.5	46	77	11	14	12	12.5
	29-30	103	108	2.5	2.6	12.7	17	73	76	ND	ND	12.7	13.1
	34-35	105	113	2.6	2.9	11.3	14	64	70	19	21	28	31
	36-37	96	102	6	6.7	47	71	94	103	19	20	28	32
	55-56	117	123	3	3.18	27.5	15	157	160	13	16	19	23
	68-69	123	133	2.7	2.7	19.6	31	124	127	18	20	13	21
	76-77	141	171	3	3.2	38	23	148	150	17	17.5	15	18
	87-88	146	174	3.3	3.8	47.8	41	226	230	24	26	27	32
	95-96	116	125	2.9	2.3	24.3	57	131	135	14	16	16	19

(1) 50% HNO_3 leach , **(2)** $HF/HClO_4/HNO_3$ digestion , ND: not detected, NA: not analyzed

D 3.0. Grain-Size Depencies of Trace Metal Concentrations Extracted by 50% HNO_3

Location	clays	very fine sand	fine sand	medium sand
		a) Pb (ppm)		
Mud Dump Site				
84.1	175	NA	NA	NA
84	159	73	52	16
86	232	NA	NA	-
86.1	222	NA	NA	NA
86.2	245	NA	NA	-
87	272	17	14	-
85	181	NA	NA	-
Sewage Sludge Dumpsite				
- South Christiaensen Basin				
89A	177	120	60	-
89C	187	-	-	
- North Christiaensen Basin				
1	-	-	34	26
1-2	-	-	39	-
1-2a	-	-	38	-
71	206	68	55	-
91	235	100	85	-
31B	204	NA	NA	-
Nearshore Mud-Patches				
Trough Mud Patches				
7a	140	33	21	16
7b	100	NA	NA	-
7-1b	17	0.9	NA	NA
13A	-	-	15	-
13B	-	-	21	-
South of Long Beach				
54A	160	113	NA	-
56	140	NA	48	14
Nearshore Mud Bank				
South of Atlantic Beach				
5	-	19	14	13
5-1	-	19	NA	NA
Buried Muds				
South of Jones Inlet				
33	120	NA	NA	-
33-1	199	NA	NA	-
South of Long Beach Island				
20A	-	24	22	-
21A	88	35	22	18
37	-	-	-	-
24	-	23	12	7
Cholera Bank				
62	-	20	13	-
63	85	30	22	-

D 3.0. Grain-Size Depencies of Trace Metal Concentrations Extracted by 50% HNO_3 (continued)

Location	clays	very fine sand	fine sand	medium sand
		b) Cr (ppm)		
Mud Dump Site				
84.1	183	-	27	ND
84	152	47	ND	ND
86	253	NA	ND	ND
86.1	223	NA	ND	ND
86.2	263	NA	ND	ND
87	138	ND	ND	ND
85	215	NA	ND	ND
Sewage Sludge Dumpsite				
-South Christiaensen Basin				
89A	142	64	ND	ND
-North Christiaensen Basin				
1	-	NA	ND	ND
1-2	-	NA	ND	ND
1-2a	-	NA	ND	ND
71	127	14	7	ND
-Christiaensen Basin Mud				
91	209	38	33	ND
33B	-	-	ND	ND
Nearshore Mud Patches				
Trough Mud Patches				
7a	123	ND	ND	ND
7b	61	ND	ND	ND
7-1b	ND	ND	ND	ND
13A	-	-	ND	ND
13B	-	-	ND	ND
South of Long Beach				
54A	103	31	ND	ND
56	39	NA	ND	ND
Nearshore Mud Bank				
South of Atlantic Beach				
	5	-	ND	ND
Buried Muds				
South of Jones Inlet				
33	74	NA	ND	ND
33-1	127	NA	ND	ND
South of Long Beach Island				
20A	-	ND	ND	ND
21A	-	ND	ND	ND
37	-	-	-	ND
24	-	-	-	ND
Cholera Bank				
62	-	ND	ND	ND
63	39	ND	ND	ND

D 3.0. Grain-Size Depencies of Trace Metal Concentrations Extracted by 50% HNO_3 (continued)

c) Zn (ppm)

Location	clays	very fine sand	fine sand	medium sand
Mud Dump Site				
84.1	182	NA	NA	NA
84	161	75	70	21
86	308	NA	NA	-
86.1	322	NA	NA	-
86.2	420	NA	NA	-
87	227	22	20	-
85	219	-	-	-
Sewage Sludge Dumpsite				
-South Christiaensen Basin				
89A	185	106	43	37
-North Christiaensen Basin				
1	-	NA	44	41
1-2	-	NA	41	-
1-2a	-	NA	28	-
71	359	61	40	2.5
-Christiaensen Basin Mud				
91	366	116	93	21
33B	-	-	ND	ND
Nearshore Mud Patches				
Trough Mud Patches				
7	133	33	33	22
7b	99	NA	NA	-
7-1b	24	4	NA	-
13	-	-	20	-
13B	-	-	19.6	-
South of Long Beach				
54A	156	93	21	-
56	145	65	48	37
Nearshore Mud Bank				
South of Atlantic Beach				
5	-	25	19	-
5-1	-	21	-	-
Buried Muds				
South of Jones Inlet				
33	106	NA	19	-
33-1	151	NA	-	-
South of Long Beach Island				
20A	-	37	21	-
21A	-	32	21	19
37	-	13	7	-
24	-	22	10	6
Cholera Bank				
62	-	-	1	-
63	250	101	-	-

D 3.0. Grain-Size Depencies of Trace Metal Concentrations extracted by 50% HNO_3 (continued)

Location	clays	very fine sand	fine sand	medium sand
		d) Cu (ppm)		
Mud Dump Site				
84.1	125	NA	NA	-
84	160	58	53	-
86	204	NA	NA	-
86.1	223	NA	NA	NA
86.2	269	NA	NA	-
87	193	10	8	-
85	176	NA	NA	NA
Sewage Sludge Dumpsite				
-South Christiaensen Basin				
89A	149	81	32	-
89C	223			
-North Christiaensen Basin				
1	-	NA	15	-
1-2	50	NA	16	-
1-2a	-	NA	15	-
71	197	33	27	-
-Christiaensen Basin Mud				
91	230	91	70	-
Nearshore Mud Patches				
Trough Mud Patches				
7	77	11	6.5	-
7b	65	NA	NA	-
7-1b	46	34	NA	-
13	-	-	3.6	-
South of Long Beach				
54A	91	55	6.5	-
56	14	NA	6	-
Nearshore Mud Bank				
South of Atlantic Beach				
5	-	13	NA	-
Buried Muds				
South of Jones Inlet				
33	88	NA	NA	-
33-1	87	NA	NA	-
South of Long Beach Island				
20A	10	6	5	-
21A	-	-	7	-
37	-	-	5	-
24	-	5	4-	-
Cholera Bank				
62	-	5.5	ND	-
63	96	45	30	-

D 3.0. Grain-Size Depencies of Trace Metal Concentrations Extracted by 50% HNO_3 (continued)

e) Ni (ppm)

Location	clays	very fine sand	fine sand	medium sand
Mud Dump Site				
84.1	12	ND	ND	ND
84	14	ND	ND	ND
86	22	ND	ND	ND
86.1	25	ND	ND	ND
86.2	30	ND	ND	ND
87	23	ND	ND	ND
85	19	ND	ND	ND
Sewage Sludge Dump Site				
-South Christiaensen Basin				
89A	26	10	ND	ND
-North Christiaensen Basin				
1	ND	ND	ND	ND
1-2	-	ND	ND	ND
1-2a	-	ND	ND	ND
71	28	ND	ND	ND
-Christiaensen Basin Mud				
91	47.5	18	2	ND
Nearshore Mud Patches				
Trough Mud Patches				
7a	27	ND	ND	ND
7b	NA	ND	ND	ND
7-1b	NA	ND	ND	ND
13A	-	ND	ND	ND
13B	-	ND	ND	ND
South of Long Beach				
54A	12.5	ND	ND	ND
56	ND	ND	ND	ND
Nearshore Mud Bank				
South of Atlantic Beach				
5	-	ND	ND	ND
Buried Muds				
South of Jones Inlet				
33	8	ND	ND	ND
33-1	12	ND	ND	ND
South of Long Beach Island				
20A	ND	ND	ND	ND
21A	-	ND	ND	ND
37	-	-	-	ND
24	-	-	-	ND
Cholera Bank				
62	-	ND	ND	ND
63	31	ND	ND	ND

D 3.0. Grain-Size Depencies of Trace Metal Concentrations Extracted by 50% HNO_3 (continued)

Location	clays	very fine sand	fine sand	medium sand
		f) Cd (ppm)		
Mud Dump Site				
84.1	5.2	ND	ND	ND
84	4	ND	ND	ND
86	10.4	ND	ND	ND
86.1	7	ND	ND	ND
86.2	10	ND	ND	ND
87	6.8	ND	ND	ND
85	6	ND	ND	ND
Sewage Sludge Dumpsite				
-South Christiaensen Basin				
89A	6	64	ND	ND
89C	7.5			
-North Christiaensen Basin				
1	-	ND	ND	ND
1-2	-	ND	ND	ND
1-2a	-	ND	ND	ND
71	10.6	ND	ND	ND
-Christiaensen Basin Mud				
91	13.3	ND	ND	ND
33B	-	ND	ND	ND
Nearshore Mud Patches				
Trough Mud Patches				
7a	4.8	ND	ND	ND
7b	2.5	ND	ND	ND
7-1b	6.6	ND	ND	ND
13A	-	ND	ND	ND
13B	-	ND	ND	ND
South of Long Beach				
54A	7	ND	ND	ND
56	4.5	ND	ND	ND
Nearshore Mud Bank				
South of Atlantic Beach				
5	-	ND	ND	ND
Buried Muds				
South of Jones Inlet				
33	3.3	ND	ND	ND
33-1	6	ND	ND	ND
South of Long Beach Island				
20A	3.5	ND	ND	ND
21A	5	ND	ND	ND
37	-	ND	ND	ND
24	-	ND	ND	ND
Cholera Bank				
62	-	ND	ND	ND
63	8.5	ND	ND	ND

Appendix E

The Results of Statistical Analysis

E 1.0. Mud Dump Site

E.1.1. The Result of OneWay Analysis of Variance (ANOVA) of Trace Metals

Oneway Analysis of Pb by Station

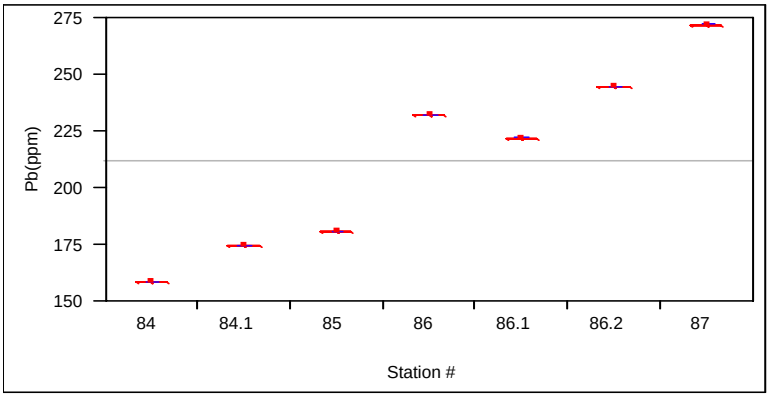

Oneway Anova

Summary of Fit

Rsquare	.
Adj Rsquare	.
Root Mean Square Error	.
Mean of Response	212.2857
Observations (or Sum Wgts)	7

Analysis of Variance

Source	DF	Sum of Squares	Mean Square
Station #	6	10327.429	1721.24
Error	0	0.000	.
C. Total	6	10327.429	

Means for Oneway Anova

Level	Number	Mean
84	3	159.000
84.1	3	175.000
85	3	181.000
86	3	232.000
86.1	3	222.000
86.2	3	245.000
87	3	272.000

Oneway Analysis of Cr by Station

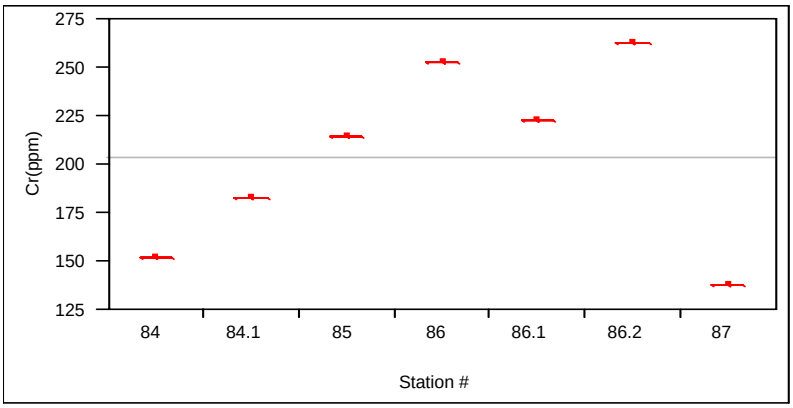

Oneway Anova

Summary of Fit

Rsquare	.
Adj Rsquare	.
Root Mean Square Error	.
Mean of Response	203.8571
Observations (or Sum Wgts)	7

Analysis of Variance

Source	DF	Sum of Squares	Mean Square
Station #	6	13864.86	2310.81
Error	0	-1.819e-12	.
C. Total	6	13864.86	

Means for Oneway Anova

Level	Number	Mean
84	3	152.000
84.1	3	183.000
85	3	215.000
86	3	253.000
86.1	3	223.000
86.2	3	263.000
87	3	138.000

Oneway Analysis of Zn by Station

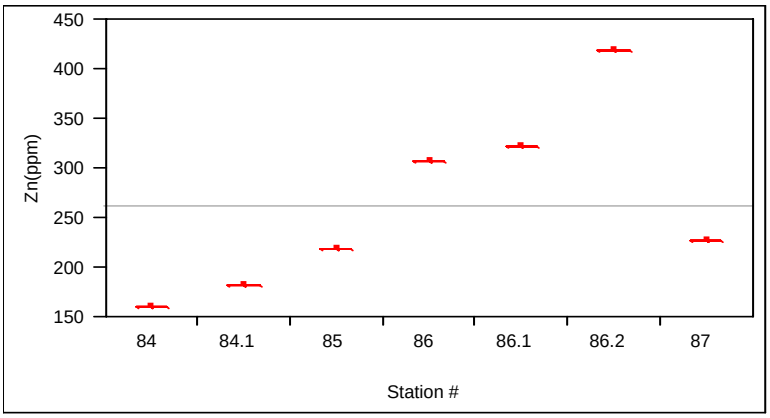

Oneway Anova

Summary of Fit

Rsquare	.
Adj Rsquare	.
Root Mean Square Error	.
Mean of Response	262.7143
Observations (or Sum Wgts)	7

Analysis of Variance

Source	DF	Sum of Squares	Mean Square
Station #	6	50351.429	8391.90
Error	0	0.000	.
C. Total	6	50351.429	

Means for Oneway Anova

Level	Number	Mean
84	3	161.000
84.1	3	182.000
85	3	219.000
86	3	308.000
86.1	3	322.000
86.2	3	420.000
87	3	227.000

Oneway Analysis of Cu by Station

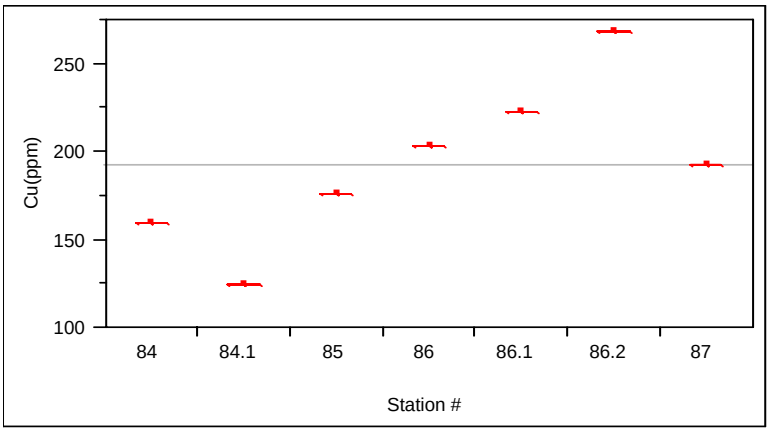

Oneway Anova

Summary of Fit

Rsquare	.
Adj Rsquare	.
Root Mean Square Error	.
Mean of Response	192.8571
Observations (or Sum Wgts)	7

Analysis of Variance

Source	DF	Sum of Squares	Mean Square
Station #	6	12798.86	2133.14
Error	0	-1.819e-12	.
C. Total	6	12798.86	

Means for Oneway Anova

Level	Number	Mean
84	3	160.000
84.1	3	125.000
85	3	176.000
86	3	204.000
86.1	3	223.000
86.2	3	269.000
87	3	193.000

Oneway Analysis of Ni by Station

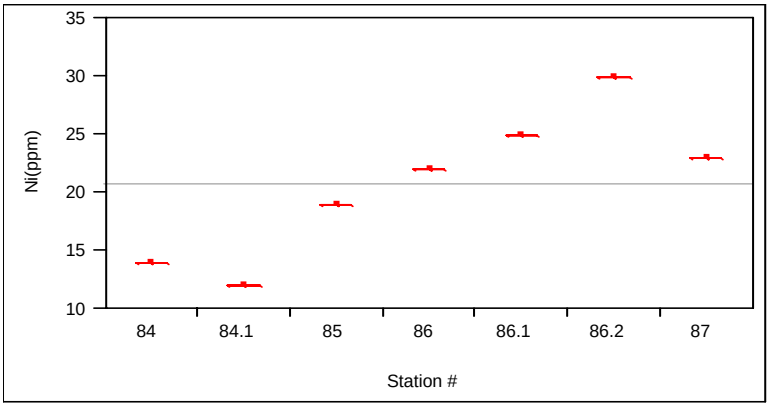

Oneway Anova

Summary of Fit

Rsquare	.
Adj Rsquare	.
Root Mean Square Error	.
Mean of Response	20.71429
Observations (or Sum Wgts)	7

Analysis of Variance

Source	DF	Sum of Squares	Mean Square
Station #	6	235.42857	39.2381
Error	0	2.8422e-14	.
C. Total	6	235.42857	

Means for Oneway Anova

Level	Number	Mean
84	3	14.0000
84.1	3	12.0000
85	3	19.0000
86	3	22.0000
86.1	3	25.0000
86.2	3	30.0000
87	3	23.0000

Oneway Analysis of Cd by Station

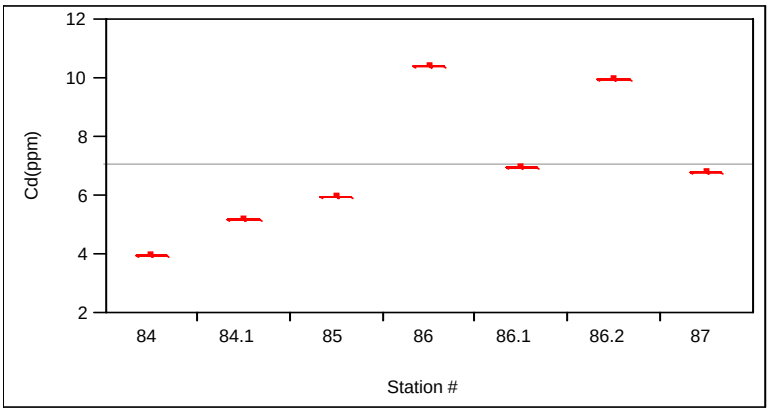

Oneway Anova

Summary of Fit

Rsquare	.
Adj Rsquare	.
Root Mean Square Error	.
Mean of Response	7.057143
Observations (or Sum Wgts)	7

Analysis of Variance

Source	DF	Sum of Squares	Mean Square
Station #	6	33.817143	5.63619
Error	0	0.000000	.
C. Total	6	33.817143	

Means for Oneway Anova

Level	Number	Mean
84	3	4.0000
84.1	3	5.2000
85	3	6.0000
86	3	10.4000
86.1	3	7.0000
86.2	3	10.0000
87	3	6.8000

E.1.2. Pairwise, Spearman's Rho and Kendall Tau-b Correlations between Trace Metals

Pairwise

Variable	by Variable	Correlation	Count	Signif Prob
Cu(ppm)	Pb(ppm)	0.6802	7	0.0927
Zn(ppm)	Pb(ppm)	0.6262	7	0.1325
Zn(ppm)	Cu(ppm)	0.9383	7	0.0018
Cr(ppm)	Pb(ppm)	0.1963	7	0.6731
Cr(ppm)	Cu(ppm)	0.6418	7	0.1202
Cr(ppm)	Zn(ppm)	0.8132	7	0.0261
Ni(ppm)	Pb(ppm)	0.7975	7	0.0317
Ni(ppm)	Cu(ppm)	0.9746	7	0.0002
Ni(ppm)	Zn(ppm)	0.9156	7	0.0038
Ni(ppm)	Cr(ppm)	0.5838	7	0.1688
Cd(ppm)	Pb(ppm)	0.6963	7	0.0822
Cd(ppm)	Cu(ppm)	0.7659	7	0.0447
Cd(ppm)	Zn(ppm)	0.8638	7	0.0122
Cd(ppm)	Cr(ppm)	0.7881	7	0.0353
Cd(ppm)	Ni(ppm)	0.7768	7	0.0399
Mn(ppm)	Pb(ppm)	0.9370	3	0.2272
Mn(ppm)	Cu(ppm)	0.9239	3	0.2499
Mn(ppm)	Zn(ppm)	0.8926	3	0.2978
Mn(ppm)	Cr(ppm)	-0.6686	3	0.5338
Mn(ppm)	Ni(ppm)	0.9644	3	0.1704
Mn(ppm)	Cd(ppm)	0.9938	3	0.0710

Spearman's Rho

Variable	by Variable	Spearman Rho	Prob>|Rho|
Cu(ppm)	Pb(ppm)	0.7143	0.0713
Zn(ppm)	Pb(ppm)	0.7500	0.0522
Zn(ppm)	Cu(ppm)	0.9643	0.0005
Cr(ppm)	Pb(ppm)	0.2500	0.5887
Cr(ppm)	Cu(ppm)	0.7143	0.0713
Cr(ppm)	Zn(ppm)	0.7500	0.0522
Ni(ppm)	Pb(ppm)	0.7857	0.0362
Ni(ppm)	Cu(ppm)	0.9643	0.0005
Ni(ppm)	Zn(ppm)	0.9286	0.0025
Ni(ppm)	Cr(ppm)	0.5357	0.2152
Cd(ppm)	Pb(ppm)	0.7500	0.0522
Cd(ppm)	Cu(ppm)	0.8571	0.0137
Cd(ppm)	Zn(ppm)	0.8929	0.0068
Cd(ppm)	Cr(ppm)	0.7500	0.0522
Cd(ppm)	Ni(ppm)	0.7500	0.0522
Mn(ppm)	Pb(ppm)	1.0000	0.0000
Mn(ppm)	Cu(ppm)	1.0000	0.0000
Mn(ppm)	Zn(ppm)	1.0000	0.0000
Mn(ppm)	Cr(ppm)	-0.5000	0.6667
Mn(ppm)	Ni(ppm)	1.0000	0.0000
Mn(ppm)	Cd(ppm)	1.0000	0.0000

Kendall's Tau-b

Variable	by Variable	Kendall Tau b	Prob>|Tau b|
Cu(ppm)	Pb(ppm)	0.5238	0.0985
Zn(ppm)	Pb(ppm)	0.6190	0.0509
Zn(ppm)	Cu(ppm)	0.9048	0.0043
Cr(ppm)	Pb(ppm)	0.4286	0.1765
Cr(ppm)	Cu(ppm)	0.5238	0.0985
Cr(ppm)	Zn(ppm)	0.6190	0.0509
Ni(ppm)	Pb(ppm)	0.6190	0.0509
Ni(ppm)	Cu(ppm)	0.9048	0.0043
Ni(ppm)	Zn(ppm)	0.8095	0.0107
Ni(ppm)	Cr(ppm)	0.4286	0.1765
Cd(ppm)	Pb(ppm)	0.6190	0.0509
Cd(ppm)	Cu(ppm)	0.7143	0.0243
Cd(ppm)	Zn(ppm)	0.8095	0.0107
Cd(ppm)	Cr(ppm)	0.6190	0.0509
Cd(ppm)	Ni(ppm)	0.6190	0.0509
Mn(ppm)	Pb(ppm)	1.0000	0.1172
Mn(ppm)	Cu(ppm)	1.0000	0.1172
Mn(ppm)	Zn(ppm)	1.0000	0.1172
Mn(ppm)	Cr(ppm)	-0.3333	0.6015
Mn(ppm)	Ni(ppm)	1.0000	0.1172
Mn(ppm)	Cd(ppm)	1.0000	0.1172

E.2.0. Sewage Sludge Dumpsite

E.2.1. The Results of Oneway Analysis of Variance (ANOVA) of Tace Metals

Oneway Analysis of Pb by Station

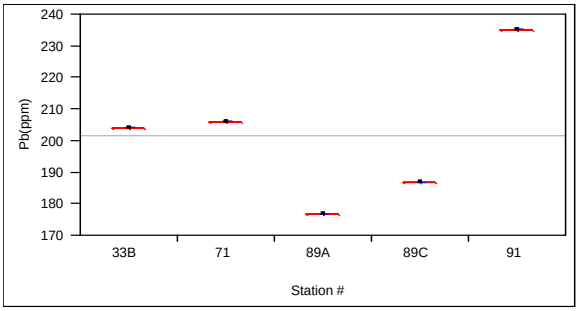

Oneway Anova

Summary of Fit

Rsquare	.
Adj Rsquare	.
Root Mean Square Error	.
Mean of Response	201.8
Observations (or Sum Wgts)	5

Analysis of Variance

Source	DF	Sum of Squares	Mean Square
Station #	4	1958.800	489.700
Error	0	-2.274e-13	.
C. Total	4	1958.800	

Means for Oneway Anova

Level	Number	Mean
33B	3	204.000
71	3	206.000
89A	3	177.000
89C	3	187.000
91	3	235.000

Oneway Analysis of Cu by Station

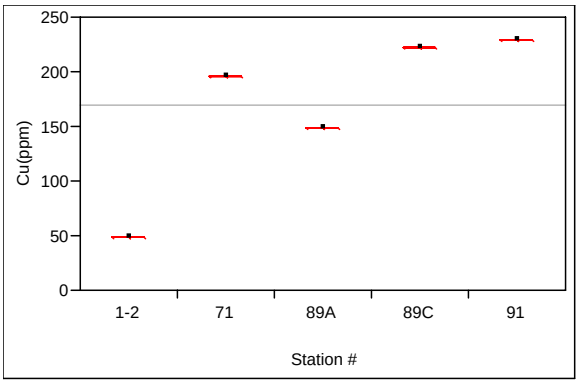

Oneway Anova

Summary of Fit

Rsquare	.
Adj Rsquare	.
Root Mean Square Error	.
Mean of Response	169.8
Observations (or Sum Wgts)	5

Analysis of Variance

Source	DF	Sum of Squares	Mean Square
Station #	4	21978.800	5494.70
Error	0	0.000	.
C. Total	4	21978.800	

Means for Oneway Anova

Level	Number	Mean
1-2	3	50.000
71	3	197.000
89A	3	149.000
89C	3	223.000
91	3	230.000

Oneway Analysis of Zn by Station

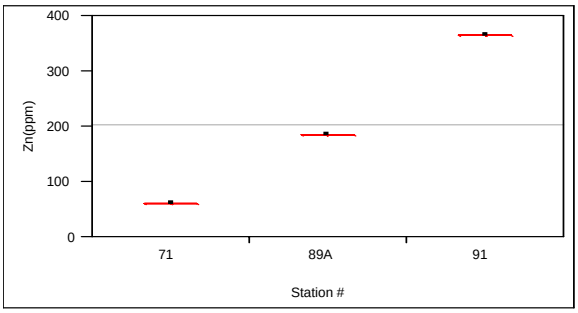

Oneway Anova

Summary of Fit

Rsquare	.
Adj Rsquare	.
Root Mean Square Error	.
Mean of Response	204
Observations (or Sum Wgts)	3

Analysis of Variance

Source	DF	Sum of Squares	Mean Square
Station #	2	47054.000	23527.0
Error	0	0.000	.
C. Total	2	47054.000	

Means for Oneway Anova

Level	Number	Mean
71	3	61.000
89A	3	185.000
91	3	366.000

Oneway Analysis of Cr by Station

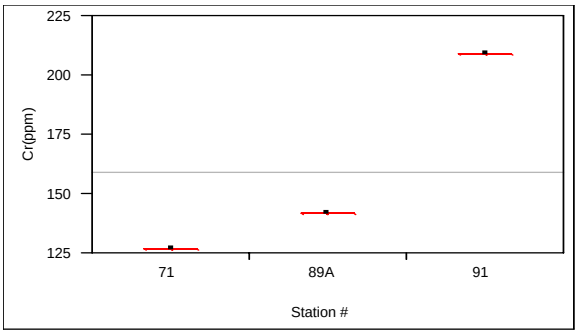

Oneway Anova

Summary of Fit

Rsquare	.
Adj Rsquare	.
Root Mean Square Error	.
Mean of Response	159.3333
Observations (or Sum Wgts)	3

Analysis of Variance

Source	DF	Sum of Squares	Mean Square
Station #	2	3812.6667	1906.33
Error	0	0.0000	.
C. Total	2	3812.6667	

Means for Oneway Anova

Level	Number	Mean
71	3	127.000
89A	3	142.000
91	3	209.000

Oneway Analysis of Ni by Station

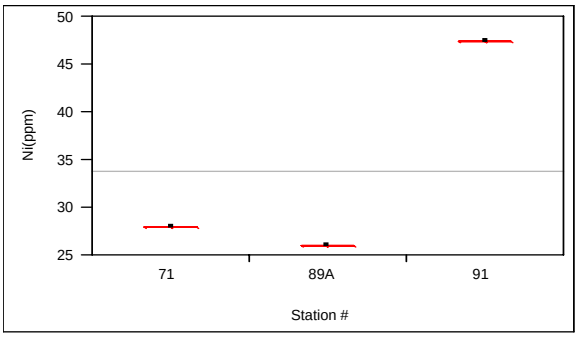

Oneway Anova

Summary of Fit

Rsquare	.
Adj Rsquare	.
Root Mean Square Error	.
Mean of Response	33.83333
Observations (or Sum Wgts)	3

Analysis of Variance

Source	DF	Sum of Squares	Mean Square
Station #	2	282.16667	141.083
Error	0	0.00000	.
C. Total	2	282.16667	

Means for Oneway Anova

Level	Number	Mean
71	3	28.0000
89A	3	26.0000
91	3	47.5000

Oneway Analysis of Cd by Station

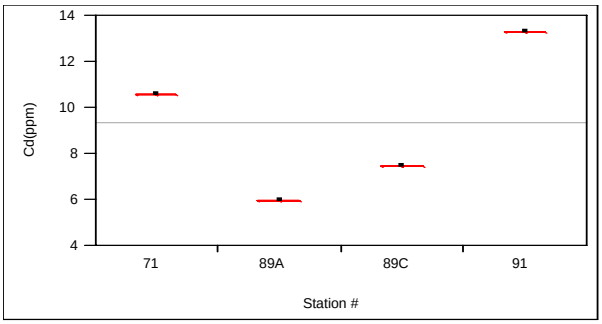

Oneway Anova

Summary of Fit

Rsquare	.
Adj Rsquare	.
Root Mean Square Error	.
Mean of Response	9.35
Observations (or Sum Wgts)	4

Analysis of Variance

Source	DF	Sum of Squares	Mean Square	F Ratio	Prob > F
Station #	3	31.810000	10.6033	.	.
Error	0	0.000000	.		
C. Total	3	31.810000			

Means for Oneway Anova

Level	Number	Mean
71	3	10.6000
89A	3	6.0000
89C	3	7.5000
91	3	13.3000

Oneway Analysis of Mn by Station

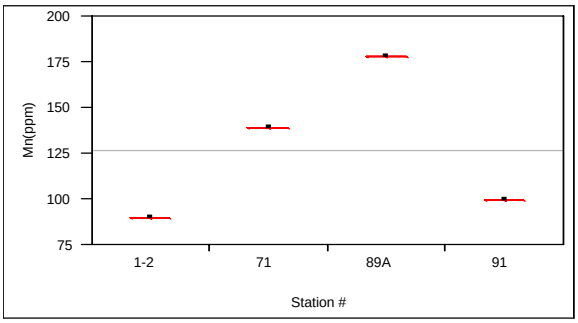

Oneway Anova

Summary of Fit

Rsquare	.
Adj Rsquare	.
Root Mean Square Error	.
Mean of Response	126.75
Observations (or Sum Wgts)	4

Analysis of Variance

Source	DF	Sum of Squares	Mean Square
Station #	3	4842.7500	1614.25
Error	0	0.0000	.
C. Total	3	4842.7500	

Means for Oneway Anova

Level	Number	Mean
1-2	3	90.000
71	3	139.000
89A	3	178.000
91	3	100.000

E.2.2.0. Pairwise, Spearman's Rho and Kendall Tau-b Correlations of Trace Metals

Pairwise

Variable	by Variable	Correlation	Count	Signif Prob
Cu(ppm)	Pb(ppm)	0.6791	4	0.3209
Zn(ppm)	Pb(ppm)	0.5900	3	0.5982
Zn(ppm)	Cu(ppm)	0.5008	3	0.6660
Cr(ppm)	Pb(ppm)	0.7673	3	0.4432
Cr(ppm)	Cu(ppm)	0.6947	3	0.5110
Cr(ppm)	Zn(ppm)	0.9705	3	0.1550
Ni(ppm)	Pb(ppm)	0.9050	3	0.2797
Ni(ppm)	Cu(ppm)	0.8547	3	0.3475
Ni(ppm)	Zn(ppm)	0.8774	3	0.3186
Ni(ppm)	Cr(ppm)	0.9672	3	0.1636
Cd(ppm)	Pb(ppm)	0.9904	4	0.0096
Cd(ppm)	Cu(ppm)	0.6781	4	0.3219
Cd(ppm)	Zn(ppm)	0.4635	3	0.6932
Cd(ppm)	Cr(ppm)	0.6634	3	0.5382
Cd(ppm)	Ni(ppm)	0.8318	3	0.3746
Mn(ppm)	Pb(ppm)	-1.0000	3	0.0000
Mn(ppm)	Cu(ppm)	0.2179	4	0.7821
Mn(ppm)	Zn(ppm)	-0.5900	3	0.5982
Mn(ppm)	Cr(ppm)	-0.7673	3	0.4432
Mn(ppm)	Ni(ppm)	-0.9050	3	0.2797
Mn(ppm)	Cd(ppm)	-0.9889	3	0.0950

Spearman's Rho

Variable	by Variable	Spearman Rho	Prob>|Rho|
Cu(ppm)	Pb(ppm)	0.8000	0.2000
Zn(ppm)	Pb(ppm)	0.5000	0.6667
Zn(ppm)	Cu(ppm)	0.5000	0.6667
Cr(ppm)	Pb(ppm)	0.5000	0.6667
Cr(ppm)	Cu(ppm)	0.5000	0.6667
Cr(ppm)	Zn(ppm)	1.0000	0.0000
Ni(ppm)	Pb(ppm)	1.0000	0.0000
Ni(ppm)	Cu(ppm)	1.0000	0.0000
Ni(ppm)	Zn(ppm)	0.5000	0.6667
Ni(ppm)	Cr(ppm)	0.5000	0.6667
Cd(ppm)	Pb(ppm)	1.0000	0.0000
Cd(ppm)	Cu(ppm)	0.8000	0.2000
Cd(ppm)	Zn(ppm)	0.5000	0.6667
Cd(ppm)	Cr(ppm)	0.5000	0.6667
Cd(ppm)	Ni(ppm)	1.0000	0.0000
Mn(ppm)	Pb(ppm)	-1.0000	0.0000
Mn(ppm)	Cu(ppm)	0.2000	0.8000
Mn(ppm)	Zn(ppm)	-0.5000	0.6667
Mn(ppm)	Cr(ppm)	-0.5000	0.6667
Mn(ppm)	Ni(ppm)	-1.0000	0.0000
Mn(ppm)	Cd(ppm)	-1.0000	0.0000

Kendall's Tau b

Variable	by Variable	Kendall Tau b	Prob>|Tau b|
Cu(ppm)	Pb(ppm)	0.6667	0.1742
Zn(ppm)	Pb(ppm)	0.3333	0.6015
Zn(ppm)	Cu(ppm)	0.3333	0.6015
Cr(ppm)	Pb(ppm)	0.3333	0.6015
Cr(ppm)	Cu(ppm)	0.3333	0.6015
Cr(ppm)	Zn(ppm)	1.0000	0.1172
Ni(ppm)	Pb(ppm)	1.0000	0.1172
Ni(ppm)	Cu(ppm)	1.0000	0.1172
Ni(ppm)	Zn(ppm)	0.3333	0.6015
Ni(ppm)	Cr(ppm)	0.3333	0.6015
Cd(ppm)	Pb(ppm)	1.0000	0.0415
Cd(ppm)	Cu(ppm)	0.6667	0.1742
Cd(ppm)	Zn(ppm)	0.3333	0.6015
Cd(ppm)	Cr(ppm)	0.3333	0.6015
Cd(ppm)	Ni(ppm)	1.0000	0.1172
Mn(ppm)	Pb(ppm)	-1.0000	0.1172
Mn(ppm)	Cu(ppm)	0.0000	1.0000
Mn(ppm)	Zn(ppm)	-0.3333	0.6015
Mn(ppm)	Cr(ppm)	-0.3333	0.6015
Mn(ppm)	Ni(ppm)	-1.0000	0.1172
Mn(ppm)	Cd(ppm)	-1.0000	0.1172

E.3. Nearshore Mud-Patches

E.3.1. The Results of Oneway Analysis of Variance (ANOVA)

Oneway Analysis of Pb by Station

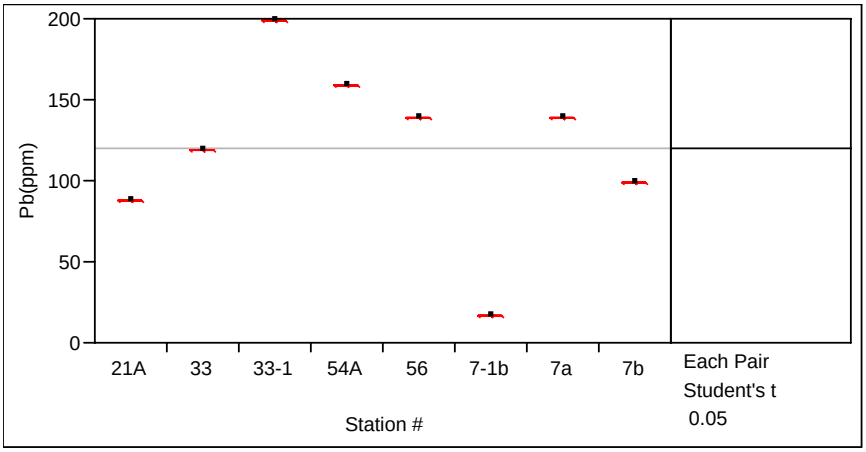

Oneway Anova

Summary of Fit

Rsquare	.
Adj Rsquare	.
Root Mean Square Error	.
Mean of Response	120.5
Observations (or Sum Wgts)	8

Analysis of Variance

Source	DF	Sum of Squares	Mean Square
Station #	7	20672.000	2953.14
Error	0	0.000	.
C. Total	7	20672.000	

Means for Oneway Anova

Level	Number	Mean
21A	3	88.000
33	3	120.000
33-1	3	199.000
54A	3	160.000
56	3	140.000
7-1b	3	17.000
7a	3	140.000
7b	3	100.000

Oneway Analysis of Cu by Station

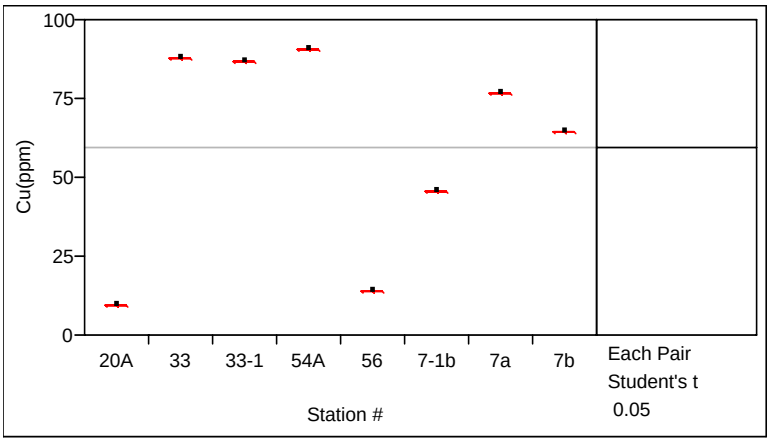

Oneway Anova

Summary of Fit

Rsquare	.
Adj Rsquare	.
Root Mean Square Error	.
Mean of Response	59.75
Observations (or Sum Wgts)	8

Analysis of Variance

Source	DF	Sum of Squares	Mean Square
Station #	7	7599.5000	1085.64
Error	0	0.0000	.
C. Total	7	7599.5000	

Means for Oneway Anova

Level	Number	Mean
20A	3	10.0000
33	3	88.0000
33-1	3	87.0000
54A	3	91.0000
56	3	14.0000
7-1b	3	46.0000
7a	3	77.0000
7b	3	65.0000

Oneway Analysis of Zn by Station

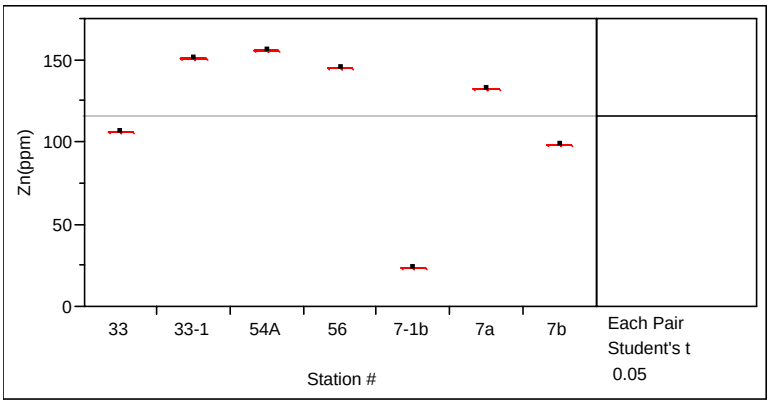

Oneway Anova

Summary of Fit

Rsquare	.
Adj Rsquare	.
Root Mean Square Error	.
Mean of Response	116.2857
Observations (or Sum Wgts)	7

Analysis of Variance

Source	DF	Sum of Squares	Mean Square
Station #	6	12807.43	2134.57
Error	0	-1.819e-12	.
C. Total	6	12807.43	

Means for Oneway Anova

Level	Number	Mean
33	3	106.000
33-1	3	151.000
54A	3	156.000
56	3	145.000
7-1b	3	24.000
7a	3	133.000
7b	3	99.000

Oneway Analysis of Cd by Station

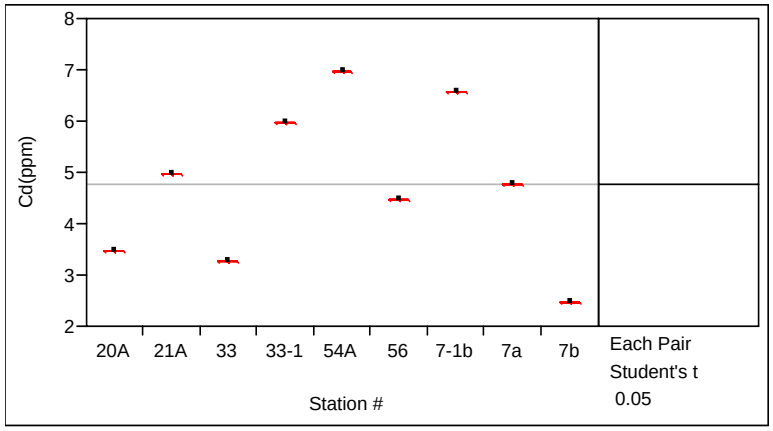

Oneway Anova

Summary of Fit

Rsquare	.
Adj Rsquare	.
Root Mean Square Error	.
Mean of Response	4.8
Observations (or Sum Wgts)	9

Analysis of Variance

Source	DF	Sum of Squares	Mean Square
Station #	8	18.88000	2.36000
Error	0	-3.553e-15	.
C. Total	8	18.88000	

Means for Oneway Anova

Level	Number	Mean
20A	3	3.50000
21A	3	5.00000
33	3	3.30000
33-1	3	6.00000
54A	3	7.00000
56	3	4.50000
7-1b	3	6.60000
7a	3	4.80000
7b	3	2.50000

Oneway Analysis of Cr by Station

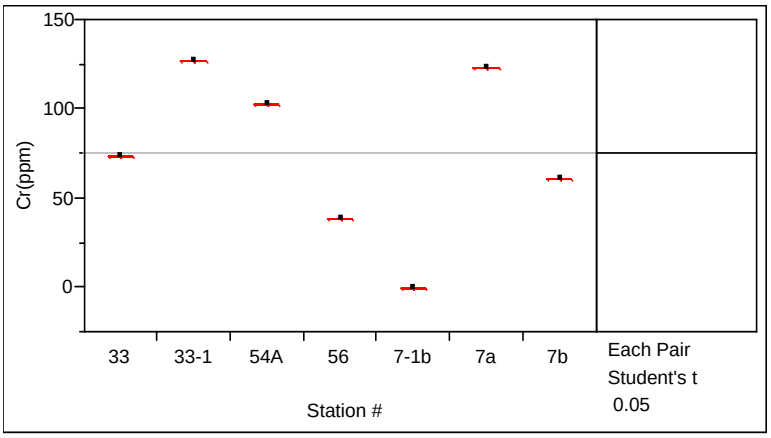

Oneway Anova

Summary of Fit

Rsquare	.
Adj Rsquare	.
Root Mean Square Error	.
Mean of Response	75.28571
Observations (or Sum Wgts)	7

Analysis of Variance

Source	DF	Sum of Squares	Mean Square
Station #	6	12909.43	2151.57
Error	0	-3.638e-12	.
C. Total	6	12909.43	

Means for Oneway Anova

Level	Number	Mean
33	3	74.000
33-1	3	127.000
54A	3	103.000
56	3	39.000
7-1b	3	0.000
7a	3	123.000
7b	3	61.000

Oneway Analysis of Ni by Station

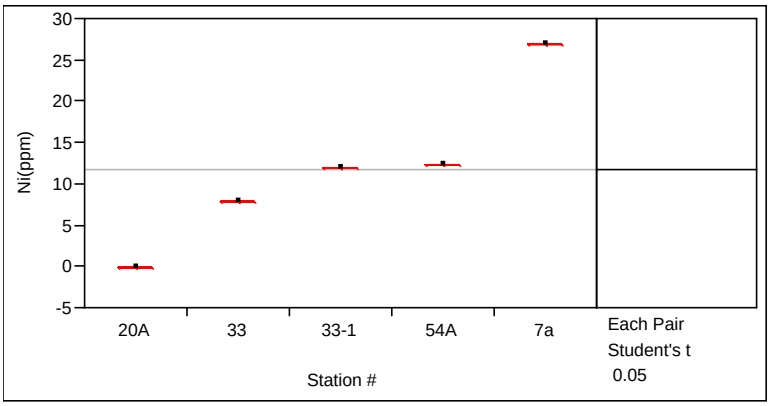

Oneway Anova

Summary of Fit

Rsquare	.
Adj Rsquare	.
Root Mean Square Error	.
Mean of Response	11.9
Observations (or Sum Wgts)	5

Analysis of Variance

Source	DF	Sum of Squares	Mean Square
Station #	4	385.20000	96.3000
Error	0	0.00000	.
C. Total	4	385.20000	

Means for Oneway Anova

Level	Number	Mean
20A	1	0.0000
33	1	8.0000
33-1	1	12.0000
54A	1	12.5000
7a	1	27.0000

Oneway Analysis of Mn by Station

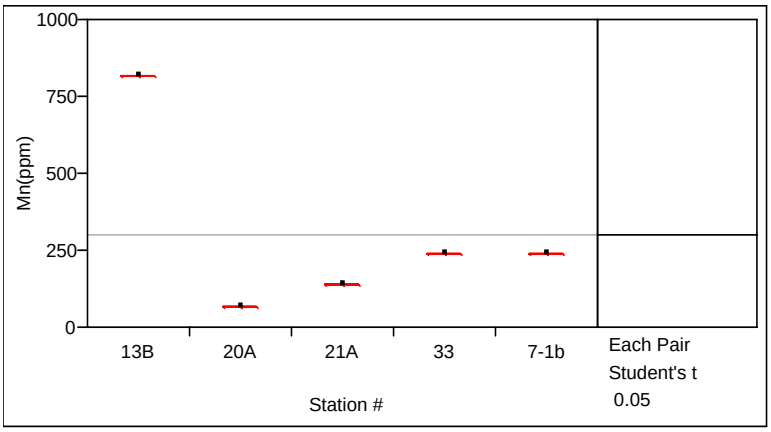

Oneway Anova

Summary of Fit

Rsquare	.
Adj Rsquare	.
Root Mean Square Error	.
Mean of Response	300.8
Observations (or Sum Wgts)	5

Analysis of Variance

Source	DF	Sum of Squares	Mean Square
Station #	4	354376.80	88594.2
Error	0	0.00	.
C. Total	4	354376.80	

Means for Oneway Anova

Level	Number	Mean
13B	3	817.000
20A	3	67.000
21A	3	140.000
33	3	239.000
7-1b	3	241.000

E.3.2. Pairwise, Spearman's Rho and Kendall Tau-b correlations of Trace Metals

Pairwise

Variable	by Variable	Correlation	Count	Signif Prob
Cu(ppm)	Pb(ppm)	0.4035	7	0.3694
Zn(ppm)	Pb(ppm)	0.9558	7	0.0008
Zn(ppm)	Cu(ppm)	0.2622	7	0.5701
Cr(ppm)	Pb(ppm)	0.8493	7	0.0156
Cr(ppm)	Cu(ppm)	0.7241	7	0.0658
Cr(ppm)	Zn(ppm)	0.7668	7	0.0443
Ni(ppm)	Pb(ppm)	-0.0945	4	0.9055
Ni(ppm)	Cu(ppm)	0.5676	5	0.3183
Ni(ppm)	Zn(ppm)	0.1403	4	0.8597
Ni(ppm)	Cr(ppm)	0.6159	4	0.3841
Cd(ppm)	Pb(ppm)	0.0512	8	0.9041
Cd(ppm)	Cu(ppm)	0.2660	8	0.5242
Cd(ppm)	Zn(ppm)	0.0203	7	0.9655
Cd(ppm)	Cr(ppm)	0.0709	7	0.8800
Cd(ppm)	Ni(ppm)	0.3640	5	0.5470
Mn(ppm)	Pb(ppm)	-0.2305	3	0.8520
Mn(ppm)	Cu(ppm)	0.8376	3	0.3680
Mn(ppm)	Zn(ppm)	-1.0000	2	.
Mn(ppm)	Cr(ppm)	-1.0000	2	.
Mn(ppm)	Ni(ppm)	1.0000	2	.
Mn(ppm)	Cd(ppm)	0.3961	4	0.6039

Spearman's Rho

Variable	by Variable	Spearman Rho	Prob>|Rho|
Cu(ppm)	Pb(ppm)	0.4865	0.2682
Zn(ppm)	Pb(ppm)	0.9550	0.0008
Zn(ppm)	Cu(ppm)	0.5000	0.2532
Cr(ppm)	Pb(ppm)	0.7928	0.0334
Cr(ppm)	Cu(ppm)	0.6786	0.0938
Cr(ppm)	Zn(ppm)	0.6429	0.1194
Ni(ppm)	Pb(ppm)	0.2000	0.8000
Ni(ppm)	Cu(ppm)	0.3000	0.6238
Ni(ppm)	Zn(ppm)	0.4000	0.6000
Ni(ppm)	Cr(ppm)	0.4000	0.6000
Cd(ppm)	Pb(ppm)	0.2036	0.6287
Cd(ppm)	Cu(ppm)	0.3095	0.4556
Cd(ppm)	Zn(ppm)	0.4286	0.3374
Cd(ppm)	Cr(ppm)	0.1786	0.7017
Cd(ppm)	Ni(ppm)	0.6000	0.2848
Mn(ppm)	Pb(ppm)	-0.5000	0.6667
Mn(ppm)	Cu(ppm)	0.5000	0.6667
Mn(ppm)	Zn(ppm)	-1.0000	.
Mn(ppm)	Cr(ppm)	-1.0000	.
Mn(ppm)	Ni(ppm)	1.0000	.
Mn(ppm)	Cd(ppm)	0.4000	0.6000

E.4. 0. Pairwise, Spearman's Rho and Kendall Tau b Trace Metal Correlation from NYB

Kendall's Tau b

Variable	by Variable	Kendall Tau b	Prob>|Tau b|
Cu(ppm)	Pb(ppm)	0.3904	0.2243
Zn(ppm)	Pb(ppm)	0.8783	0.0062
Zn(ppm)	Cu(ppm)	0.4286	0.1765
Cr(ppm)	Pb(ppm)	0.6831	0.0334
Cr(ppm)	Cu(ppm)	0.5238	0.0985
Cr(ppm)	Zn(ppm)	0.5238	0.0985
Ni(ppm)	Pb(ppm)	0.0000	1.0000
Ni(ppm)	Cu(ppm)	0.2000	0.6242
Ni(ppm)	Zn(ppm)	0.3333	0.4969
Ni(ppm)	Cr(ppm)	0.3333	0.4969
Cd(ppm)	Pb(ppm)	0.1818	0.5330
Cd(ppm)	Cu(ppm)	0.2857	0.3223
Cd(ppm)	Zn(ppm)	0.4286	0.1765
Cd(ppm)	Cr(ppm)	0.1429	0.6523
Cd(ppm)	Ni(ppm)	0.4000	0.3272
Mn(ppm)	Pb(ppm)	-0.3333	0.6015
Mn(ppm)	Cu(ppm)	0.3333	0.6015
Mn(ppm)	Zn(ppm)	-1.0000	0.0000
Mn(ppm)	Cr(ppm)	-1.0000	0.0000
Mn(ppm)	Ni(ppm)	1.0000	0.0000
Mn(ppm)	Cd(ppm)	0.3333	0.4969

Pairwise Correlations

Variable	by Variable	Correlation	Count	Signif Prob
Zn(ppm)	Cu(ppm)	0.8671	17	0.0000
Cd(ppm)	Cu(ppm)	0.7016	18	0.0012
Cd(ppm)	Zn(ppm)	0.8400	16	0.0000
Cr(ppm)	Cu(ppm)	0.8485	17	0.0000
Cr(ppm)	Zn(ppm)	0.6840	17	0.0025
Cr(ppm)	Cd(ppm)	0.5102	16	0.0435
Ni(ppm)	Cu(ppm)	0.7149	17	0.0013
Ni(ppm)	Zn(ppm)	0.7189	16	0.0017
Ni(ppm)	Cd(ppm)	0.8016	16	0.0002
Ni(ppm)	Cr(ppm)	0.4226	16	0.1029
Mn(PPM)	Cu(ppm)	0.0035	12	0.9914
Mn(PPM)	Zn(ppm)	-0.3396	10	0.3370
Mn(PPM)	Cd(ppm)	-0.0260	12	0.9361
Mn(PPM)	Cr(ppm)	-0.1340	10	0.7121
Mn(PPM)	Ni(ppm)	-0.1334	10	0.7132
Pb(ppm)	Cu(ppm)	0.7151	19	0.0006
Pb(ppm)	Zn(ppm)	0.6631	17	0.0037
Pb(ppm)	Cd(ppm)	0.5496	18	0.0182
Pb(ppm)	Cr(ppm)	0.8017	17	0.0001
Pb(ppm)	Ni(ppm)	0.3806	16	0.1458
Pb(ppm)	Mn(PPM)	-0.0158	11	0.9633

Spearman's Rho Correlation

Variable	by Variable	Spearman Rho	Prob>|Rho|
Zn(ppm)	Cu(ppm)	0.9240	<.0001
Cd(ppm)	Cu(ppm)	0.7676	0.0002
Cd(ppm)	Zn(ppm)	0.7542	0.0007
Cr(ppm)	Cu(ppm)	0.8454	<.0001
Cr(ppm)	Zn(ppm)	0.7043	0.0016
Cr(ppm)	Cd(ppm)	0.4461	0.0833
Ni(ppm)	Cu(ppm)	0.6614	0.0038
Ni(ppm)	Zn(ppm)	0.7373	0.0011
Ni(ppm)	Cd(ppm)	0.7317	0.0013
Ni(ppm)	Cr(ppm)	0.2881	0.2792
Mn(PPM)	Cu(ppm)	0.1958	0.5419
Mn(PPM)	Zn(ppm)	-0.3576	0.3104
Mn(PPM)	Cd(ppm)	0.1471	0.6482
Mn(PPM)	Cr(ppm)	-0.1273	0.7261
Mn(PPM)	Ni(ppm)	-0.0243	0.9468
Pb(ppm)	Cu(ppm)	0.7428	0.0003
Pb(ppm)	Zn(ppm)	0.7664	0.0003
Pb(ppm)	Cd(ppm)	0.7381	0.0005
Pb(ppm)	Cr(ppm)	0.7802	0.0002
Pb(ppm)	Ni(ppm)	0.3652	0.1642
Pb(ppm)	Mn(PPM)	-0.0818	0.8110

Kendall's Tau b Correlations

Variable	by Variable	Kendall Tau b	Prob>|Tau b|
Zn(ppm)	Cu(ppm)	0.7941	<.0001
Cd(ppm)	Cu(ppm)	0.5847	0.0008
Cd(ppm)	Zn(ppm)	0.6103	0.0011
Cr(ppm)	Cu(ppm)	0.6371	0.0004
Cr(ppm)	Zn(ppm)	0.5482	0.0023
Cr(ppm)	Cd(ppm)	0.3149	0.0939
Ni(ppm)	Cu(ppm)	0.5482	0.0023
Ni(ppm)	Zn(ppm)	0.6109	0.0010
Ni(ppm)	Cd(ppm)	0.5641	0.0028
Ni(ppm)	Cr(ppm)	0.2279	0.2227
Mn(PPM)	Cu(ppm)	0.1212	0.5833
Mn(PPM)	Zn(ppm)	-0.2889	0.2449
Mn(PPM)	Cd(ppm)	0.1679	0.4496
Mn(PPM)	Cr(ppm)	-0.1111	0.6547
Mn(PPM)	Ni(ppm)	-0.0449	0.8575
Pb(ppm)	Cu(ppm)	0.5706	0.0007
Pb(ppm)	Zn(ppm)	0.6421	0.0003
Pb(ppm)	Cd(ppm)	0.5449	0.0018
Pb(ppm)	Cr(ppm)	0.6320	0.0004
Pb(ppm)	Ni(ppm)	0.2689	0.1488
Pb(ppm)	Mn(PPM)	-0.0909	0.6971

Appendix F

F. Summary of Clay Mineral Structures

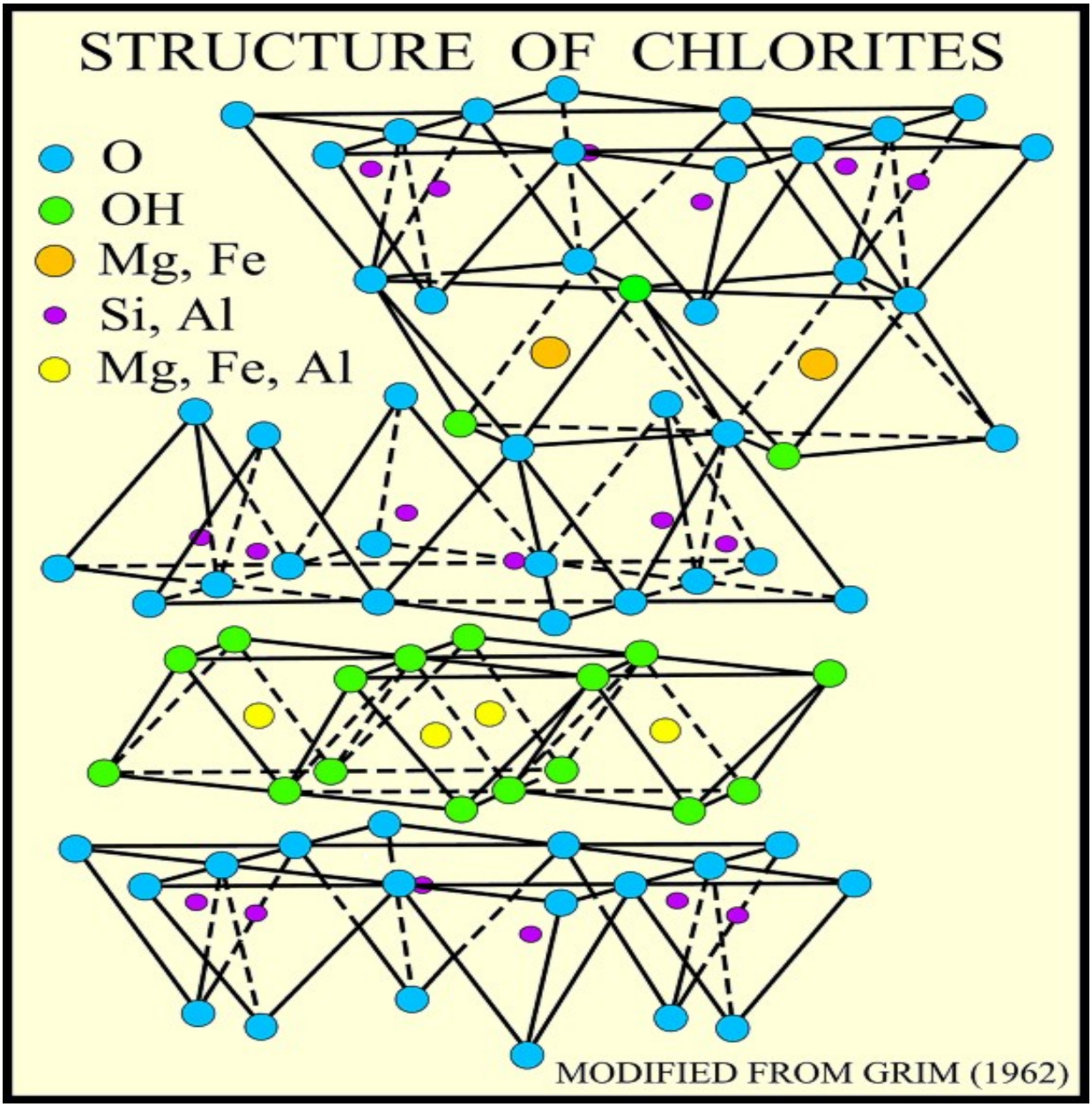
STRUCTURE OF CHLORITES
O
OH
Mg, Fe
Si, Al
Mg, Fe, Al
MODIFIED FROM GRIM (1962)

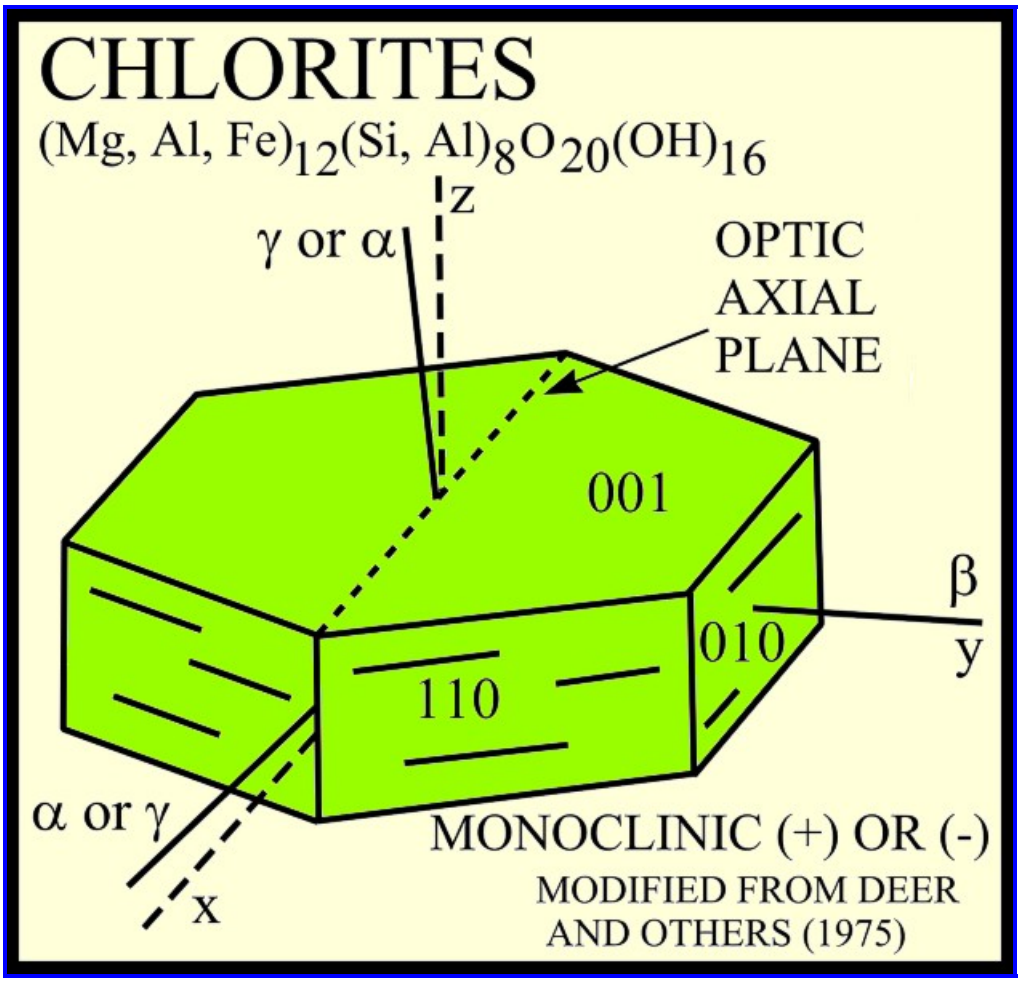
CHLORITES
(Mg, Al, Fe)12(Si, Al)8O20(OH)16
z
γ or α
OPTIC
AXIAL
PLANE
001
β
010
y
110
α or γ
x
MONOCLINIC (+) OR (-)
MODIFIED FROM DEER
AND OTHERS (1975)

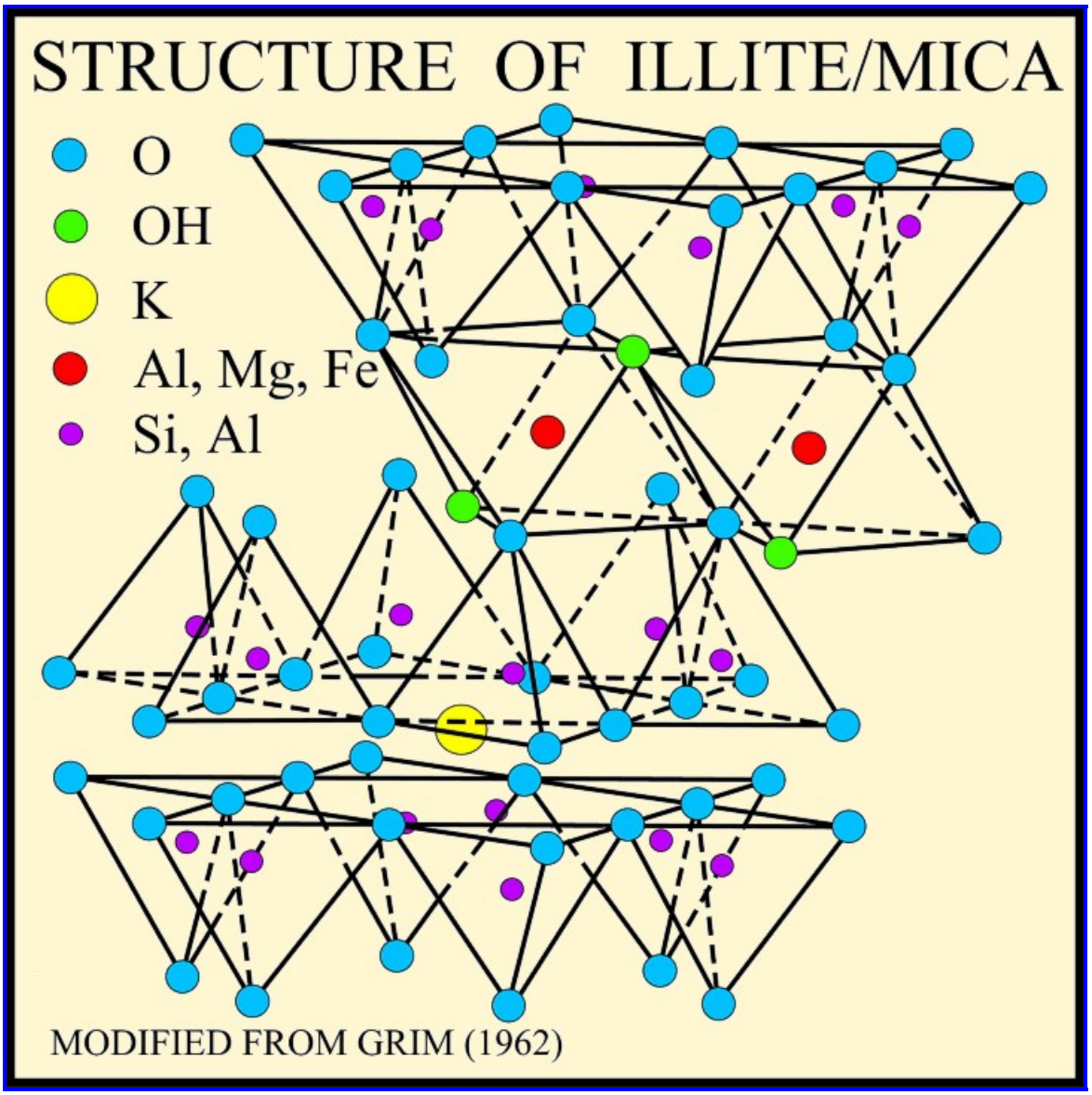
STRUCTURE OF ILLITE/MICA
O
OH
K
Al, Mg, Fe
Si, Al
MODIFIED FROM GRIM (1962)

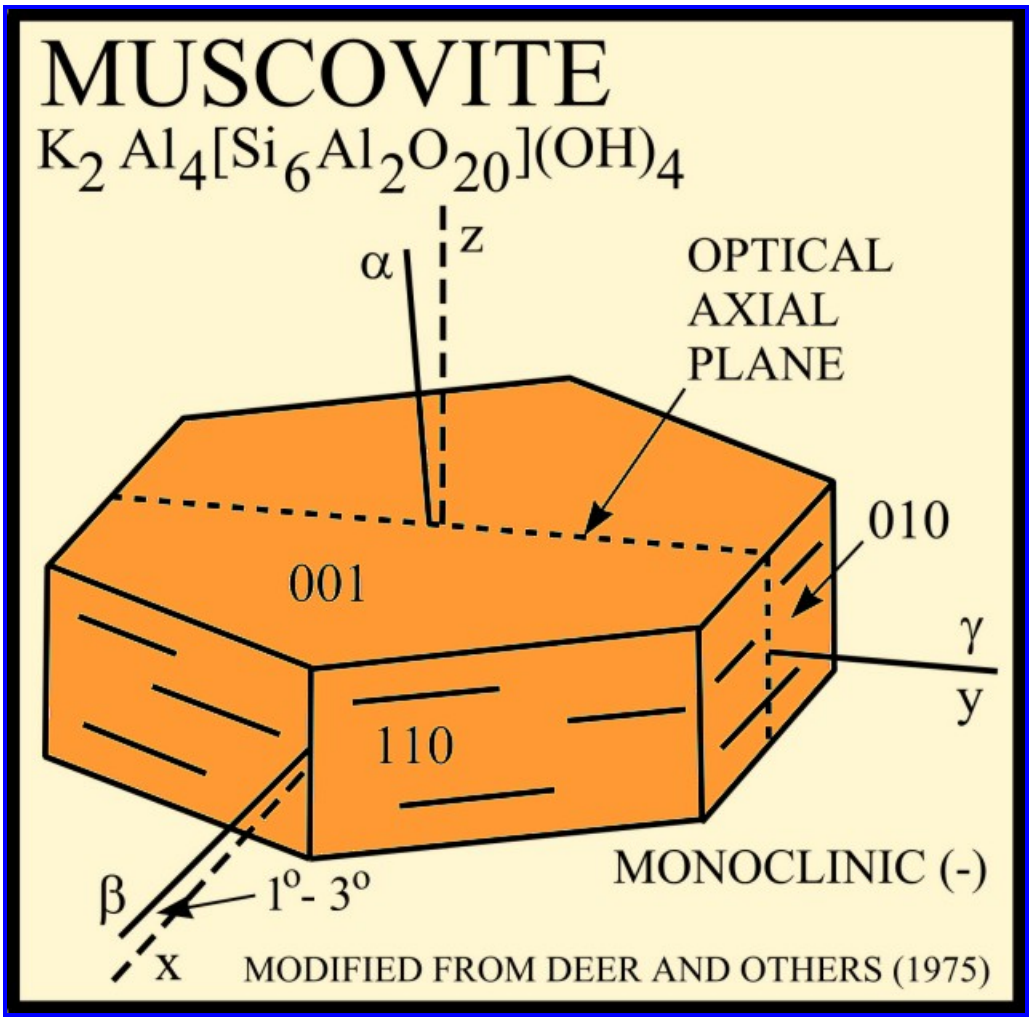
MUSCOVITE
$K_2 Al_4[Si_6Al_2O_{20}](OH)_4$
α
z
OPTICAL
AXIAL
PLANE
010
001
γ
y
110
β
1°- 3°
MONOCLINIC (-)
x
MODIFIED FROM DEER AND OTHERS (1975)

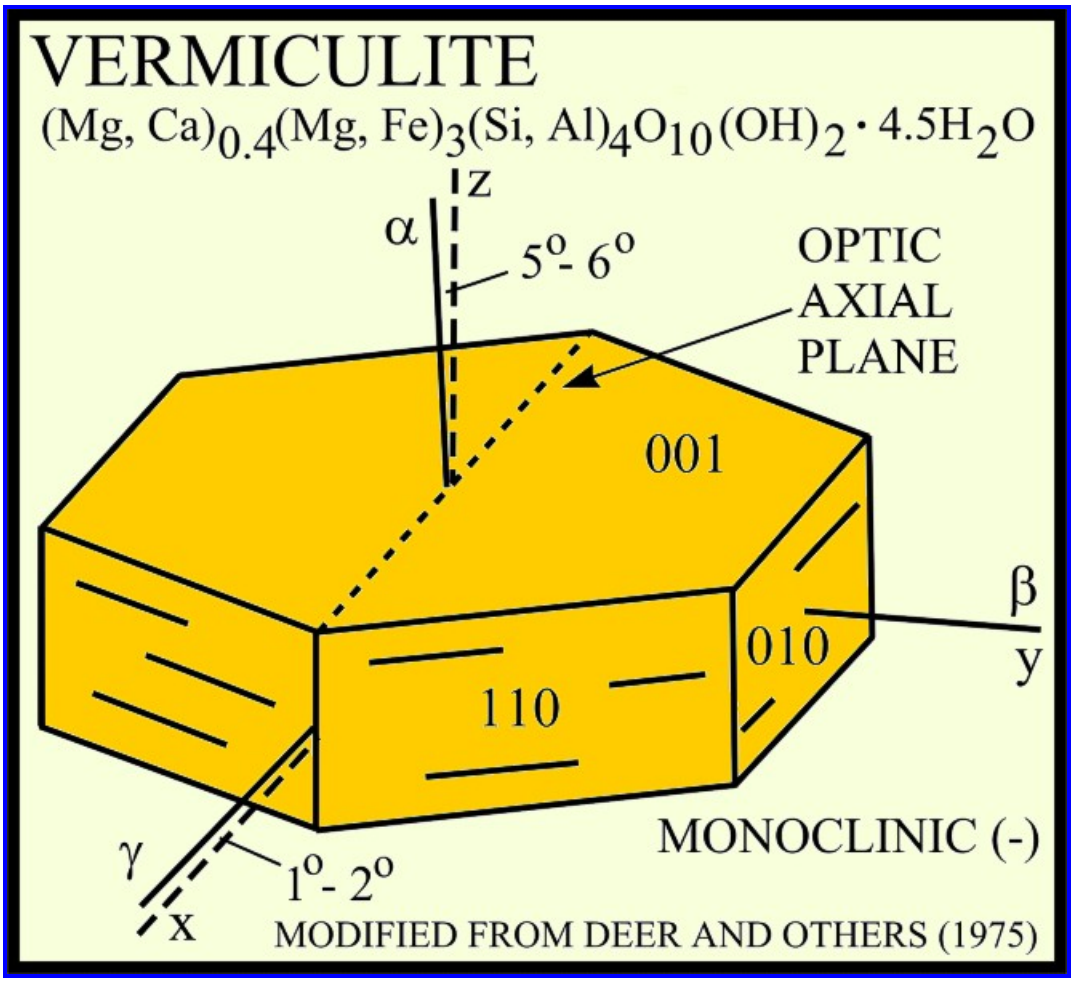
VERMICULITE
$(Mg, Ca)_{0.4}(Mg, Fe)_3(Si, Al)_4O_{10}(OH)_2 \cdot 4.5H_2O$
z
α
5°- 6°
OPTIC
AXIAL
PLANE
001
β
010
y
110
γ
1°- 2°
x
MONOCLINIC (-)
MODIFIED FROM DEER AND OTHERS (1975)

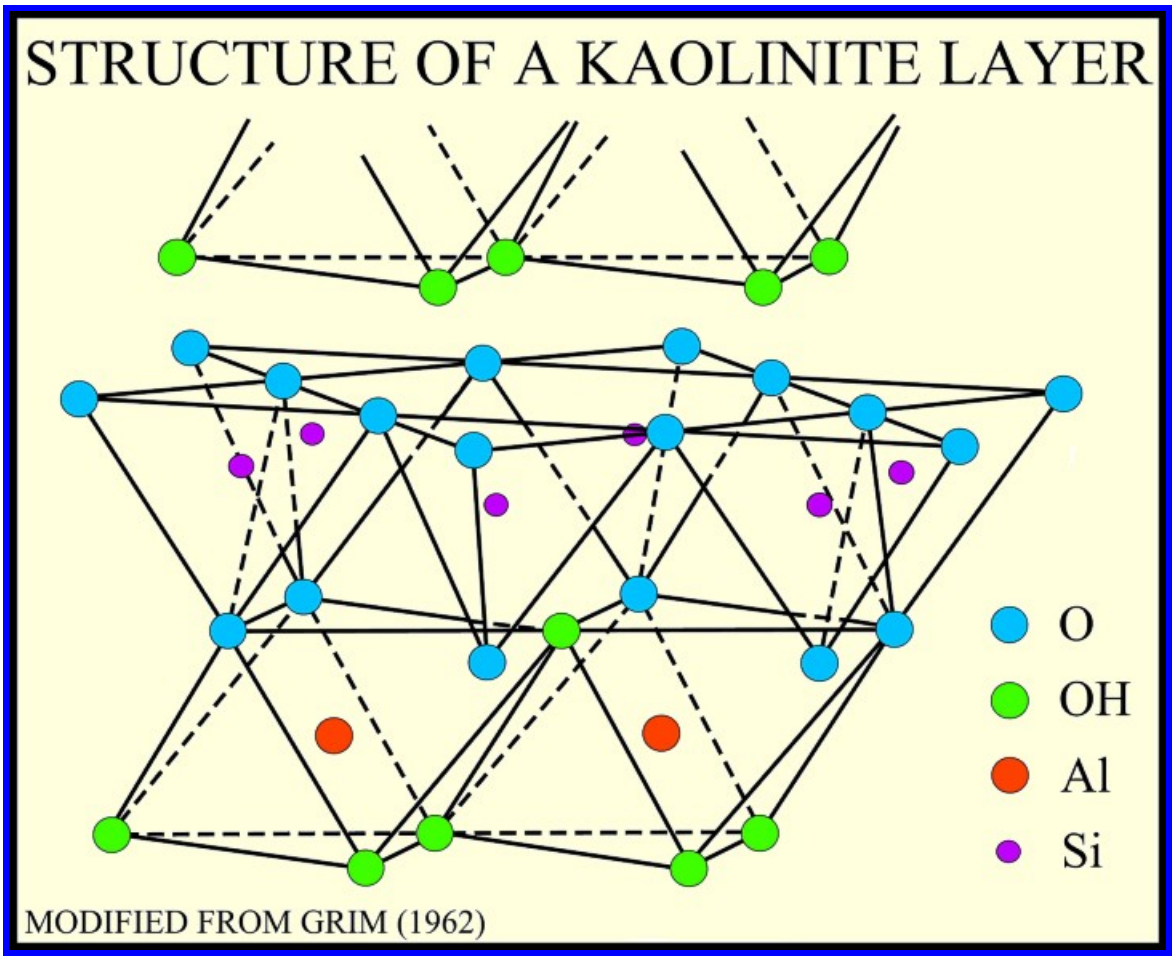
STRUCTURE OF A KAOLINITE LAYER
O
OH
Al
Si
MODIFIED FROM GRIM (1962)

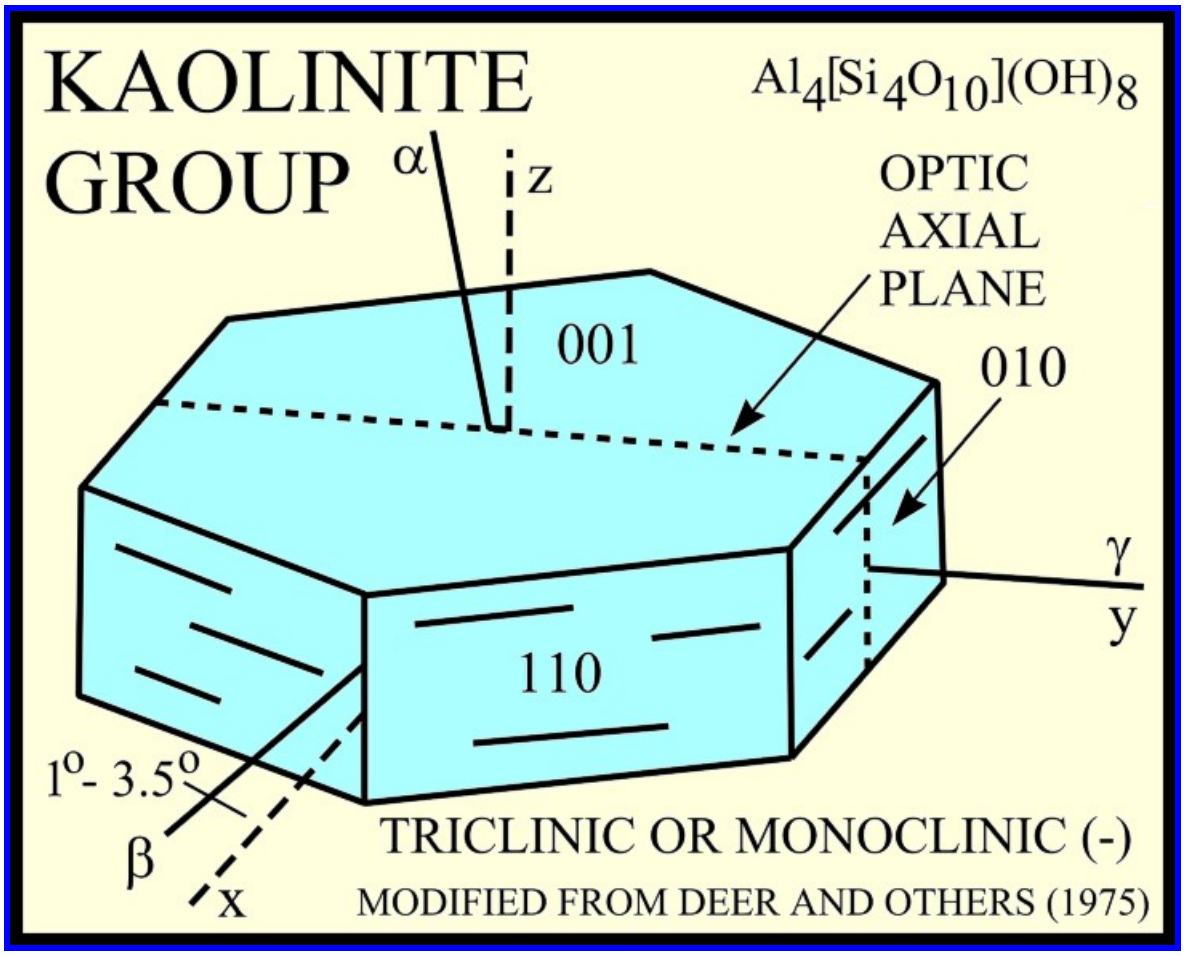
KAOLINITE
GROUP
$Al_4[Si_4O_{10}](OH)_8$
α
z
OPTIC
AXIAL
PLANE
001
010
γ
y
110
1°- 3.5°
β
x
TRICLINIC OR MONOCLINIC (-)
MODIFIED FROM DEER AND OTHERS (1975)

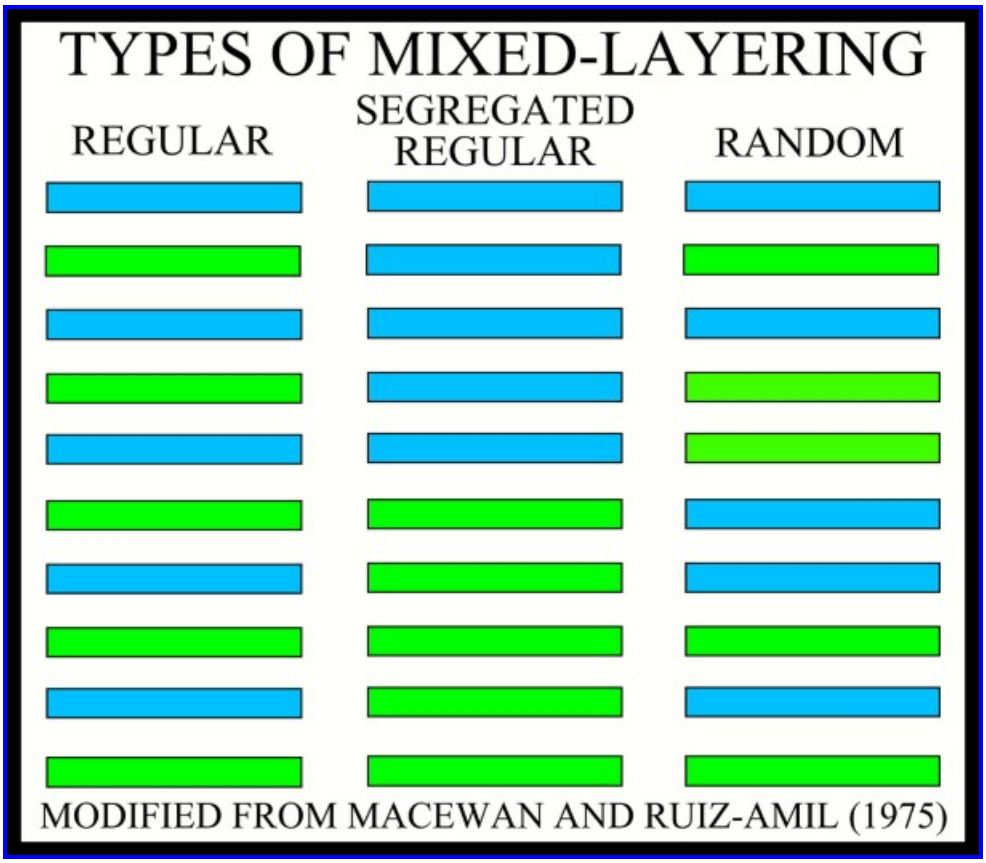
TYPES OF MIXED-LAYERING
REGULAR
SEGREGATED REGULAR
RANDOM
MODIFIED FROM MACEWAN AND RUIZ-AMIL (1975)

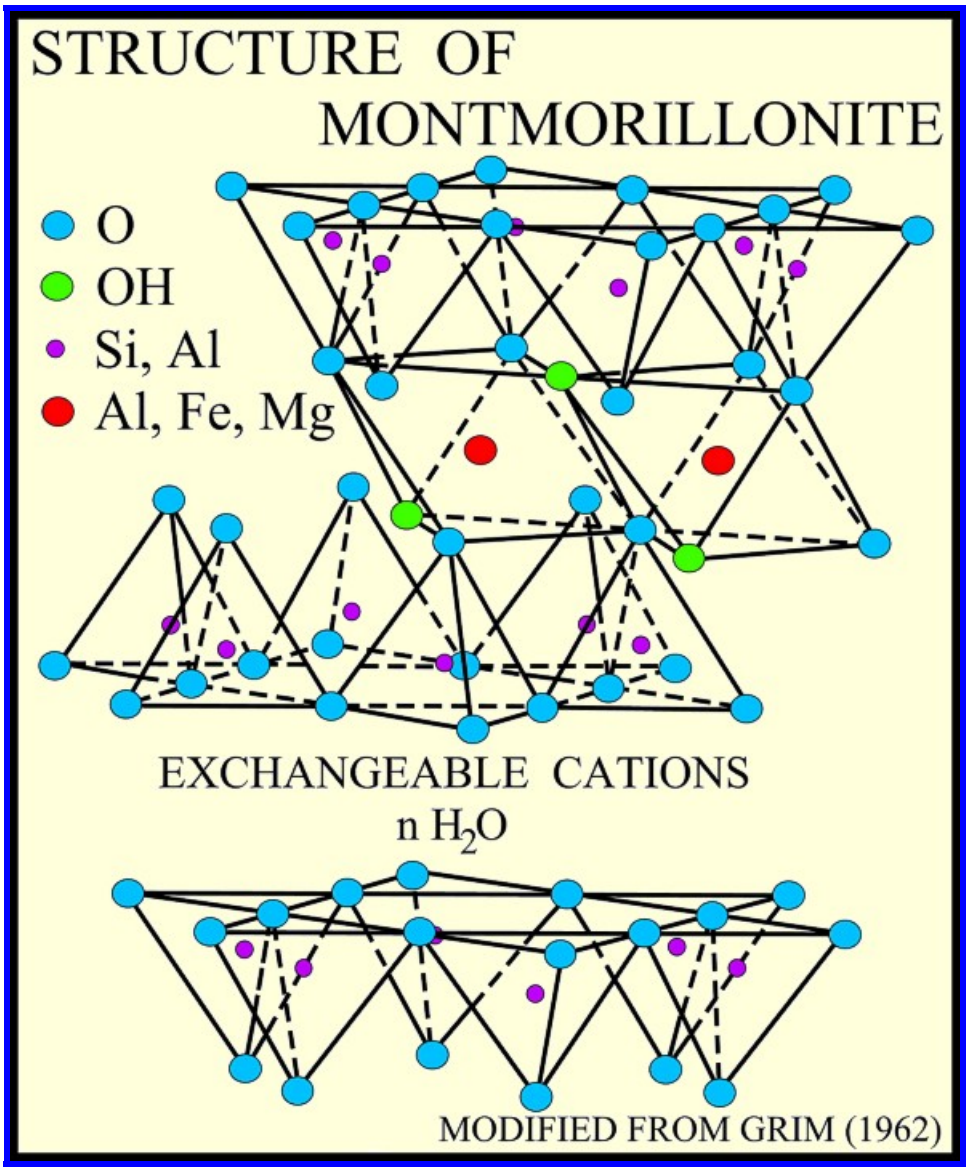
STRUCTURE OF
MONTMORILLONITE
O
OH
Si, Al
Al, Fe, Mg
EXCHANGEABLE CATIONS
n H_2O
MODIFIED FROM GRIM (1962)

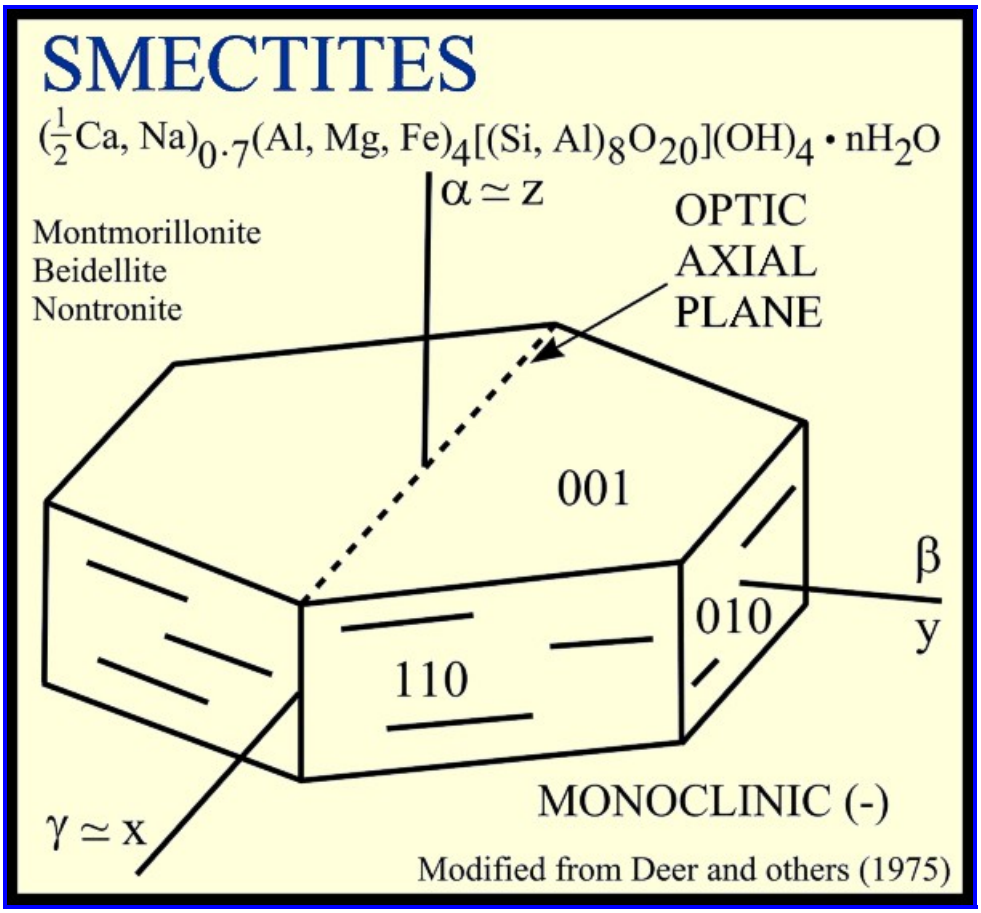
SMECTITES
$(\frac{1}{2}Ca, Na)_{0.7}(Al, Mg, Fe)_4[(Si, Al)_8O_{20}](OH)_4 \cdot nH_2O$
Montmorillonite
Beidellite
Nontronite
$\alpha \simeq z$
OPTIC
AXIAL
PLANE
001
010
110
β
y
$\gamma \simeq x$
MONOCLINIC (-)
Modified from Deer and others (1975)

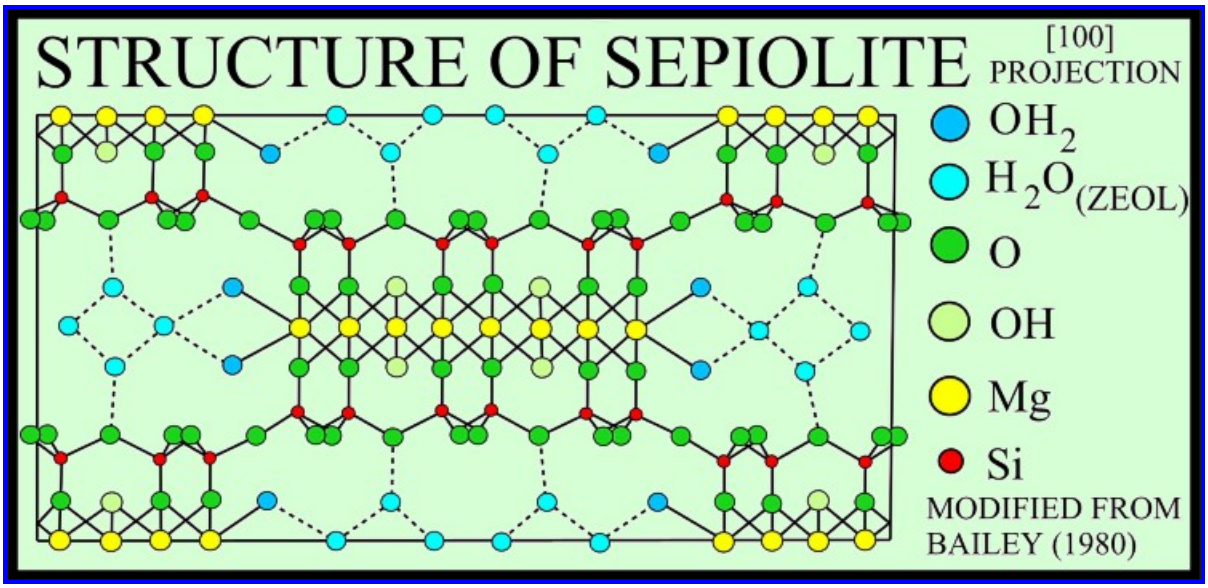
STRUCTURE OF SEPIOLITE
[100]
PROJECTION
OH_2
$H_2O_{(ZEOL)}$
O
OH
Mg
Si
MODIFIED FROM
BAILEY (1980)

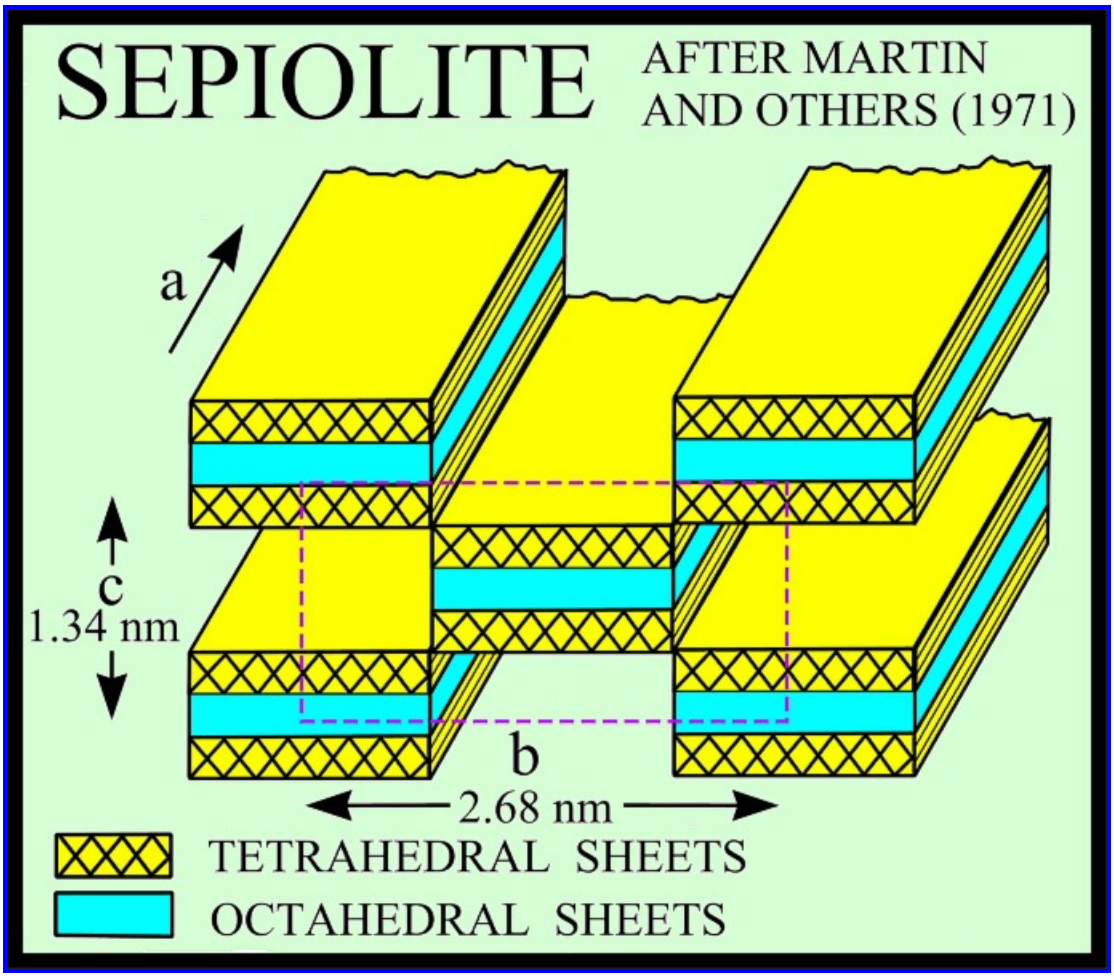
SEPIOLITE
AFTER MARTIN AND OTHERS (1971)
a
c
1.34 nm
b
2.68 nm
TETRAHEDRAL SHEETS
OCTAHEDRAL SHEETS

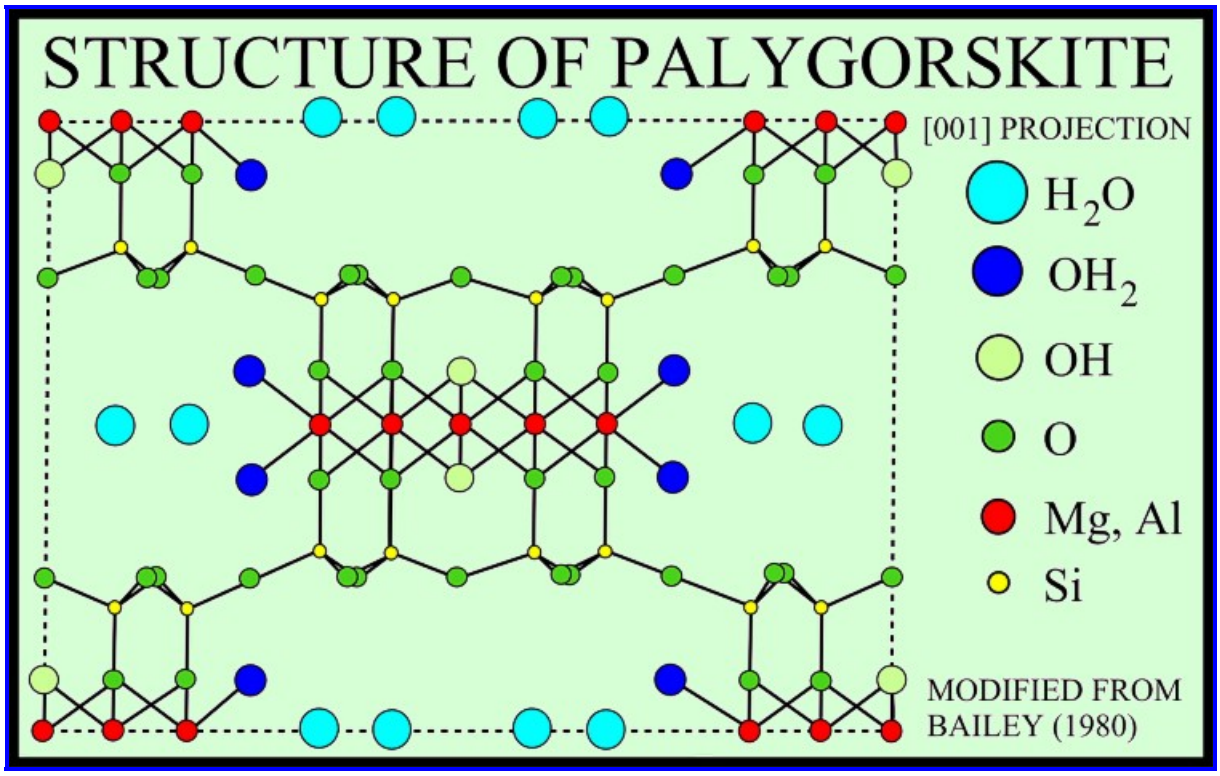
STRUCTURE OF PALYGORSKITE
[001] PROJECTION
H_2O
OH_2
OH
O
Mg, Al
Si
MODIFIED FROM
BAILEY (1980)

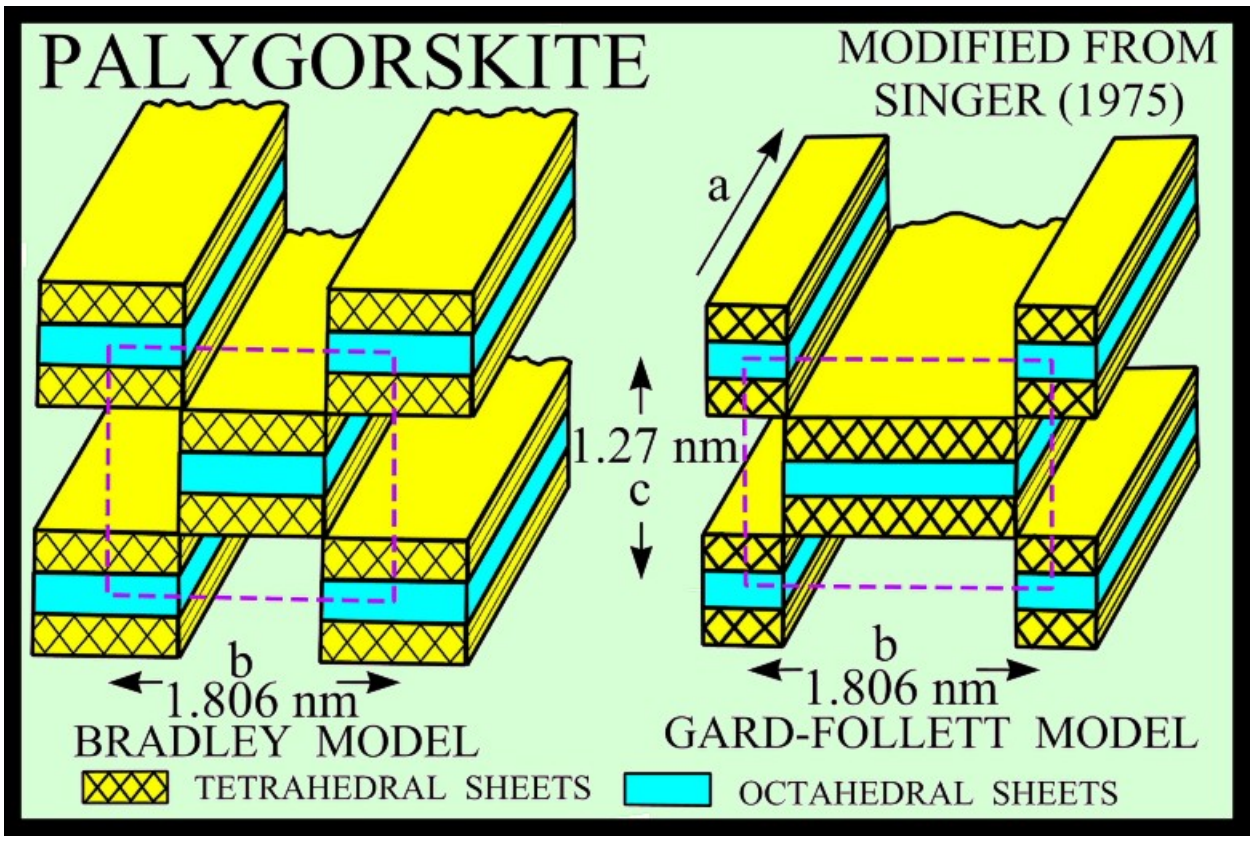
PALYGORSKITE
MODIFIED FROM
SINGER (1975)
a
1.27 nm
c
b
1.806 nm
BRADLEY MODEL
b
1.806 nm
GARD-FOLLETT MODEL
TETRAHEDRAL SHEETS
OCTAHEDRAL SHEETS

Appendix G

G. A Summary of Metal Mobility and its Biological Importance

Sources of Trace Elements in Aquatic Systems

Trace element may be derived from the weathering of rocks or, increasingly, they may be introduced into the atmosphere and hydrosphere by human activities.

Weathering

Weathering of terrestrial materials (ultimately, rocks) followed by introduction into aquatic system via surface or subsurface flow; can result in input of metals in either particulate or dissolved form. The natural sources of trace metals and elements are metallic or nonmetallic minerals (oxides, carbonates, sulphides, silicates, arsenides and others), mineral water spring and mine drainage. Biological link to weathering occurs by virtue of microbial respiration (which produces carbonic acid and in some cases oxidative weathering of minerals such as sulfides which can contain high TM concentrations. Complexation of metals by biologically-produced organic materials may be important in transmission of metals weathered from terrestrial material to aquatic realm.

Redox processes at land-water interfaces

Potential exist for reductive mobilization of TMs during anaerobic metabolism (e.g. reductive dissolution of Fe/Mn oxides) in soils/sediments that reside in land water interface regions. Released metals may enter aquatic system proper via surface or subsurface water flow. Surface water is generally more influenced by trace metals than groundwater. From this point of view gravel pits is similar to surface water.

Human activity

Human activities introduce trace metals to the hydrosphere in many ways. Burning of fossil fuels and smelting of ores put metals into the atmosphere, where they are washed out by rain into surface waters. Municipal sewage and industrial effluent introduce metals directly. Mining activities can cause release of metals by breaking up impermeable rocks and subjecting them to water and oxidative weathering/dissolution. Underground disposal of toxic wastes, including radionuclides, has the potential to release metals into groundwater, and hence to surface waters. In many rivers, lakes and oceans, the human input of trace elements is many times greater than the natural input (Stumm and Baccini, 1978; Nriagu et al., 1979; Galloway, 1979). Average concentrations of some selected trace elements in rocks and waters are shown in **Table 1.**

Table 1: Selected trace metal concentrations in rocks (ppm) and waters (ppb)

Element	Granite	Basalt	Shale	Sandston	Limestone	Streams	Ocean
Cr	10	170	90	35	11	1	0.2
Mn	50	1500	850	50	1100	8	0.2
Fe	major	major	major	major	major	40	2
Ni	10	130	68	2	20	2	0.5
Cu	20	87	45	2	4	7	0.5
Zn	50	105	95	16	20	30	2
Pb	17	6	20	7	9	1	0.03

From Drever 1988 (The Geochemistry of Natural Waters)

Biological Importance of Trace Metals and Overview of their Properties

It has been known for several decades that trace quantities of certain elements exert a positive or negative influence on plant, animal, and human life. Trace elements are defined as those elements that generally occur in waters at concentrations of less than 1 mg/l, which generally means molar concentrations of 10^{-4} M or less (Drever, 1988).

Major Metals

These elements, which include Na, K, Ca and Mg, are known as "hard" metal I ions based on their tendency to participate in electrostatic rather than covalent interactions with complexants. Hard cations tend to not be strongly complexed in either fresh water or sea water, except when they are present in high concentration in which case they tend to be complexed by major anions (referred to as "simple ligand") and to some degree by OH and COOH groups on organic macromolecules (referred to as "hard" organic complexant sites). Under some conditions formation of Ca and Mg carbonate minerals precipitates is associated with biological activity – very important in oceanic C cycle since sinking of carbonates is potentially a major mechanism for transfer of C from surface to deep ocean**.**

Trace Metals

Fe(III), Mn(IV), and Al(III) oxides-These metals are strongly hydrolyzed under circuneutral pH conditions typical of most natural waters; as a result, are generally found as highly insoluble hydrous oxides (e.g. $Fe(OH)_3$, MnO_2, $Al(OH)_3$ in well-oxygenated natural waters; over time can become converted to relatively well-crystalline oxide minerals. Due to their low solubility, Fe (III), Mn (IV) oxides are generally present at very low concentrations in natural waters and as generally included as trace metals. Complexation by organic substances can be important in maintaining these metals in solution in organic-rich aquatic environment. However, these metal oxides can be present at relatively high concentrations (e.g. 10^{-1} mole per L) in sediments and soils; therefore in these systems are sometimes referred to as the "major metals" in natural system. Whether present suspended in water column or in soil/sediment, Fe/Mn/Al hydroxide surfaces are highly reactive, with strong tendency to adsorb both cations and anions. As such, they constitute one of the important "simple ligands", and are important scavengers of other trace

metals in aquatic systems. Fe, Mn, and Al oxides are *carrier phases*, whose behavior (e.g. in terms of acid-base and redox chemistry) exert a fundamental control on the behavior of other trace metals. These metal oxides are soluble in acidic conditions; behave as "hard" cations thus are relatively mobile under these conditions.

Transition metals

These metals are generally divalent cations, they possess appreciable affinity for both "hard" and "soft" complexation sites on organic molecules. Soft complexation sites, at least in terms of aqueous complexation, are generally comprised of organic N and organic S group. Transition metals are also generally strongly complexed by inorganic solid surface sites (surface hydroxyl groups). These transition metals are also subject to formation of mineral precipitates with simple inorganic ligand such as carbonate (CO^{2-}) and or sulfide (S^{2-}); trace metals can form either discrete phases or coprecipitates with major metals, i.e. Fe and Mn phases. Fe^{2+} and Mn^{2+} are important as enzyme cofactors in many biochemical pathways; most commonly redox-reaction; most autotrophic organisms and bacteria have enzymes which allow them to acquire Fe^{2+} and Mn^{2+} from Fe and Mn oxides through use of strong Fe(III) and Mn(IV) binding molecules called siderophores which complex and thereby dissolve the Fe(III) or Mn(IV), and (usually) through the use of reductive enzymes which convert Fe(III) and Mn(IV) to Fe(II) and Mn(II). Fe^{2+} and Mn^{2+} also are end products of microbial Fe (III) and Mn (IV) oxide reduction; as such can sometimes be present at no-trace levels, particularly in interstitial waters of aquatic sediments. Fe^{2+} and Mn^{2+} are highly redox sensitive, they are subject to abiotic or biologically-catalyzed oxidation under aerobic conditions.

Cu^{2+}, Ni^{2+}, Co^{2+}, and Cr^{2+} are commonly involved in biochemical pathway as cofactors, or as co-enzymes; sometimes involved in maintenance of macromolecular

structures; can be toxic at high concentrations as they interfere with structures.

Cu^{2+} and Ni^{2+} are generally not subject to major redox transformation, although some possibilities for enzymatic reduction of these compounds exist. Co is subject to redox transformation between Co^{3+} and Co^{2+} ; redox transformation may be biological or abiotic. Cr is also subject to redox transformations; main one is from soluble chromate ion (e.g. CrO_4^{2-}, = Cr (VI) to insoluble Cr (III) = Cr (III) hydroxide, to Cr^{2+} which is involved in certain biochemical pathways. Redox transformation of Cr may be either enzymatic or abiotic.

Soft metal ions

Soft metal ions are primarily divalent cations with high affinity to soft sites on organic macromolecules.

The major soft metal ions are, Zn^{2+}, Cd^{2+}, Hg^{2+}, Pb^{2+}, Sn^{2+}, Ag^{2+}, Sn^{2+}, $Ag^{+}$and Au^{+}/Au^{3+} . These metals sometimes referred to "toxic metals" because they can form complexes with "soft" groups on biological molecules and thereby replace them and block action or modify vital structure. Of all these metals only Zn is important in biochemical pathways. Like transition metals, soft metals can form either discrete phases or coprecipitates with metals, i.e. Fe and Mn phases such as, carbonates and sulfides.

Two of soft metal ions, Hg^{2+} and Sn^{2+}, are subject to biological ethylation; are even more toxic in this from and this is of considerable environmental concern.

Most of trace metals and many major elements are transported in surface and ground waters chiefly in complexed form. For example, the cation Cu^{2+}, Hg^{2+}, Pb^{2+} and U^{4+} are found chiefly in complexes rather than as the free ions. The mobilities and other environmental properties of such elements are, therefore, chiefly those of their complexes. Adsorption of metals and or anions may be greatly favored or inhibited when

they occur as complexes rather than as free ions. For instance, the hydroxide complexes of uranyl ion (UO_2^{2+}) are strongly adsorbed by oxide and hydroxide minerals, whereas uranyl carbonate complexes poorly adsorbed by these minerals (Hsi and Langmuir 1985). The toxicity and bioavailability of metals in natural water depends on the aqueous speciation or complexation of the metals. The toxicities to aquatic life of Cu^{2+}, Cd^{2+}, Zn^{2+}, Ni^{2+}, Hg^{2+} and Pb^{2+} are a function of the activity of the metal ions and their complexes, not of total metal concentrations (Morel and Hering 1993; Manahan 1994). The bioavailability of essential metals such as Fe, Mn, and Cu to plants is also a function of their metal speciation (Morel and Hering 1993). According to Manahan (1994), a toxic substance or toxicant "is harmful to living organisms because of it detrimental effects on tissues, organs, or biological processes." Mechanisms by which toxic metals poison plants and animals relate to their tendency to form strong complexes with the generally soft functional groups on biomolecules (Sposito 1989; Moral and Herring 1993). Shown in **Table 2** are observed toxicity sequences for some plants.

Table 2: Representative metal toxicity sequences

Organisms	Sequence of decreasing toxicity*
Algae	**Hg** > *Cu* > **Cd** > *Fe* > Cr > *Zn* > *Co* > Mn
Flowering plants	**Hg** > *Pb* > *Cu* > **Cd** > Cr > *Ni* > *Zn*
Fungi	**Ag** > **Hg** > *Cu* > **Cd** > *Cr* >*Ni* > *Pb* > *Co* > *Zn* > *Fe*
Phytoplankton (freshwater)	**Hg** > *Cu* > **Cd** > *Zn* > *Pb*

Note: Elements in bold are soft acids
Italized elements are borderline hard-soft acids.
Cr (III) and Mn (II) are hard acids
* Hg = Hg(II), Fe = Fe(II), Cr = Cr(III), Co(II), Mn = Mn(II), Pb = Pb(II)
Source: From the Chemistry of Soil, by G. Sposito (1989)

Another reason for the biochemical importance of heavy metals is the fact that some are essential as macronutrients and micronutrients for various organisms. According to Manahan (1994), C, H, O, N, S, P, K, Ca and Mg are essential for plants. Of these elements, C, H, and O are

constituents of biomass, N and P are in proteins, S in Proteins and enzymes, and K, Mg, and Ca have metabolic functions. Plants essential trace elements (micronutrients) include B, Cl, Co, Cu, Fe, Mn, Mo, Na, Si, V, and Zn. It has been known for many decades that trace quantities of certain elements exert a positive or negative effect on plant, animal, and human life. Therefore, it is important to consider heavy metal contamination.

REFERENCES

ABOOD, K.A., 1974. Circulation in the Hudson River. In: Roels, O.A. (Ed.), The Hudson River Colloquium. Annals of the nEw York Academy of Sciences 250, 39-111.

ADRIANO, D. C., 1992. Biogeochemistry of Trace Metals. Lewis Publishers, New York p. 513.

AJA, S.U., and P.E. ROSENBERG. 1992. Thermodynamic status of compositionally-variable clay minerals: A discussion. Clays and Clay Minerals 40(3): 292-99.

ALLEN, H. E., 1995. Metal Contaminated Aquatic Sediments. Ann Arbor Press, INC. Michigan p. 292.

ALLEN, J.R.L., 1991, Fine sediment and its sources, Severn Estuary and inner Bristol Channel, southwest Britain: Sedimentary Geology, v. 75, p. 57-65.

AMAACH, N.H., 1996, Geochemical Study of Trace Metals in Soils of the Williamsburg Area, Brooklyn ,NewYork. MA, Thesis, Department of Geology, Brooklyn College NY., p.87

AMOS, C.L., KING. E.L., 1984. Bedforms of the Canadian eastern seaboard: a comparison with global occurrences. Mar. Geol. 57, 167-208.

ANDERSON. J.R., 2004, Sand Sieve Analysis, http://gpc.edu./~janderso/historic/labman/sievean.htm

ARLEN, L., and MOUNTAIN, D.G., 1996, Oceanographic Conditions in the Inner New York Bight During the 12-Mile Dumpsite Study. NOAA Tech. Repo. NMFS 124, pp. 21-31.

AUSTIN, J.R., JR., CHRISTIE-BLICK, N., MALONE, M.J., et al., 1998, Proceddings of the Ocean Drilling Program , Initial reports, Volume 174A: College Station, Texas, Ocean Drilling program, 324p.

BISCAYE, J.I., 1965, Mineralogy and sedimentation of recent deep-sea clay in the Atlantic Ocean and adjacent seas and oceans: Geological Society of America Bulletin, v. 77, p. 183-196.

BOCZAR-KRAKIEWICZ, B., BONA, J.L., 1986. Wave-dominated shelves: A model of sand-ridge formation by progressive, infragravity waves. In: Knight, R.J., McLean, J.R., (Eds.), Shelf Sands and Sandstones, Canadaian Society of Petroleum Geologists, Memoir II, pp. 163-179.

BOKUNIEWICZ, H., GOLDSMITH, V., CLARK, H.W., 1991. The New York Bight Information System: Devolopment, Results, and Future effects. March.

BOTHNER, M.H., and GRASSLE, J.F., 1996, Sewage contamination in Sediments Beneath a Deep-Ocean Dumpsite. Northeastern Geology and Environmental Sciences, v. 18, no. 4, 1996, p.292.

BUCHHOLTZ TEN BRINK, M.B., ALLISON, M.A., SCHLEE, J.S., CASSO, M., LOTTO, L., and BOPP, R.F., 1996. Sewage sludge and sedimentary processes in the New York Bight: where does it go from here? EOS Transactions 76, 14, abstract.

BUCHHOLTZ TEN BRINK, M.B., BOTHNER, M.H., MANHHEIM, F.T., and BUTMAN, B., 1997, Contaminant Metals in Coastal marine Sediments: A Legacy for the Future and a Tracer of Modern Sediment Dynamics: http://water.usgs.gov/osw/techniques/workshop/brink.html

BUTMAN, B., HARRIS, C. K., and TRAYKOVSKI, P., 2003, Winter-Time Circulation and sediment transport in the Hudson Shelf valley. Elsevier Science Ltd. v.23, issue 8, pp. 801-820.

CARMODY, D.J., 1972. The Distribution of Five Heavy Metals in the Sediments of the New York Bight. PhD dissertation, Columbia University Teachers College University Microfilms, Ann Arbor Mich.

CARMODY, D.J., PEARCE, J.B., and YASSO, W.E., 1973, Trace Metals in Sediments of New York Bight: Mar. Poll. Bull., v. 4, pp. 132-135

CHAVE, K. L., 1960, Evidence on history of sea water from chemistry of deeper subsurface waters and ancient basins: American Association of Petroleum Bulletin, v. 44, p. 357-370.

CHEN, M., AND MA, L.Q., 2001, Comparison of Three Aqua Regia Digestion Methods for Twenty Florida Soils: Soil Sci.Soci. Am. J. 65:491-499

CHRISTIE-BLICK, N., MOUNTAIN, D.S., GHOSH, A., MCHUGH. C.M.G., PEKAR, S.F., and SCHOCK, S.G., 2002, New insights on late Pliestocene sedimentation at the New Jersey magin based on CHIRP sonar prophiles and Vibracore: Eos (Transactions, American

COCH, N.K., BOKUNIEWICZ, H.J., 1986. Oceanographic and geologic framework of the Hudson system. Northeastern Geology 8, 96-108.

CONNER, W.G., AURAND, D., LESLIE, M., SLAUGHTER, J., AMER., and ROVENSCROFT, F.I., 1979, Disposal of dredged material within the New York Bight District. *In* Present Practices and Candidate Alternatives, v. 1. Technical Report MTR-7808, MITRE Corporation, McLean, Virginia, p. E-31.

COOPER, J.C., CANTELMO, F.R., NEWTON, C.E., 1988. Overview of the Hudson River Estuary. *In*: BARNTHOUSE, L.W., KLAUDA, R.J., VAUGHAN, D.S., KENDAL, R.L. (Eds.), Science, law and Hudson River Power Plants. American Fisheries Society Monography 4. American Fisheries Society, Bethsda, Maryland, USA.

DARLYMPLE, R.W., ZAITIN, B.A., B.A., and BOYD, R., 1992. Estuarine facies models; conceptual basis and stratigraphic implications. Journal of sedimentary Petrology 62, 1130-1146.

DARLYMPLE, R.W., HOOGENDOORM, E.L., 1997. Erosion and deposition on migrating shoreface-attached ridges, Sable-Island, eastern Canada. Geosci. Can. 24, 25-36.

DAYAL, R., HEATON, M.G., FUHRMANN, M., and DUEDALL, I.W., 1981, A Geochemical and Sedimentological Study of Dredged Material Deposit in the New York Bight. Technical Memorandum OMPA-3, U.S. National Oceanic and Atmospheric Administration, Stoony Brook, New York, 265p.

DRAKE, D.E., and CHACCHIONE, D.A., 1985. Seasonal variation in sediment transport on the Russian river Shelf, California. Continental Shelf Research 4, pp. 495-514. Abstract

DRAXLER, A.F.J., STUDHOLME, A.L., ZDANOWICZ, V.S., REID, R.N., VITALIANO, J.J., WILK, S.J., KATZ, I. AND O'REILLY, J.E., 1996, Closure of the New York Bight 12-Mile Sewage Sludge Dumpsite: Ecosystem Responses with implications for Resource Management. Northeastern Geology and Environmental Sciences, v. 18, no.4, p. 293-303.

DREVER , J.I. 1988. The Geochemistry of Natural Waters, second edition. Prentice Hall. New Jersey p. 437.

DUANE, D.B., FIELD. M.E., MEISBURGER, E.P., SWIFT, D.J.P., and WILLIAMS, S.J., 1972. Linear shoal on the Atlantic inner continental shelf, Florida to Long Island. In: Swift, D.J.P., Duane, D.B., Pilkey., O.H. (Eds.), Shelf Sediment Transport: Process and Pattern. Dowden, Hutchinson and Ross, Stroudsburg, Penn., pp. 447-498.

ELRICK, K. A., and HOROWITZ, A.J., 1986, Analysis of Rocks and Sediments for Arsenic, Antinomy, Selinium, by wet Digestion and hydride Generation Atomic Absorption. Varian Instrument at Work. No. AA-56, p.5

EMERY, K.O., and RITTENBURG, S.C., 1952. Early diagenesis of California basin sediments in relation to origin oil: American Association of Petroleum Geologists Bulletin, v. 36, p. 735-806.

ENVIRONMENTAL SCIENCES, v. 21, nos. 1/2, pp. 18-34.

EPA and USACE, 1977, Ecological evaluation of proposed discharge of dredged material into ocean waters (implementation manual for section 103 of Public Law 92-352 (MPRSA of 1972)): Environmental Effects Laboratory, Army Engeneer Waterways Experiment Station, Vicksburg, Mississippi, 19p., plus appendices.

EPA and USACE, 1991, Evaluation of dredged material proposed for ocean disposal (testing manual): EPA, Office of marine and Estuarine Protection, Whashington, D.C. under Contract No. 68-C8-0105, variously paged.

EPA, 1979, Draft Environmental impact Statement (EIS) for New York Bight Acid Waste Disposal Designation, Contract 68-01-4610.

EPA, 1980b, Final Environmental Impact Statement for New York Bight Acid Waste Disposal Site designation: EPA, Oil and Special Material Control Division, Marine Protection Branch, Whashington, D.C. 20460 variously paged.

EPA, 1996, Personal communication on sludge dumpers report with A. Roufaeal, Region 2, EPA, NY, NY.

EWING, J., LEPICHON, X., and EWING, M., 1963, Upper stratification of Hudson Apron region: Journal of geophysical Research, v. 68, p. 6303-6316.

FIGUEIREDO, A.G., SWIFT, D.J.P., STUBBLEFIELD, W.L., and CLARKE, T.L., 1981. Sand ridges on the inner Atlantic shelf of North America: Geo-Mar. Lett. 1, 187-191.

FOLK, R.L., 1966, A Review of Grain Size Prameters: Sedimentology, v.6, pp. 73-93

FÖRSTNER, U., and WITMAN, G.T.W., 1981. Metal Pollution in the Aquatic Environment, second revised edition. Sringer-Verlag, Berlin Heidelberg New York. 486p.

FRANK, W.M., MCKINNEY, T.F., FRIEDMAN, G.M., 1972. Atlantic continental shelf - a comparison of areas north and south of the Hudson River submarine canyon. Marine Geology and Geophysics, section 8, International geological congress, pp. 231-236.

FREELAND, G. and SWIFT, D., 1978. Surficial Sediments, MESA New York Bight Atlas Monograph 15. P.182.

FREELAND, G.L., STANLEY, D.J., SWIFT, D.J.P. and LAMBERT, D.N., 1981. The Hudson Shelf Valley: its role in shelf sediment transport. Mar. Geol. 42, 399-427.

FRIEDMAN, G.M., FABRICANAD, B.P., IMBRIMBO, E.S., BREY, M.E., and SANDERS., J.E., 1968, Chemical changes in interstitial water from continental shelf sediments: Journal of Sedimentary Petrology, v. 38, p. 1313-1319.

FRIEDMAN, G.M., MUKHOPADHYAY, P.K., MOCH, A., AHMED, A., 2000. Waters and organic-rich waste near dumping grounds in the New York Bight. International Journal of Coal Geology, v. 43, pp. 325-355.

FRIEDMAN, G.M., 1996a. Waste management and dredged-material disposal in the nearshore environment: a symposium. Northeastern Geol. Environ. Sci. 18, i.

FRIEDMAN, G.M., 1996b. Waste management and dredged-material disposal in the nearshore environment: case history of the New York Bight. Northeastern Geol. Environ. Sci. 18, 257-264.

FRIEDMAN, G. M., 1999, Dredging Harbors: What to do with Toxic Waste: A Symposium, Northeastern Geology and Environmental Sciences, v. 21, nos. 1/2, pp. 1-11.

FRIEDMAN, G.M., SANDERS,J.E., and KOPASKA-MERKEL, D.C., 1992, Principles of Sedimentary deposits. Macmillan Publishing Company, New York, p.717.

FROELICH, P.B., GOLDEN, B., and PILKEY, O.H., 1971, Organic Carbon in sediment of the North Carolina continental rise: Southeastern Geology, v. 13, p. 91-97.

GARDNER, J.V., 1975. Late Pleistocene carbonate dissolution cycles in the eatern equatorial Atlantic. Cushman found. Foramineferal Res. Spec. Publ. 13, 129-141. Geophysical Union), v. 83, p. F727.

GEYER, W.R., WOODRUFF, J.D., and TRAYKOVSKI, P., 2001, Seiment transport and trapping in the Hudson River estuary: Estuaries. v.24, p. 670-679.

GIBBS, R. J., JHA, P.K., and CHAKRAPANI, G.J., 2000, Clay Mineralogy of the Hudson River Estuary. Northeastern geology and Environmental Sciences, v. 22, no. 1, pp. 26-30.

GOFF. J.A., SWIFT. D.J.P., DUNCAN. C.S., MAYER. L.A., and HUGHES-CLARKE. J., 1999. High-resolution swath sonar investigation of sand ridge, dune and ribbon mophoplogy in the offshore environment of the New Jersey margin. Marine Geology 161, 307-337.

GREIG, R.A., REID, R.N., and WENZLOFF, D.R., 1977, Trace Metal Concentrations in sediments from Long Island Sound: Marine Pollution Bulletin, v.8, no. 8, pp. 183-188.

GRIFFIN, G.M., and INGRAM, R.L., 1955, Clay minerals of the Neuse River Estuary: Journal Sedimentary Petrology, v. 25, p. 194-200.

GRIM, R. E. 1968. Clay Mineralogy. New York: Mc Graw Hill.

GROSS, M.G., 1970, Preliminary Analysis of Urban Waste, New York metropolitan Region. Technical report No. 5, Marine Science Research Center, State University of New York, Stony Brook, p.35

GROSS, M.G., 1976, Middle Atlantic Continental Shelf and the New York Bight, Special Symposia, v.2, p.441

HARRIS, W.H., 1976, Spatial and Temporal Variation in Seidementary Grain-Size facies and Sediment Heavy Metal Ratios in the New York Bight apex, p102-123, in Gross, M.G. (ed.) , Middle Atlantic Continental Shelf and the New York Bight. Am. Soc. Limnol. and Oceanog. Spec. Symp., v.2, Allen Press, Lawrence, Kansas.

HARRIS, W.H., 1977, Distribution of Surficial Sediments, Total Organic Carbon, Heavy Metals and Heavy-Metal ratios in the New York Bight Apex and LINS Areas. NOAA-MESA Progress Rept. Grant No. 04-6-022-44014, national Oceanic and Atmospheric Administration. MESA-New York Bight Office, Stony Brook, p.25

HARRIS, W.H., and WASCHITZ, M., 1982, Bulk Organic Geochemistry and Trace Metals in Sewage-derived Sediments from the New York Bight Apex: Northeastern Environmental Science, v. 1, No. 1, pp. 19-32.

HOROWITZ, A.J., 1984, Major Element Analysis pf Rocks and Sediments by atomic Absorption Spectroscopy. Varian Instrument at Work. No. AA-42, p.5.

HOUSTEN, L.J. 1999, Preparing a Dredging material Management Plan for the Port of New York/New Jersey: Northeastern Geology and Environmental Sciences, v. 21, nos. 1/2, 1999, pp. 12-17.

HSI, C-K. D., and LANGMUIR. 1985. Adsorption of uranyl onto ferric oxyhydroxides: Application of the surface complexation site binding model. Geochim, Cosmochim. Acta 49(11):2423-32.

HUNT, J.M., 1961, Distribution of Hydrocarbons in Sedimentary Rocks: Geochemica et Cosmochimica Acta, v. 22, p. 37-49.

HUNTLEY, S.L., BONNEVIE, N.L., WENNING, R.J., and BEDBURY, H., 1993, Distribution of Polycyclic Aromatic Hydrocarbons (PAHs) in Three Northern New Jersey Waterways: Bulletin of Environmental Contamiants and Toxicology, v. 51, p. 865-873

HYDROQUAL, INC., 1989, Assessment of pollutant inputs to the New York Bight: NY Bight Restoration Plan, Phase 1 report, Attachment III: Prepared for EPA Region 2 by Dynamac Corp., Rockville, MD, variously paged.

INTERSTATE ELECTRONICS CORPORATION, 1973, Ocean Waste Disposal in Selected Geographics Areas. Report No. 4460C1541, Cointract 68-01-0796.

ISACHSEN, Y.W., LANDING, E., LAUBER, J.M., RICKARD, L.V., and ROGERS, W.B., 2000. Geology of New York: a simplifies account. New state Museum Educational Leaflets, 28. The New York State Geological survey, New York State Museum, Albany, New York, USA, 294 pp.

KLITGORD, K.D., HUTCHINSON, D.R., and SCHOUTEN, H., 1988. U.S. Atlantic continental margin; structural and tectonic framework. *In* Sheridan, R.E., and Grow, J.A. (Eds.), The Atlantic Continental Margin. Geol. Soc. Am., Geol. North Am. Ser., I-2: 19-53.

KRUGE, S. L. 1999, Molecular Organic geochemistry of the New York Bight sediments: Sources of the Biogenic Organic matter and Polycyclic Aromatic hydrocarbon: Northeastern and Environmental Sciences, v, 21, nos. 1/2 ,pp.121-128

KUSKOPF, K.B., and BIRD, D.K., 1995, Introduction to Geochemisty, third edition. McGraw-Hill Book Co., New York p. 647.

LANGMUIR, D. 1997, Aqueous Environmental Geochemistry. Pentice Hall Book Co., New Jersey p. 600.

LAVELLE, J.W., KELLER, G.H. and CLARKE, T.L., 1975. Possible bottom current response to surface winds in the Hudson Shelf Channel. Journal of Geophysical Research 80 15, pp. 1953-1956. Abstact-INSPEC

LI, X., SHEN, Z., WAI, O.W.H., and LI, Y-SHEUNG, 2000, Chemical Partitioning of Heavy Metals Contaminants in Sediments of the PeaL River Estuary: Chemical Speciation and Bioavailability, v.12, no.1, pp. 17-25

LITTEN, S., 1999, Toxic Chemical in New York Harbor: Northeastern geology and environmental Sciences, v. 21, nos. 1/2, pp. 18-34

LYNE, V.D., BUTMAN, B. and GRANT, W.D., 1987. sediment movement along the US east coast continental shelf-I. Estimates of bottom stress using the Grant-Madsen - Glenn model and near-bottom wave and current measurements. Continental Shelf Research 10 5, pp.397-428.

MANAHAN, S.E. 1991. Environmental chemistry. 6th ed. Chelsea, MI: Lewis Pub.Co.

MANNING, J., OEY, L., PACKER, D., VITALIANO,. FINNERAN, T., YOU, K. and FROMM, S., 1994. Observations of bottom currents and estimates of resuspended sediment transport at the New York Bight 12-mile dumpsite. Journal of Geophysical Research 99 C5, pp. 10221-1`0239. Abstract-INSPEC

MASSA, A.A., DEL VICARIO, MARIO, PABST, DOUGLAS, PECHKO, PATRICIA, LECHICH, ALEX, STERN, E.A., DIETERICH, ROBERT, and MAY,B., 1996, Disposal

of Waste and Dredged Sediments in the New York Bight: Northeastern Geology and Environmental Sciences, v. 18 pp. 265-285.

MAY, H.M., D.G. KINNIBURGH, P.A. HELMKE, and M.L. JACKSON. 1986. Aqueous dissolution, solubilities and thermodynamics stabilities of common aluminosilicate caly minerals: kaolinite and smectites. Geochim. Cosmochim. Acta 50: 1667-77.

MAYER, G.F., 1982, Ecological stress and the New York Bight: Science and management: Estuarine Research Federation, Columbia, SC, 715 p.

MCBRIDE, M.B. 1994. Environmental chemistry of soils. Oxford University Press. New York.

MCBRIDE, R.A., MOSLOW, T.F., 1991. Origin, evolution and distribution of shoreface sand ridges, Atlantic inner shelf, USA. Mar. Geol. 97, 57-85.

MCHUGH, C.M.G, PEKAR, S.F. CHRISTIE-BLICK, N., RYAN, W.B.F., CARBOTTE, S., and BELL, R., 2004. Spatial Varaiation in a Condensed Interval between Estuarine and Open-Marine Settings: Holocene Hudson River Estuary and Adjacent Continantal Shelf. Geology, v. 32; No.2 , p. 169-172.

MCHUGH, C.M.G., and OLSEN, H.C., 2002. Pleistocene chronology of continental margin sedimentation: New insights into traditional models, New Jersey. Mar. Geol. 186, 389-411.

MCHUGH, C.M.G., DAMUTH, J.E., and MOUNTAIN. 2001. Cenozoic mass-transport facies and their correlation with sea-level change, New Jersey continental margin. Mar. Geol. 184, 295-334.

METZGER, S., 1998. The New York Harbor dilemma, currents. Hudson River Environmental Society 29, 2-3.

MILLER, K.G., et al., 1994. Proc. ODP, Inti. Repts., 150X: College Station, TX (Ocean Drilling Program).

MILLER, K.G., et al., 1996a. Proc. ODP, Inti. Repts., 150X: College Station, TX (Ocean Drilling Program).

MILLER, K.G., SUGARMAN, P.J., BROWNING, J.V., et al., 1998. Proc. ODP, Inti. Repts., 174AX: College Station, TX (Ocean Drilling Program).

MONAHAN, R.K., MAYER, G.F., and STANFORD, H.M. 1987, Thirty-five Years of dumping Titanium Dioxide. NOAA/Ocean Assessments Division, Stoony Brook, New York, p.12-43.

MOREL, F.M.M., and J.G. HERING. 1993. Principles and applications of aquatic chemistry. New York: John Wiley & Sons.

MOUNTAIN, G.S., MILLER, K.G., and BLUM, P., et al., 1994. Proc. ODP Int. Rep. 150. ODP, College Station, TX.

MUELLER, J. A., ANDERSON, A. R., and JERIS, J. R., 1975, Contaminants entering the New York Bight: Sources, mass loads, significance, p. 162-172, *in* CROSS, M. G. (ed.), Middle Atlantic Continental Shelf and the New York Bight. Am. Soc. Limnol. Oceanog. Spec. Symp., v. 2, Allen Press, Lawrence, Kansas.

MUNNS, W.R. JR., and RUBINSTEIN, N.I., 1990, Environmental risks of ocean disposal: p. 515-531 *in* Cleaning up Our Coastal Waters: An unfinished Agenda, A regional conference co-sponsored by Manhattan College and the Management conferences for the Long Island Sound Study, the NY-NJ Harbor Estuary program, aqnd the NY Bight Restoration Program, March 12-14, 1990: Prepared for EPA by Dynamac Corporation under Contract 68-C8-0052.

NELSEN, T.A., GADD, P.E. and CLARKE, T.L., 1978. Wind-induced current flow in the upper Hudson Shelf Valley. Journal of Geophysical Research 83 C12, pp. 6073-6081.

NEWMAN, W.S., THURBER, D.H., ZEISS, H.S., ROCKACH, A., MUSICH, L., 1969. Late Quaternary geology of the Hudson River Estuary: a preliminary report. Transactions of the New York Academy of Sciences 31, 548-569.

NITSCHE, F.O., RYAN, W.B.F., CARBOTTE, S.M., BELL, R.E., SLAGLE, A., BERTINADO. C., FLOOD, R., KENNA. T., and M HUGH. C.M.G., 2007. Regional patterns and local variations of sediment distribution in the Hudson River Estuary. Estuarine, Coastal and Shelf Science 71, 259-277.

NOAA, 1985. National Estuarine Inventory: Data Atlas. In: Physical and Hydrologic Characteristics, vol. 1. National oceanic and Atmospheric Administration, Strategic assessment Branch, Ocean Assessment Division, Rockville, MD, 104 pp.

NOAA, 1995, Effects of the cessation of the sewage sludge dumping at the 12-Mile Site: Proceeding of the 12-Mile Dumpsite Symposium, Long Branch, NJ 18-19 June 1991, NOAA Technical Report NMFS 124, a technicalreport of the *Fishery Bulletin*, U.S. Department of Commerce, Seattle, WA, 257 p.

OLSEN, C.R., LARSEN, I.L., MULHOLLAND, P.J., VON. D.K.L., GREBMEIER, J.M., SCHAFFNER, L.C., DIAZ., R.J., and NICHOLS, M.M., 1993. The concept of an equilibrium surface applied to particle sources and contaminat distribution in estuarine sediments. Estuaries 16, 683-696.

OLSEN, C.R., SIMPSON, H.J., BOPP, R.F., WILLIAMS, S.C., PENG, T.H., and DECK, B.L., 1978. A geochemical analysis of the sediments and sedimentation in the Hudson Estuary. Journal of Sedfimentary Petrology 48, 401-418.

OLSEN, C.R., SIMPSON, H.J., PENG, T.H., BOPP, R.F., and TRIER, R.M., 1981. Sediment Mixing and accumulation rate Effects on Radionuclide Depth profile in Hudson Estuary Sediments. J. Geophy. Res. 86, 11020-11028.

PARKER, A., RAE, J.E., 1998. Environmental Interaction of clays. Springer, p. 271

PARKER, C.A., LANFREDI, N.W., and SWIFT, D.J.P., 1982. Seafloor response to flow in a southern hemisphere sand-ridge field: Argentine inner shelf. Sediment. Geol. 33, 195-216.

PAZZAGLIA, F.J., and GARDNER, T.W., 1994. Late Cenozoic flexural deformation of the middle US: Atlantic passive margin. J. Geophys. Res. 99, 12143-12157.

PEARCE, J.B., 1972, The Effects of Solid Waste Disposal on Benthic Communities in the New York Bight: Marine Pollution and sea life. Fish News, P. 404-411.

PELTIER, W.R., 1982. Dynamics of the ice age Earth. Advances in Geophysics 24, 1-146.

POAG, C.W., and WARD, L.W., 1993. Allostratigraphy of the US Middle Atlantic Continental margin – Characteristics, Distribution, and Depositional History of Principal Unconformity-Bounded Upper Cretaceous and Cenozoic Sedimentary Units. US Geol. Surv. Prof. Pap. 1542. US Gov. Printing Office, Whashington, DC, 81 pp.

RAYMOND, S.U., (Ed.), 1998. Industrial Ecology and the Environment: Applications to the New York Harbor. Report on a Workshop of the New York Academy of Sciences. September 29-30, 1997. Subsequent Observations on Action. New York Acadeny of Sciences, New York.

RIDGE, J.C., FRANZI, D.A., and MULLER, E.H., 1991, Late Wisconsin, pre-Valley Heads glaciation in the western Mohawk Valley, central New York, and its region implications: Geological Society of America Bulletin, v. 1032-1048.

RINE, J.M., TILLMAN, R.W., CULVER, S.J., and SWIFT, D.J.P., 1991. Generation of late Holocene ridges on the middle continental shelf of New Jeresy, USA - evidence for formation in a mid-shelf setting based on comparison with nearshore ridge. Spec. Publs. Int. Ass. Sediment. 14. 395-423.

SAIC, 1995. Analysis of waves and near-bottom currents during major storms at the New york mud dump site. report #20 of the New York mud dump site studies. Technical Report Science Applications International Corporation, New Port, RI.

SANDERS, J.E., 1974. Geomorphology of the Hudson Estuary. In: Roels, O.A. (Ed.), Hudson River Collquium. Annals of the New York Academy of Sciences, pp. 5-38.

SAS INSTITUTE, INC., 2002, JMP the Statistical Discovery Software: Statistics and Graphics Guide, v.5, p.707

SCHIMMEL, S.C., MELZIAN, B.D., CAMPBELL, D.E., STROBEL, C.J., BENYI, S.J., ROSEN, J.S., and BUFFAM, H.W., 1994, Statistical Summary: EMAP-Estuaries Virginia Province-1991. (EPA/620/R-94/005) U.S. Environmental Protection Agency, ORD, ERL-Narragansett, RI, p. 14-63.

SCHLEE, J., 1973. atalntic continental shelf and slope of the U.S. sediment texture of the northeast part. U.S. Geol. Surv. Prof. Pap. 529-L. 64p.

SCHWAB, W.C., THIELER, E.R., BUTMAN, B., and TEN BRINK, M.R.B., 2004, Regional Geologic Framework of the Inner-Continental Shelf off New York: Baseline Information for Environmental and Resource Management, http://pbisotopes.ess.sunusb.edu/lig/Conferences/abstracts_00/schwab/Schwab_abst.htm.

SCHWERTMANN, U., and TAYLOR, R.M., 1989. Iron oxides. p. 379-438. *In* DIXON, J.B., and WEED, S.B., (ED.) Minerals in soil environments. ASA and SSSA, Madison, WI.

SCOTT, J., BERRY, W., COBB, D., KEITH, D., TRACY, G., and RUBINSTEIN, N., 1990, The Application of the Amphipode Ten-day Toxicity Test for Dredged Material Evaluations. Contribution # 11881. U.S. EPA-ERL, Narragansett, RI, p. 55-62.

SHEPARD, F.P., and COHEE, G.V., 1936, Continental Sediments off the Mid-Atlantic Shelf: Geological Society of America Bulletin, v. 47, p. 441-456

SHERIDAN, R.E., GRADSTEIN, F.M., et al., 1983. Init. Repts. DSDP, 76: Whashington (U.S. Govt. Printing Office).

SIMPSON, H.J., OLSEN, C.R., TRIER, R.M., and WILLIAMS, S.C., 1976. Man-made radionuclides and sedimentation in the Hudson River estuary. Science 194, 179-183.

SINDERMAN, C.J., and SWANSON, R.L., 1979, Oxygen depletion and associated Benthic Mortalities in the New York Bight, 1976: NOAA professional paper 11, U.S. Department of Commerce, National Oceanic Atmospheric Administration, p. 1-16.

SPOSITO, G. 1989. The chemistry of soils. Oxford University Press, New York.

SQUIRES, D. F., 1983, The ocean dumping quandary waste disposal in the New York Bight: State University of New York Press, Albany, NY, 226p.

STAELENS, N., PARKPIAN, P., and POLPRASERT, C., 2000, Assessment of Metals Speciation Evolution in sewage sludge Dewatered in Vertical Flow Reed Beds Using a Sequential Extraction Scheme, Chemical speciation and BioAvailability, v. 12, no.3, pp. 97-107

STECKLER, M.S., and WATTS, A.B., 1978. Subsidence of the Atalantic-type continental margin off New York. Earth Planet. Sci. Lett. 41, 1-13.

STECKLER, M.S., MOUNTAIN, G.S., MILLER, K.G., and CHRISTIE-BLICK, N., 1999. Reconstructiong the geometry of Tertiary sequences on the New Jersey passive margin by 2-D backstripping: the interplay of sedimentation, eustacy and climate. Mar. Geol. 154, 399-420.

STEVENSON, F.J., and FITCH, A., 1986. Chemistry of complexation of metal ions with soil solution organics. p. 29-58. *In* P.M. Huang et al. (ed.) Interactions of soil minerals with natural organics and microbes. ASA and SSSA, Madison, WI.

STOFFER, P., and MESSINA, P., 2004, Introduction to the Geologic History of the New York Bight, http://www.geol.hunter.cuny.edu/bight/geologyhtml.

STUBBLEFIED, W.L., MCGRAIL, D.W., and KERSEY, D.G., 1984a. Recognition of transgressive and post-transgressive sand ridges on the New Jersey continental shelf. In: Tillman, R.W., Siemers, C.T. (Eds.), Siliciclastic Shelf sediments. Soc. Econ. Pleaontologists and Mineralogists, Tulsa, pp. 1-23.

STUMM, W., and MORGAN, J.J., 1996. Aquatic Chemistry, third edition. John Wiley & Sons, INC. New York p. 1022.

STUMM, W., 1992. Chemistry of the Solid-Water Inerface. John Wiley & Sons, INC. New York p.428.

SWANSON, R.L., BELL, T.M., KHAN, J., and OLHA, J., 1991, Use impairment and ecosystem impacts of the New York Bight: *Chemistry and Ecology*, V. 5, p. 99-127.

SWIFT, D.J.P., and FREELAND, G.L., 1978. Current lineations and sand waves on the inner shelf, middle atlantic bight of North America. J. Sediment. Petrol. 48, 1257-1266.

SWIFT, D.J.P., KOEFOED, J.W., SAULSBURY, F.P., and SEARS, P., 1972, Holocene evolution of the shelf surface, central and southern Atlantic shelf ofr North America, *in* Swift , D.J.P., et al., eds., Shelf sediment transport: Process and pattern: Stroudsburg, Pennsylvania, Dowden, Hutchinson & Ross, p. 499-514.

SWIFT, D.J.P., 1976. Continental shelf sedimentation. In Stanley, D.J., Swift, D.J.P., (Eds.), Marine sediment Transport and Environmental Management. Wiley, New York, pp. 311-350.

SWIFT, D.J.P., 1985. Response of the shelf floor to flow. In: Tillman, R.W., Swift, D.J.P., Walker, R.G. (Eds.), Shelf Sands and Sandstone Reservoirs. SEPM short Course Notes No. 13, pp. 135-241.

SWIFT, D.J.P., DUANE, D.B., and MCKINNEY, T.F., 1973. Ridge and swale topography of the middle atalantic bight, North America: secular response to the Holocene hydraulic regime. Ma. Geol. 15, 227-247.

SWIFT, D.J.P., MOIR, R., and FREELAND, G.L., 1980, Quaternary Rivers on the New Jersey: Relation of Seafloor to Buried Valleys. Geology, v. 8, pp. 276-280

TAVOLARO, J.F., 1989, A Sediment Budget study of Clamshell Dredging and Ocean Disposal Activities in The New York Bight. Environ Geol Water Sci Vo. 6, No.3, pp. 133-140

TROWBRIDGE, J.H., 1995. A mechanism for the formation and maintenance of shore-oblique sand ridges on storm dominated shelves. J. Geophys. Res. 100, 16071-16086.

UCHUPI, E., DRISCOLL, N., BALLARD, R.D., BOLMER, S.T., 2001. Drainage of late Wisconsin glacial lakes and the morphology and late Quaternary stratigraphy of the New Jersey-southern New England continental shelf and slope. Mar. Geol. 1972, 117-145.

USACE NEW YORK DISTRICT and EPA REGION 2, 1992, Guidance for performing tests on dredged material proposed for ocean disposal: Issued by USACE NY District, variously paged.

USACE and EPA, 1994, Long-term management plan for the NY/NJ Harbor region: USACE, New York District, NY, NY.

USACE, 1995, New York Harbor Dredged Material Management Plan: Phase I Report - Plan Study. US Army Corps of Engineers, New York district, New York, 72p.

VINCENT, C. E., SWIFT, D. J. P. and HILARD, B., 1981, Sediment Transport in the New York Bight, North American Atlantic Shelf: Marine Geology. 42:369-398.

WAKEMAN, T.H., KNOESEL, E., and KNUSTON, L., 1996, Dredged Material Disposal in Subaqueous Pits: Northeastern Geology and Environmental Sciences, v. 18. No.4, pp. 286-291.

WEISS, D., 1974. Late Pleistocene stratigraphy and Paleoecology of the Lower Hudson River Estuary. Geological Society of America Bulletin 85, 1561-1570.

WILLIAMS, S.J., and DUANE, D.B., 1974, geomorphology and sediments of the inner New York bight continental shelf: USACE, Coastal engeneering Research Center, Fort Belvoir, VA, Technical Memorandum no. 45-81p.

YOUNG, R.A., SWIFT, D.J.P., CLARKE, T.L., HARVEY, G., and BETZER, P.A., 1995, Dispersal pathways for particle-associated polluttants: Science, v. 229, no. 4712, p. 431-435.